Characterization of the Innate and Adaptive Immune Systems during Active TB Disease and during Treatment.

by

Leigh Ann Kotzé

Dissertation presented for the degree of Doctor of Philosophy (Molecular Biology) in the Faculty of Medicine and Health Sciences at Stellenbosch University.

The financial assistance of the National Research Foundation (NRF) towards this research is hereby acknowledged. Opinions expressed, and conclusions arrived at, are those of the author and are not necessarily to be attributed to the NRF.

Supervisor: Prof Gerhard Walzl

Co-supervisor: Dr Nelita du Plessis

April 2019

Declaration

By submitting this dissertation electronically, I declare that the entirety of the work contained therein is my own, original work, that I am the sole author thereof (save to the extent explicitly otherwise stated), that reproduction and publication thereof by Stellenbosch University will not infringe any third party rights and that I have not previously in its entirety or in part submitted it for obtaining any qualification.

Signature: ...  .....

Date: 12/10/2018

Summary

Individuals presenting with symptoms of active tuberculosis (TB) disease currently undergo a lengthy diagnostic procedure, followed by an intense six-month treatment regimen. Delays in accurate diagnoses and severe treatment side effects contribute to low treatment adherence and drive the emergence of drug resistant *Mycobacterium tuberculosis* (*M.tb*) strains. Improvements in diagnostic technologies have allowed for same day diagnoses, however the roll-out of such devices are limited to settings with stable infrastructure. Additionally, many patients do not require the full treatment regimen when diagnosed early or when presenting with mild disease, however few reliable methods are available for identifying fast-responders. Immune biomarkers show great promise in addressing the need for improved diagnostic and treatment response prediction techniques.

This study aimed to investigate multiple promising biomarkers, including (1) promising host diagnostic biomarkers for accurate discrimination of active TB disease from other diseases at point-of-care level; (2) promising host cell surface biomarkers for identifying treatment response shortly after treatment initiation; and also (3) functional host biomarkers for elucidating host-pathogen interaction responses for translation into diagnostic or treatment response biomarkers.

Host diagnostic biomarkers were investigated (Chapter 2) in individuals presenting with symptoms suggestive of active TB disease, stratified according to an algorithm based on a combination of clinical, radiological and laboratory findings. Nine acute-phase proteins were investigated in participants' serum, and a biosignature comprising the biomarkers C-reactive protein (CRP) and serum amyloid A (SAA), accurately discriminated between participants with and without active TB disease with a sensitivity of 87.4% and specificity of 75.7%, irrespective of human immunodeficiency virus (HIV) co-infection. The validated biosignature performance in *Ascaris lumbricoides* sensitized participants remained relatively stable (Chapter 3; Sensitivity of 78%; Specificity of 75%). Validation of this biosignature in scenarios where both HIV- and *Ascaris* co-infection were considered, identified a robust and reliable biosignature suitable for use in high-burden settings.

Individuals with confirmed active TB disease and healthy controls were recruited to investigate cell surface biomarkers of treatment response (Chapter 4). Markers of interest (CD126, CD120b, CD62L, CD197, and CD58) were investigated via flow cytometry on various immune cell subsets across three time points (diagnosis, month 1, end of treatment). No markers were differentially expressed at month 1, whereas CD120b and CD58 were upregulated the end of treatment on $CD4^+$ and $CD8^+$ T-cells, limiting their use as early treatment response biomarkers. Innate and adaptive response cytokines were then investigated from isolated cell subsets (neutrophils, monocytes, T-cells, combination) and compared to whole blood under unstimulated and antigen-stimulated conditions (Chapter 5). The downregulation of protective innate cytokines in the whole blood compared to the culture of monocytes with T-cells, suggested an active suppressive mechanism. A potential innate suppressive immune cell, myeloid-derived suppressor cells (MDSC), was then investigated in TB patients and healthy controls.

MDSC were significantly upregulated in peripheral blood mononuclear cells (PBMC) from active TB patients, and cytokine production from MDSC co-cultured with T-cells displayed T-cell-specific downregulation of IFN-γ (Chapter 6). MDSC should be considered as a potential TB diagnostic biomarker, and future studies investigating frequency changes during treatment will inform on their value as treatment response biomarker.

Opsomming

Individue wat met simptome van aktiewe tuberkulose (TB)-siekte aanbied moet tans deur ‘n lang diagnostiese prosedure ondergaan, gevolg deur ‘n intensiewe ses-maande lank behandelingskema. Vertragings in akkurate diagnose en slegte behandeling newe-effekte dra by tot lae behandeling nakoming en verhoog die opkoms van middelweerstandige *Mycobacterium tuberculosis (M.tb)* stamme. Verbeterings in diagnostiese tegnologieë het vir dieselfde dag diagnose toegelaat, maar die uitrol van sulke toestelle is egter beperk tot instellings met stabiele infrastruktuur. Daarbenewens benodig baie pasiënte nie die volle behandelingskema wanneer hulle vroeg gediagnoseer word, of wanneer hulle met sagte siekte aanbied nie, maar min betroubare metodes is beskikbaar vir die identifisering van vinnige genesing. Immuun biomerkers toon ‘n groot belofte om die behoefte aan verbeterde diagnostiese en behandelings reaksie voorspelling tegnieke aan te spreek.

Hierdie studie het daarop gemik om kandidaatbiomerkers te ondersoek, insluitend (1) gasheer diagnostiek kandidaatbiomerkers vir die akkurate onderskeiding van aktiewe TB-siekte van ander siektes, op die punt van sorg; (2) sel-oppervlak kandidaatbiomerkers vir die identifisering van behandelings reaksie kort na die begin van behandeling; asook (3) funksionele kadidaatbiomerkers vir die verduideliking van gasheer-patogeen interaksie uitkomste.

Kandidaatbiomerkers is ondersoek (Hoofstuk 2) in individue wat met simptome van aktiewe TB-siekte aan gebied het, wat gestratifiseer was volgens ‘n algoritme gebaseer op ‘n kombinasie van kliniese, radiologiese en laboratoriums bevindinge. Nege akute-fase proteïene was ondersoek in die pasiënte se serum, en ‘n biosignature bestaande uit die biomerkers C-reactive proteïen (CRP) en serum amyloid A (SAA) het akkuraat tussen deelnemers met en sonder aktiewe TB-siekte onderskei, met ‘n sensitiwiteit van 87.4% en spesifisiteit van 75.7%, ongeag menslike immunogebreksvirus (MIV) mede-infeksie. Die prestasie van die biomerk in *Ascaris lumbricoides* sensitiseerde deelnemers was gevalideer en het relatief stabiel gebly (Hoofstuk 3; Sensitiwiteit van 78%; Spesifisiteit van 75%). Validering van hierdie biomerk in gebiede waar beide MIV- en *Ascaris* mede-infeksie oorweeg is, het ‘n betroubare biomerk geïdentifiseer wat geskik is vir gebruik in hoë-las instellings.

Individue met bevestigde aktiewe TB-siekte en gesonde kontroles is gewerf om sel-oppervlak biomerkers van behandelings reaksie te ondersoek (Hoofstuk 4). Merkers van belangstel (CD126, CD120b, CD62L, CD197, en CD58) is deur middel van vloeisitometrie op verskeie immuunstelsel onderafdelings oor drie tydpunte (diagnose, maand 1, behandeling einde) ondersoek. Geen merkers is op maand 1 differensieel uitgedruk nie, terwyl CD120b en CD58 aan die einde van behandeling opgerig op $CD4^+$ en $CD8^+$ T selle is, wat hulle gebruik as behandelings reaksie biomerkers beperk. Aangebore en aanpasbare immuunstelsel-sitokiene is dan ondersoek uit geïsoleerde sel onderafdelings (neutrofiele, monosiete, T selle, kombinasies) en met heelbloed onder nie-gestimuleerde en antigeen-gestimuleerde toestande vergelyk (Hoofstuk 5). Die af-regulering van beskermende aangebore sitokiene in die heelbloed, in vergelyking met die kultuur van monosiete met T selle, het ‘n aktiewe

onderdrukkende meganisme voorgestel. ‘n Potensiële aangebore onderdrukkende immuun sel, myeloïde-afgeleide onderdrukker selle, is dan ondersoek in TB-pasiënte en gesonde kontroles. Myeloïde-afgeleide onderdrukker selle was beduidend opgerig in perifere bloed mononukleêre selle van aktiewe TB-pasiënte, en sitokien produksie van myeloïde-afgeleide onderdrukker selle gekultuur saam met T selle het T sel spesifieke af-regulering van IFN-γ vertoon (Hoofstuk 6). Myeloïde-afgeleide onderdrukker selle behoort dus beskou as ‘n potensiële TB-diagnostiese biomerker, en toekomstige studies wat die frekwensie veranderings tydens behandeling ondersoek, sal op hulle waarde as biomerkers vir behandelings reaksie inlig.

Acknowledgements

This has by no means been an easy journey, but it has taught me the value of surrounding yourself with like-minded individuals – a PhD cannot be completed without a stellar team. My team at SU Immunology Research Group (SU-IRG), my team of supervisors, my team of family, and my team of friends have all guided and supported me along this path, and I could not have done it without them.

To the colleagues who became friends at SU-IRG, thank you for the wealth of knowledge you shared with me, for the countless “stupid questions” asked during training, and for perhaps just as many hours of expressing my troubles and concerns. Thank you all for being selfless teachers and for constantly encouraging critical thinking. A few special mentions: Bronwyn Smith, thank you for taking me under your wing so early on in my education. Your calm approach to the crazy world we live in taught me the patience I never had, your assistance with the early FACS experiments taught me to think critically, and your honest friendship is so treasured. Devon Allies, thank you for reminding me to come down to earth when my head was so lost in the clouds. Your friendship helped me through many a troubling time, even though you still manage to irritate me sometimes. To the rest of the group, your words of encouragement and bear hugs when things were difficult will never be forgotten. I appreciate you all.

A heartfelt thank you to the clinical team who daily collected samples that contributed to the work in this dissertation. Thank you for always being willing to help and for the smiles that accompanied it.

To my friends, I thank you for your constant support and mostly your understanding. Thank you for your objective advice and the reprieve from the study environment. A few special mentions: Ilana van Rensburg, you never give yourself the credit you are due. Girl, you are a genius! Thank you for being the friend I could always count on (especially when things got a bit too crazy) and for being the person that has always inspired me most, both intellectually and personally. You are going to go far, my friend. Lastly, Melisse Erasmus. Life tends to deal us cards we would otherwise wish could not be played. Thank you for showing me true strength, and even though our PhD’s have kept us apart you have always been there to guide and encourage, and sometimes even help troubleshoot. Thank you.

To my supervisor’s, Prof Gerhard Walzl and Dr Nelita du Plessis. I imagine I was quite a handful…especially in these last few weeks. Thank you for always being patient and showing me so much kindness. Thank you for imparting on me your skills and expertise, your passion for science, and your work ethic. Most importantly, thank you for taking a chance on me and trusting me with your research interests. I have learned so much under your guidance and will be forever grateful. You inspire those around you on a daily basis and I am so privileged to have been student to both of you. Prof, thank you for setting aside time in your busy schedule to make sure I got this far. I will always appreciate the opportunities and wisdom you afforded me. Nelita, thank you for being the calm in the storm. You are definitely the expert of time management; a quality I aspire to achieve. Thank you for always being there.

To my mentor, Prof Hazel Dockrell. Thank you for our hour-long Skype calls once a month. Thank you for your patience when schedules were too busy, thank you for your constructive criticism, your encouragement, support and belief from afar. I thank you.

To my parents, Peter and Toni, and my brother and sister, Jamie and Robyn. Thank you for always believing in me even when I did not believe in myself. I am forever grateful for the sacrifices you made along the way for me to achieve my dreams, and I could not ask for more loving and giving parents. I am proud to be your daughter. To my siblings, we often get caught up in our own lives and forget to remove the blinkers. I hope this long journey you have walked with me has taught you that nothing is impossible, but also that the greater the input the greater the reward. You have both been there when I have stumbled and lost my way, and I thank you for your gentleness and kindness in those times. I would also thank my grandparents: Ouma and Oupa, and Nan and Grandad. The four of you have been such a precious blessing throughout my life. Thank you for teaching me resilience and kindness and thank you for pushing me when I was tired. I would never have made it to this point without your support. Lastly, to my godmother. You instilled in me the love I have for reading, a quality I treasure beyond measure and one we can share together with mum, which likely put me on the path of discovery that stopped at the Science station somewhere along the way. Both your career-driven focus and your passion for our family has been a wonderful example throughout my life. I love you all.

To Justin. You have been my partner in crime since day one. You celebrated with me at my career highs and loved me at my lows. Thank you for being my pillar of strength through thick and thin and thank you for being my biggest supporter. You have always inspired me with your dedication to your own studies and I am so proud of you. Thank you for everything. I am so excited for our future!

To end it all off, I would like to thank the funders, without whom this would never have been possible. I would like to thank the National Research Foundation Freestanding, Innovation and Scarce Skills Bursary Fund and Stellenbosch University for personal funding and support, as well as all the funding bodies involved in the larger studies through which these studies would not have been possible.

If you can’t fly, then run.
If you can’t run, then walk.
If you can’t walk, then crawl,
But by all means, keep moving.
-Martin Luther King Jr.

Table of Contents

CHARACTERIZATION OF THE INNATE AND ADAPTIVE IMMUNE SYSTEMS DURING ACTIVE TB DISEASE AND DURING TREATMENT. I
DECLARATION I
SUMMARY II
OPSOMMING IV
ACKNOWLEDGEMENTS VI
TABLE OF CONTENTS VIII
LIST OF TABLES X
LIST OF FIGURES XIII
SUMMARY OF RESEARCH 1
CHAPTER 1 4
LITERATURE REVIEW 4
TUBERCULOSIS PATHOGENESIS 4
INNATE IMMUNE RESPONSE TO TB 6
ADAPTIVE IMMUNE RESPONSE TO TB 11
TUBERCULOSIS DIAGNOSIS 16
TREATMENT REGIMENS AND OUTCOMES 19
BIOMARKERS IN TUBERCULOSIS 20
COMORBIDITIES OF TUBERCULOSIS 23
CONCLUSION 26
CHAPTER 2 27
INVESTIGATION OF HOST SERUM BIOMARKERS FOR THE DIAGNOSIS OF TB DISEASE. 27
2.1 STUDY DESIGN 28
2.2 METHODS 29
2.3 RESULTS 36
2.4 DISCUSSION 44
CHAPTER 3 52
EVALUATION OF THE POTENTIAL INFLUENCE OF *ASCARIS LUMBRICOIDES* CO-INFECTION ON THE ACCURACY OF A RECENTLY IDENTIFIED HOST IMMUNE BIOSIGNATURE FOR THE DISCRIMINATION BETWEEN INDIVIDUALS WITH ACTIVE TB DISEASE AND THOSE WITHOUT *M.TB* INFECTION. 52
3.1 STUDY DESIGN 55
3.2 METHODS 56
3.3 RESULTS 59
3.5 DISCUSSION 75
3.6 ADDENDUM 85
CHAPTER 4 88

Investigation of PBMC surface marker expression as indicators of treatment response. 88
4.1 Study Design 89
4.2 Methods 90
4.3 Results 100
4.4 Discussion 124
CHAPTER 5 139
Evaluation of the Contribution of Individual Leukocyte Subsets Towards the Overall Immune Response. 139
5.1 Study Design 140
5.2 Methods 141
5.3 Results 152
5.4 Discussion 164
5.5 Addendum 169
CHAPTER 6 178
Investigation into the role of Myeloid-Derived Suppressor Cells in peripheral blood during the immune response to TB disease. 178
6.1 Study Design 181
6.2 Methods 182
6.3 Results 193
6.4 Discussion 217
CHAPTER 7 229
Conclusion 229
REFERENCE LIST 237

List of Tables

Table 2.1: *Harmonized classification criteria of participants based on combinations of clinical and microbiological findings.* _____ *30*

Table 2.2: *Luminex Immunoassay kits used for the investigation of the nine cytokines of interest.* _ *31*

Table 2.3: *Participant demographics according to the harmonised classification algorithm.* _____ *36*

Table 2.4: *Median concentrations of the top four host serum analytes detected in participants with active TB disease (n = 221) and those without TB disease (n = 489), independent of HIV infection status.* _____ *37*

Table 2.5: *Median concentrations of the top four host serum analytes detected in participants with active TB disease (n = 221) and those latently infected (n = 221), independent of HIV infection status.* _____ *38*

Table 2.6: *Median concentrations of host serum analytes detected in HIV negative participants with active TB disease (n = 163) and those without TB disease (n = 376), as well as their diagnostic accuracy and optimum cut-off values to achieve this.* _____ *40*

Table 2.7: *Median concentrations of host serum analytes detected in HIV positive participants with active TB disease (n = 58) and participants without TB disease (n = 114), as well as their diagnostic accuracy and optimum cut-off values to achieve this.*_____ *40*

Table 2.8: *Superlearner model building outcomes using the Training and Test set approach for the combination of the biomarkers CRP and SAA for the optimal combined sensitivity and specificity.* _ *42*

Table 2.9: *Superlearner model building outcomes using the Training and Test set approach for the combination of the biomarkers CRP and SAA for a sensitivity kept greater than or equal to 90%.* _ *43*

Table 3.1: *Multiplex kit details for the assessment of Ascaris exposure.* _____ *57*

Table 3.2: *Ascaris-specific IgE ImmunoCAP® ranges and clinical significance in terms of diagnosing Ascaris sensitization.*_____ *59*

Table 3.3: *Classification of the Luminex analysis participants according to their TB and Ascaris infection statuses, as well as the general demographics for each classification group.* _____ *62*

Table 3.4: *Classification of the Luminex analysis participants according to their Ascaris infection status alone, as well as the general demographics for each classification group.*_____ *62*

Table 3.5: *Median concentrations of the nine APP as detected in participants with active TB disease only (n = 6), and participants without either disease (n = 11).*_____ *66*

Table 3.6: *Median concentrations of the nine APP as detected in participants with active TB disease and Ascaris co-infection (n = 15), and participants with Ascaris infection only (n = 16).*_____ *67*

Table 3.7: *Training/Test set statistical output of the assessed biosignature candidates for the discrimination between participants with and without active TB disease in a cohort for which Ascaris sensitization status is known.* _____ *71*

Table 3.8: *Training/Test set statistical output of the assessed biosignature candidates for the discrimination between participants with and without active TB disease in a cohort for which Ascaris sensitization status is known.* _____ *72*

Table A3.1: *Classification of all study participants according to their TB and Ascarisinfection statuses.* _____ *85*

Table A3.2: *Classification of all study participants according to their Ascaris infection status alone..* *85*

Table 4.1: *The reagents and respective manufacturers and lot numbers used for the sample preparation of Aim 1.* _____ *92*

Table 4.2: *The antibodies chosen to investigate the markers of interest on the surface of immune cells, and their respective catalogue numbers and clones.* _____ *94*

Table 4.3: *Participant demographics for the active TB and healthy control participants enrolled into Aim 1 of this study.* _____ *100*

Table 4.4: *Participant demographics for the active TB and healthy control participants enrolled into Aim 2 of this study.* _____ *101*

Table 4.5: *Summary of the significant results observed for each marker's frequency in each cell subset assessed.* _____ *113*

Table 5.1: *General reagents prepared for use during this study, their manufacturers and catalogue numbers.* _____ *142*

Table 5.2: *Details of the Antibodies used for the Determination of Cell Subset Purities.* _____ *142*

Table 5.3: *MACS® Column specifications for the MS and LS column types used for positive selection.* _____ *144*

Table 5.4: *The number of cells required per stimulation and in total for each isolated cell subset.* *147*

Table 5.5: *Staining conditions and single stain specifications for the purity check samples.* _____ *149*

Table 5.6: *Demographics of the six healthy volunteer participants.* _____ *152*

Table 5.7: *Expected cell frequencies and yields from a standard Ficoll-Paque density media gradient centrifugation experiment (based on literature estimates) for total PBMC, lymphocytes and monocytes alike.* _____ *153*

Table 5.8: *Fraction purities (given as a percentage) obtained for each isolated cell subset, as well as the frequency (given as a percentage) of PBMC that these cells make up.* _____ *156*

Table 5.9: *Cytokines produced in the whole blood compartment and by the isolated subsets investigated in this study in the unstimulated condition.* _____ *159*

Table 5.10: *Cytokines produced in the whole blood compartment and by the isolated subsets investigated in this study in the stimulated condition.* _____ *160*

Table 5.11: *Significance values for each of the cytokines that were downregulated in whole blood compared to the combined culture of monocytes and T lymphocytes after non-specific stimulation.* *161*

Table A5.1: *Significance values for each of the cytokines that were downregulated in whole blood compared to the combined culture of monocytes and T lymphocytes after non-specific stimulation.* *160*

Table 6.1: *General reagents prepared for use during this study.* _____ *183*

Table 6.2: *Co-stimulatory antibody working solution preparation details.* _____ *184*

Table 6.3: *Outline of the stimulation conditions used and the cell numbers used for each.* _____ *186*

Table 6.4: *Staining conditions and single stain specifications for the purity check samples.* _____ *188*

Table 6.5: *The antibodies chosen to investigate the phenotype of MDSC's in terms of their TLR4 and potential Cav-1 expression.* _____ *188*

Table 6.6: *The two multiplex kit details for the assessment of human cytokines and chemokines.* *190*

Table 6.7: *Active TB and Healthy Control Participant Demographics.* *193*

Table 6.8: *Individual participant data on the yield and purity for each cell subset isolated during this study, namely MDSC, monocytes and T cells.* *195*

Table 6.9: *Normalization methods employed to ensure the normal distribution of raw data for each cytokine, prior to statistical analyses.* *212*

List of Figures

Figure 1.1: *A summary illustration of the immune response to Mycobacterium tuberculosis infection up to the point at which the granuloma is established.* 5

Figure 1.2: *A revised view of T cell mediated immunity to TB following T cell activation, proliferation and migration to the site of infection.* 12

Figure 2.1: *Diagram of the 5-Plex Standard Dilution Series to be made.* 33

Figure 2.2: *Diagram of the 4-Plex Standard Dilution Series to be made.* 33

Figure 2.3: *Receiver Operating Characteristic (ROC) curves representing acute phase proteins used during univariate analyses.* 39

Figure 2.4: *Histogram depicting the AUC values for each marker when assessed irrespective of HIV infection status, as well as when assessed in HIV negative and positive population groups respectively.* 41

Figure 2.5: *ROC curves of the superlearner model using the (a) Training and (b) Test datasets for the evaluation of the model's performance.* 42

Figure 3.1: *The reproductive lifecycle of Ascaris lumbricoides from the ingestion of fertilized eggs from contaminated soil, until the worms mature and themselves are able to reproduce, with specific interest in their maturation stage in the human lungs.* 53

Figure 3.2: *Comparison of Ascaris Sensitization Frequencies in the South African Sample Community from Fisantekraal, Western Cape (blue bars), and the Sensitization Frequencies in a subset of Multiple Sample Communities in South Africa (specifically from the AE-TBC, grey bars).* 60

Figure 3.3: *Comparison of the distribution of Ascaris sensitization in male and female participants.* 60

Figure 3.4: *Overall Ascaris-specific IgE sensitization results stratified according to the ImmunoCAP®'s suggested ranges.* 61

Figure 3.5: *Ascaris co-infection with TB significantly alters the circulating concentrations of CRP and SAA.* 63

Figure 3.6: *Ascaris co-infection with TB significantly alters the circulating concentrations of CRP and SAA.* 64

Figure 3.7: *Active TB alters circulating CRP and SAA independently of Ascaris co-infection.* 65

Figure 3.8: *Individual biomarker diagnostic accuracies when stratified according to Ascaris infection status.* 68

Figure 3.9: *Combination of the biomarkers CRP and SAA for the diagnosis of TB from No TB in QFT Nil and QFT Antigen conditions.* 69

Figure 3.10: *Combination of the biomarkers CRP, SAA, SAP, PCT, tPA, A2M, Ferritin, Fibrinogen, and Haptoglobin for the diagnosis of TB from No TB in QFT Nil and QFT Antigen conditions.* 70

Figure 3.11: *Combination of the biomarkers SAA, tPA and PCT for the diagnosis of TB from No TB in QFT Nil and QFT Antigen conditions.* 73

Figure 3.12: *Combinations of biomarkers assessed for the discrimination between active TB disease and No TB in Ascaris infected participants only.* 74

Figure A3.1: *Ascaris and active TB disease coinfection influence on the remaining seven acute phase proteins.* _____ *86*

Figure A3.2: *Ascaris and active TB disease coinfection influence on the remaining seven acute phase proteins under unstimulated (Nil) and antigen-stimulated (Antigen) conditions.* _____ *87*

Figure 4.1: *Demonstration of the FSC and SSC settings during instrument setup.* _____ *96*

Figure 4.2: *Demonstration of the gating strategy used to ensure true lymphocyte and granulocyte populations could be distinguished.* _____ *98*

Figure 4.3: *The gating strategy developed using the FMO for Panel 1 for the investigation of CD4+ and CD8+ T cell subsets.* _____ *102*

Figure 4.4: *The gating strategy developed using the FMO for Panel 1 for the investigation of CD19+ B cells.* _____ *103*

Figure 4.5: *The gating strategy developed using the FMO for Panel 2 for the investigation of NK cells.* _____ *104*

Figure 4.6: *The gating strategy developed using the FMO for Panel 2 for the investigation of NKT cells.* _____ *105*

Figure 4.7: *The gating strategy developed using the FMO for Panel 2 for the investigation of Neutrophils.* _____ *106*

Figure 4.8: *The gating strategy developed using the FMO for Panel 2 for the investigation of classical and intermediate monocyte subsets.* _____ *107*

Figure 4.9: *The gating strategy for the investigation of the markers of interest on all cells, developed using the FMO for Panel 1 and 2.* _____ *108*

Figure 4.10: *Comparison between the CD3 expression frequencies of Panels 1 and 2 for both TB patients and healthy controls (p = 0.015).* _____ *109*

Figure 4.11: *Representative dot plots of the frequency of (a) CD126, (b) CD120b and (c) CD62L on all cells acquired by flow cytometry over the course of TB treatment and in healthy controls (HC).* __ *111*

Figure 4.12: *Representative dot plots of the frequency of (a) CD58 and (b) CD197 on all cells acquired by flow cytometry over the course of TB treatment and in healthy controls (HC).* _____ *111*

Figure 4.13: *Frequency of (a) CD126, (b) CD62L, (c) CD120b, (d) CD58 and (e) CD197 expressing $CD4^+$ T lymphocytes represented as a frequency of total cells at the baseline (BL), month 1 (M1), and month 6 (M6) time points compared to healthy controls (HC).* _____ *114*

Figure 4.14: *Frequency of (a) CD126, (b) CD62L, (c) CD120b, (d) CD58 and (e) CD197 expressing $CD8^+$ T lymphocytes represented as a frequency of total cells at the baseline (BL), month 1 (M1), and month 6 (M6) time points compared to healthy controls (HC).* _____ *115*

Figure 4.15: *Frequency of (a) CD126, (b) CD62L, (c) CD120b, (d) CD58 and (e) CD197 expressing B lymphocytes represented as a frequency of total cells at the baseline (BL), month 1 (M1), and month 6 (M6) time points compared to healthy controls (HC).* _____ *116*

Figure 4.16: *Frequency of (a) CD126, (b) CD62L, and (c) CD120b expressing NK cells represented as a frequency of total cells at the baseline (BL), month 1 (M1), and month 6 (M6) time points compared to healthy controls (HC).* _____ *116*

Figure 4.17: *Frequency of (a) CD126, (b) CD62L, and (c) CD120b expressing NKT cells represented as a frequency of total cells at the baseline (BL), month 1 (M1), and month 6 (M6) time points compared to healthy controls (HC).* _____ *117*

Figure 4.18: *Frequency of (a) CD126, (b) CD62L, and (c) CD120b expressing Neutrophils represented as a frequency of total cells at the baseline (BL), month 1 (M1), and month 6 (M6) time points compared to healthy controls (HC).* _____ *117*

Figure 4.19: *Frequency of (a) CD126, (b) CD62L, and (c) CD120b expressing intermediate monocytes represented as a frequency of total cells at the baseline (BL), month 1 (M1), and month 6 (M6) time points compared to healthy controls (HC).* _____ *118*

Figure 4.20: *Frequency of (a) CD126, (b) CD62L, and (c) CD120b expressing classical monocytes represented as a frequency of total cells at the baseline (BL), month 1 (M1), and month 6 (M6) time points compared to healthy controls (HC).* _____ *118*

Figure 4.21: *The median frequency of expression of the markers (a) CD58 and (b) CD197 which were assessed in the $CD4^+$ T lymphocyte (red data point), $CD8^+$ T lymphocyte (orange data point) and B lymphocyte (yellow data point) subsets, as well as on all cells (green data point).*_____ *119*

Figure 4.22: *The median frequency of expression of the markers (a) CD126, (b) CD62L, and (c) CD120b which were assessed in the $CD4^+$ T lymphocyte (red data point), $CD8^+$ T lymphocyte (orange data point), B lymphocyte (yellow data point), neutrophil (green data point), NK cell (turquoise data point), NKT cell (light blue data point), classical monocyte (dark blue data point), and intermediate monocyte (purple data point) subsets, as well as on all cells (pink data point).* _____ *120*

Figure 4.23: *Absolute counts of innate and adaptive immune cell subsets as seen in the peripheral blood of thirteen active TB participants at four time points during TB treatment, i.e. baseline, week 2, month 1, and month 6.*_____ *121*

Figure 4.24: *Absolute counts of innate and adaptive immune cell subsets as seen in the peripheral blood of 112 active TB participants at two time points during TB treatment, i.e. baseline (BL) and month 6 (M6), as well as 52 healthy controls.* _____ *123*

Figure 5.1: *An example of the general gating strategy used for all samples prior to fluorochrome-specific gating.*_____ *149*

Figure 5.2: *Morphological characteristics of the isolated cellular fractions.* _____ *152*

Figure 5.3: *Comparison between the flow cytometry data for PBMC and isolated monocyte cell fractions stained with the CD14-PE antibody.*_____ *155*

Figure 5.4: *The seven cytokines that had a significantly lower production in whole blood compared to when monocytes and T lymphocytes were co-cultured in response to non-specific stimulation.* __ *163*

Figure A5.1: *The 26 cytokines assessed during this study, under unstimulated conditions.* _____ *170*

Figure A5.2: *The 26 cytokines assessed during this study, under stimulated conditions.* _____ *173*

Figure A5.3: *SPICE pie charts representing the relative contributions of each cytokine to the overall individual cell subset cytokine profile of* ***unstimulated*** *samples, expressed as a proportion.* ____ *176*

Figure A5.4: *SPICE pie charts representing the relative contributions of each cytokine to the overall individual cell subset cytokine profile of* ***antigen stimulated*** *samples, expressed as a proportion.* *177*

Figure 6.1: *Morphological characteristics of the isolated immune cell populations.*_____ *197*

Figure 6.2: *A visual comparison between a (a) stable and (b) unstable sample acquisition where an interruption in the sample flow (b) may be observed around 12.5 on the Time axis.* _____ *199*

Figure 6.3: *Gating strategy employed for the identification of eMDSC from enriched HLA-DR$^-$CD33$^+$ MDSC isolated from PBMC.* _____ *201*

Figure 6.4: *Gating strategy employed for the identification of M-MDSC from enriched HLA-DR$^-$CD33$^+$ MDSC isolated from PBMC.* _____ *202*

Figure 6.5: *Gating strategy employed for the identification of PMN-MDSC from enriched HLA-DR$^-$CD33$^+$ MDSC isolated from PBMC.* _____ *203*

Figure 6.6: *Gating strategy employed for the identification of CD14$^+$ Monocytes from the enriched CD14$^+$ Monocyte population isolated from PBMC.* _____ *204*

Figure 6.7: *Frequencies of MDSC subsets as a percentage of the total number of isolated PBMC in TB patients compared to QFT positive and negative healthy controls.*_____ *205*

Figure 6.8: *Comparison between the frequencies of the different MDSC subsets (as a percentage of the total number of isolated PBMC) in (a) TB patients and (b) healthy controls.*_____ *206*

Figure 6.9: *Median fluorescent intensities of the surface markers CD14 and CD15, comparing their expression in (a) TB patients ($p < 0.0001$), and (b) healthy controls ($p < 0.0001$).* _____ *207*

Figure 6.10: *Comparison of the frequency of isolated autologous HLA-DR$^+$CD14$^+$ monocytes, as a percentage of the total number of isolated PBMC, (a) between TB patients and healthy controls ($p = 0.26$).* _____ *208*

Figure 6.11: *Median fluorescent intensity of the surface marker CD14, comparing its expression between total MDSC and Monocytes in (a) TB patients ($p = 0.09$), and (b) healthy controls ($p = 0.0013$).* _____ *208*

Figure 6.12: *Comparison of the frequency of cells, both MDSC and monocyte, expressing the surface markers Caveolin-1 and TLR4 between TB patients and healthy controls.*_____ *209*

Figure 6.13: *Median fluorescent intensities of the surface markers (a) Cav-1 ($p = 0.051$) and (b) TLR4 ($p = 0.102$), measuring their expression on the surface of MDSC TB patients and healthy controls.* *210*

Figure 6.14: *Comparison between the frequency of MDSC and monocytes expressing the surface markers Caveolin-1 and TLR4 in TB patients and healthy controls.* _____ *211*

Figure 6.15: *Cytokines involved primarily in the induction of HLA-DR$^-$CD33$^+$ MDSC were upregulated following stimulation of MDSC with PPD, compared to unstimulated HLA-DR$^-$CD33$^+$ MDSC.* ____ *213*

Figure 6.16: *Upregulated cytokines involved in the recruitment and regulation of HLA-DR$^-$CD33$^+$ MDSC following stimulation with PPD, compared to unstimulated HLA-DR$^-$CD33$^+$ MDSC.* _____ *213*

Figure 6.17: *Upregulated cytokines involved in unconventional induction and immunosuppressive functions of HLA-DR$^-$CD33$^+$ MDSC following stimulation with PPD, compared to unstimulated HLA-DR$^-$CD33$^+$ MDSC.* _____ *214*

Figure 6.18: *Co-culture of PPD stimulated CD3$^+$ T cells with (+MDSC) and without (-MDSC) HLA-DR$^-$CD33$^+$ MDSC resulted in the significant (a) upregulation of soluble Fas ($p = 0.0454$), and (b) upregulation of IL-1β ($p = 0.0223$) concentrations in the* ***presence*** *of MDSC, when co-cultured in a ratio of 1:2.5 (error bars represent the median and interquartile range).*_____ *215*

Figure 6.19: *Co-culture of PPD stimulated $CD3^+$ T cells with (+MDSC) and without (-MDSC) HLA-DR^- $CD33^+$ MDSC resulted in the significant (a) downregulation of T cell-specific IFN-γ ($p = 0.0334$), and (b) upregulation of C-C Motif Chemokine Ligand 2 (CCL2) ($p = 0.0129$) concentrations in the **presence** of MDSC, when co-cultured in a ratio of 1:1 (error bars represent the median and interquartile range).* _____ *215*

Figure 7.1: *Graphical simplification of the pipeline through which patients with active TB disease go, and the biomarker types employed during each phase.* _____ *230*

SUMMARY OF RESEARCH

The overarching theme of this manuscript was the investigation of biomarkers in the context of active TB disease. Biomarkers serve a dual function in research: they are most commonly investigated for use as discriminatory tests but may also function to unearth important questions about the biology of a disease.

As a research community, we have still not established a robust set of biomarkers for use across multiple geographical regions, which highlights the importance of continued biomarker research. In this dissertation we aimed to investigate and explore various biomarker avenues; including diagnostic biomarkers, treatment response biomarkers, and functional biomarkers which may elucidate further biological mechanisms for active TB disease.

Firstly, host serum biomarkers were investigated for potential use in a rapid diagnostic tool. It was hypothesized that the levels of acute phase proteins would be significantly different in active TB disease patients in comparison to patients without active TB disease but who present to primary healthcare clinics with symptoms compatible thereto, and that these proteins would be useful as a diagnostic biosignature for active TB disease. Thus, we aimed to investigate nine host serum biomarkers as potential contributors to a future rapid diagnostic. This study successfully identified a serum-based biosignature made up of C-reactive protein (CRP) and serum amyloid A (SAA) which accurately discriminated between individuals with active TB disease and those without with a high sensitivity and diagnostic accuracy, irrespective of HIV infection. While not suited as a diagnostic tool based on World Health Organization guidelines, this finding is important because of its ability to be developed as a point-of-care, rule-out triage test, particularly in high-burden settings where HIV co-infection is prevalent. While CRP and SAA are considered general inflammatory proteins and therefore not specific for active TB disease, the observation that the production of these proteins are significantly higher than seen during other respiratory diseases makes them worthy non-specific biomarker candidates for active TB disease.

It is well known that in highly endemic settings HIV is not the only co-infection present compromising the immune response against active TB disease. The stability of the two-biomarker biosignature was therefore validated under other co-infection settings. Literature revealed that soil-transmitted helminth infections are significantly underreported and represented in southern- and South Africa, particularly in the adult population. *Ascaris lumbricoides,* the most common soil-transmitted helminth in South Africa, is known to drive type 2 mediated T cell responses that overshadow protective type 1 T cell responses during active TB disease. Thus, it was hypothesized that the diagnostic accuracy of the two-biomarker biosignature would not be significantly influenced by the presence of concurrent *Ascaris lumbicoides* sensitization, and the study aimed to investigate the potential influence of helminth co-infections on the diagnostic accuracy of the biosignature. Besides a drop in biomarker sensitivity, the performance of the

biosignature (CRP and SAA) remained relatively the same, which shows great promise for use in regions where helminth (*Ascaris lumbricoides* specifically) and *Mycobacterium tuberculosis* co-infections are prevalent, such as in southern- and South Africa.

With the successful identification of a blood-based diagnostic biosignature (for use as a triage test), alternative blood-based biomarkers were investigated for use as indicators of treatment response. Previous studies in our research group identified three biomarkers with potential promise as treatment response biomarkers, with significant differences being observed between treatment timepoints, namely at diagnosis, month 1 after treatment and at the end of treatment. These biomarkers were surface markers identified on the surface of peripheral blood mononuclear cells (PBMC) and were CD126, CD120b, and CD62L. The hypothesis for this chapter was then that the evaluation of the three identified surface markers on individual cell types from patients with active TB disease during anti-TB therapy would allow for the identification of cell-specific biomarkers of treatment response. This study aimed to investigate the three biomarkers identified previously, as well as an additional two promising biomarkers (CD58 and CD197), in whole blood instead of PBMC at various time points in relation to treatment in order to elucidate which immune subsets are responsible for the differential expression of these markers. Expression of the five markers was assessed on all cells and found to not significantly change across the treatment period, except for CD58, contrary to previous findings. This observation is particularly important as it highlighted the notion that PBMC are not good representatives of the whole blood environment in terms of surface marker expression. Individual subset expression supported this finding, as only two markers changed over the treatment period on various immune subsets, contrary to previous findings. These findings support the belief that PBMC cannot be used as a proxy for whole blood surface marker expression, as many immune subsets may be excluded during isolation steps and bias results.

The diagnostic and treatment response biomarker investigations focused on marker of the innate immune system, a host defense mechanism that has recently proven to be of more importance than historically thought. In order to better understand the biology of *Mycobacterium tuberculosis* infection and the innate immune response towards it, the next chapter investigated differences in cytokine production, the products produced by innate immune subsets which elicit protective effects and adaptive immune activation. The hypothesis postulated that the differential expression of innate immune response proteins, in an antigen-stimulated manner, is dependent on the presence of both innate and adaptive immune subsets. This study aimed to evaluate and compare the differential expression profiles of various innate cytokines in culture conditions with single immune subsets and combinations of such subsets, in order to determine the contribution of each immune subset to the cytokine signature. Antigen-stimulation resulted in the downregulation of important cytokines in the whole blood compartment which are crucial for adequate control of *M.tb* infection. This was in comparison to their production by isolated T cells cultured in the presence of isolated monocytes in latently infected participants and eluded to suppressive immune cell types within the whole blood compartment. In

particular, the downregulation of TNF-α drove the investigation of suppressive innate immune cell types not frequently investigated in active TB disease.

One such subset considered was the myeloid-derived suppressor cell (MDSC) subset owing to their limited, yet interesting research availability. A subset of immature myeloid cells, MDSC present with suppressive properties in cancer and active TB disease, to a lesser extent. This study hypothesized that MDSC alter immune responses during *M.tb* infection and disease. MDSC have previously been investigated in the context of active TB disease only in whole blood, however literature has shown that PBMC are the most suited for MDSC investigation. This study, therefore, aimed to investigate the immunomodulatory role of MDSC in PBMC on the immune response during active TB disease compared to latent *M.tb* infection. Considering the novelty of these cells in TB research, this study had a secondary aim of investigating the presence or absence of caveolin (a protein associated with lipid rafts) and TLR4 (a receptor on the surface of most innate immune subsets for the detection of lipopolysaccharide proteins) on the surface of MDSC as a theoretical proof-of-concept for future studies. In agreement with previous literature, this study observed an upregulation of total MDSC in active TB disease patients compared to controls, however the most prevalent MDSC subset was the monocytic subset, contrary to previous literature. While caveolin and TLR4 are not novel markers, they have not been investigated on the surface of MDSC, and this study confirmed their presence via flow cytometry – a first for human TB research. These findings raise important questions as to the biological functions of these markers in MDSC during active TB disease, potentially acting as alternative mechanisms of *M.tb* entry into MDSC to bypass traditional phagolysosome destruction, thus creating a reservoir for MDSC survival. Finally, cytokine production investigations revealed that purified protein derivative (PPD)-stimulated MDSC produced multiple cytokines associated with MDSC expansion and effector functions in cancer, while PPD-stimulated MDSC co-cultured with T cells resulted in a significant downregulation of T cell-specific IFN-γ which is very important for bacterial clearance and control during active TB disease. These findings highlight the potential role of MDSC as functional biomarkers for biological responses observed during diagnosis and response to treatment.

CHAPTER 1

Literature Review

The human immune system, like all other biological systems in the human body, aims to maintain homeostasis to preserve the internal equilibrium when external challenges are met. One such challenge that threatens homeostasis involves the entry of *Mycobacterium tuberculosis* (*M.tb*) into the lungs, following the inhalation of aerosol droplets containing the bacteria, and entry across the mucosal barrier which provides the primary defense mechanism against invasion from foreign pathogens. Although the host immune system destroys *M.tb* shortly after entry for a minority of individuals, the largest number of individuals are latently infected while *M.tb* is contained by the immune system in micro-granulomas and its pathogenic effects kept at bay, or it evades the host immune system entirely to develop into active disease. *M.tb*, an acid-fast bacillus, has recently been ranked the leading cause of death worldwide alongside HIV, killing approximately 1.3 million people (HIV negative), of an estimated 10 million people predicted to have contracted the disease in 2017 alone which highlights the urgent requirement for improved focus on tuberculosis (TB) research[1].

Tuberculosis Pathogenesis

The World Health Organization (WHO) estimates that approximately a quarter of the world's population is infected with *M.tb*, yet only about 10% of these individuals ever progress to active disease[1]. 90% of individuals who are infected with *M.tb*, therefore remain asymptomatic and control the infection so that it never has the chance to progress to active disease. Many hypotheses have been suggested as to why this figure exists as it does, but owing to both the invading bacteria as well as the human immune response being widely heterogeneous, stratification of patients according to their exposure to *M.tb* becomes complicated[2].

Upon inhalation of infected droplets, the bacteria breach the mucosal barrier in the lungs and enters the alveolar space. Here, the bacteria is recognized by pattern recognition receptors (PRR's) of the innate immune system which are expressed on the surfaces of alveolar epithelial cells, alveolar and interstitial macrophages, as well as dendritic cells (DC's) which engulf the bacteria via phagocytosis[3–5]. These cells are known as antigen-presenting cells (APC's) as they present the phagocytosed antigen to antigen-specific adaptive immune cells to trigger the adaptive immune response. Inside these phagocytes, the bacteria are encased in phagosomes which are capable of fusing with lysosomes to create the phagolysosome – an acidic and hypoxic environment not favorable for the survival of the bacteria[3]. The enzymes released by the lysosome degrade the bacteria into smaller peptides/antigens which may then be loaded onto major histocompatibility complex (MHC) class-II molecules which subsequently display these peptides to antigen-specific $CD4^+$ T lymphocytes (and to some degree $CD8^+$ T lymphocytes via MHC class I molecules) to initiate an adaptive immune response when these APC's circulate into the lymph nodes[5]. The T cells are thus activated and release various pro-inflammatory

cytokines and chemokines to further activate macrophages presenting *M.tb* antigens to initiate their innate anti-mycobacterial killing mechanisms. Should the infected APC's not be able to eradicate the bacteria successfully, activated T cells migrate to the site of infection in the lung and stimulate the formation of granulomas – an organized structure containing infected macrophages at the center which are surrounded by central memory T cells, fibroblasts, lymphocytes, foamy macrophages, granulocytes, and other mononuclear phagocytes in order to contain the infection and limit the replication and dissemination of the bacteria[2,3,5]. A summarized illustration is provided in Figure 1.1.

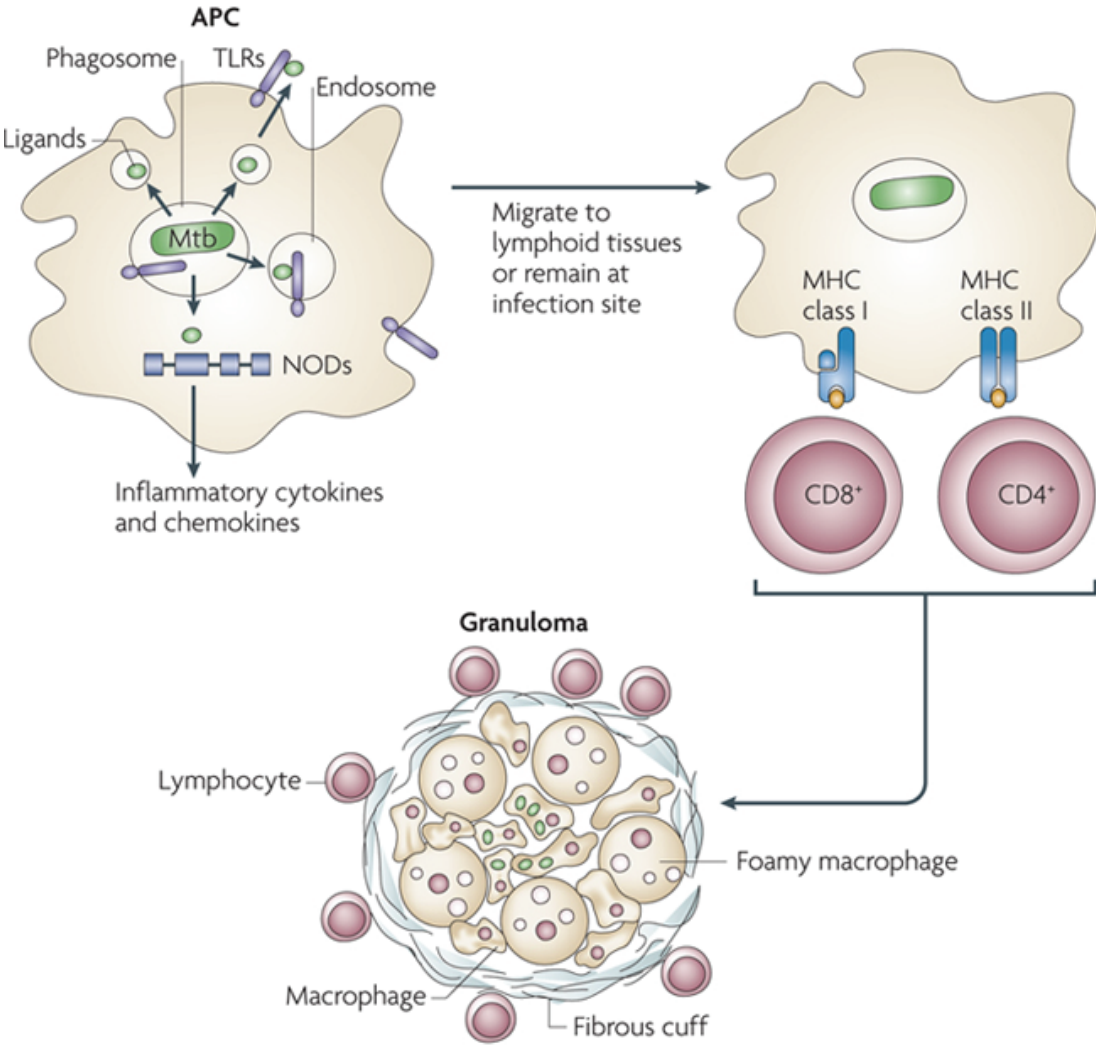

Figure 1.1: A summary illustration of the immune response to Mycobacterium tuberculosis infection up to the point at which the granuloma is established. M.tb is phagocytosed by APC's such as alveolar and interstitial macrophages, and dendritic cells which recognize mycobacterial structures specific to M.tb (M.tb ligands) via their TLR's. M.tb-specific ligands are also recognized by nucleotide-binding oligomerization domain (NOD) proteins resulting in the secretion of inflammatory cytokines and chemokines. Phagocytosed bacteria are housed in phagosomes which fuse with lysosomes to create a hypoxic and acidic phagolysosome. In the phagolysosome, proteolysis of M.tb takes place to produce antigenic peptides which are loaded on to MHC class I or II molecules to activate the adaptive immune response through the activation of naïve T cells, either at the site of infection or in the secondary lymphoid organs. Effector T cells as well as memory T cells then migrate back to the site of infection to control M.tb replication via the formation of granulomas through their secretion of TNF and other effector cytokines. (Adapted from Harding & Boom, 2010, Nature Reviews Microbiology[6]).

The activated macrophages within the granuloma (activated through T cell produced interferon (IFN)-γ) release tumor necrosis factor (TNF)-α to keep *M.tb* replication restricted within[3]. The ideal situation, however, is very rarely the most common. The most common occurrence is that infected individuals remain latently infected as a result of a continuous cycle of endogenous reinfection.

Following exposure to *M.tb*, different clinical outcomes of disease are observed due to the aforementioned individual heterogeneity in immune responses and this observation is the cause for complication of efforts to utilize biomarkers in the diagnosis and treatment response of TB disease. Walzl *et al*.[2] comprehensively describes the various clinical outcomes following exposure in which the immune system may, in short, (1) eradicate the disease completely, (2) adequately control the infection, or (3) fail to control infection to develop active disease[2]. In the first scenario, the host is able to successfully mount an innate immune response without the need for an adaptive immune response and therefore memory response; in the second scenario the host may successfully mount an adaptive response that recruits T cells and B cells to perform effector functions to control the bacteria in quiescent granulomas, during which the bacteria are unable to replicate and the host is termed “latently” infected; in the third scenario the bacteria is able to escape the immune system and replicate successfully. In this third scenario, active disease ensues and pro-inflammatory responses are upregulated significantly[2,4,5,7]. While this explains host infection outcome in a simple manner, *M.tb* infection presents as a complex spectrum of disease states, the detail of which is beyond the scope of this review[8].

Innate Immune Response to TB

The innate immune response is a fast-acting machine that is capable of carrying out protective strategies within minutes/hours without the adaptive immune response being alerted to infection. It is becoming more and more apparent that the innate response is more specific and vital for bacterial control than once believed and is now respected as the mediator of early *M.tb* infection control as well as the key role player in the maintenance of the adaptive T cell response[9]. Contrary to these roles, it has been shown that innate immune cells may also act as a niche for bacterial replication and potentially act as a reservoir for the evasion of the immune response by *M.tb*[3,9].

The innate immune cells recognize their targets through a limited yet highly effective repertoire of PRR’s which recognize pathogen-associated molecular patterns (PAMP’s) – unique to microbial structures. The primary PRR employed by the innate immune system is the Toll-like receptor (TLR). Signaling via TLR’s triggers an inflammatory cascade and the maturation of various innate cell types in order for a successful immune response[10,11]. The immune cells of the innate immune system also express numerous other receptors on their surfaces such as nucleotide oligomerization domain (NOD)-like receptors or NLR’s, but for application purposes will only be discussed briefly in this review.

Toll-like Receptors

Toll-like receptors (TLR’s) are a family of ten receptors that are capable of recognizing a distinct but limited repertoire of microbial structures both extracellularly and intracellularly where the lumen of

endocytic vesicles is concerned[10]. The cell types which primarily express these receptors are macrophages and dendritic cells, but neutrophils, eosinophils, epithelial cells and keratinocytes also express TLR's[12]. TLR's are capable of recognizing structures such as: flagellin, lipoproteins (e.g. lipopolysaccharide), double-stranded (ds)RNA, single-stranded (ss)RNA, and bacterial and viral DNA[11]. During *M.tb* infection, signaling is achieved specifically through the TLR2 pathway. *M.tb* cell wall constituents (glycolipids and lipoproteins) are the predominant ligands of TLR2 which activate the innate immune system and enhance the adaptive[6]. Other signaling pathways activated during *M.tb* infection include signaling via TLR4 and TLR9. The TLR4 pathway is capable of recognizing the LPS of gram negative bacteria[11], and is largely activated by the heat shock proteins 60/65 secreted by *M.tb*[13]. TLR9, on the other hand, specifically recognizes the unmethylated CpG DNA motifs of bacteria[11,13], and all three pathways lead to the induction of inflammatory cytokine production.

Nucleotide Oligomerization Domain (NOD)-like Receptors

NLR's are a family of 23 receptors who survey the intracellular environment and drive the formation of inflammasomes – a structure in the cytoplasm of cells that activates the production of Interleukin (IL)-1β and IL-18, as well as inflammatory caspases. They recognize microbial structures just as TLR's do, but also sense metabolic stress to drive inflammation. Lastly, the characteristic that makes them unique compared to other PRR's is the recent finding that they have the ability to recognize and bind more conserved microbial structures. This has highlighted their importance in contributing to the initiation of a successful immune response[12].

Macrophages

The first responders in the lung are the alveolar macrophages which, ironically, are also the key reservoirs for persistent replicating bacteria. Derived from resident monocytes, alveolar macrophages phagocytose *M.tb* that they encounter in the lung to initiate a pro-inflammatory and anti-microbial response via the TLR2 signaling pathway[3]. Inside the macrophages the bacteria is controlled in the phagosome, and the macrophage releases the cytokines TNF-α, IL-1, IL-6 and IL-12 along with the chemokines CCL2 (Chemokine (C-C Motif) Ligand 2) and CXCL10 (Chemokine (C-X-C Motif) Ligand 10)[3]. This gradient of chemokine and cytokine production recruits neutrophils, dendritic cells and T lymphocytes to the site of infection[9]. In doing so, the macrophages initiate the formation of the granuloma[3] and the recruited T cells produce IFN-γ to continue stimulating the macrophages as well as activate peripheral macrophages to recruit more macrophages to the granuloma[2,7]. Consistent TNF-α production is paramount for the maintenance and integrity of the established granuloma, and is, therefore, the key cytokine involved in the control of *M.tb* infection, alongside IFN-γ[7,14]. Contrariwise, *M.tb* is capable of manipulating the macrophage and the response it triggers to favor its own survival[3,9]. When the innate response is stimulated for prolonged periods of time, regulatory T cells are recruited to the site of infection to produce IL-10 and reduce the macrophage IFN-γ sensitivity[15] among other things, in order to prevent host tissue damage resulting from abnormal inflammation. IL-10, a regulatory cytokine produced by regulatory T cells (T_{Reg}) that would normally be an important cytokine necessary

for the prevention of host immunopathology, now becomes an inhibitor of macrophage effector functions, reducing their capability to kill the bacteria and maintain granuloma promoting cytokines/chemokines, thereby unintentionally allowing the phagocytosed bacilli to become protected inside the macrophage[3,7,16].

Neutrophils

Following the signal for neutrophil recruitment, neutrophils migrate to the site of infection and later the draining lymph nodes where they are able to interact with APC's and lymphocytes to influence the inflammatory response[17]. Neutrophils function to clear infections and debris from the circulatory system. They are, therefore, also responsible for phagocytosing free *M.tb* and also have potent anti-microbial properties in the form of stored granules which are discharged upon *M.tb* phagocytosis and apoptosis. These granules have both antimicrobial effects on the bacteria, but also detrimental effects on the host immune system owing to their pro-inflammatory nature[5,7,9]. In order to avoid prolonged inflammation, infected apoptotic neutrophils are phagocytosed by passing macrophages, thereby successfully clearing destroyed neutrophil contents and resolving neutrophil-induced inflammation. During the phagocytosis of apoptotic neutrophil debris, macrophage cell death outcomes are also determined – macrophages become either apoptotic, favoring the host immune response; or necrotic, favoring *M.tb* survival and dissemination[16] – thereby influencing the outcome of *M.tb* control[18]. They may also limit the amount of available antigen for antigen presentation by the professional antigen presenting cells, thereby limiting the magnitude of the adaptive immune response the APC's are able to establish[17]. Neutrophils are therefore both a protective and limiting cell type in the innate response, being mostly protective during the early stages of infection, but becoming a limitation further into infection where they are associated with the loss of *M.tb* containment and the progression to active disease[19].

Dendritic Cells

Dendritic cells (DC's) belong to the phagocyte group which includes macrophages and neutrophils, from the innate immune system. DC's therefore play an important role in the phagocytosis of *M.tb* and happens to be the primary APC for the induction of the adaptive immune response in the case of TB[3]. DC's are classified as such due to their ability to co-stimulate adaptive immune cells and secrete T-helper polarizing cytokines such as IL-12 upon phagocytosis of *M.tb*, apart from their obvious ability to present antigen[3,7,9]. This cell type is very similar to the macrophage cell type because of its *M.tb* recognition mechanism: TLR-mediated antigen recognition. Antigen presentation occurs in the same way as seen in macrophages where *M.tb* peptides are loaded onto MHC II molecules and presented to T lymphocytes in the draining lymph nodes. The T lymphocytes then proliferate and polarize to elicit their effector functions, known as T cell priming[9]. Primed T cells return to circulation and to the lung where they produce IFN-γ to further activate more macrophages in order for them to produce cytokines and anti-microbial factors[7]. Another receptor of particular importance, also found on the surface of DC's, is DC-SIGN (dendritic cell-specific intercellular adhesion molecule-3-grabbing non-integrin), a receptor that is responsible for the recognition of a single *M.tb* glycolipid, mannosylated lipoarabinomannan

(ManLAM), compared to TLR's which are capable of recognizing multiple *M.tb* peptides; and which that leads to the production of IL-10, an immune suppressor, to block T cell priming[9]. In this way, *M.tb* is again able to influence the outcome of the immune response mounted against it in both the innate and adaptive pathways.

Natural Killer and Natural Killer T Cells

Natural Killer and Natural Killer T cells also play an important role in the innate immune response to TB in terms of the inhibition of *M.tb* growth, particularly in instances where sufficient T cell responses are lacking.

Natural Killer (NK) cells are a population of non-phagocytic innate immune cells which are known to have potent cytotoxic properties. Following activation by cytokines like IL-2 and IL-12, NK cells firstly release perforin to perforate target cell membranes, followed by various granzyme molecules which enter the perforated cell and initiate apoptosis of the infected cell[20–23]. A recent study published by Chowdhury *et al.* reported that NK cell frequencies are upregulated during latency only, and decrease during active disease, disputing the expansion of NK cells during chronic inflammatory conditions[24]. While NK cells express no T cell receptors, NKT cells, in contrast, express intermediate levels of the T cell receptor. This is because NKT cells are a population of CD1d-restricted, unconventional T cells that respond to antigen presented by the CD1d major histocompatibility complex class I (MHC I) receptor. The antigens presented by this receptor are specifically lipids, glycolipids or highly hydrophobic peptides which induce the production of immunoregulatory cytokines[25–27]. The available research on the NKT cell population is very limited owing to its relatively recent discovery. Data that is available has identified the presence of these cells predominantly within the thymus, as well as its scarcity within draining lymph nodes[28]. Other studies have also demonstrated a significantly low presence of NKT cells during active TB disease specifically[25].

Myeloid-Derived Suppressor Cells

Undoubtedly the most under-studied suppressive cell type known to immunologists, myeloid-derived suppressor cells (MDSC) are considered an enigma that, although comprehensively characterized in the field of murine tumor biology, have not been properly defined in the human system. Having been studied extensively in mice with cancerous tumors[29], this innate immune cell type still requires in depth analysis into their functional roles in human subjects. What is known about MDSC is their ability to suppress T cell functions as well as induce the differentiation of other suppressive regulatory cell types such as T_{Reg}[30,31]. Shipp *et al.*[29] skillfully reviewed and summarized the literature on MDSC suppressive capabilities in the human immune system. A simple conclusion was drawn that a suppressive effect could be observed by MDSC and attributed to a specific pathway in humans but attempts to show that the inhibition of these pathways lead to the full reversal of MDSC-mediated suppression were few and far between, suggesting that various alternative MDSC-mediated immunosuppressive pathways can be triggered as substitutes during loss-of-function of suppressive potential.

It is known that during hematopoietic stem cell (HSC) maturation, myeloid cells develop to further differentiate into either dendritic cells, macrophages or granulocytes. These cells are rapidly activated and mobilized to produce proinflammatory cytokines, upregulate MHC class II- and costimulatory molecules, in response to relatively strong signals produced by pathogens, primarily through PAMPs. This classically activated myeloid response is however of short duration as the pathogen is effectively eliminated. However, in the case of chronic infections, leading to relatively weak, protracted and unresolved inflammation, myelopoiesis is skewed towards the generation of immature immune cells with a suppressive phenotype, jointly characterized as MDSC. Accumulation of MDSC in chronic inflammatory environments requires two distinct sets of signals: (1) expansion-related signals which are predominantly tumor-derived growth factors that interfere with the terminal differentiation pathway of myeloid cells, and (2) activation-related signals that are responsible for the development of the suppressive MDSC functions otherwise absent in immature myeloid cells[32]. While these two sets of signals undoubtedly overlap somewhat, each signal is governed by its own unique set of transcription factors and intermediates that initiate the development of fully suppressive MDSC. Known intermediates include cytokines and chemokines like granulocyte-macrophage colony-stimulating factor (GM-CSF), vascular endothelial growth factor (VEGF), and IL-6 for the first signal; and IL-1β, IL-13, and prostaglandin E_2 (PGE_2) for the second signal. Other secreted factors known to influence MDSC generation and accumulation include transforming growth factor (TGF)-β, IL-10, various alarmins and polyunsaturated fatty acids[29,31,33,34]. The role of MDSC during *M.tb* infection has not been well defined. The handful of studies performed in human volunteers display increased frequencies of MDSC in the peripheral blood[30,31] and broncho-alveolar lavage samples from TB patients, as well as a reduction in frequency following successful TB treatment[30]. In mice, these cells were also observed to phagocytose the *M.tb* bacilli as well as produce both pro-inflammatory and immunomodulatory cytokines such as IL-6 and IL-10 respectively, suggesting a role for MDSC in providing an immune evasion strategy for the bacteria while simultaneously acting in an immune modulatory fashion to dampen the immune response[35].

MDSC show potential as a new suppressive cell type involved in the immune response to TB disease. With the previously mentioned data, it could be hypothesized that MDSC reduction may play a role in the restoration of protective immunity and, therefore, potentially act as a biomarker of treatment response if the point during treatment at which they begin to be downregulated could be identified.

The innate immune system has proven itself to be a resilient and important weapon in the human immune arsenal. It is capable of both triggering a cascade of events, mostly pro-inflammatory, aimed at initiating and assisting a successful adaptive immune response, as well as restricting the replication and dissemination of *M.tb* bacilli during primary infection. The innate immune system is even capable, in many cases, of destroying *M.tb* bacilli before it has the chance to alert the adaptive system. *M.tb* is, however, able to evade multiple mechanisms aimed at its eradication due to its ability to manipulate the various key control mechanisms. The most important mechanism in question is the ability of *M.tb* to

collapse the pro-inflammatory response that is required for *M.tb* control, and its inverse ability to amplify this response to the point where the pro-inflammatory environment instead becomes damaging to the host and favorable for *M.tb* survival.

Adaptive Immune Response to TB

The adaptive immune response to TB in the past has been the focus of research for the development of new vaccines, treatments, diagnostics, and biomarker discovery owing to the crucial role of T cells in the protection against *M.tb* infection. It has, however, been shown that the adaptive and innate responses are tightly dependent on one another.

The adaptive response can either be humoral or cell-mediated, where in the humoral immune response, B lymphocyte antibodies are the effector cell type, while in cell-mediated immunity T- and B-lymphocytes are the effector cell types[10]. Adaptive responses are initiated upon presentation of *M.tb* antigens to naïve *M.tb*-specific $CD4^+$ T cells in the draining lymph node via presentation on MHC class II molecules on dendritic cells (the primary antigen presenting cell), a process which may take up to 11 days post innate immune challenge[7]. These T cells then proliferate and migrate to the site of infection.

The most important T cell response during TB disease is the T_H1 response during which IFN-γ and TNF-α is produced and released to ensure the maintenance of the granuloma and the control of *M.tb* replication[14,36,37]. The T_H1 response's production of IFN-γ stimulates further production of TNF-α from activated macrophages to ensure strong infection control[14]. In an application example, individuals with HIV infection exhibit an extensive loss of $CD4^+$ T cells (predominantly the T_H1 subtype) which results in a heightened susceptibility to *M.tb* infection[38]. As stated previously, the production of the cytokine IL-10 reduces T_H1 responses through the direct inhibition of macrophage and DC function as well as the cytokines/chemokines necessary for the migration of T_H1 cells from the lymph node to the lung[7] to indirectly reduce the integrity of the granuloma and permit *M.tb* dissemination[36]. A more detailed illustration of the adaptive immune response is given in Figure 1.2.

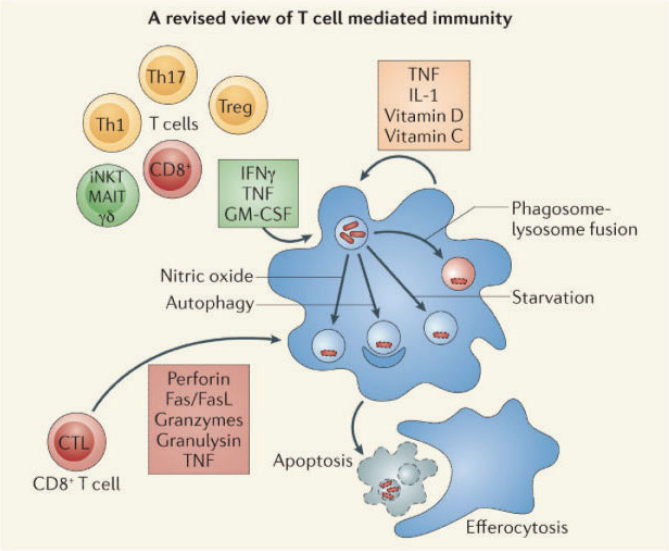

Figure 1.2: A revised view of T cell mediated immunity to TB following T cell activation, proliferation and migration to the site of infection. M.tb is capable of activating various T cell subsets, namely T_H1, T_H17 or T_{Reg} responses, as well as CD8+ cytolytic T cells and unconventional T cells: γδ T cells, mucosal-associated invariant T cells, and inducible Natural Killer-like T cells. These T cell subsets produce cytokines that may induce either of the following mycobacterial killing pathways: autophagy, starvation, the nitric oxide killing mechanism, or phagosome-lysosome fusion. Any of the mentioned mechanisms may lead to the programmed cell death (apoptosis) of the infected macrophage and its contents which are subsequently phagocytosed by uninfected macrophages through the process of efferocytosis. (Adapted from Nunes-Alves et al. *2014[5])*

T helper cells are the subsets of effector $CD4^+$ T cells and each display an almost unique repertoire of cytokines and effector functions. T helper cells differentiate from a T helper cell precursor known as T_H0 to the various subsets depending on the cytokine stimulus. Examples of the T helper subsets include: T_H1, T_H2, T_H17, and T_{Reg}. There exist a few "new" T helper subsets, T_H9 and T_H22, but these subsets have not been well defined and have particularly not been researched in the context of TB disease so will not be discussed in this review.

T Helper 1/T Helper 2 Response Balance

The T Helper 1 (T_H1) immune response is the primary protective response to *M.tb* infection and is traditionally activated during intracellular bacterial or viral challenge to initiate cell-mediated immunity and inflammation[39]. The selective differentiation of T_H0 cells into T_H1 cells is established during the initial priming of these cells and is influenced by extracellular factors, such as cytokine environment and the source of co-stimulatory signal. Naïve T_H0 precursors differentiate into the T_H1 subset upon stimulation with the pro-inflammatory cytokines IL-12 and IFN-γ to produce predominantly IL-2 and IFN-γ, along with IL-12 and TNF-α[40]. The cytokines produced by this subset direct the immune response to one of a cell-mediated nature, characterized by the activation of macrophage microbicidal activity, the induction of acidification and maturation of phagosomes, as well as autophagy and vitamin D receptor signaling via IFN-γ mediated signaling[2,5,40,41]. Through this response cells such as mononuclear

phagocytes, Natural Killer cells and cytotoxic T lymphocytes ($CD8^+$ T cells) are activated for their intracellular killing mechanisms to hopefully clear *M.tb* infection[40].

The T Helper 2 (T_H2) immune response is the antagonist of the T_H1 immune response in that it is primarily activated during immune challenges from extracellular parasites as well as during allergic responses in order to drive antibody-mediated response types with the production of antigen-specific antibodies[39–41]. Naïve T_H0 cells are stimulated to differentiate into T_H2 $CD4^+$ T cells when they encounter the likes of IL-4 and to some extent IL-5, and function to produce the cytokines IL-4, IL-5, IL-10 and IL-13[2,39,40] . The function of T_H2 related cytokines are to activate the growth and differentiation of B cells, eosinophils and mast cells, as well as to inhibit a handful of macrophage functions especially autophagy so that antigen presentation is impaired, along with the clonal expansion of T cells resulting in the loss of granuloma organisation[39,41], although the primary function of this subset during TB disease is to limit immune pathology during chronic infection[2]. The detrimental effects the T_H2 response is shown to have during *M.tb* infection may very well be a cause for reactivation of disease or the progression of disease from latent infection to active, but this correlation has not yet been fully identified.

The primary difference between T_H1 and T_H2 responses is the cytolytic capabilities of the T_H1 response and the ability of the T_H2 response to induce the synthesis of Immunoglobulin (Ig)M, IgG, IgA and IgE antibodies[39] in autologous B cells, highlighting yet another potential role for B cells during *M.tb* infection which has not yet been investigated thoroughly. It is common for the response type to be redirected, for example during helminth infection the T_H1 response is redirected to a T_H2 response in order to combat the parasitic challenge, with the consequence of losing the production of crucial pro-inflammatory *M.tb* control cytokines.

The balance between the T_H1 and T_H2 responses during *M.tb* is crucial for the successful control and containment of infection. Tipping the balance in either direction results in the loss of immune regulation and subsequent dissemination of disease. It is still unclear what factors exactly are responsible for tipping the balance or why some individuals maintain a perfect balance throughout infection so that they never progress, but the elucidation of this paradigm is likely the key to unlocking a comprehensive understanding of this elusive disease.

T Helper 17 Response

The T_H17 response is one of two immune regulatory responses initiated via immune challenge with extracellular bacteria and/or fungi, which in some cases may lead to autoimmunity should there be a chronic stimulation[39]. This response is characterized by the production of IL-17 as well as IL-21, IL-22 and TNF-α in some cases, following a differentiation course driven by the cytokines IL-6 and TGF-β[40–42]. It is known that the production of TGF-β during active disease is abundant, to the point of excess, and that it is expressed at the site of infection and for these reasons is given the role of driving T_H17 differentiation[41]. During TB disease, the production of IL-17 initiates the recruitment of neutrophils to the lung where neutrophils drive inflammation and other cytokines like IL-23 are produced to ensure a

successful IL-17 functioning[2,5,43]. The importance of IL-23 is highlighted during Bacillus Calmette-Guérin (BCG) vaccine studies where without IL-23, the IL-17 response is ineffective and protective T_H1 responses are not induced[44], although this cytokine is not necessary for the initial differentiation of T_H17 cells[42]. When T_H17 $CD4^+$ T cells are adoptively transferred, as observed by Gallegos *et al*.[45], the IL-17 producing cells only partially inhibit bacterial growth while the transferred T_H2 cells had no effect on bacterial growth, eliminating these two immune response types as the primary effector pathways that control *M.tb* infection.

IFN-γ is known to inhibit the production of IL-17 by IL-17-producing $CD4^+$ T cells[5,7], and through this inhibition is able to impede the accumulation of pathogenic neutrophils recruited by IL-17 in the lung, as well as impair their survival. In doing so, IFN-γ reduces the level of inflammation in the lung and improves the host's disease outcome[7,41]. This interaction between T_H1 and T_H17 responses supports the suggestion made by Wozniak *et al*.[46] that cross-regulation occurs between the two response types to provide robust protection against *M.tb* infection and simultaneously ensure no excessive damage occurs as a result[46].

Regulatory T Cell Response

Regulatory T cells, the second immune regulatory response, are induced by the cytokines IL-2 and TGF-β[40], are the cell type responsible for surveillance of the immune system and the maintenance of immune tolerance and homeostasis. They are mainly responsible for ensuring the successful execution of a T_H1 response, simultaneously regulating the response to prevent immune pathology and lung damage arising from excessive inflammation. Should T_{Reg} cell activity be over active, immune regulation would be overpowering and detrimental to the host response as it would suppress the protective actions of the inflammatory response[2,5]. T_{Reg} cells are responsible for the production of the immunosuppressive cytokines IL-10, IL-35 and TGF-β which are responsible for eliciting the immune regulatory actions of this cell type[5,7,40,41], i.e. inhibiting and/or delaying the production of IFN-γ and IL-17[7], and suppressing the T_H1 immune response.

Although the cytokine functions of this immune response can be inferred from previously done studies, the role of T_{Reg} cells in the immune response during TB disease remains controversial owing to various contrasting studies. The most probable role, however, is the reactivation of latent disease and the development of active disease through the action of decreasing the production of IFN-γ[47] while simultaneously producing IL-17. The resultant action is the accumulation of polymorphonuclear leukocytes at the site of infection in the lung which function to dampen the predominantly pro-inflammatory response and the loss of *M.tb* infection control along with decreased macrophage killing activity[41,47].

In keeping with the theme of homeostasis within the immune system, there are both activating as well as suppressive immune cell types. The majority and most common of these have already been

discussed above, and focus been placed on how each suppressive cell type plays a role to balance out a pro-inflammatory cell type so that homeostasis is maintained. The main function of the suppressive cell types is to limit immune pathology and ensure that activating responses do not get out of hand[2,7,47]. These regulatory mechanisms can, however, get out of hand themselves should their regulation become more extensive than required. In such cases, the protective pro-inflammatory responses are inhibited and dissemination of *M.tb* from the granuloma permitted due to the loss of control[2,5,7]. The two main types of regulatory cell types (T_H17 and T_{Reg}) have been discussed, but an emerging role for Myeloid-Derived Suppressor Cells appears to be coming to the forefront in pulmonary disease research as a vital suppressive cell type.

$CD8^+$ T Cells

Textbook definitions of cytotoxic T cells ($CD8^+$ T cells) describe them as a cell type that is mobilized during chronic viral infections and generally is not involved during bacterial infections. Understandably the function of $CD8^+$ T cells during the immune response to TB disease is, therefore, not well described. It has been observed, however, that there is indeed such a response during infection, although it is of a much lower magnitude and does not seem to play a pivotal role in control. What is known about this cell type during the immune response to TB disease, is that it produces molecules such as granulysin and perforin which may be directly cytotoxic to the mycobacterium and/or restrict its growth[2,5]; it may also modulate phagocyte activity[2] but further studies are required to elucidate this. The three mechanisms by which these cells may be cytotoxic include pathways involving TNF production, the initiation of the Fas and Fas Ligand signaling system which mediates cell death signaling, and finally and most frequently the exocytosis of cytotoxic granules containing lysis proteins such as perforin, granulysin and granzymes which induce apoptosis of the target cell[5], a known mechanism to control/inhibit bacterial replication. As described previously in the review, infected cells that have undergone apoptosis are themselves phagocytosed by uninfected macrophages through the process of efferocytosis to trap the bacteria and force an interaction with the macrophage lysosome to facilitate the killing of the bacteria[5].

There have been a few studies that suggest *M.tb*-specific $CD8^+$ T cells may also secrete IFN-γ along with IL-2, a mechanism which is proposed to facilitate enhanced macrophage activation at the site of infection, but the function of these IL-2^+/IFN-γ^+ cells is seen to be reduced in TB patients compared to latently infected individuals[48]. This finding suggests that the functional profile of these cells is highly restricted to *M.tb*. Even though these cell types display potential as minor role players during *M.tb* infection, it has been shown that this cell type and the others described above can definitely not compensate for a lack of $CD4^+$ T cells in terms of adaptive protection.

B cells and Antibodies

Little is known about the role of B cells and the antibodies they produce, i.e. the humoral immune response, during *M.tb* infection. However, B cells are observed in the granuloma structure during latent

infection alongside important central memory T cells[2,7] and follicle-like B cell aggregates have also been observed in the lungs of TB patients[7,49]. Traditionally, the humoral response is capable of being activated by antigen-specific T helper cells to act as APC's, and produce antigen-specific antibodies which may opsonize extracellular microbes and neutralize their toxins, thereby facilitating enhanced phagocytosis of these microbes[39,49,50]. There does exist evidence that *M.tb*-specific B cells and antibodies are produced during TB disease to possibly perform this opsonizing function, but the capacity for the *M.tb*-specific antibodies to opsonize extracellular *M.tb* was limited to recognize some but not all *M.tb* antigens[51]. Their significant presence in the granuloma and capability to opsonize some extracellular mycobacteria, therefore, suggests a key role during disease, but this role remains elusive. O'Garra *et al*.[7] suggests that B cells and their antibodies may play a role in modulating immune activation and susceptibility to infection through the possible induction of immunomodulatory mechanisms and their cytokines, but further work is necessary before we can better our understanding of the humoral response during TB disease.

As the immune system requires a continuous state of homeostasis, following a successful immune response, the number of innate and adaptive immune cells specific for the activating bacteria need to be controlled. Non-essential cells may either be removed via apoptosis pathways or differentiate into a memory phenotype where the cells remain in circulation or in resident tissues for future activation. Here TNF-α once again plays an incredibly important role in the clearance of such cells in preparation for future infections through the activation of the apoptotic cell death pathway[12].
Homeostasis between pro-inflammatory and anti-inflammatory immune cell types has been shown to be a delicate system that requires constant surveillance and modulation. The key protective mechanism behind *M.tb* infection control and/or clearance may, therefore, lie in the balance and regulation of the host immune response, and should become the focus of TB research.

Tuberculosis Diagnosis

Individuals with suspected TB present with a combination of symptoms which may include one or more of the following: a persistent cough lasting two weeks or more, persistent fever, night sweats, unexplained weight loss, fatigue, and hemoptysis. In some cases, traditional clinical symptoms are not presented in patients with active disease, for example in immunocompromised patients in the case of human immunodeficiency virus (HIV), in children/infants who are known to be unable to produce viable sputum samples, as well as patients with extra-pulmonary TB, which complicates accurate diagnosis further[4,52,53]. Diagnosis is time consuming and labour intensive which may take weeks, especially where resources and facilities are scarce, delaying the initiation of treatment considerably. Misdiagnosis and delayed diagnosis is also a common setback due to socio-economic and geographic limitations, and in some instances due to the fear of social exclusion from society should individuals seek medical attention and be diagnosed with TB[54–56]. The diagnosis of TB is based on a combination of clinical observations and microbiological assay results owing to there being no definitive and adequately accurate diagnostic test[57]. Diagnosis is, however, not as steadfast as we would like it to be with a case detection rate of only 63% as of the year 2014 proving to be the most limiting factor in TB control[54,58]. Alterations in

disease presentation in individuals with secondary infections such as HIV or Type II Diabetes further hampers efforts for accurate diagnoses[57].

Sputum-based assays

Sputum-based assays are currently the gold-standard in TB diagnostics and include sputum smear microscopy as well as automated liquid cultures (BD BACTEC™ MGIT™). Smear microscopy remains the gold-standard diagnostic tool in many high-burden settings, and is well known for its poor sensitivity (approximately 50%; specificity of approximately 95%) and high limit of detection (approximately 10^4 bacilli per mL) resulting in poor diagnostic yields[4,59]. While automated liquid cultures have greatly improved sensitivities (approximately 81.5%; specificity of approximately 99.6%) and require less than 10 bacilli per mL of sputum, this tool is more costly than smear microscopy, is limited by a long time to positive result (2-3 weeks), as well as high rates of media contamination, often resulting in high rates of patient drop-out[4,60,61]. Assays based on the collection of sputum samples provides a problem due to the difficulty in acquiring quality sputum samples, especially in children and infants[53]. Individuals with extrapulmonary infection are also incapable of producing sputum as often, no *M.tb* is present in their pulmonary tissue[53]. As an aside, TB in children presents as a paucibacillary disease which results in a lower bacterial load than found in adults – sputum-based methods rely on high bacterial loads for *M.tb* detection[53,62]. The Xpert® MTB/RIF assay (Cepheid, Sunnyvale, USA), a variant of a nucleic acid amplification tests (NAAT)[4], is the latest development making a significant impact on TB diagnosis as it is able to detect the presence of *M.tb* in sputum samples as well as identify strain sensitivity/resistance to rifampicin through the amplification and detection of mutations in the *rpoB,* the gene responsible for conferring rifampicin resistance[57,63]. In terms of performance, the Xpert® MTB/RIF assay has provided a fast and reliable assay that is capable of producing results within two hours, displaying a high specificity of approximately 98% and a high sensitivity in smear positive individuals (98-100%), but only moderate sensitivity in smear negative individuals (68-72%)[64–66] which is a known limitation of NAATs[4]. This assay is limited by its high running costs, the need for a stable electricity supply and the short shelf life of its consumables[57,67,68]. For this reason, this assay as well as other sputum-based assays upon which we rely, are not suited as a point-of-care test which is urgently needed in resource limited and high burden settings.

Radiological Methods

Should an individual present with suggestive symptoms, confirmatory chest radiographs (CXR) are preformed to determine the extent of infection in the lungs, although they are only used as a supportive diagnostic tool to consolidate the microbiological findings but only when resources allow[57]. X-ray Computed Tomography (CT) and Positron Emission Tomography-Computed Tomography (PET-CT) scans provide more confidence in radiological diagnoses as they are far more accurate than CXR but are not realistic options in most developing countries[69].

Immunological Assays

Interferon-Gamma Release Assays (IGRA's) are important for the diagnosis of latent TB infection, a state of disease in which the bacterial replication is inhibited, or the bacteria lays dormant, and include the QuantiFERON TB Gold Plus assay (QFT-Plus) which uses the enzyme-linked immunosorbent assay (ELISA) technique to quantify IFN-γ production in response to stimulation by *M.tb*-specific antigens. Other IGRA's include the ELISPOT-based T-SPOT.TB test that enumerates *M.tb*-specific IFN-γ producing cells as spot forming units in a plate[70]. The Tuberculin skin test (TST) is a measure of the delayed-type hypersensitivity (DTH) response following the administration of purified protein derivative (PPD) just under the top layer of skin and is known for its use in the diagnosis of latent disease[70]. When compared to the skin test, IGRAs such as QFT and T-SPOT.TB are significantly more accurate and specific in the diagnosis of *M.tb* infection. However, IGRA limitations include the incapability of these assays to discriminate between active and latent disease, the limited utility in high burden settings where latent infection prevalence is high, and overall poor sensitivity and specificity[71–73]. In addition, the use of TST is limited by the high false-positivity rate observed in individuals who have had previous BCG vaccinations or those infected with non-tuberculous Mycobacteria (NTM), however the latter is still a contested belief[74–76]. These assays are, however, important for the indication of previous exposure to *M.tb* proteins or current challenge that is being controlled[63].

There are currently no diagnostic methods available that are capable of being used at point-of-care, and none are appropriate for use with all patients around the world due to the various limitations described above. For this reason, an affordable, easy to use, *M.tb*-specific, point-of-care diagnostic test is urgently required, especially for use in low- to middle-income countries where resources and skilled health care workers capable of conducting the required tests are scarce. One option being explored is the use of highly sensitive biomarkers, but more research is necessary to evaluate their viability as a point-of-care option.

Drug Susceptibility Testing (DST)

Drug susceptibility tests are tests done in order to determine possible *M.tb* strain resistance to any of the first-line drugs and are more frequently being done in tandem with diagnosis owing to the development of improved technology in the field. In some instances, where facilities and resources are limited, advanced diagnosis and concurrent DST are not an option. Here, DST are not performed routinely, only when treatment of individuals fails even though it has been well adhered to.

As stated previously, the Xpert® MTB/RIF assay is capable of detecting drug sensitivity/resistance to rifampicin through the detection of mutations in the *rpoB.* This DST is potentially the most preferred method due to its concurrent determination of resistance alongside *M.tb* infection confirmation, and it is able to give a result within two hours but is not the gold standard. The gold standard of DST relies on sputum culture in Lowenstein-Jensen media using the proportional method[77], and is limited by the slow growth rate of *M.tb*, limiting the time to result. A phenotypic resistance measurement test, this culture requires that less than 1% of inoculum grows on culture media that contains a high concentration of

any one of the anti-TB drugs in circulation[78]. Along with the Xpert® MTB/RIF assay, the GenoType®MTBDR*plus* (Hain Lifescience GmbH, Nehren, Germany) line probe assay and INNO LIPA Rif.TB (Innogenetics, Ghent, Belgium) assays are also available as rapid detection assays. The former is capable of providing a diagnosis that is equally as accurate as the Xpert® MTB/RIF assay with the added benefit of isoniazid resistance detection[79] as well as rifampicin resistance detection through the detection of mutations in the *inhA* promoter and *katG*[80]. The latter is also capable of detecting rifampicin resistance to TB[81], but where resources are limited the rapid detection assays are not a feasible option.

Treatment Regimens and Outcomes

The treatment success rate of newly diagnosed patients is estimated at 85% and the first-line drugs utilized are estimated to result in cure in approximately 90% of cases[82]. The remaining 10% may develop a recurrence from reinfection or relapse due to improper suppression of the mycobacteria during treatment. Why do these estimates then not instill confidence in the current global TB standing? The estimates are based on cases that are reported to the World Health Organization and are in most cases situations where the diagnosed patients have access to proper health care and TB treatment. Many cases remain unreported to the WHO mainly due to lack of infrastructure and improper diagnosing. Mortality rates remain disturbingly high in high burden, low-income countries as inadequate facilities and access to proper treatment are not available. Following diagnosis, a standard course of treatment is followed for patients who show no drug resistance. Treatment includes an initial two-month intensive phase regimen of four first-line drugs: isoniazid, rifampicin, pyrazinamide and ethambutol; followed by a four-month continuation phase treatment regimen of two first line drugs which involves the continued administration of isoniazid and rifampicin[83]. Treatment often fails and may be due either to: low patient adherence from disagreeable side effects, multi-drug resistant (MDR-TB) strains of *M.tb* most commonly to rifampicin and isoniazid, and/or HIV co-infection as a result of the interaction of TB drugs and antiretroviral therapy (ART) and it's resultant compromise of the immune system[4].

The response to TB treatment is monitored through the conversion of sputum samples to smear negative two months into treatment and again 5 months into treatment. The conversion of sputum culture to culture negative after the course of treatment is completed, is considered an indicator of treatment success, however, these standards are not consistent as is evident through the occurrence of relapse and reinfection seen after treatment completion. This could potentially be due to immune alterations as a result of the treatment itself[84–86]. Strong preliminary evidence shows that immune reprogramming differs among TB patients based on their response to treatment, which allows for the identification of distinguishing biomarkers for rapid versus slow response, failed treatment and relapse.

Biomarkers in Tuberculosis

As defined by Doherty *et al.,* a biomarker is a "characteristic that is objectively measured and evaluated as an indicator of normal biological processes, pathogenic processes or pharmacologic responses to a therapeutic intervention". Biomarkers are, therefore, crucial research elements in attempts to rapidly and accurately diagnose active TB disease from latent infection and other similarly presenting infectious diseases, for the indication of individual risk profiles in terms of their progression to active TB disease, for the prediction of treatment outcome, as well as for the determination of true correlates of risk and/or protection, to name a few.

Progress towards the identification of successful TB biomarkers has been stunted owing to the complexity of active TB disease which makes accurate diagnosis a challenge, treatment outcome unpredictable and complete elimination of the bacterium not possible in the majority of cases. As of yet, there is a lack of reliable biomarkers specific to TB that display good predictive value in their individual capacity[87]. Focus has now turned toward researching the use of multiple biomarkers in combinations that portray unique biosignatures for the identification of TB disease[2]. The challenges faced with biomarker discovery in TB have been reviewed previously in Wallis *et al*.[88], and the most challenging aspect of these biomarkers that we currently face is the influence of treatment which can either up- or down-regulate biomarkers during treatment and/or disease. Most importantly, a validated biomarker or biosignature that is *M.tb*-specific, and not readily influenced by alternative inflammatory conditions or diseases that alter the immune response, is required for the TB pandemic to be resolved. Differentiating biomarkers are currently being studied for the purpose of identifying reliable diagnostic biomarker candidates and biomarkers of response to treatment candidates. These may include cytokines, chemokines, cell surface receptors, soluble receptors, inflammatory markers (other than cytokines and chemokines), antibodies and their markers, and antibodies to *M.tb* antigens; factors that are essential for the understanding of the underlying pathological process of TB and the host response[2,88].

Diagnostic Biomarkers

Traditional diagnostic methods for TB disease, such a sputum smear microscopy and sputum culture, lack sensitivity and rapid result delivery, respectively, as highlighted elsewhere. Rapid diagnosis is crucial for timeous treatment initiation, prevention of transmission and further dissemination of disease. This has driven the development of rapid, efficient diagnostic tools such as the GeneXpert® MTB/RIF which significantly reduces the turnaround time for a concise diagnosis to about two hours. The limited availability of GeneXpert® MTB/RIF technology in resource-limited, sometimes inaccessible, rural regions inhibits proper beneficial use in cases where such tests are needed most. Sputum samples can also be a difficult sample to obtain for the GeneXpert® MTB/RIF test as many patients are unable to produce sputum samples of good quality, especially in children, in HIV coinfection, or where the disease has disseminated from the lungs to other organs[4,52]. The need for a rapid, point-of-care diagnostic tool that is preferably handheld is obvious, and while efforts are being made to improve systems like the GeneXpert® MTB/RIF for such purposes, a blood-based point-of-care device based off of host

biomarkers would greatly improve swift diagnosis and access to treatment in resource-limited settings, especially in patients who have disseminated disease.

Previous attempts have investigated the use of IGRA's as diagnostic biomarker candidates, however their inability to discriminate between latent infection and active disease limits their use and negates their potential as future diagnostic biomarker candidates. The principle of IGRA read-outs should not, however, be discarded from future biomarker discovery studies as the release of IFN-γ and the quantification thereof has been shown to still be of importance as a diagnostic biomarker candidate in a study performed by Casey *et al.*. Here they concluded that the presence of T cells that produce IL-2 and/or IFN-γ in latently infected individuals differs in actively diseased patients whose T cells secrete only IFN-γ[89]. Serological biomarkers for active disease are also being studied. These biomarkers are antibodies which detect against *M.tb*-specific antigens and are so desirable due to them being simple and cheap for use at point of care[2]. They are proving disadvantageous however in terms of their sensitivity and specificities[89,90], but combinations of serological biomarkers involved in different *M.tb* pathways should be investigated further in biomarker discovery efforts. The use of phenotypic biomarkers for diagnosis have also been studied, the most promising results being seen in *M.tb*-specific $CD4^+$ T cell populations when immune activation and proliferation markers were under investigation. As such, these markers have been shown to display high sensitivities and specificities for diagnosing between active disease and latent infection, and require further validation[37].

Lastly, transcriptional diagnostic biosignatures are also currently under investigation. Studies performed by Sutherland *et al.* and Maertzdorf *et al.* have successfully highlighted host gene signatures capable of discriminating between individuals with active TB disease and latent *M.tb* infection, however the samples required to develop/investigate these signatures require extensive laboratory processing and are very costly experiments, limiting their current practicality in high-burden settings where latent infection pressure is high[91,92].

Biomarkers of Treatment Response

The hope for treatment response biomarker candidates is that they will provide a method for predicting each individual's potential treatment outcome during the early stages of treatment; facilitate the shortening of treatment regimens, and the shortening of anti-tuberculosis drug clinical trials; and also, be able to give an indication of the individual's risk of relapse following the end of treatment. Such work is important to add to the existing biomarker discovery efforts[2]. Studies evaluating cell surface markers as indicators of treatment response, such as those carried out by Veenstra *et al.*[93], have shown promise, but predicting response to treatment, treatment failure or risk of relapse is proving to be incredibly difficult. Previously, bacterial load at the beginning of treatment has been an indication of the required length of treatment and sputum culture conversion has been indicative of treatment success[2,37].

The outcome classification of an individual's response to treatment for active pulmonary TB disease is normally dependent on the culture status of that individual at the end of the treatment period. The gold

standard tool available for the prediction of ultimately favorable or unfavorable outcomes is the conversion of sputum culture from *M.tb* positive to negative after two months of treatment. This technique falls short as a predictor of treatment outcome and treatment response, however it is currently the only available option to have been validated[94]. Sputum culture conversion as a biomarker of treatment response, however, has many shortfalls which include the well-known delay in result generation, as well as its limited use in drug-susceptible samples only. In order to overcome the delay in result time, sputum smears for acid-fast bacilli have acted as a surrogate for sputum culture in recent years, but unfortunately have high false positivity rates due to the presence of dead bacteria, which limit their use in clinical settings. It is, therefore, important to investigate alternative methods for the prediction of individual responses to treatment. Blood-based tests that do not rely on the direct detection of the *M.tb* bacilli are attractive alternatives for sputum-based techniques and recent studies in viral infections have supported their use as indicators of treatment response. Such studies have demonstrated that the phenotypes and frequencies of virus-specific $CD4^+$ and $CD8^+$ T lymphocyte phenotypes correlate with viral antigen load, which may be translated into *M.tb*-specific bacterial loads upon further investigation[95,96].

Previous studies have investigated various TB-specific blood-based alternatives with varying success rates. Such alternatives include serum-based studies centered around cytokine secretion[97] and proteomic signatures[98] for the prediction of month 2 culture status and subsequent end of treatment outcome, while others have investigated plasma-based cytokine secretion for the discrimination between fast and slow responders to anti-TB treatment[99]. Interestingly, a study performed by Adekambi *et al*. identified three T cell specific biomarkers ($CD38^+IFN\text{-}\gamma^+$, $Ki\text{-}67^+IFN\text{-}\gamma^+$, and $HLA\text{-}DR^+IFN\text{-}\gamma^+$ T cells) that are capable of discriminating between active TB and latent infection cases, while two of the three ($CD38^+IFN\text{-}\gamma^+$ and $Ki\text{-}67^+IFN\text{-}\gamma^+$ T cells) were capable of monitoring treatment response with substantial decreases in frequencies at the point at which sputum culture converted to negative[37]. While these studies have all proven promising, they are limited by the need for further validation and the lack of consistent sample types being used for biomarker investigations. Additionally, it would appear that the prediction of treatment outcome is complicated by observations that individual variable readouts are not necessarily associated with month 2 culture status. As seen in a study performed by Jayakumar *et al*., combinations of both measurable variables as well as demographic factors, such as age, need to be combined as a biosignature for improved predictive accuracy[97]. Alternatively, blood-based transcriptomic signatures have shown recent promise as predictors of treatment response, as is evident from the study performed by Cliff *et al.*[86]. The ability to predict an individual's response to treatment at an early time point would provide clinicians with the ability to potentially shorten treatment regimens for those with a predicted favorable outcome or change the treatment regimen early on to include more intensive drugs for those with predicted unfavorable outcomes in order to improve patient adherence and reduce the risk of developing drug resistance.

Predictive Biomarkers

Considering the difficulties faced with developing diagnostic and treatment response biomarkers, attention has recently changed to the potential prediction of progression to active disease in high risk cases, i.e. latently infected controls, in order to predict future incidence and potentially prevent this through the initiation of preventative therapies. Multiple large-scale studies have recently been completed investigating various gene expression profiles for the identification of individual risk of progression to active disease. Sloot *et al.* identified a two-gene signature that was capable of predicting progression to active disease up to 8 months before the first reported incidence in adult, *M.tb*-exposed controls[100]. Likewise, Zak *et al.* went on to identify a 16-gene signature capable of predicting progression to active disease up to 12 months before the first reported incidence in both *M.tb*-exposed adults, and adolescents[101]. Lastly, the most recent discovery was the identification of a four-gene signature by Suliman *et al.* capable of predicting progression to active disease in multiple sites across Africa with little population-associated variability[102]. While all of these signatures demonstrate great promise, current implementations of PCR- and transcriptomic-based assays are not feasible in high-burden settings. However, should national legislature address the need for household contact exposure to *M.tb* infection programs, such assays would be of great value for the swift identification of high-risk individuals, especially adolescents, thereby limiting future incidence and economic burden in the health care system.

While there are yet many different biomarker investigations underway, more detailed reviews on more specific biomarker targets have been published elsewhere. Walzl et al.[2] has reviewed the advances in immunological TB biomarkers pertaining to most aspects of the immune response to TB, while Tucci et al.[103] and John et al.[104] have reviewed the pathogen-derived biomarkers in terms of their gene/protein expression.

Comorbidities of Tuberculosis

In South Africa, there is a high multi-morbidity (MM) presence between TB, HIV and non-communicable diseases (NCD) that is sadly highly prevalent in resource-limited communities. The concept of multi-morbidities is complex, one that is accepted as fact but that has not been investigated thoroughly. Multi-morbidities are, however, becoming a clear threat in countries where prevalent infectious diseases are presenting alongside first-world lifestyle NCD's and result in reduced quality of life, poorer health outcomes from disease, and the increased requirement to seek out health care[105]. Examples of such comorbidities (NCD as well as chronic infectious diseases) that are compounding in MM include: hypertension, obesity, Type II Diabetes, cardiovascular disease, HIV, hepatitis C virus, cancer, chronic obstructive pulmonary disease (COPD), and helminth infection. These are exacerbated by the high prevalence of smoking and malnutrition in these regions[106].

The importance of studying comorbidities lies in the knowledge that each environmental influence, foreign stimulus or co-infection alters the immune response, often resulting in the discontinuation of one response in order to focus on another, limiting overall immune control.

Human Immunodeficiency Virus

HIV is a well-known, highly virulent virus that up until recently held the title of the most deadly disease in the world, killing approximately 1.2 million people in 2014 but was surpassed by TB which had a death toll of approximately 1.5 million people in the same year[58]. In sub-Saharan Africa HIV has had the most significant impact, with estimates showing that annually 70% of all new HIV cases are accounted for in this region, and 70,5% of the global population living with HIV/AIDS is from this region[107] The number of co-infection related deaths has risen to approximately 0.4 million HIV positive, active TB individuals, and the overall number of TB patients co-infected with HIV stands at 77%, highlighting the close correlation between the two diseases[106].

HIV and TB co-infections play a dubious game, with each disease causing the exacerbation of the other. It is known that individuals with HIV are much more likely to develop active TB than an HIV uninfected individual due to the severe disruption of the control of *M.tb* infection by HIV, the tentative nature of which has been discussed previously in this review[36]. Concurrent TB infection in HIV positive individuals causes the exacerbation of the HIV viral load as well as diminished CD4 count[108]. In the case of individuals who already have latent TB infection, concurrent diagnosis with HIV results in a much higher risk of progression to active disease and/or reactivation owing to the HI virus's characteristic weakening of cell mediated immunity and therefore the integrity of granulomas; HIV is also well known to alter the pathogenesis of *M.tb* infection as well as its clinical presentation[7,109].

Two opposing observations have been made with regards to the control of TB disease in the presence of HIV co-infection, emphasizing the lack of understanding of the immune response to complex co-infections. The first and most frequently seen observation is that HIV is responsible for the reduction in the $CD4^+$ T cell pool, especially *M.tb*-specific $CD4^+$ T cells, a defect that is known to increase the risk of developing active TB disease, increases the risk for failed *M.tb* infection control, and increases the chances of the infection disseminating to extra-pulmonary disease[7,108]. This is caused by the activation of the circulating $CD4^+$ T cells via the high viral loads to induce T cell apoptosis[36,110]. The second observation, although not widely understood, opposes the first. In a few studies there have been findings that *M.tb*-specific $CD4^+$ T cell volumes are higher in co-infected patients even though they had lower total $CD4^+$ T cell counts[111,112]. A study inspired by these two observations performed by Siddiqui et al.[36] aimed to compare the immune responses between individuals with mono or coinfection with TB and/or HIV. In this study they observed findings concurrent with the first observation mentioned above and postulated that there may exist a competitive imbalance between T_H1 and T_H2 immune response types in co-infected individuals. From this, they postulated further that this may result in an intense inflammatory response, but one that lacks control owing to their observation of high levels of IL-10 and IL-13, prevalent T_H2 response cytokines[36].

HIV co-infected patients being treated with ART or highly active antiretroviral therapy (HAART) again show altered effects on the immune control of *M.tb* infection. Should ART be started promptly following HIV diagnosis, it has been shown that these individuals display a partial immune restoration, allowing

the depleted $CD4^+$ T cell pool to be replenished somewhat; in latently infected individuals, ART suppresses the virus to the point where susceptibility to TB disease progression or reactivation is reduced[7,36]. It has been noted, however, that should a co-infected individual start ART within the first few weeks or months of TB treatment - during which the bacterial burden is still relatively high – intense T cell and T_H1 responses are triggered because of the partial immune restoration, resulting in a condition known as TB immune reconstitution inflammatory syndrome (TB-IRIS). TB-IRIS is a hyper-inflammatory condition resulting from various risk factors, including short intervals between commencement of TB treatment and ART, disseminated TB, and low CD4 counts which all play key roles in allowing for extensive *M.tb* antigen recognition following the restoration of the immune system[7,36,109].

Helminth Infections – *Ascaris lumbricoides*

Parasitic intestinal worms, also known as helminths, frequently plague the intestinal tracts of children and adults in developing countries. Many helminths are intestinal worms and belong to the phylum nematode, transmitted via soil contaminated with infected faeces or faecal contaminated water sources, and the most common genus is *Ascaris,* with the species *Ascaris lumbricoides* often affecting humans. It is estimated that approximately one third of the world's population may be infected with helminths, a statistic that is all too familiar in the TB community[113]. The population group for which the highest burden of disease is seen, is in children and adolescents owing to them being more frequently in contact with sand with their bare feet as well as unwashed fruit. Studies have shown that chronic helminth infection in children and adolescents, resulting from their "immature" immune systems among other things, causes impaired cognitive function and memory, stunted growth as well as diminished physical fitness, a crippling consequence for future economic growth and survival[114].
Should a parasitic infection have such an impact on a child's physical wellbeing during the early stages of development, it stands to reason that it would potentially wreak havoc on the immune system as well, both in children and in adults.

It is well known that TB prevalence is high in areas where helminth infection is endemic, predominantly developing countries in poverty stricken and/or rural regions[115–118]. It is interesting to note that these two coinfections are also highly prevalent in areas endemic for HIV infection, highlighting the clear association between these three infectious diseases[113]. In terms of the immune response to helminth infection, it is quite the opposite to the type of response that dominates during *M.tb* infection. *M.tb* infection elicits a predominantly T_H1 immune response along with the activation of the T_H17 response for regulatory control during chronic infection. During helminth infection, however, a T_H2 response is activated along with T_{Reg} cells for inflammatory control during chronic infection, a response that is known to be associated with enhanced susceptibility to TB disease[113,117,118]. It has been hypothesized that these two opposite responses, if activated in the same individual due to co-infection, would lead to the suppression or at least weakening of the T_H1 response in favor of the T_H2 response, thus resulting in the control of *M.tb* infection being less effective and potentially lost[118].

The term “helminth” groups various types of helminths together but does not consider the widely differing immune responses each type elicits in the host. For this reason, it is unclear which helminth type, if any, has a significant impact on host protection to *M.tb* during co-infection, or whether another helminthic factor such as helminth load or stage of reproduction/development may be playing a significant role in host protection development. The effect of helminth co-infection during *M.tb* infection as such is still not widely agreed upon. It has been shown that helminth infection does interrupt the development of strong immune responses to vaccines such as BCG, tetanus toxin, and cholera vaccine[115,117], but in a study performed by Hübner *et al*.[117], rats infected with *Litomosoides sigmodontis* (a filarial nematode) showed no difference in immune response when challenged with *M.tb*, and their control of *M.tb* infection did not differ to that of control rats, which contradicts the aforementioned hypothesis[117]. In a study by Abate *et al.*[113], the aforementioned hypothesis was instead supported by findings that helminth-induced production of IL-10 and induction of the T_{Reg} response played an immunosuppressive role; increased levels of IL-10 were found in helminth infected TB patients and IL-10 production was down-regulated during anti-helminth treatment to decrease worm burden and also improve cellular immunity to *M.tb* infection[113]. Rafi *et al*.[119] concluded through their review that there is strong evidence that helminth-induced T cell responses impair defenses against *M.tb* infection, once again supporting the aforementioned hypothesis[119].

It is abundantly clear that the association between the host immune control of *M.tb* infection and the exposure to/infection with helminths is poorly understood and requires a substantial amount more investigation. However, it is also clear that co-infections, such as helminth co-infection or co-infection with HIV, do drastically alter the immune response following exposure and the influence this alteration has on the control of *M.tb* infection, is crucial for our understanding of immune control and modulation of this disease.

Conclusion

Tuberculosis remains a steadfast pathogen that influences multiple facets of life, both in the universal and human sense. It is clear from the literature described above that this is a highly heterogeneous pathogen capable of exploiting highly heterogeneous host organisms. This hampers efforts to identify correlates of risk and correlates of protection, as well as efforts to translate species-dependent findings into the human model for which many structures and pathways are not homologous. Tuberculosis incidence, and more specifically that of drug-resistant case incidence, is sharply on the rise despite renewed efforts towards developing accurate and reliable tools for use at the point-of-care in high burden settings for improved case detection and monitoring. Biomarkers for diagnosis and/or treatment response, while few, lack specificity and reliability in geographical regions other than those in which the biomarkers were originally developed. While the urgency to develop improved diagnostic and treatment methods is clear, it is also important for research to employ a multi-disciplinary approach for the elucidation of pathogen evasion methods, as well as to perform research that encompasses multiple aspects involved in active TB disease, i.e. biomarkers of both diagnosis, treatment response and even the restoration of protective immunity.

CHAPTER 2

Investigation of host serum biomarkers for the diagnosis of TB disease.

New non-sputum host biomarkers for active Tuberculosis (TB) diagnosis are required for global control. Sputum-based diagnostics are accompanied by severe limitations which include long turn-around times to diagnosis, and difficulty obtaining samples from patients with early infection, extrapulmonary infection or those with disseminated disease such as children. Serum-based biomarker discovery holds the potential to provide early active TB disease diagnosis, however many serum biomarkers currently under evaluation require skilled and expensive technology, particularly proteomics technologies such as mass spectrometry[120–122]. While these methods are essential for novel biomarker discovery, they are not able to be implemented in a clinical setting at the point of care in high burden regions. Therefore, easily accessible serum biomarkers that are measurable in a simplified manner, such as with lateral flow devices, are required to reach the global goal of quickly and accurately diagnosing active TB disease in high burden regions at primary healthcare clinics. During initial microbial infection, the host immune cells release pro-inflammatory cytokines such as Interleukin (IL)-6, IL-1, tumour necrosis factor (TNF)-α, and interferon (IFN)-γ as part of their protective response[2,7]. These cytokines activate other immune mediators and induce the production of acute phase proteins: innate, non-specific responders to immunological stress. Acute phase proteins serve an important function early during infection as they are responsible for opsonisation of microorganisms, activating the complement system, as well as scavenging free haemoglobin, among others, all of which are crucial in early clearance of *M.tb* infection[123,124]. These markers could potentially serve as early biomarkers of TB disease. Keeping in mind the global desire for a robust, cost-effective point-of-care (POC) diagnostic tool, various options are being investigated as diagnostic biomarker readouts, including the use of lateral flow devices. These devices are handheld, easily transported, easily operated, affordable to produce, have low operational costs, and provide results within minutes; ideal for resource-limited regions[125]. In order to develop a lateral flow device for TB diagnostic purposes, target analytes need to first be identified and validated in highly endemic settings, with special attention paid to the types of endemic coinfections prevalent in such settings. The Luminex® multiple analyte analysis platform is one that allows for the measurement and identification of multiple soluble target analytes, as well as their validation, that may later be used in the development of a lateral flow device, one such tool that currently does not exist. This study, therefore, aimed to investigate host serum biomarkers capable of discriminating between participants with and without active TB disease, without the need for complex proteomic approaches.

2.1 Study Design

Hypothesis

We hypothesise that the levels of multiple acute phase proteins will be significantly different in TB patients in comparison to individuals without active TB, but who present with symptoms compatible with active TB, and that these proteins will be useful as a diagnostic signature for TB disease when used in combination.

Aims

The aim of this study is to investigate 9 different host serum biomarkers as potential contributors to a future diagnostic tool to aid in the swift diagnosis of TB, especially in resource-limited settings.

Objectives

- Measure multiple target analytes by performing Luminex immunoassays on serum samples from study participants presenting with symptoms compatible with active TB in whom active TB was subsequently confirmed or ruled out
- Identify serum biomarkers that display high sensitivity and strong diagnostic potential in univariate analysis, even in the context of HIV infection
- Construct a multi-marker diagnostic model that may most effectively discriminate between active TB cases and individuals without active TB, but that presented to the clinics with symptoms compatible with active disease, amongst all population groups

2.2 Methods

2.2.1 Participant Recruitment

As part of the African European-Tuberculosis Consortium (AE-TBC) for TB diagnostic biomarkers (http://www.ae-tbc.eu), approximately 718 individuals (mixed race or black Africans) who presented with symptoms suggestive of pulmonary TB were prospectively recruited by investigators from five field site clinics in five African countries (Stellenbosch University (SUN), South Africa; Makerere University (UCRC), Uganda; Medical Research Council Unit (MRC), The Gambia; Karonga Prevention Study (KPS), Malawi; and the University of Namibia (UNAM), Namibia). To ensure reproducibility and consistency, all five sites made use of the same harmonised Standard Operating Procedures.

All of the experiments outlined in this thesis were performed by myself. The data generated from this chapter in particular, in additional to data generated by other member of the Stellenbosch University Immunology Research Group, contributed to the development of a larger biomarker biosignature for which Dr Novel N. Chegou was the lead researcher.

Ethical Considerations

Ethical approval was obtained from the Human Research Ethics Committee of Stellenbosch University under the ethics number: N10/08/274 for the larger AE-TBC study, under which this sub-study was approved. Each participating site also obtained approval from their local or national ethics review boards. This study was performed in accordance with the Helsinki Declaration.

Inclusion Criteria

Participants were considered eligible for enrolment into the study if they presented with a persistent cough lasting more than 2 weeks, and any of the following: fever, malaise, weight loss, night sweats, shortness of breath, chest pain, or close contact with a TB patient. Participants were required to be above 18 years of age and willing to give written informed consent for participation, including consent to HIV testing.

Exclusion Criteria

Participants were excluded from enrolment if they presented with severe anaemia with a haemoglobin (HB) level of less than 10 g/l, were already on anti-TB treatment or had been during the ninety days preceding recruitment, had used quinolone or aminoglycoside antibiotics in the past sixty days, or had been residing outside of the study community for more than three months during the past year.

2.2.2 Diagnosis of Tuberculosis

Each individual had sputum and blood samples collected and had a chest X-ray (CXR). Serum was collected and stored at minus 80ºC until analysis. The sputum samples were cultured using the MGIT method (BD Biosciences) or the Lowenstein Jensen method depending of the method available for use at the study site. Positive MGIT cultures were stained using the Ziehl-Neelsen method to inspect for acid-fast bacilli, followed by one of the following two *M.tb* complex confirmation tests: Capilia TB testing (TAUNS, Numazu, Japan), or standard molecular methods (PCR for *M.tb* genes). Together, the clinical, radiological and laboratory findings were used to classify individuals into disease status groups (Table 2.1). The developed classification algorithm was harmonised across all study sites in conjunction with the standard operating procedures. For individuals in whom active TB was ruled out, treatment for alternate diagnoses, where available, was offered and *M.tb* infection status was determined. A QuantiFERON-TB Gold In-tube test (QFT), TST or T-SPOT.TB test was performed on all study participants at the beginning of the study depending on the available facilities at the field site. These results, however, did not affect patient management but only served as an indication of prior sensitization to *M.tb*. In addition, participants without an initial diagnosis of TB were re-examined after 2 months to rule out this disease. Each individual had their HIV status determined using the Determine® HIV-1/2 (Alere, Matsudo, Japan) rapid test, and positive rapid tests were confirmed by a second rapid test from a different manufacturer or by enzyme-linked immunosorbent assays (ELISA).

Table 2.1: Harmonized classification criteria of participants based on combinations of clinical and microbiological findings.

Classification	**Definition**
Definite TB	2 positive sputum cultures, OR 1 positive culture and CXR suggestive of PTB.
Probable TB	2 positive smears or 1 culture, without documented CXR evidence, but symptoms responding to TB treatment, OR 1 positive smear with CXR consistent with PTB.
Possible TB	1 positive smear and symptoms responding to TB treatment, OR CXR suggestive of TB and symptoms and/or radiology responding to TB treatment.
Questionable	Positive smear(s), but no other supporting evidence, OR CXR suggestive of PTB, but no other supporting evidence, OR

	Treatment initiated by healthcare providers on clinical suspicion only. No other supporting evidence.
No-TB	Negative cultures, negative smears, negative CXR and treatment never initiated by healthcare providers.

Abbreviations: TB – Tuberculosis; PTB – pulmonary Tuberculosis; CXR – chest X-ray

2.2.3 *Luminex Immunoassay and Analysis*

The levels of nine acute phase proteins, selected from a larger list of markers from a recently completed pilot study that was based on their largely pro-inflammatory roles in the innate immune system, were evaluated in two separate multiplex immune assays (Luminex, Bio Rad Laboratories, Hercules, CA, USA), in serum samples from all study participants (Table 2.2). Assays on the samples were performed on the Bio-Plex 200 suspension array system, using the dual-laser, flow-based microplate reader system (Bio Rad). The beads from each sample were acquired individually and analysed using the Bio-Plex Manager™ Software version 6.1 according to the recommended settings.

Table 2.2: Luminex Immunoassay kits used for the investigation of the nine cytokines of interest.

Multiplex Kit:	**Bio Plex Pro Acute Phase Assay Kit (4- and 5-Plex)**	
Catalogue Number:	171-305050	
Manufacturer:	Bio Rad Laboratories	
Cytokines Assessed:	**4-Plex**	**5-Plex**
	C-Reactive Protein (CRP)	Ferritin
	Alpha-2-macroglobulin (A2M)	Fibrinogen
	Serum Amyloid P (SAP)	Serum Amyloid A (SAA)
	Haptoglobin	Procalcitonin (PCT)
		Tissue Plasminogen Activator (tPA)

The Bio Plex Acute Phase Assay kit is recommended for use with serum and plasma samples, and culture supernatants may also be used. A condensed version of the protocol is given below.

Kit Reagents:

Each Acute Phase Assay kit comes with 4- and 5-Plex Multiplex assays, antibody-conjugated beads (25x concentration), detection antibodies (10x concentration), acute phase standards (2 vials/lyophilized), and acute phase controls (2 vials/lyophilized). The kit also contained serum-free diluent and serum-based diluent. 96-well plates for sample dilutions and assay buffer were not provided.

Preparation of Samples, Standards, Controls, Standard Dilution Series, and Coupled Magnetic Beads:

Samples:

Prior to the start of the measurements, the samples were centrifuged at 13 200 rpm for 10 minutes to clear the samples of any precipitates. For the 5-Plex assay, 3µl of sample was diluted in 297µl of serum-free diluent in a 96-well plate according to the sample positions on the plate layout and mixed thoroughly by pipetting to achieve a 1:100 dilution. For the 4-Plex assay, 3µl of the 1:100 dilution mixture was pipetted into a second 96-well plate along with an additional 297µl of serum-free diluent and mixed thoroughly by pipetting. This achieved a final sample dilution of 1:10000.

Standards:

The lyophilized standards were reconstituted using the serum-based and serum-free diluents where indicated when using **serum** or **plasma** samples. When **culture supernatants** were used, the standards were reconstituted in the culture medium used, and replaced the serum-free and serum-based diluents where applicable.

Before the standards were reconstituted, standard/control diluent was prepared for both the 4- and 5-Plex kits as follows: 1ml of serum-based diluent was diluted in 24ml of serum-free diluent and vortexed for 10 seconds to be used as the 5-Plex standard/control diluent; while 25ml of serum-free diluent was used directly as the 4-Plex standard/control diluent.

The standards were then reconstituted with 0.5ml of the appropriate standard/control diluent prepared above, gently vortexed for 1-3 seconds and incubated on ice for 60 minutes. These were then used as **S0** in the standard dilution series explained below.

Controls:

While ensuring the lyophilised control pellet was at the bottom of each glass vial, one vial was reconstituted with 1ml of the 5-Plex standard/control diluent, while the second vial was reconstituted with 2ml of the 4-Plex standard/control diluent. Each was gently vortexed for 1-3 seconds and incubated on ice for 60 minutes. The controls were reconstituted immediately after the standards were reconstituted.

Standard Dilution Series:

Nine 1.5ml Eppendorf tubes were prepared for the 4- and the 5-Plex assay. To the first tube of the dilution series containing 200µl 5-Plex standard/control diluent, 200µl of the 5-Plex assay reconstituted standard (**S0**) was added and vortexed gently to create Standard 1 (**S1**) as identified in Figure 2.1. The dilution series was continued as illustrated in the diagram, using a clean pipette tip each time and vortexing gently after each addition.

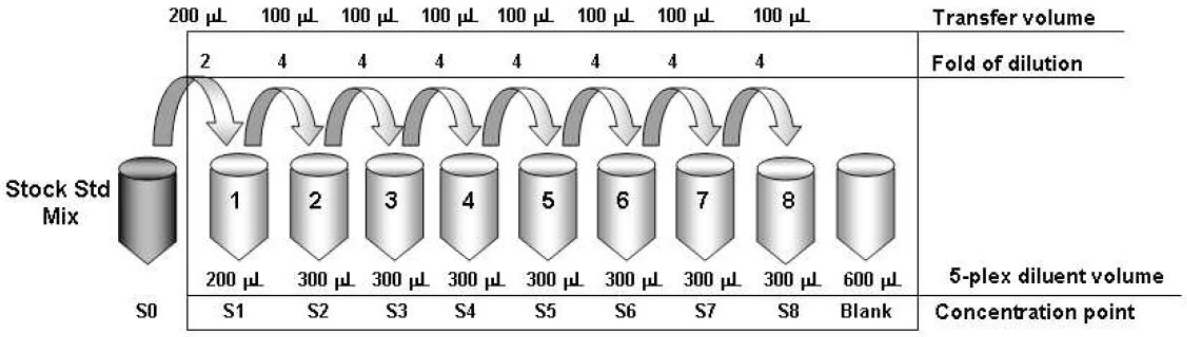

Figure 2.1: Diagram of the 5-Plex Standard Dilution Series to be made.

The standard dilution series for the 4-Plex assay is illustrated in Figure 2.2. Briefly, 50µl of the reconstituted 4-Plex standard was added to the first 1.5ml Eppendorf tube containing 350µl of the 4-Plex standard/control diluent and gently vortexed to be identified as **S1**. As before, the dilution series was continued according to Figure 2.2 and good laboratory practices observed.

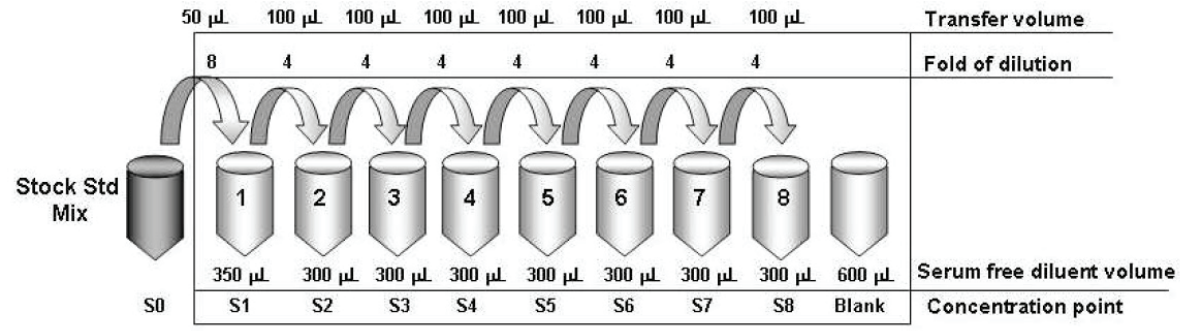

Figure 2.2: Diagram of the 4-Plex Standard Dilution Series to be made.

All reagents were reconstituted and prepared on the day of use. All samples, standards and controls were kept on ice until ready for use. It should be highlighted that each standard dilution series made use of a 0 pg/ml blank which was made up of 600µl of the appropriate standard diluent (or culture medium where culture supernatants were used). These were used to format the software to automatically subtract the background median fluorescent intensity (MFI) values from the MFI values of all the other readings to obtain a representative value lacking background influence. The standard dilution series, blanks and controls were run in duplicate on the 96-well plate, followed by the diluted samples which could either be run in duplicate or singlets depending on the study-specific criteria, mostly depending on available space.

Coupled Magnetic Beads:

The coupled magnetic beads (25x concentration) provided with the kit were vortexed for 30 seconds at medium speed and diluted to 1x concentration as follows: 120µl of the 25x concentration beads were added to 5880µl assay buffer in a 15ml Falcon tube covered with aluminium foil to protect the beads from the light and kept on ice until ready for use.

Assay Procedure

The diluted standards, samples and controls were equilibrated to room temperature for 20 minutes before use. While equilibrating, the 96-well plate was pre-wet with 100µl of assay buffer (**avoiding bubbles**), washed twice with a Bio-Plex Pro™ Wash Station plate washer and covered with sealing tape until ready for use. The coupled magnetic beads were vortexed for 15-20 seconds, of which 50µl of the beads were added to each well and washed twice. The diluted standards and control were then vortexed for 1-3 seconds, of which 50µl of each were added to the appropriate wells according to the plate template. The samples were mixed thoroughly by pipetting, and 50µl of each sample was added to the appropriate wells according to the plate template. The plate was covered with sealing tape and foil, and incubated for 1 hour in the dark on a plate shaker. For all incubation steps the plate was first covered in sealing tape followed by foil and placed on a plate shaker.

During the incubation period, the detection antibodies (10x concentration) were centrifuged for 30 seconds to collect the entire volume at the bottom of the vial. These were then diluted to a 1x concentration as follows: 150µl of the 10x detection antibody stock was added to 1350µl of detection antibody diluent. Following the incubation, the plate was washed three times after which 12.5µl of the detection antibodies were added to each well following a short vortex. The plate was then incubated for 30 minutes.

During the incubation the streptavidin-PE (100x concentration) vial was centrifuged for 30 seconds and diluted to a 1x concentration in a 15ml Falcon tube covered in foil as follows: 30µl of the 100x streptavidin-PE was added to 2970µl assay buffer. Following incubation, the plate was washed three times after which 25µl of the 1x streptavidin-PE was added to each well after a vigorous vortex. The plate was incubated for 10 minutes after which it was washed three times. Finally, 125µl of assay buffer was added to each well and the plate shaken on the plate shaker at 900 rpm for 30 seconds before the sealing tape was removed and the plate run on the Bio-Plex 200.

Sample Acquisition

The Bio-Plex 200 was switched on 30 minutes prior to use to allow for the lasers to warm up and calibrated with the Bio-Plex Calibration kit. The samples were acquired and analyzed using the low RP1 target value using the 100 beads per region option. Once all of the samples had been acquired, the data was exported to an excel spreadsheet for statistical analysis.

Statistical Analyses

Statistical data analysis was performed using GraphPad Prism version 5.0 (GraphPad Software, San Diego, CA, USA) and R version 3.2.0 (Bell Laboratories, New Jersey, USA). A p-value of < 0.05 was considered statistically significant. Univariate analysis for differences between comparison groups, e.g. TB and No TB, were evaluated using the Mann-Whitney U test for non-parametric datasets. Receiver Operating Characteristic (ROC) curve analysis assessed the diagnostic accuracy of each biomarker both when excluding and including HIV infection. Cut-off values derived from ROC curve analysis (taking into consideration their respective sensitivity and specificity values and employing Youden's

Index) show potential for use in POC triage tests in order to best discriminate between different groups of individuals. Youden's Index is one of the main summary statistics of ROC curve analysis and is primarily used for non-parametric datasets. It interprets and evaluates each of the ROC curve analysis biomarkers, and defines a maximum potential effectiveness for each, thus creating a more rigorous selection criteria for appropriate biomarkers[126]. Multivariate analyses were performed using a superlearner ensemble of statistical learning algorithms for the development of a stable predictive model. Data were assigned to Training and Test datasets. In order to build the superlearner for the predictive modelling, algorithms were selected for inclusion into a single ensemble of statistical learning algorithms. This was done by repeatedly applying the superlearner to the Test dataset and evaluating its performance. Algorithms were ranked according to their performance and those that had a coefficient or weight of greater than zero were eliminated from the ensemble. The final ensemble was made up of 8 learners/statistical learning algorithms which had a mean coefficient. Next we used a 20-fold cross-validation model to assess the performance of our biosignature on the training and test datasets. ROC curves were generated for each set and the performance of the model assessed.

It should be noted here that no corrections were made for multiple testing. The reason for this is that the process of modelling avoids the need to perform multiple tests and therefore the need to correct for them. To elaborate, modelling divides the data into two groups: the "training" and "test" sets. The "training" set can be used multiple times to generate the most suitable model without testing for significance. Once the final model is decided upon, it is tested on the "test" set only once. It is at this point that the model is tested for significance, and thus only one test for significance is performed, negating the necessity to correct for multiple testing.

2.3 Results

2.3.1 Participant Demographics

Of the 718 participants recruited for this study, 710 were included for the final analysis. Six (0.8%) participants had a questionable TB disease state diagnosis and were excluded from further statistical analysis along with one participant who was pregnant and another with incomplete clinical results. Detailed participant demographics are given in Table 2.3. The No TB participants had a range of diagnoses, including acute exacerbation of chronic obstructive pulmonary disease, upper or lower respiratory tract infections (bronchitis or pneumonia) or unknown conditions but none developed active TB during the follow-up period.

Table 2.3: Participant demographics according to the harmonised classification algorithm (Includes the participant details for those who were excluded from analysis for the reasons highlighted previously).

Study Site	SUN	MRC	UCRC	KPS	UNAM	Total
Participants (n)	169	209	172	117	50	717
Age (median)	36	33	30.5	39	35.5	34
Men, n (%)	69 (40.8)	123 (58.9)	88 (51.2)	60 (51.3)	29 (58)	369 (51.5)
HIV pos, n (%)	31 (18.3)	20 (9.6)	28 (16.3)	66 (56.4)	28 (56)	173 (24.1)
QFT pos, n (%)	105 (62.1)	83 (39.7)	120 (69.8)	44 (37.6)	35 (70)	387 (54)
Definite TB, n (%)	22 (12.6)	53 (30.3)	60 (34.3)	12 (6.9)	28 (16)	175 (79.2)
Probable TB, n (%)	2 (15.4)	0 (0)	0 (0)	5 (38.5)	6 (46.2)	13 (5.9)
Possible TB, n (%)	8 (24.2)	13 (39.4)	4 (12.1)	3 (9.1)	5 (15.2)	33 (14.9)
Total TB, n (%)	32 (14.5)	66 (29.9)	64 (29)	20 (9)	39 (17.6)	221 (100)
Latently Infected, n (%)	86 (38.9)	40 (18.1)	59 (26.7)	29 (13.1)	7 (3.2)	221 (45.2)
Uninfected, n (%)	49 (18.3)	100 (37.3)	49 (18.3)	67 (25)	3 (1.1)	268 (54.8)
Total No TB, n (%)	135 (27.6)	140 (28.6)	108 (22.1)	96 (19.6)	10 (2)	489 (100)
Questionable TB, n (%)	2 (33.3)	3 (50)	0 (0)	0 (0)	1 (16.7)	6 (100)

2.3.2 Diagnostic Accuracy of Individual Markers

The diagnostic accuracy of individual host serum markers was assessed to determine their potential value in differentiating between individuals with active TB and those without active disease, irrespective of their HIV infection status. It should be noted that the group of individuals without TB disease used in this section included individuals who were both latently infected and uninfected. Of the nine serum markers assessed as markers of TB infection state, eight showed significant differences ($p<0.05$) between the participants with TB and those without active TB disease; the only marker that showed no significant difference was alpha-2-macroglobulin (A2M). A2M was also the only marker for which the

median analyte concentration was higher in the participants **without** active TB compared to those with active TB (not significant; data not shown). The top four performing marker results are given in Table 2.4.

Table 2.4: Median concentrations of the top four host serum analytes detected in participants with active TB disease (n = 221) and those without TB disease (n = 489), independent of HIV infection status. (PCT, tPA and Ferritin measurements are in pg/mL, while the rest are in ng/mL).

TB vs No TB					
Host Marker	**Sensitivity (%)**	**Specificity (%)**	**P-value**	**AUC (95% C.I.)**	**Optimum cut-off value**
CRP	77.83 (0.72-0.83)	78.32 (0.74-0.82)	P<0.0001	0.84 (0.80-0.87)	> 1.23
SAA	84.62 (0.79-0.89)	71.37 (0.67-0.75)	P<0.0001	0.83 (0.79-0.86)	> 0.31
Ferritin	79.19 (0.73-0.84)	64.01 (0.60-0.68)	P<0.0001	0.78 (0.75-0.82)	> 5.28
Fibrinogen	84.16 (0.79-0.89)	54.60 (0.50-0.59)	P<0.0001	0.72 (0.69-0.76)	> 0.26

Abbreviations: A2M – alpha-2-macroglobulin; CRP – C-reactive protein; SAA – serum amyloid A; TB – tuberculosis; LTBI – latent tuberculosis infection; AUC – area under the curve; C.I. – confidence interval.

In terms of differentiating between individuals with active TB and those who are latently infected irrespective of their HIV status, all of the markers showed significant differences ($p<0.05$) between the two participant groups (Table 2.5). Interestingly, as was the case when differentiating between participants with active TB and those without active disease, A2M was the only marker that displayed a converse median analyte concentration compared to the remaining eight analytes. In this instance, however, A2M was the strongest performing marker for the diagnosis between the active and latent groups in terms of the area under the curve (AUC) and corresponding sensitivity and specificity values (Table 2.5), contrary to the findings in the comparison between the active TB and No TB case groups.

Table 2.5: Median concentrations of the top four host serum analytes detected in participants with active TB disease (n = 221) and those latently infected (n = 221), independent of HIV infection status (PCT, tPA and Ferritin measurements are in pg/mL, while the rest are in ng/mL).

TB vs LTBI					
Host Marker	**Sensitivity (%)**	**Specificity (%)**	**P-value**	**AUC (95% C.I.)**	**Optimum cut-off value**
A2M	82.35 (0.77-0.87)	92.76 (0.89-0.96)	P<0.0001	0.92 (0.90-0.95)	> 557.90
CRP	76.02 (0.70-0.81)	81.45 (0.76-0.86)	P<0.0001	0.85 (0.81-0.88)	< 0.85
SAA	74.66 (0.68-0.80)	84.62 (0.79-0.89)	P<0.0001	0.85 (0.81-0.88)	< 0.31
Ferritin	70.59 (0.64-0.77)	79.19 (0.73-0.84)	P<0.0001	0.82 (0.78-0.86)	< 5.26

Abbreviations: A2M – alpha-2-macroglobulin; CRP – C-reactive protein; SAA – serum amyloid A; TB – tuberculosis; LTBI – latent tuberculosis infection; AUC – area under the curve; C.I. – confidence interval.

Following Receiver Operating Characteristic (ROC curve) analysis, each marker's AUC was scrutinised for their individual diagnostic accuracies in the case of diagnosing between active disease and No TB disease, as well as diagnosing between active disease and latent infection. Markers with an AUC of 0.70 and above are considered very accurate, and the two most accurate markers for diagnosing between active TB and No TB disease (Figure 2.3(a) and (b)), and active TB and latent infection (Figure 2.3(c) and (d)) are given in Figure 2.3 below.

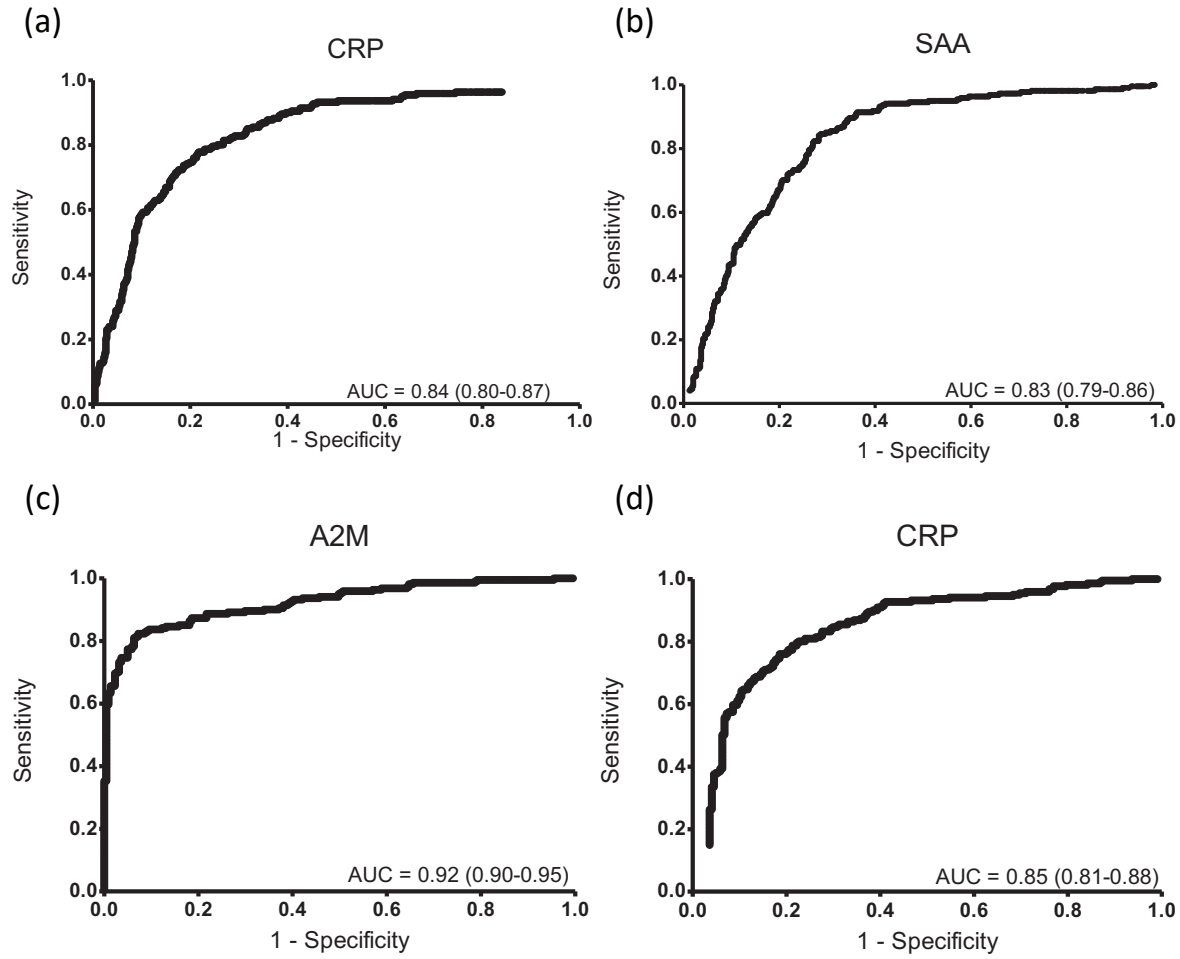

*Figure 2.3: Receiver Operating Characteristic (ROC) curves representing acute phase proteins used during univariate analyses. (a and b) The top two performing host serum analytes, CRP and SAA respectively, detected in individuals with **active TB disease** (n = 221) and individuals **without TB disease** (n = 489) that displayed the greatest potential for use in a diagnostic tool, independent of HIV infection status. (c and d) The top two performing host serum analytes, A2M and CRP respectively, detected in individuals with **active TB disease** (n = 221) and individuals with **latent infection** (n = 221) that displayed the greatest potential for use in a diagnostic tool, independent of HIV infection status.*

2.3.3 Influence of HIV co-infection on the Diagnostic Accuracy of Individual Markers

Owing to the high HIV positive TB incidence rates in the African region[58], participants were further grouped according to their HIV infection status and the accuracy of the markers re-assessed within each group to determine co-infection influence. Detailed participant demographics are given in Table 2.3, while details of the top 4 performing biomarkers for the discrimination between participants with and without active TB disease who were either HIV negative or HIV positive are given in Tables 2.6 and 2.7.

Table 2.6: Median concentrations of host serum analytes detected in HIV negative participants with active TB disease (n = 163) and those without TB disease (n = 376), as well as their diagnostic accuracy and optimum cut-off values to achieve this (PCT, tPA and Ferritin measurements presented in pg/mL, while the rest are in ng/mL).

TB vs No TB in HIV negative participants					
Host Marker	**Sensitivity (%)**	**Specificity (%)**	**P-value**	**AUC (95% C.I.)**	**Optimum cut-off value**
CRP	77.30 (0.70-0.83)	78.51 (0.74-0.83)	P<0.0001	0.83 (0.79-0.87)	> 0.86
SAA	84.05 (0.78-0.89)	76.13 (0.72-0.80)	P<0.0001	0.84 (0.80-0.87)	> 0.31
Ferritin	78.53 (0.71-0.85)	68.97 (0.64-0.74)	P<0.0001	0.79 (0.75-0.83)	> 5.28
Fibrinogen	80.37 (0.73-0.86)	60.48 (0.55-0.65)	P<0.0001	0.74 (0.69-0.78)	> 0.26

Abbreviations: CRP – C-reactive protein; SAA – serum amyloid A; tPA – tissue plasminogen activator; TB – tuberculosis; AUC – area under the curve; C.I. – confidence interval.

Table 2.7: Median concentrations of host serum analytes detected in HIV positive participants with active TB disease (n = 58) and participants without TB disease (n = 114), as well as their diagnostic accuracy and optimum cut-off values to achieve this (PCT, tPA and Ferritin measurements presented in pg/mL, while the rest are in ng/mL).

TB vs No TB in HIV positive participants					
Host Marker	**Sensitivity (%)**	**Specificity (%)**	**P-value**	**AUC (95% C.I.)**	**Optimum cut-off value**
CRP	87.93 (0.77-0.95)	70.18 (0.61-0.78)	P<0.0001	0.87 (0.80-0.92)	> 2.07
SAA	68.97 (0.55-0.80)	78.07 (0.69-0.85)	P<0.0001	0.80 (0.73-0.87)	> 0.61
Ferritin	56.90 (0.43-0.70)	92.11 (0.86-0.96)	P<0.0001	0.78 (0.70-0.85)	> 29.05
tPA	74.14 (0.61-0.85)	64.60 (0.55-0.73)	P<0.0001	0.74 (0.66-0.82)	> 0.28

Abbreviations: CRP – C-reactive protein; SAA – serum amyloid A; tPA – tissue plasminogen activator; TB – tuberculosis; AUC – area under the curve; C.I. – confidence interval.

The diagnostic accuracies (AUC values) were compared between HIV positive and HIV negative participants as well as within the complete participant group so as to visualise the possible influence of HIV infection (Figure 2.4). A one-way ANOVA was performed for each analyte to compare the different HIV criteria. From the observed results, no significant difference was seen between the HIV-, HIV+ and All groups, suggesting that HIV co-infection does not significantly affect the efficacy of the assessed biomarkers. For a few analytes, the AUC values do however show a trend towards being higher in the

HIV infected group, than in the HIV negative assessment group and in the overall population irrespective of HIV infection, which suggests that these markers would perform best when used in a diagnostic tool for HIV infected individuals. The trend displayed above is also mimicked in the case of diagnosing between participants with active TB and those who are latently infected, further supporting the non-significant effect of HIV co-infection on these select markers (Table 2.7).

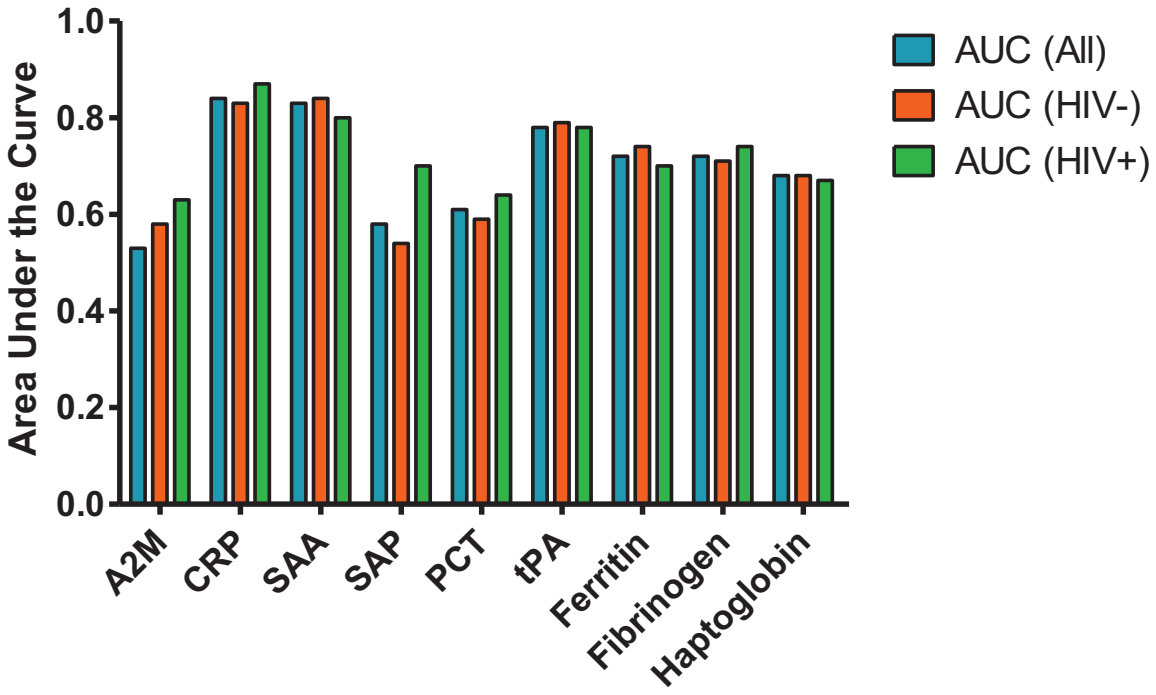

Figure 2.4: Histogram depicting the AUC values for each marker when assessed irrespective of HIV infection status, as well as when assessed in HIV negative and positive population groups respectively. The data represent the comparison of biomarkers in active TB and No TB cases for which there were no significant differences following one-way ANOVA.

2.3.4 Diagnostic Accuracy of Markers used in Combinations

A superlearner ensemble of statistical algorithms was used to build a stable diagnostic model that would not be overoptimistic in its predictions. Data were assigned to Training and Test sets on which to build the predictive model and test its actual performance, respectively, irrespective of HIV infection status and/or clinic site. Prior to multivariate analysis, the top four Youden's Index markers were selected for the final evaluation of marker combinations, namely: CRP, SAA, Ferritin and Fibrinogen. The Training set consisted of n = 406 (60%) data observations, while the Test set consisted of n = 268 (40%) data observations. The Training set was split into n = 131 TB cases and n = 275 No TB controls, while the Test set was split into n = 87 TB cases and n = 181 No TB controls (owing to data distribution, only 674 data sets were included in the multivariate analysis instead of 710).

Combinations of two biomarkers – **CRP and SAA** – resulted in the most successful combination after assessing the optimal combined sensitivity and specificity using Youden's J (Table 2.8). This resulted in a biosignature with a sensitivity and specificity of 87.4% and 75.7% respectively, with a predictive accuracy of 86.6%. The two ROC curves were nearly identical, i.e. they fell within the overlap of the 95% confidence intervals (Figure 2.5(a) and (b) for the Training and Test sets respectively).

Table 2.8: Superlearner model building outcomes using the Training and Test set approach for the combination of the biomarkers CRP and SAA for the optimal combined sensitivity and specificity.

	Sensitivity	Specificity	NPV	AUC	P-value
Training Set (n = 406)					
% (n/N)	85.5 (112/131)	75.6 (208/275)	0.916	0.844	4.91×10^{-7}
95% C.I.	(0.783-0.910)	(0.701-0.806)	(0.878-0.943)	(0.808-0.879)	
Test Set (n = 268)					
% (n/N)	87.4 (76/87)	75.7 (137/181)	0.926	0.866	9.9×10^{-6}
95% C.I.	(0.785-0.935)	(0.688-0.818)	(0.877-0.956)	(0.819-0.910)	

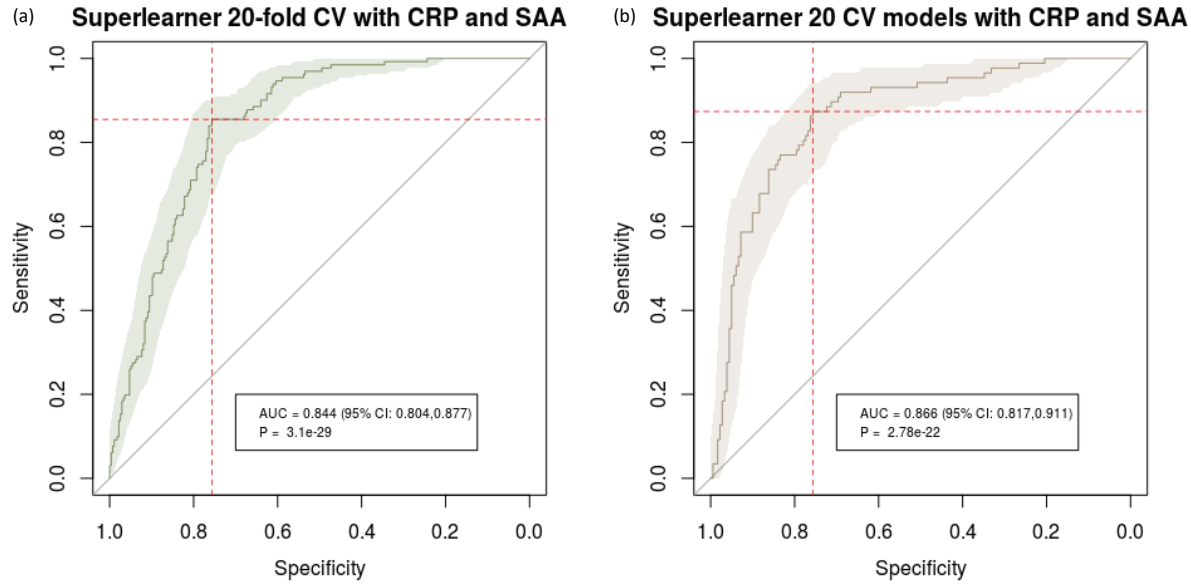

Figure 2.5: ROC curves of the superlearner model using the (a) Training and (b) Test datasets for the evaluation of the model's performance.

The best specificity was also calculated for a sensitivity of greater than or equal to 90%, for which the best outcome was a 69.6% specificity at a sensitivity of 90.8%, with a diagnostic accuracy of 76.5% (Table 2.9). Diagnostic/screening tools aim to have a sensitivity of above 90% owing to this greatly reducing the number of false negative results and thus resulting in fewer disease cases being missed. One would rather have a higher false positive rate for which those individuals require confirmatory testing, than have a high false negative rate which results in increased transmission and poor clinical outcomes for the diseased cases.

Table 2.9: Superlearner model building outcomes using the Training and Test set approach for the combination of the biomarkers CRP and SAA for a sensitivity kept greater than or equal to 90%.

	Sensitivity	**Specificity**	**NPV**	**AUC**	**P-value**
Training Set (n = 406)					
% (n/N)	90.1 (118/131)	64.0 (176/275)	0.931	0.724	0.024
95% C.I.	(0.836-0.946)	(0.58-0.697)	(0.878-0.943)	(0.678-0.767)	
Test Set (n = 268)					
% (n/N)	90.8 (79/87)	69.6 (126/181)	0.940	0.765	0.00083
95% C.I.	(0.827-0.960)	(0.624-0.762)	(0.890-0.969)	(0.710-0.814)	

2.4 Discussion

Traditional diagnostic methods for TB disease, such a sputum smear microscopy and sputum culture, lack sensitivity and rapid result delivery, respectively. Rapid diagnosis is crucial for timeous treatment initiation, prevention of transmission and further dissemination of disease resulting in the worsening of the patient's condition. This has driven the development of rapid, efficient diagnostic tools such as the GeneXpert® MTB/RIF which significantly reduces the turnaround time for a concise diagnosis to about two hours. The limited availability of GeneXpert® MTB/RIF technology in resource-limited, sometimes inaccessible, rural regions inhibits proper beneficial use in cases where such tests are needed most. Sputum samples can also be a difficult sample to obtain for the GeneXpert® MTB/RIF test as many patients are unable to produce good quality sputum samples, especially in children, in HIV coinfection, or where the disease has disseminated from the lungs to other organs[4,52]. The need for a rapid, point-of-care diagnostic tool that is preferably handheld is obvious, and while efforts are being made to improve systems like the GeneXpert® MTB/RIF for such purposes, a blood-based point-of-care device would greatly improve swift diagnosis and access to treatment in resource-limited settings, especially in patients who have disseminated disease.

This project investigated the circulating serum levels of nine acute phase proteins that play mainly pro-inflammatory roles during the innate immune response during TB disease. The aim was to identify an individual or combination of acute phase proteins that could successfully discriminate between individuals with and without confirmed TB disease, with strong sensitivity and specificity (Optimally: >80% and 98% respectively in a pooled smear-negative/smear-positive population both with and without HIV infection, according to the High-Priority Target Product Profile for new Tuberculosis Diagnostics proposed by the W.H.O. in 2014)[127] for the long term goal of identifying blood-based biomarkers that could be used in a rapid point-of-care device such as a lateral flow test. Current near-to-patient devices include the GeneXpert® MTB/RIF assay, for which a desirable sensitivity performance is already achieved, however, the assay is dogged by limitations, specifically when used in high-burden regions. Meta-analyses performed on the performance of the GeneXpert® MTB/RIF assay in multiple studies and settings have identified the pooled sensitivity of the assay to be 89% (95% Credible Interval (CrI) 85%-92%) and pooled specificity to be 99% (95% CrI 98%-99%) in instances where GeneXpert® MTB/RIF was used as an initial diagnostic test, replacing traditional smear microscopy[128,129]. During a meta-analysis of 7 studies, when HIV was taken into consideration the pooled sensitivity for individuals with HIV infection was only 79% (95% CrI 70%-86%), but was 86% (95% CrI 76%-92%) for individuals without HIV infection[128,129]. Based on these data, the GeneXpert® MTB/RIF is a great front-line diagnostic tool, however the test is not a point-of-care diagnostic in many locations and the need for a second clinic visit prior to initiation of treatment poses a serious limitation to its implementation across Africa. In addition, the challenge to collect good quality sputum samples from all patients, especially children, as well as the high likelihood of false positive diagnoses in persons

with known previous episodes of TB, limits the reliable use of this platform in many cases. It should be noted here that the credible interval (CrI) is the Bayesian equivalent of the confidence interval (CI).

We also aimed to investigate the influence of HIV co-infection with TB on the diagnostic accuracy and efficacy of these acute phase proteins. A combination of two markers, CRP and SAA, displayed robust sensitivity when diagnosing between TB cases and No TB cases with and without HIV infection. However, due to the low specificity of the biosignature it would be better suited as a triage test, rather than a primary diagnostic tool. The TPP formulated by the W.H.O. for the End TB strategy strongly suggests the investigation of alternative forms of diagnostic approaches, and as such we proposed the development of a point-of-care triage test for our own biosignature. Triage tests or screening tests help narrow down the number of people who need culture-based confirmatory diagnoses. Owing to the complexity of TB and slow technological advances, many individuals suspected of having the disease are falsely diagnosed - a triage test would allow for a swift ruling out of active TB disease in suspected patients and thus allow confirmatory culture-based test turnaround times on screened positive patients to be improved significantly. The negative predictive value of 92.3% for the identified biosignature comprising of CRP and SAA would thus be a prime candidate for such an application and would confidently allow for the exclusion of ~92% of suspected patients who do not have the disease and would therefore not require redundant and additional testing.

The two-marker biosignature discriminated between patients with active TB disease and those without disease.

Instead of using univariate parameters for the development of robust and stable diagnostic tools, the use of multiple parameters appears more promising. Univariate parameters often display exceptional sensitivity or specificity results, but usually lack the combination of both. For this reason, multiple parameters, or biomarkers in this case, are the preferable option for the development of diagnostic tools, as these combinations of well performing individual biomarkers provide greatly improved sensitivities **and** specificities with more robust readouts.

In order to streamline the process of combining multiple biomarkers and assessing their diagnostic accuracies, the top four individually performing biomarkers of this study were selected using Youden's Index. The top four biomarkers for this study were thereby selected (CRP, SAA, Ferritin, and Fibrinogen) using this method. Their predictive abilities in combination were then investigated by building a predictive model using a superlearner ensemble of eight statistical learning algorithms and following the training/test set approach. The result was a biosignature composed of the analytes CRP and SAA that accurately discriminate TB disease from No TB cases ~87% of the time (AUC 0.866, 95% C.I. 0.82-0.91) with an optimal combined sensitivity of 87.4% and specificity of 75.7%. Should the sensitivity be optimised to greater than or equal to 90%, the biosignature was capable of performing at a sensitivity and specificity of 90.8% and 69.6%, respectively, which would be the ideal optimization of a biosignature for use as a screening tool (higher sensitivity is more valuable as a screening tool). The combined sensitivity was much greater than the sensitivities for both biomarkers in their individual capacities,

although the combined specificity is greatly reduced. As mentioned previously, this is disadvantageous for our desired application of a robust diagnostic test, but owing to the high sensitivity of the biosignature it could be alternatively used as a screening test.

C-reactive protein (CRP) and Serum amyloid A (SAA) are serum-based proteins that are associated with the acute phase of the inflammatory response, and their circulating concentrations are known to increase significantly during bacterial infections[130–132]. Their secretion from hepatocytes and innate immune cells is induced by IL-6, mainly from monocytes at the site of inflammation[133]. These two proteins function as opsonins, activating the complement response, as well as recruiters of innate immune cells to the site of infection[123]. Circulating CRP concentrations are known to reflect the severity of disease as the highest levels are seen during active TB of untreated patients, and the circulating concentrations return to normal over the course of treatment, as do those of SAA[132,134,135]. SAA may, however, be a more sensitive indicator of inflammation than CRP[53]. Although only mildly elevated CRP levels have been observed in HIV infected individuals, studies have shown circulating CRP concentrations to be highest in individuals with TB co-infected with advanced HIV disease, highlighting its suitability for use in this study's setting since HIV co-infections are known to impair host immune responses[135]. Since HIV infected individuals often present as sputum-smear negative when suspected of having TB disease, they are not properly diagnosed and increase the pool of overall missed cases, possibly resulting in the generation of drug resistance following isoniazid monotherapy[136] as part of preventative treatment that is often offered to HIV infected patients with either positive tuberculin skin tests or positive interferon gamma release assays. Although CRP level testing has proven to be less sensitive than culture-based tests (as seen in this study and others[135,136]), culture-based diagnostic methods are not always feasible in endemic settings. Additionally, sensitive tests such as the GeneXpert® MTB/RIF[137] have limited value in ruling out TB disease, highlighting the large gap in accurate case-finding. With this said, circulating CRP concentrations could be very useful for diagnosing smear-negative TB disease in patients with HIV infection or severely immunocompromised individuals using a rule-out screening approach as this study and others show that median concentrations of CRP are not significantly influenced by an individual's HIV status[135]. The use, therefore, of CRP together with the highly homologous SAA in a rule-out screening test for TB in settings where HIV prevalence is high (such as South Africa) would be a significant benefit to the health sector in reducing missed cases, reducing possible drug resistance development, as well as possible transmission of drug-resistant strains in those who are severely immunocompromised, and those who present with smear-negative TB disease.

Alpha-2-macroglobulin is highly accurate for discriminating between participants with active TB and latent infection.

As the poorest performing marker in the diagnosis between active TB and No TB, alpha-2-macroglobulin (A2M) was not expected to be a valuable marker for further development. It was thus surprising when it could very successfully discriminate between latently infected participants and those with active disease 92% of the time (95% C.I. 0.90-0.95) with very high sensitivity and specificity

outcomes (82.35%, 95% C.I. 0.77-0.87; and 92.76%, 95% C.I. 0.89-0.96 respectively) in a univariate capacity. A2M is a non-immunoglobulin acute phase protein that is not only produced by the liver, but also by local macrophages. One of its main functions during homeostasis is to act as a carrier protein that binds growth factors and cytokines such as platelet-derived growth factor, transforming growth factor (TGF)-β, TNF-α, IL-6, low-density lipoprotein receptor-related protein-1 (LRP-1) and IL-1β[138]. IL-6, IL-1β and TNF-α are crucial cytokines for a successful host response and infection control.

In bacterial sepsis studies, it is well known that A2M is a crucial role player in the host response, and it is postulated that neutrophils produce and release A2M from internal microvesicles during sepsis-induced systemic inflammation[139]. Neutrophil microvesicle-derived A2M binds the cell membranes of endothelial cells where they are made available for binding to LRP-1 on neighbouring neutrophils. Through this mechanism, A2M is able to enhance neutrophil adhesion, chemotaxis and anti-bacterial effects, allowing for a swift migration to the site of infection and containment of the pathogen. Knockout studies in mice further support this as the lack of the LRP-1 receptor on neutrophils has been shown to reduce the protective effect of A2M[140]. Whether this hypothesis stands true for hepatocyte-produced A2M is unknown. The observation that A2M is much higher in our latently infected population suggests that A2M may be crucial for pathogen control in the lungs during latent infection, possibly through the improved recruitment and migration capacity of circulating neutrophils to the site of infection. This may, however, prove to be detrimental to the host in the long term as it is unknown for how long circulating A2M levels are increased following initial/during latent infection considering there is no way to tell when the person became infected. Chronic inflammation and possible conversion to active disease may be a consequence of this added pathogen control during the initial stages of latent infection, and no studies aimed at assessing the follow-up of latently infected patients have been conducted with the purpose of monitoring circulating A2M concentrations and its correlation with conversion to active disease.

A2M is clearly a useful biomarker for the distinction between latent infection and active disease even when used in univariate analysis. For this reason, it should be assessed further for use as a screening tool in high-burden areas where preventative strategies such as isoniazid preventative therapy may be an option in appropriate cases. Considering the aims and objectives of this study, a diagnostic discriminant for active disease and latent infection was not initially part of the scope of the project, but it should be noted for future work. In addition, all nine biomarkers assessed in this study were markers of general systemic inflammation and were thus non-specific for active TB disease. Considering the criteria that the latently infected participants in this study presented to the clinic with symptoms suggestive of active TB disease, while not having active TB disease, would still have been diagnosed with other respiratory illnesses. In such cases, our selected markers would still be elevated as we did not have a participant group that was asymptomatically latently infected. This is a limitation to the study, however we are confident that our selected biosignature markers, albeit non-specific, were produced in significantly larger quantities compared to other respiratory illnesses which makes them worthy candidate biomarkers.

HIV co-infection does not alter the diagnostic efficacy of the selected biomarkers.

Quite possibly the most influential risk factor for the predisposition of *M.tb* infection and/or progression to active disease, the deleterious effects of HIV co-infection not only on circulating *M.tb*-specific CD4+ T cells, but also primary macrophage functions is well known and has been characterised many times over[108,141]. The ability of HIV to alter the pathogenesis and clinical presentation of *M.tb* infection would consequently alter many correlates of risk and/or diagnostic biomarkers of TB through the increase or decrease of marker expression during co-infection. It should be noted that even though only 8.2% of all our participants tested HIV positive, this percentage is annually increasing in the African region despite global effort at lowering the incidence in high-burden areas, thus the need for a robust diagnostic test whose results are not skewed by the influence of HIV infection.

In this study, we assessed the influence of HIV co-infection on our biomarker/biosignature stability and predictive efficacy. We observed with confidence that HIV co-infection does indeed not alter the performance of our biosignature, a strong positive in the further development of the biosignature as a diagnostic screening/triage test. Additionally, some of the assessed analytes displayed marginally stronger (non-significant) diagnostic accuracies in our HIV infected group compared to the HIV uninfected group without compromising the overall differentiating ability. This enhances our desire to utilise these markers specifically in our high HIV-TB burden setting where mainstream diagnostic methods may be strongly influenced by HIV co-infection, as these markers perform better in HIV infected persons, however this shall not be discussed as biosignatures for TB diagnosis in HIV infected population groups falls outside of the scope of this project, but is an important aside.

Ethnicity influence considerations.

Participants in this study were recruited from sites located in five different African countries, bringing in to question the influence of ethnic backgrounds on research findings. While it is commonly known that host genetics play a large role in immune response profiles to multiple diseases, when assessed in the larger study towards which this Chapter's work contributed, an influence of ethnicity on biosignature performance was not observed. Since the two-biomarker biosignature evaluated in Chapter was assessed using the same participant cohort, we can deduce that ethnicity did not influence the performance of the biosignature. Previous studies have indeed identified differences in cytokine profiles between ethnic groups, but these studies investigated diseases such as cancer and viruses for the most part. Tuberculosis-specific studies investigating the influence of ethnicity on cytokine profiles have recently begun to surface and largely focus on broad ethnic groups, i.e. African, Eurasian etc. One such study performed by Coussens *et al.* investigated differences between African and Eurasian ancestry on the overall inflammatory profile of active TB patients[142]. Indeed, patients with African ancestry displayed lower neutrophil counts and lower serum concentrations of certain chemokines which became more pronounced upon treatment initiation and correlated with poorer outcome, but this study did not take in to account geographical location on the African continent. Based on the development of our two-biomarker biosignature on a cohort of participants from multiple countries gives the confidence that this biosignature is robust enough to overcome such ethnic differences. We do, however, believe that

socioeconomic status should in future be considered owing to its apparent influence on inflammatory profiles, more so than ethnicity, especially since Tuberculosis is a disease that burdens low socioeconomic status communities[125,143].

The use of serum samples instead of antigen-stimulated samples.

Many diagnostic studies make use of antigen-stimulated samples for the investigation and development of biomarkers. In this experimental chapter, we chose to instead use serum samples due to the clinical relevance this sample type holds. Serum, compared to antigen-stimulated samples, is readily available at the point-of-care following a short phlebotomy into the correct vacutainer and requires little to no processing, whereas antigen-stimulated samples require overnight stimulation in skilled laboratories often long distances from primary healthcare clinics. In order to create a point-of-care diagnostic tool, one requires the use of an easily available sample that would not require lengthy processing by skilled personnel, as with serum, to ensure same-day/same-consultation diagnoses of active TB disease. This would improve patient treatment adherence, reduce delays in treatment initiation significantly, and avoid the potential loss of patient's to follow-up because of the delay in diagnosis. In addition to this, antigen-stimulation assays would be very costly and, therefore, not suitable for use at the point-of-care.

Dr Novel Chegou and colleagues have published many research papers in which antigen-stimulated samples were evaluated instead of plasma and/or serum. In one such research article, a 7-day stimulation assay was used which resulted in an astounding 100% accuracy in discriminating active TB disease from household contacts[73]. Other studies have reported similar, but less accurate results using antigen-stimulated samples, however the translation of such assays into the clinical setting lacks credence[72,144,145]. Turn-around time for diagnostic results would be too slow, skilled laboratory personnel would be required to perform the assays and interpret results, and such assays would impose a heavy financial burden.

With that said, antigen-stimulated samples would likely have shown a different outcome in this instance. Antigen-stimulation of whole blood would elicit an antigen-specific response from the repertoire of immune cells found within peripheral blood, likely improving diagnostic accuracy of measured analytes. This would be beneficial for research purposes; however, serum samples represent a snapshot of the host immunological response without additional stimulation/interference that is a true representation of the biological processes occurring at the time of phlebotomy. Therefore, serum would be a more suitable candidate for the translation of scientific findings into the clinical setting, regardless of improved diagnostic accuracy in antigen-stimulated samples. Lastly, owing to the known heterogeneous response to M.tb, antigen-stimulated samples may not be the most suitable sample type.

Limitations.

Considering the limitations of this study, the largest would be that the biosignature described above is not suited as a diagnostic tool for TB disease – our original aim – due to the limiting specificity values, as hoped for in our stated hypothesis. It does, however, provide us with an indication that serum-based

screening tests may be of value in future efforts towards more rapid diagnosis of patients and the reduction of demand for culture-based tests through the development of a Point-of-Care screening test. These screening tests have the potential to provide healthcare workers with the means to test patients who are suspected of having TB disease and receiving a result within a few minutes. Due to the high negative predictive values (NPV) seen with the above biosignature, healthcare workers could be confident that the overwhelming majority of patient who's test result are negative do not have TB disease and can be assessed for alternative conditions. For those patients who have a positive screening test result, culture-based diagnostics may be performed to confirm or deny the suspicion of disease, thereby dramatically reducing the burden on national health laboratory services and streamlining the output of culture results. Our findings have been included and further validated in a seven-biomarker biosignature developed by Dr Novel N. Chegou[125] who investigated additional biomarker candidates other than the nine acute phase proteins investigated in this study. This seven-biomarker biosignature is now undergoing continued development into a lateral flow screening tool for use in high burden settings.

Another limitation of this study is that only one co-infection was evaluated in tandem. Disease co-infections are complex scenarios. While HIV is most likely the most concerning co-infection worldwide owing to its extreme host response manipulation, other co-infections specific to the target populations need to be scrutinized and assessed in validation studies for such biosignatures going forward. Parasitic infections, for example, are a great burden in low income regions, and the nature of the host response to such infection in tandem with TB disease may severely influence the accuracy and reliability of the proposed screening biosignature. It is, however, important to remember that the proposed biosignature from this study is not influenced by HIV co-infection. Going forward, this biosignature will be validated in a cohort of participants with soil-transmitted helminth (STH) co-infections plus *M.tb* infection, specifically the roundworm *Ascaris lumbricoides* (*Ascaris*). *Ascaris* is responsible for a large proportion of STH infections in South Africa, with the national prevalence estimated to be approximately 13% from survey data collected during 2010[146]. Owing to a lack of policy guidelines, robust STH distribution statistics are widely unavailable in South Africa, especially for individual STH species, while general STH infections as a collective are more easily accessible. However, these statistics are largely based off prevalence prediction models, not raw data, and are severely outdated[146,147]. This gap in knowledge and apparent high burden in South Africa highlights the importance of investigating STH co-infections with TB, as the prevalence of these co-infections are likely very high. For this reason, Chapter 3 will further investigate STH co-infections on the accuracy and reliability of the proposed biosignature.

In conclusion, the two biomarker biosignature comprising CRP and SAA shows great promise for further development as a triage test, especially since the influence of HIV co-infection does not significantly reduce the accuracy and reliability of the biosignature. These two biomarkers are currently being investigated further in the seven biomarker biosignature mentioned previously since the combination of additional biomarkers improved the reliability of the biosignature. Of more practical importance would be the identification of A2M as a robust univariate biomarker capable of distinguishing between active

disease and latent infection. Current blood-based tools like IGRA's are capable of detecting infection, but not distinguishing between active disease and latent infection. It would, therefore, be of great value to investigate this marker further as a potential screening tool in settings where latent infection with *M.tb* is high. In such settings, the high exposure pressure drives the progression from latent infection to active TB disease, thereby providing a "reservoir" for potential active TB disease cases. As such, screening tests using biomarkers such as A2M could potentially improve the uptake of isoniazid preventative therapies (IPT). Additionally, A2M should be further investigated for potential use as a predictor of disease progression, since a blood-based read-out of A2M would be a much more feasible POC tool than the current gene-based biosignatures being developed[101,102].

CHAPTER 3

Evaluation of the potential influence of *Ascaris lumbricoides* co-infection on the accuracy of a recently identified host immune biosignature for the discrimination between individuals with active TB disease and those without *M.tb* infection.

The performance of the host serum biosignature identified in Chapter 2 (capable of discriminating between individuals with active TB disease and those without infection) has been successfully evaluated in a scenario where HIV co-infection is prevalent and where such co-infection poses the risk of influencing the biosignature performance. We have successfully reported on the biosignature stability when used in such an environment and set out to test the stability of the biosignature when faced with helminth co-infection. *Ascaris lumbricoides* (*Ascaris*) infection is of specific interest, as this roundworm infection is highly prevalent in South Africa[148]. This warrants further assessment as it is clear that the extent of helminth exposure and co-infection in Southern Africa, South Africa specifically, is considerably greater than previously expected and far outweighs the HIV prevalence statistics for South Africa[149,150]. Helminthiasis is also a serious global health concern, when considering that as much as 24% of the global population is infected with these soil-transmitted parasites that are excessively transmitted in the tropical and sub-tropical regions of the globe (this includes sub-Saharan Africa, Americas, China and East Asia)[151]. Helminth infection is a prevalent environmental influence predominantly in children and adolescents, and former studies have focused the majority of efforts on research in this population. The frequency of infection in the adult population is therefore not well documented. The major concern surrounding helminth infections is the knowledge that infections are easily controlled and/or eliminated when treated properly, but obstacles like poor sanitation and restricted access to proper healthcare in developing countries where the burden is high, fuels the transmission, re-infection and reproduction cycle of these parasites[151,152].

Ascaris lumbricoides, a species of the nematode phylum (roundworms), is a soil-transmitted helminth that has a complex life-cycle, yet one that does not employ an intermediate host. Transmission occurs through the ingestion of mature eggs from soil that has been contaminated by infected feces. After ingestion, the eggs hatch into larvae within the small intestine of the human host and penetrate the intestinal wall where they travel through the bloodstream to the lungs for further maturation. After about 2 weeks in the lungs, the matured larvae penetrate the alveolar walls to ascend the bronchial tree to reach the throat where they are swallowed to return to the small intestine. Here they develop into mature worms which continue the reproductive cycle, as displayed in Figure 3.1[153]. The key event during the life cycle of *Ascaris* is the migration of the larvae through the lungs. This event possibly allows for the direct exposure of alveolar macrophages to larval excretory/secretory (E/S) proteins and/or other *Ascaris* antigens[154]. Since alveolar macrophages are the most important responders to *M.tb* infection in the lungs, the long-term exposure of these cells to *Ascaris* larvae threaten the polarization of these macrophages to alternatively activated (M2) macrophages instead of the required classically activated

(M1) macrophages necessary for the successful clearance of *M.tb* infection[119,154,155]. The immunological consequences of helminth infection are very well known in terms of the polarization of the immune system to a T_H2 response characterized by a prevalent T_{Reg} response[155–158].

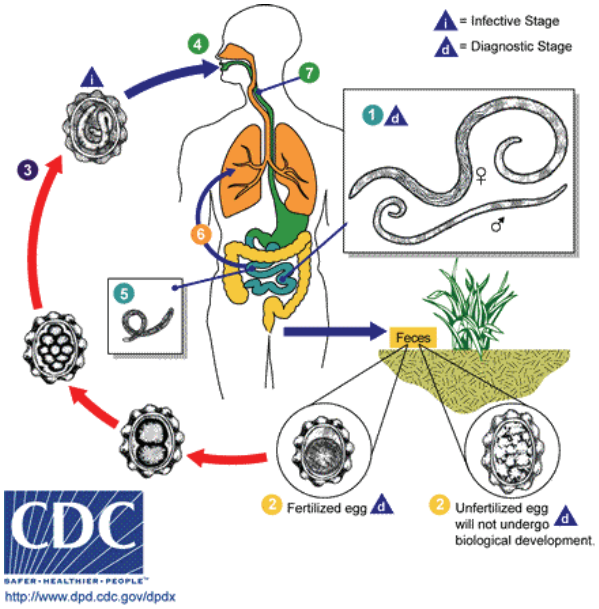

Figure 3.1: The reproductive lifecycle of Ascaris lumbricoides from the ingestion of fertilized eggs from contaminated soil, until the worms mature and themselves are able to reproduce, with specific interest in their maturation stage in the human lungs. (Image reproduced from https://www.cdc.gov/parasites/images/ascariasis/ascariasis_lifecycle.gif)

Traditionally, infection with *M.tb* requires a T_H1 immune response for successful clearance, however, studies conducted in TB-helminth co-infections have identified that the preferred polarization of the immune response during co-infection is to that of T_H2 accompanied by T_{Reg}[119,155,157]. This T_H2-skewed response has been shown to dampen the response to *M.tb* infection through the reduction of IFN-γ production, as well as an increase in production of the cytokines IL-10, IL-4, IL-5 and IL-13 which are known to dampen T_H1 responses[154]. While helminth infection remains a state of chronic inflammation without medical intervention much like *M.tb* infection, parallel treatment of intestinal helminths with albendazole during *M.tb* challenge and treatment has been documented to restore the T_H1-type response alongside a downregulation of the T_{Reg} response[157,159,160]. This eludes to a very possible restoration of the T_H1-type immune response following anthelminthic treatment in active TB and helminth co-infection, however, clinical studies investigating the relationship between anthelminthic treatment during active TB is very limited, as highlighted by Abate *et al.*[159].

The limited number of clinical investigations into this relationship are not the only contentious factors. No conclusive evidence exists in the literature about true helminth infection resolution and immune restoration owing to the heterogeneity of intestinal helminth species and the visibly unique immune responses they elicit in the host. Some studies even suggest that resolved helminth infection could result in a permanently skewed T_H2 polarized immune response, threatening the effective clearance of *M.tb* infection and possibly increasing the risk for progressing to active disease in latent infection[154,157].

In terms of the effects of helminth co-infection on bacillary load and clearance, conclusive evidence is also lacking to draw a consensus as some researchers observe no influence of helminth co-infection on bacillary load[116,161], while others report a noticeable increase in bacilli[154]. These findings suggest that these effects and/or responses could very well be a species-specific phenomenon, thereby complicating translation of TB-helminth co-infection results to the clinical setting. With that being said, *Ascaris* co-infection with TB disease is a highly understudied field of research in terms of TB-helminth co-infections, even though it is ranked as one of the three main species responsible for the majority of infection worldwide[151,162,163]. The geographical distribution of *Ascaris* infection has also been shown to largely overlap with endemic *M.tb* infections, as well as endemic HIV infections, which highlights the importance of this co-infection and its lack of understanding in our setting[163–166].

In summary, *Ascaris lumbricoides* was chosen because of (1) its high prevalence in developing countries, (2) its known direct influence on the lungs during the larval stage of its maturation, and (3) its nature to elicit a strong T_H2 response which has been shown to override the natural protective T_H1 responses required for adequate M.tb infection control. Considering that *Ascaris lumbricoides* infects the lungs and this study will use samples originating from blood one can only infer what is occuring at the site of disease from results obtained in the blood, however blood is a convenient sample for research purposes and one would expect to observe a spillover effect from the site of disease to the blood. Theoretically, what is observed in the blood is likely cells and/or secreted proteins in the process of migration from the site of infection to the lymph nodes, or the inverse – soluble factors produced in response to antigen recognition in the lymph nodes being attracted to the site of infection by chemoattractants produced there. *Ascaris lumbricoides* larvae migrate through the lungs during the maturation cycle and damage the epithelium of both the lungs and lumen (upon exit from the small intestine) which results in the release of many alarmin molecules from both sites. Therefore, *Ascaris lumbricoides* infection would result in there being many soluble factors and immune cells from both sites of infection which would make it difficult to elucidate the origin of these molecules. Compound this with active TB disease in the lungs, the profile of peripheral blood would largely consist of a combination of both T_H1 and T_H2 immune factors, but not be directly representative of the sites of infection (lungs and small intestine). Therefore, for both *Ascaris lumbricoides* infection and active TB disease we can only infer what soluble products are being produced and what immune responses are being activated at the site of disease.

The data this investigation hopes to provide is relevant and novel, and important in our immediate setting, especially considering the surprising preliminary screening results, and has the ability to shed light on a defining co-infection. The importance of co-infections in severe infectious diseases such as tuberculosis should not be underestimated and detrimental co-infection consequences swiftly addressed in order to realise our efforts of producing an effective, robust and unbiased screening test. Owing to the sample types required to complete this aim, the host immune biosignature's performance will also be assessed when applied to sample types such as QuantiFERON (QFT) plasma, and not only serum.

3.1 Study Design

Hypothesis

We hypothesise that the diagnostic accuracy of the two biomarker host serum biosignature of the biomarkers C-Reactive Protein (CRP) and Serum Amyloid A (SAA) shall not be significantly influenced by the presence of concurrent *Ascaris lumbricoides* sensitization. It shall, therefore, still be able to discriminate between individuals with and without active TB disease without detrimentally altering performance, further validating the robust nature of this novel biosignature.

Aims

The aim of this study is to investigate the potential influence of helminth co-infections on the diagnostic accuracy of the two biomarker host serum biosignature identified in Chapter 2, as it has already been validated in the context of HIV co-infections; as well as validate the use of the biosignature in predicting TB disease from a sample type (QFT plasma) other than serum.

Objectives

- Characterise *Ascaris* sensitization status on a subset of participants that were evaluated during the identification of the previous biosignature.
- Perform Luminex immune assays on the QFT plasma samples of this subset.
- Characterise the contribution of *Ascaris* co-infection influence on the biosignature identified previously.
- Assess the performance of the host immune biosignature when QFT plasma samples are used instead of serum samples alone.

3.2 Methods

3.2.1 Participant Recruitment

The pilot study that lead to the hypothesis of this chapter selected 40 participant (mixed race or black Africans) samples from the Stellenbosch University clinical field site, specifically the Fisantekraal clinical site, of the larger AE-TBC study (mentioned in Chapter 2). These were selected for the assessment of the rate of *Ascaris* sensitization in the South African Community, and the results displayed in this chapter. An additional subset of 48 participants (mixed race or black Africans) who presented with symptoms suggestive of pulmonary TB were selected from the same clinical field site mentioned above, and only the clinical samples for these participants were used for further cytokine analysis. As done in Chapter 2, participants were primarily grouped according to the harmonized classification criteria based on a combination of radiological, microbiological and clinical findings, as defined in Table 2.1 of Chapter 2.

The inclusion and exclusion criteria remained the same as for Chapter 2.

Ethical Considerations

Ethical approval was obtained from the Human Research Ethics Committee of Stellenbosch University under the ethics number: N10/08/274 for the larger AE-TBC study, under which this sub-study was also approved. This study was performed in accordance with the Helsinki Declaration.

3.2.2 Sample Preparation

For each of the 48 participants, among other study-related samples, 3ml of venous blood was drawn into an EDTA vacutainer along with 3 X 1ml into each of the QFT-Gold TB QuantiFERON (QFT) tubes (Nil, Antigen, Mitogen). The EDTA vacutainer was centrifuged following phlebotomy, plasma harvested and stored at -80°C until use. Selected aliquots were sent to the University of Cape Town for further analysis. The QFT tubes were inverted ten times after phlebotomy and incubated at 37°C for 20 hours. Following incubation, the plasma supernatant was harvested and stored at -80°C until use. These plasma supernatants were then used for Luminex immunoassays to measure the levels of cytokines produced.

3.2.3 ImmunoCAP® Specific IgE Test

In order to determine participant sensitization to helminth antigens, 1ml of plasma was submitted to the University of Cape Town for *Ascaris*-specific IgE level testing. The ImmunoCAP® Specific IgE Test (ImmunoCAP®) is the gold standard for specific IgE determination and is the most common technique employed in South Africa, especially for allergy-specific IgE testing. In short, this radioallergosorbent

test (RAST) employs the binding of fluorescently labelled anti-human immunoglobulins to specific IgE antibodies which have bound to specific antigens/allergens coupled to the cellulose solid phase of the assay. Any unbound or non-specific IgE antibodies are washed from the assay after a sufficient incubation time to allow for specific IgE-allergen binding. The fluorescently labelled immunoglobulins then emit light following excitation with a laser, and the higher the intensity of the emitted light, the higher the concentration of bound antibodies which is translated into a reading of kUA/L for experimental interpretation.

3.2.4 Luminex Immunoassay and Analysis

The levels of the two acute phase proteins of interest identified in Chapter 2, C-Reactive Protein (CRP) and Serum Amyloid A (SAA), were re-evaluated with seven other acute phase proteins, indicated in Table 3.1. All nine were evaluated using Luminex multiplex kits (Luminex, Bio Rad Laboratories, Hercules, CA, USA; MILLIPLEX®, Massachusetts, USA). QFT plasma supernatants were used for the 48 participants selected after the pilot study, from both the Nil (unstimulated) and Antigen (*M.tb*-antigen stimulated) tubes, instead of serum samples as used in Chapter 2. Plasma was selected in order to assess the response to *M.tb* stimulation in active TB and non-TB participants who are known to be sensitized to *Ascaris* compared to the response to *M.tb* stimulation in those who show no sensitization to *Ascaris*. These results were compared to the *M.tb*-stimulated response in healthy controls, who themselves had been sensitized to *Ascaris* or not. The use of QFT plasma samples instead of serum, allowed for the assessment of the stability of the candidate biosignature other sample types.

Table 3.1: Multiplex kit details for the assessment of Ascaris exposure.

Multiplex Kit:	**Bio Plex Pro Acute Phase Assay Kit (4- and 5-Plex)**	
Catalogue Number:	171-305050	
Manufacturer:	Bio Rad Laboratories	
Cytokines Assessed:	**4-Plex**	**5-Plex**
	C-Reactive Protein (CRP)	Ferritin
	Alpha-2-macroglobulin (A2M)	Fibrinogen
	Serum Amyloid P (SAP)	Serum Amyloid A (SAA)
	Haptoglobin	Procalcitonin (PCT)
		Tissue Plasminogen Activator (tPA)

Assay Preparation and Procedure

The samples, standards and controls were prepared as mentioned in Chapter 2 for the 4- and 5-Plex kits. Please refer to Chapter 2 “Methods”.

Sample Acquisition

Acquisition was performed on the Bio-Plex 200 suspension array system, using the dual-laser, flow-based microplate reader system (Bio Rad). The beads from each sample were acquired individually and analysed using the Bio-Plex Manager™ Software version 6.1 according to recommended settings.

Statistical Analysis

Statistical data analysis was performed using GraphPad Prism version 5.0 (GraphPad Software, San Diego, CA, USA), and Statistica version 12.0 (Statsoft, Ohio, USA). A p-value of < 0.05 was considered statistically significant. Univariate analysis for differences between comparison groups, e.g. TB with *Ascaris* (TBAs) and TB without *Ascaris* (TB), were evaluated using the Mann-Whitney U test for non-parametric datasets. Receiver Operating Characteristic (ROC) curve analysis assessed the diagnostic accuracy of each biomarker both when excluding and including *Ascaris* sensitization. Cut-off values derived from ROC curve analysis (taking into consideration their respective sensitivity and specificity values) show potential for use in POC triage tests in order to best discriminate between different groups of individuals. Candidate biomarkers were tested for normality using the Shapiro-Wilks normality test. Selected candidates were then assessed for diagnostic accuracy in multivariate analyses using Leave-One-Out Cross Validation (a discriminant analysis approach). ROC curve analyses were performed for the biosignature combinations. Chapter 2 employed the general discriminant analysis (GDA) training/test set approach, however, owing to the significantly smaller sample size used here in Chapter 3, this approach would result in the overestimation of the model accuracy. The Kruskal-Wallis test for nonparametric data was used to compare between infection groups. Dunn's post-test was used to correct for multiple comparisons.

3.3 Results

3.3.1 Specific IgE Tests

Plasma samples for the 48 study participants (referred to as "**Study Data**"), as well as the 40 pilot study participants (referred to as "**Collective Data**"), were sent for *Ascaris*-specific IgE testing using the ImmunoCap® assay. The ranges and their criteria are shown in Table 3.2; these criteria were used to develop a sample stratification method based upon helminth sensitization status. While the ImmunoCAP® does not diagnose **current** *Ascaris* infection, it gives an indication of **exposure** to *Ascaris* antigens; whether or not this exposure was recent is not clearly documented in literature as far as we know (please refer to the discussion for more detail).

Table 3.2: Ascaris-specific IgE ImmunoCAP® ranges and clinical significance in terms of diagnosing Ascaris sensitization.

kUA/L Measured Range:	**Sensitization Outcome:**	**Ascaris Sensitization Status:**
0.0 - 0.09	Undetectable	Negative
0.1 - 0.49	Very Low	Positive
0.5 - 1.9	Low	Positive
2.0 - 14.9	Moderate	Positive
15.0 - 49.9	High	Positive
>50.0	Very High	Positive

Of the total 88 participant samples tested, 54 (~61%; **Collective Data**) participants tested positive for *Ascaris* sensitization (exposure but not necessarily infection) (Figure 3.2). Figure 3.2 compares the collective data of all 88 participants and indicates a comparable degree of *Ascaris* sensitization rates across the South African cohort of the AE-TBC study population. Approximately 67% (32 participants; **Study Data**) of the samples used for the cytokine analysis were positive for *Ascaris* sensitization. These data highlight the clearly undefined nature of adult *Ascaris lumbricoides* sensitization in South Africa.

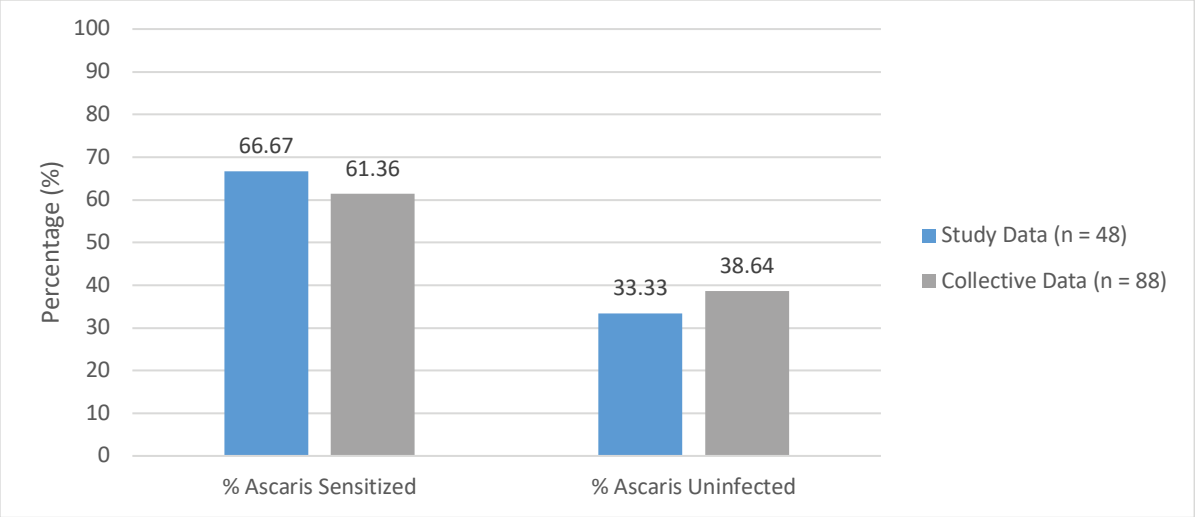

Figure 3.2: Comparison of Ascaris Sensitization Frequencies in the South African Sample Community from Fisantekraal, Western Cape (blue bars), and the Sensitization Frequencies in a subset of Multiple Sample Communities in South Africa (specifically from the AE-TBC, grey bars).

We thought it prudent to assess the distribution of *Ascaris* sensitization among male and female participants since gender-specific statistics for South African adults is currently lacking. Figure 3.3 outlines this distribution. Most notably, female participants displayed higher sensitization rates than males, with 36/54 (~67%) of the overall number of *Ascaris* **sensitized** participants being female. Similarly, 20/34 (~59%) of the overall number of *Ascaris* **uninfected** participants were female (Figure 3.3). This could well be explained by the skewed ratio of males:females which occurred purely by chance. When the data were stratified further according to *M.tb* infection status, female participants displayed higher rates of *Ascaris* infection regardless (data not shown). Owing to the small sample sizes following stratification, however, no conclusive conclusion can be drawn from this stratification.

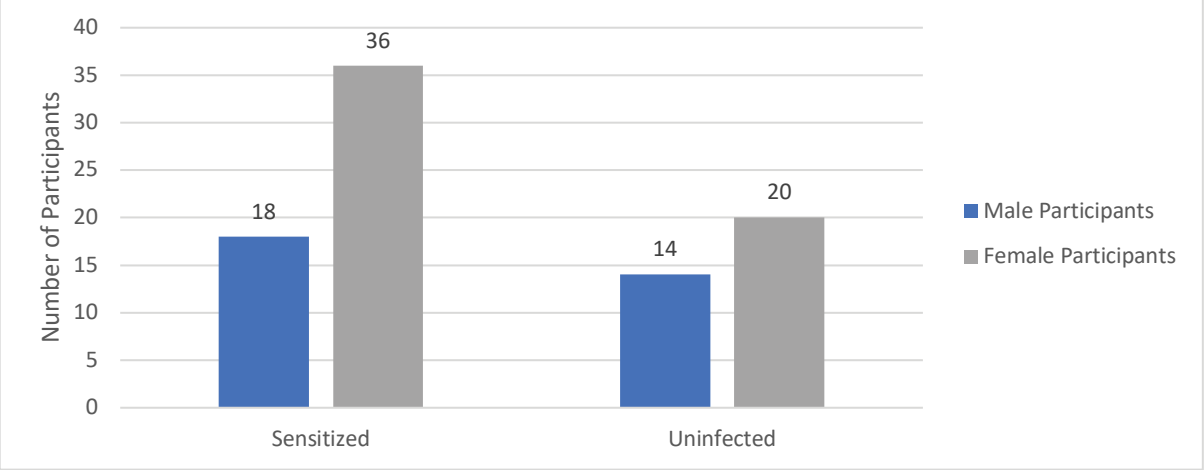

Figure 3.3: Comparison of the distribution of Ascaris sensitization in male and female participants. Female participants (grey bars) display a higher proportion of Ascaris sensitization to their male counterparts (blue bars).

Figure 3.4 expands the distribution of TB and No TB cases based on the ImmunoCAP®'s *Ascaris*-specific IgE range. In our sample population there were no "High" or "Very High" *Ascaris* IgE results,

and the majority of the participants without *M.tb* infection were uninfected with *Ascaris lumbricoides* according to the *Ascaris*-specific IgE range definition.

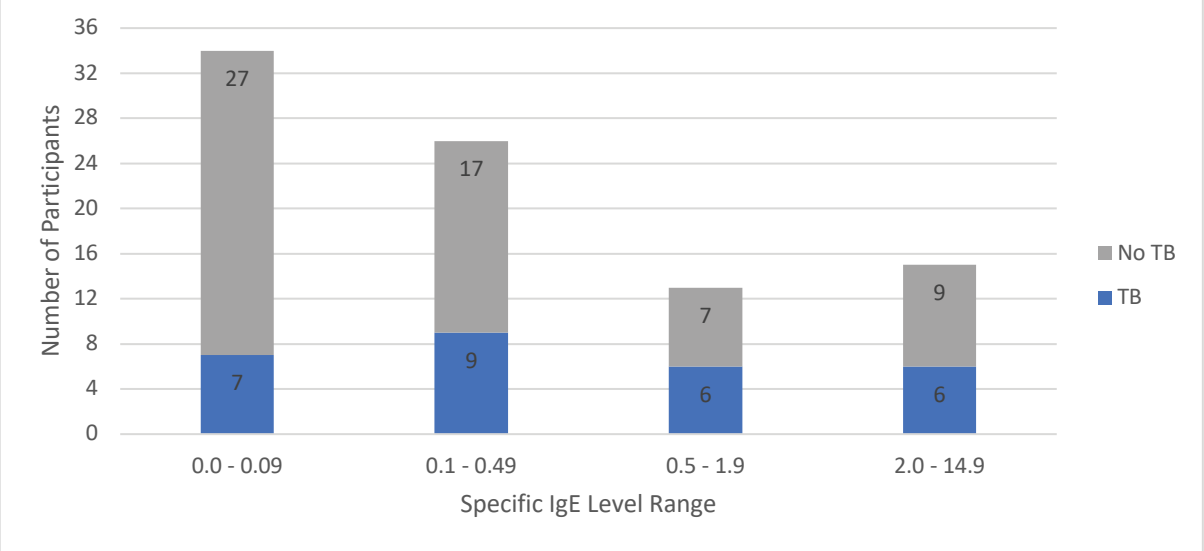

Figure 3.4: Overall Ascaris-specific IgE sensitization results stratified according to the ImmunoCAP®'s suggested ranges. M.tb infection status was taken into consideration for the stratification: blue bars represent the TB participant group while grey bars represent the No TB participant group. Total participant numbers for each group are given in the relevant section of each bar.

3.3.2 Participant Demographics

Of the total 88 participants that were tested using an IgE sensitive ELISA during the pilot study, only 48 participant samples (QFT supernatants) were selected for use in the Luminex analyses. This was due to a lack of correct sample types still available in long-term storage, as well as limited available space on the Luminex plates. The selected 48 were classified into two main groups: TB or No TB for which each group was further sub-grouped according to *Ascaris* sensitization in order to complete the main objective of characterising the contribution of *Ascaris* co-infection influence on the previously identified biosignature from the same population group. A third classification group – *Ascaris* – was created independently of the TB or No TB groups and further sub-grouped into *Ascaris* sensitized (As+) or *Ascaris* uninfected (As-) in order to investigate the differences in analyte concentrations and diagnostic accuracies of the analytes irrespective of TB infection and then to compare these to the accuracies identified in Chapter 2 of the study. Participant demographics for each of the three classification groups are given in Table 3.3 and 3.4 (complete demographics for all 88 participants, pilot and analysed sample sets combined, can be found in the Addendum (A3.1 and A3.2)). It should be reiterated from Chapter 2 that the "No TB" participants had a range of diagnoses, including acute exacerbation of chronic obstructive pulmonary disease, upper or lower respiratory tract infections or unknown conditions, but none developed active TB during the follow-up period.

Table 3.3: Classification of the Luminex analysis participants according to their TB and Ascaris infection statuses, as well as the general demographics for each classification group (this excludes those participants who were selected for the pilot sensitization rate study due to limiting factors described previously).

TB Classification Group (n = 21)				
	With *Ascaris* (n = 15) **(TBAs)**		Without *Ascaris* (n = 6) **(TB)**	
	Male:	Female:	Male:	Female:
Gender:	n = 4	n = 11	n = 2	n = 4
Median Age (Years):	35		35	
HIV Positive:	n = 0	n = 3	n = 0	n = 0
Total HIV Positive:	3		0	
Ascaris kUA/l range:	0.12 – 4.20		0.02 – 0.09	
No TB Classification Group (n = 27)				
	With *Ascaris* (n = 17) **(NoTBAs)**		Without *Ascaris* (n = 10) **(NoTB)**	
	Male:	Female:	Male:	Female:
Gender:	n = 8	n = 9	n = 6	n = 4
Median Age (Years):	36		34.5	
HIV Positive:	n = 1	n = 5	n = 0	n = 0
Total HIV Positive:	6		0	
Ascaris kUA/l range:	0.16 – 6.77		0.02 – 0.08	

Table 3.4: Classification of the Luminex analysis participants according to their Ascaris infection status alone, as well as the general demographics for each classification group (this excludes those participants who were selected for the pilot sensitization rate study due to limiting factors described previously).

***Ascaris* Classification Group (n = 48)**				
	Ascaris Positive (n = 32) **(As+)**		*Ascaris* Negative (n = 16) **(As-)**	
	Male:	Female:	Male:	Female:
Gender:	n = 12	n = 20	n = 8	n = 8
Median Age (Years):	35		35	
HIV Positive:	n = 1	n = 8	n = 0	n = 0
Total HIV Positive:	9		0	

3.3.3 Diagnostic Accuracy of Individual Markers

Coincident Ascaris sensitization is associated with an increase in the acute phase proteins CRP and SAA in active TB, while other acute phase proteins remain unaffected.

As done in Chapter 2, individual acute phase cytokines were assessed for their ability to discriminate between individuals with TB disease and those without using the Luminex immunoassay platform. The levels of nine acute phase protein concentrations were measured from both unstimulated (Nil) and antigen stimulated (Ag) QFT culture supernatants. Unstimulated values were subtracted from the antigen stimulated values to correct for background protein levels to obtain a "true" antigen response. The nil values were used for most analyses owing to their clinical relevance in this study – a clinic would readily benefit from a tool that did not need overnight processing. Ag results were used in some instances to compare *M.tb*-specific responses for a more detailed outline of immunological events. When the unstimulated (Nil) results were scrutinized, it was observed that the concentrations of CRP and SAA were increased in the TB group (TB and TBAs) compared to the No TB controls (NoTB and NoTBAs); however, when *Ascaris* co-infection was taken into consideration, the concentrations of both these proteins was significantly up regulated in *Ascaris* co-infected individuals (TBAs), while no change was observed in the No TB controls across *Ascaris* infection status (Figure 3.5(a), p = 0.059; and (b), p = 0.044). Displayed above each error bar on the graphs to follow are lower-case letters. These letters indicate the absence of statistical significance for differences in marker expression between groups when the group designation includes a common letter, i.e. when the cytokine concentrations for CRP are compared in *Ascaris* positive and negative participants with active TB disease (Figure 3.5(a)), there is no statistical significance as both groups are labeled with the letter "a". Groups that do not share a letter are statistically significantly different.

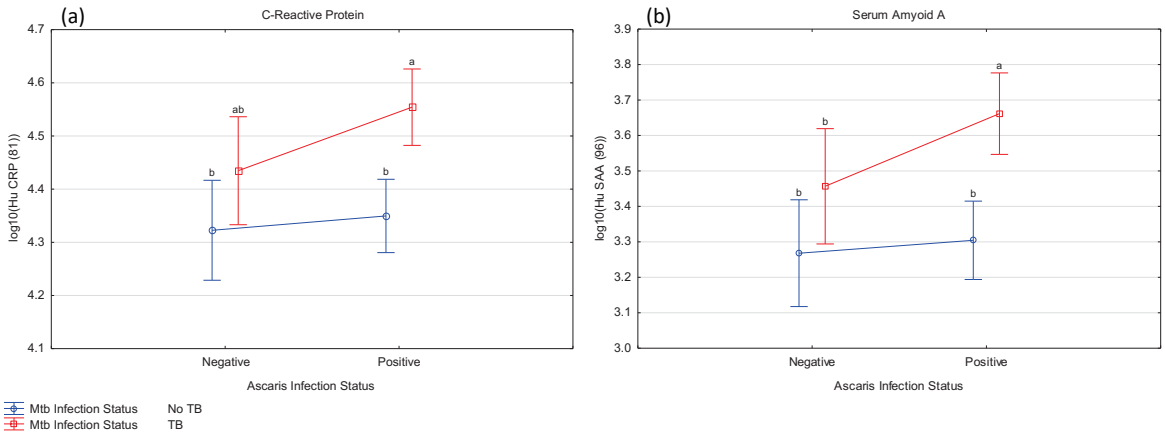

*Figure 3.5: Ascaris co-infection with TB significantly alters the circulating concentrations of CRP and SAA. Ascaris co-infection with TB significantly increases the concentrations of the proteins CRP (**a**) and SAA (**b**), while the concentrations of these proteins remain the same in both Ascaris infected and uninfected individuals when they do not have active TB. The represented data (cytokine concentrations) were log transformed and measured in ng/ml.*

Compared to Figure 3.5, Figure 3.6 demonstrates the differences between unstimulated and stimulated conditions for both CRP (Figure 3.6(a)) and SAA (Figure 3.6(b)). Here antigen stimulation resulted in a significant down regulation to that of basal control levels when stratifying according to *M.tb* infection status as well as *Ascaris* infection status (Figure 3.6(a) Nil vs Ag (TB infection status) p = 0.00036; Figure 3.6(b) Nil vs Ag (TB infection group) p = 0.0027). It is also observed that basal levels of both of these proteins remain constant in the No TB control group regardless of antigen stimulation and/or *Ascaris* and *M.tb* infection statuses. While the levels of these proteins are higher, but not significantly, in the TB group (except for the unstimulated CRP condition), there is a significant upregulation of these proteins in *Ascaris* positive individuals in the TB group compared to the *Ascaris* positive No TB group (except for CRP in the antigen stimulated group (Figure 3.6(a)). None of the other nine acute phase proteins were upregulated in this manner, and as such the data is not shown. It is, therefore, reasonable to suggest that *Ascaris* co-infection may well improve the discrimination between TB and No TB, more specifically under unstimulated conditions. Lastly, while *Ascaris* infection alone does not significantly alter SAA concentrations, *Ascaris* co-infection with TB results in significantly elevated concentrations of the proteins CRP and SAA compared to *Ascaris* only infection alone and healthy individuals without both TB or *Ascaris* infection.

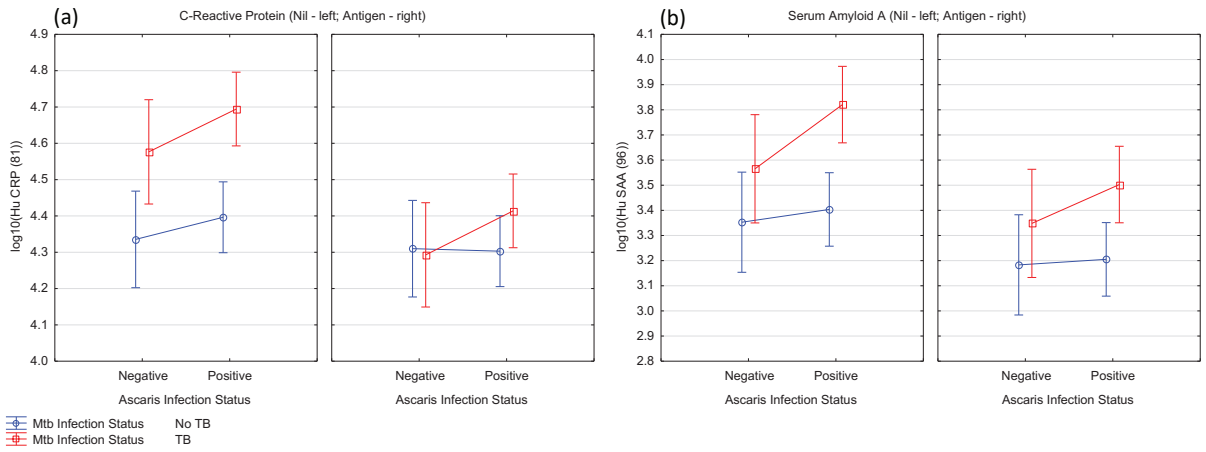

*Figure 3.6: Ascaris co-infection with TB significantly alters the circulating concentrations of CRP and SAA. Ascaris co-infection with TB significantly increases the concentrations of the proteins CRP (**a**) and SAA (**b**) when both unstimulated and stimulated with TB antigens. The represented data (cytokine concentrations) were log transformed and measured in ng/ml.*

The data was then grouped into four groups as indicated in Table 3.3, in order to compare the TBAs group to the NoTBAs group. This was done to determine the contribution of *Ascaris* infection to the changes in the biomarkers of interest in active TB versus No TB controls. Here, the "Nil" results were assessed owing to their ability to be practically applied in the clinical setting compared to the "Ag" results. One-Way ANOVA was performed to assess these differences and no significant differences were observed for the following acute phase proteins: SAP, PCT, tPA, A2M, Haptoglobin, Ferritin, and Fibrinogen, for which the data is not shown. Significant differences were, however, observed for the proteins CRP and SAA (Figure 3.7). The levels of SAA were significantly elevated in the TBAs (both TB

and *Ascaris* infection) group compared to all other groups, most significantly so compared to the NoTBAs (only *Ascaris* infection) group. While CRP levels were significantly elevated in the TBAs group compared to both groups that did not have TB, there was no significant difference between the *Ascaris* infected and uninfected TB groups. The significant increase of both biomarkers in TBAs compared to NoTBAs suggests that active TB is responsible for altering the circulating levels of inflammatory biomarkers independently of *Ascaris* co-infection.

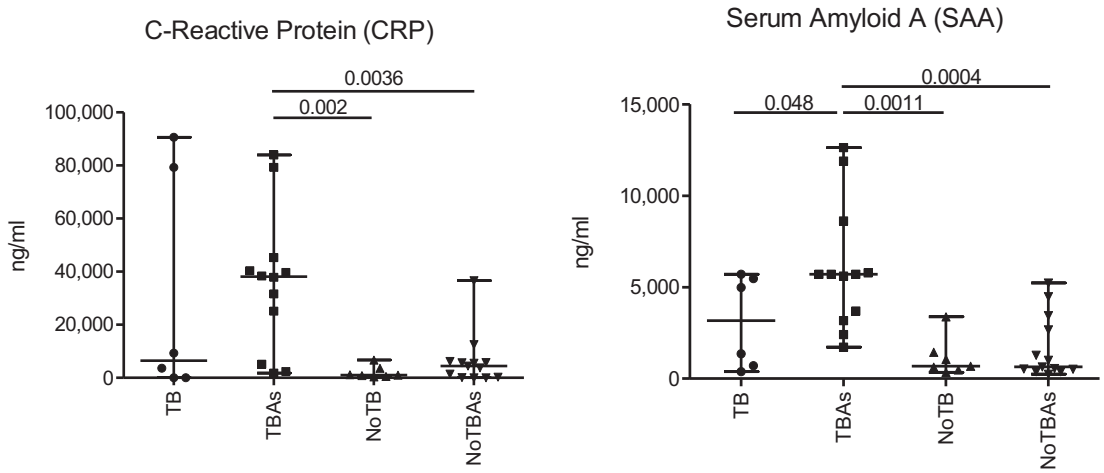

Figure 3.7: Active TB alters circulating CRP and SAA independently of Ascaris co-infection. The above graphs display one-way ANOVA results comparing the different infection groups for the acute phase proteins CRP (left) and SAA (right). TB: active TB but no Ascaris infection; TBAs: active TB with Ascaris co-infection; NoTB: no active TB disease and no Ascaris infection; NoTBAs: no active TB disease but Ascaris infection. The y-axis represents the concentration of each biomarker in ng/ml.

Individual acute phase proteins display poor diagnostic sensitivities and specificities in discriminating between TB and No TB when stratified according to Ascaris infection status.

The diagnostic accuracy of individual host markers was assessed using the unstimulated (Nil) results to determine their potential value in differentiating between individuals with active TB and those without active disease, when stratified according to their *Ascaris* infection status. Of the nine markers assessed as markers of TB infection state, all displayed no significant difference between the participants with TB and those without active disease when looking at the *Ascaris* uninfected group (Table 3.5); when looking at the *Ascaris* infected group, again none of the markers showed a significant difference (Table 3.6).

Table 3.5: Median concentrations of the nine APP as detected in participants with active TB disease only (n = 6), and participants without either disease (n = 11). (PCT, tPA and Ferritin measurements are in pg/ml, while the rest are in ng/ml).

TB vs No TB in *Ascaris* Uninfected participants					
Host Marker	**% Sensitivity (95% CI)**	**% Specificity (95% CI)**	**P-value**	**AUC (95% C.I.)**	**Optimum cut-off value**
CRP	50% (0.21-0.79)	93% (0.66-0.99)	P = 0.4106	0.60 (0.35-0.84)	≥4.37
SAA	50% (0.21-0.79)	93% (0.66-0.99)	P = 0.0719	0.71 (0.49-0.93)	≥3.44
Ferritin	42% (0.15-0.72)	86% (0.57-0.98)	P = 0.1650	0.66 (0.44-0.88)	≥5.44
Fibrinogen	67% (0.35-0.90)	71% (0.42-0.92)	P = 0.2917	0.62 (0.40-0.84)	≤7.89
tPA	33% (0.10-0.65)	79% (0.49-0.95)	P = 0.8370	0.52 (0.29-0.75)	≥4.48
PCT	17% (0.02-0.48)	93% (0.66-0.99)	P = 0.7773	0.53 (0.30-0.76)	≥4.83
SAP	42% (0.15-0.72)	86% (0.57-0.98)	P = 0.3820	0.60 (0.37-0.84)	≥4.76
Haptoglobin	75% (0.43-0.95)	64% (0.35-0.87)	P = 0.4106	0.60 (0.37-0.83)	≤8.33
A2M	25% (0.05-0.57)	93% (0.66-0.99)	P = 0.7188	0.54 (0.31-0.78)	≤6.54

Abbreviations: A2M – alpha-2-macroglobulin; CRP – C-reactive protein; SAA – serum amyloid A; TB – tuberculosis; AUC – area under the curve; C.I. – confidence interval.

Table 3.6: Median concentrations of the nine APP as detected in participants with active TB disease and Ascaris co-infection (n = 15), and participants with Ascaris infection only (n = 16). (PCT, tPA and Ferritin measurements are in pg/ml, while the rest are in ng/ml).

TB vs No TB in *Ascaris* Infected participants					
Host Marker	**% Sensitivity (95% CI)**	**% Specificity (95% CI)**	**P-value**	**AUC (95% C.I.)**	**Optimum cut-off value**
CRP	50% (0.29-0.71)	83% (0.52-0.98)	P = 0.1399	0.65 (0.45-0.86)	≥4.53
SAA	50% (0.29-0.71)	92% (0.62-0.99)	P = 0.0537	0.70 (0.53-0.87)	≥3.83
Ferritin	50% (0.29-0.71)	83% (0.52-0.98)	P = 0.3061	0.61 (0.41-0.80)	≥5.49
Fibrinogen	17% (0.05-0.37)	92% (0.62-0.99)	P = 0.7120	0.54 (0.34-0.73)	≥7.90
tPA	42% (0.22-0.63)	83% (0.52-0.98)	P = 0.5347	0.56 (0.36-0.77)	≥4.49
PCT	46% (0.26-0.67)	83% (0.52-0.98)	P = 0.2023	0.63 (0.42-0.84)	≥4.77
SAP	25% (0.10-0.47)	92% (0.62-0.99)	P = 0.9198	0.51 (0.31-0.71)	≥4.84
Haptoglobin	42% (0.22-0.63)	75% (0.43-0.95)	P = 0.7626	0.53 (0.33-0.73)	≥8.33
A2M	71% (0.49-0.87)	50% (0.21-0.79)	P = 0.7884	0.53 (0.30-0.75)	≤6.70

Abbreviations: A2M – alpha-2-macroglobulin; CRP – C-reactive protein; SAA – serum amyloid A; TB – tuberculosis; AUC – area under the curve; C.I. – confidence interval.

Following Receiver Operating Characteristic (ROC curve) analysis, each marker's AUC was evaluated for their individual diagnostic accuracies in diagnosing between active disease and No TB disease. Markers with an AUC of 0.70 and above are considered very accurate. SAA was the strongest performing maker for distinguishing between individuals with active TB disease and those without disease in both the *Ascaris* infected (As+) (Figure 3.8(a)) and uninfected groups (As-) (Figure 3.8(c)) with an area under the curve (AUC) of 0.70 (95% C.I. 0.53-0.87) and 0.71 (95% C.I. 0.49-0.93) respectively. CRP, however, did not perform as well in distinguishing between individuals with active TB disease and those without disease in both the *Ascaris* infected and uninfected groups. For CRP the AUC values were 0.65 (95% C.I. 0.45-0.86; Figure 3.8(b)) and 0.60 (95% C.I. 0.35-0.84; Figure 3.8(d)) respectively. As in Chapter 2, it was observed that the combination of the sensitivities and specificities of these markers were less than optimal when used as individual predictors of disease. For example, a biomarker with an optimal specificity but poor sensitivity would result in few TB cases being detected, even though we would be confident that they do indeed have TB.

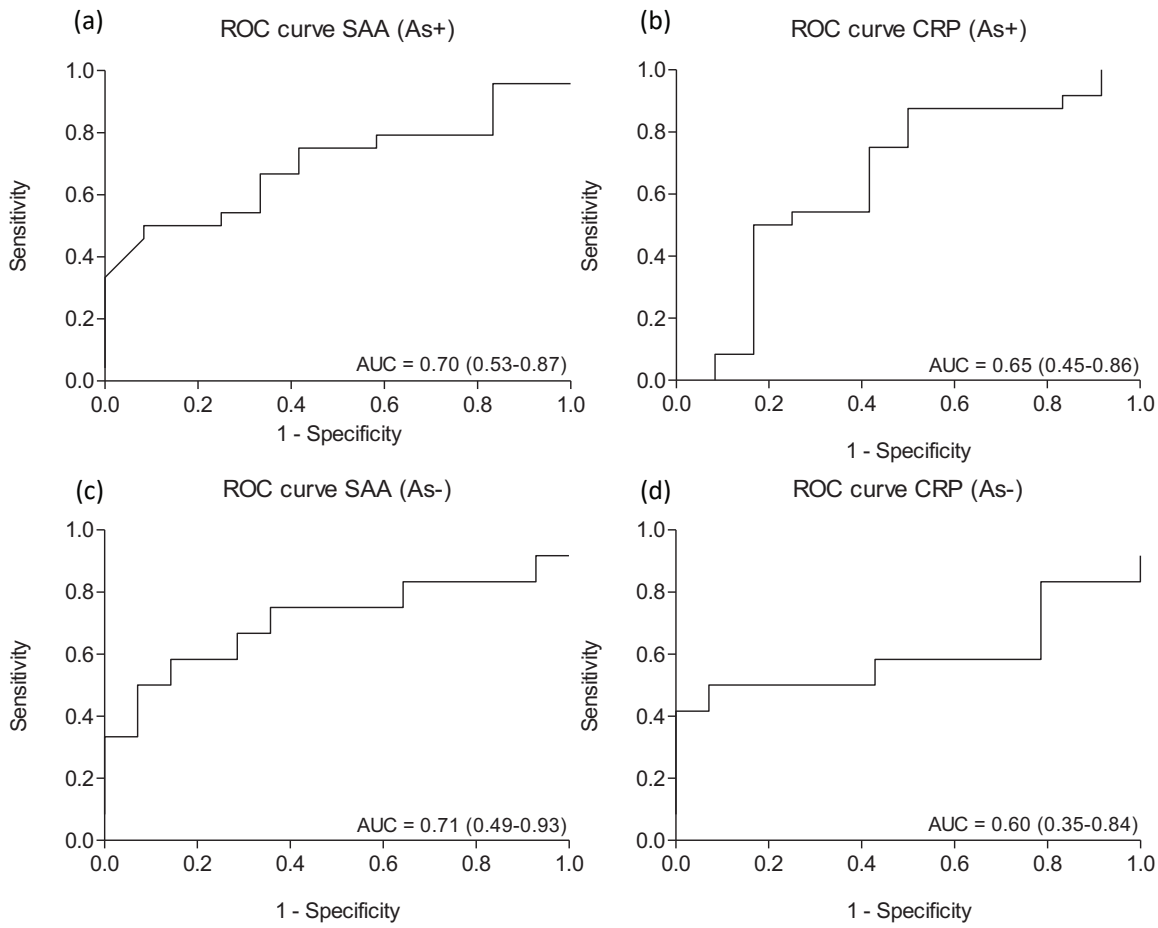

Figure 3.8: Individual biomarker diagnostic accuracies when stratified according to Ascaris infection status. ROC curve analyses of the two biomarkers of interest from our previously identified biosignature, SAA and CRP, when assessed in Ascaris infected (As+) and Ascaris uninfected (As-) individuals when assessing their ability to distinguish between persons with active TB disease and those without active disease.

3.3.4 Diagnostic Accuracy of Markers in Combination

The candidate biosignature comprising CRP and SAA may not provide as robust a screening tool as originally proposed due to less than optimal diagnostic accuracies in the proposed model.

The combinatory diagnostic ability of the nine acute phase proteins were investigated using the General Discriminant Analysis (GDA) model employing the Leave-One-Out Cross validation (LOOCV) method owing to the apparent lack of diagnostic abilities when the markers are used individually to discriminate between TB and No TB. From this, a ROC curve was generated for each biomarker combination. The LOOCV method was employed for this validation study owing to the significantly smaller sample size compared to that of Chapter 2. While employing a training (50%) and test (50%) set data partitioning approach, the LOOCV method is preferentially employed in this case owing to there not being enough data available to adequately partition the groups without losing significant modelling capabilities. While conventional validation methods, such as Random Forest prediction, partition the data into two independent sets of 50% for training and 50% for test, the LOOCV method uses multiple variations of

the 50% training and 50% test set data partitions for multiple rounds of cross-validation. Each cross-validation round simultaneously "leaves out" a single independent variable, i.e. one biomarker candidate, in order to include the variability of the model prediction without certain variables on the averaged prediction model - the results of each cross-validation round are combined to produce an average measure of fit used estimate a final predictive model. The Nil and Ag stimulation conditions were assessed separately in order to assess the effects of *M.tb*-antigen stimulation on the accuracy of the combined biomarkers. Briefly, participant QFT Nil and QFT Antigen data were independently and randomly assigned to a training and test set, regardless of *Ascaris* infection status, by the built-in Statistica algorithm.

The biosignature comprising the biomarkers CRP and SAA identified in serum samples (Chapter 2) was re-assessed for its diagnostic accuracy in the current cohort using QFT supernatants. While the previous sensitivity and specificity of this biosignature was 87.4% and 75.7% respectively, with a diagnostic accuracy of 86.6% (AUC 0.866; 95% C.I. 0.819-0.910), the diagnostic accuracy in the current cohort remained stable at 86% (AUC 0.86; 95% C.I. 0.73-0.99) in the QFT Nil condition (Figure 3.9(a)). While the specificity of the biosignature remained stable, the sensitivity declined from ~87% to ~78%. In the QFT Ag condition, however, the diagnostic accuracy dropped from ~87% to 72%, while the specificity also remained the same alongside a decline in sensitivity compared to the original biosignature data from Chapter 2 (Figure 3.9(b)). It should be noted that the Posterior P(TB) mentioned in the following ROC curves represents the optimum cut-off value for which the given AUC was extrapolated and for which the best performing sensitivity and specificity values corresponding to this. The data can be compared in Table 3.7 and 3.8.

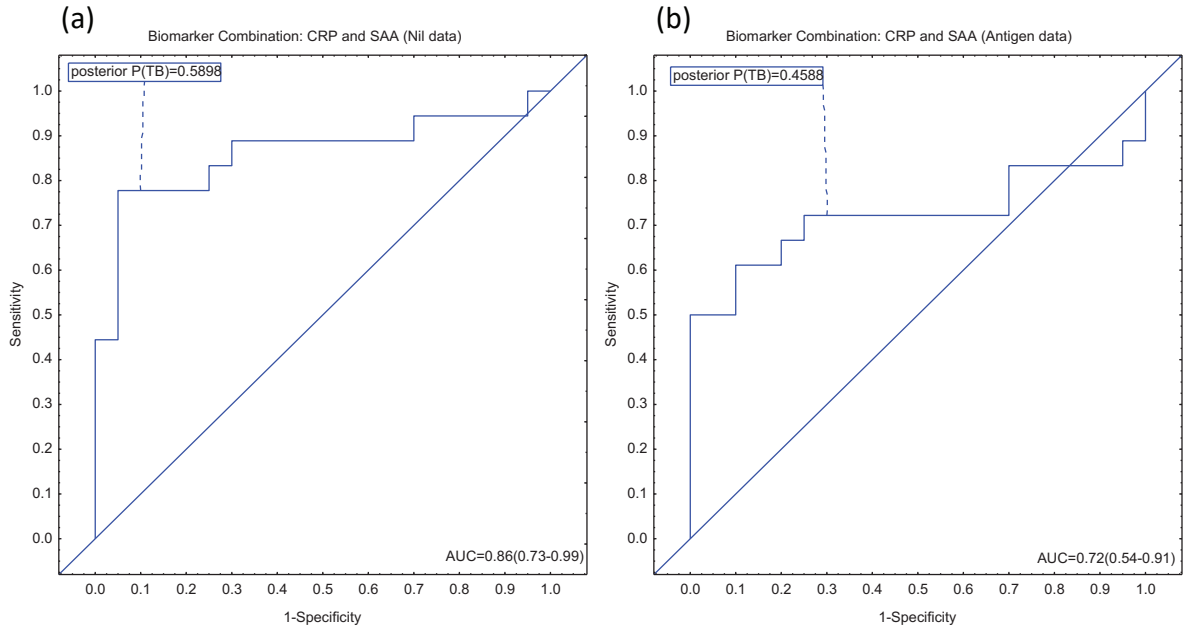

*Figure 3.9: Combination of the biomarkers CRP and SAA for the diagnosis of TB from No TB in QFT Nil and QFT Antigen conditions. Area under the curve values extrapolated from the Receiver Operating Characteristics Curve analysis for the QFT Nil (**a**) and QFT Antigen (**b**) conditions when the previously identified biosignature of CRP and SAA was used for the discrimination between TB and No TB in QFT supernatant samples.*

Interestingly, when all 9 biomarkers were assessed together as an alternative biosignature candidate, the diagnostic accuracy was improved to 94% and 88% for the QFT Nil (Figure 3.10(a)) and QFT Ag (Figure 3.10(b)) conditions respectively.

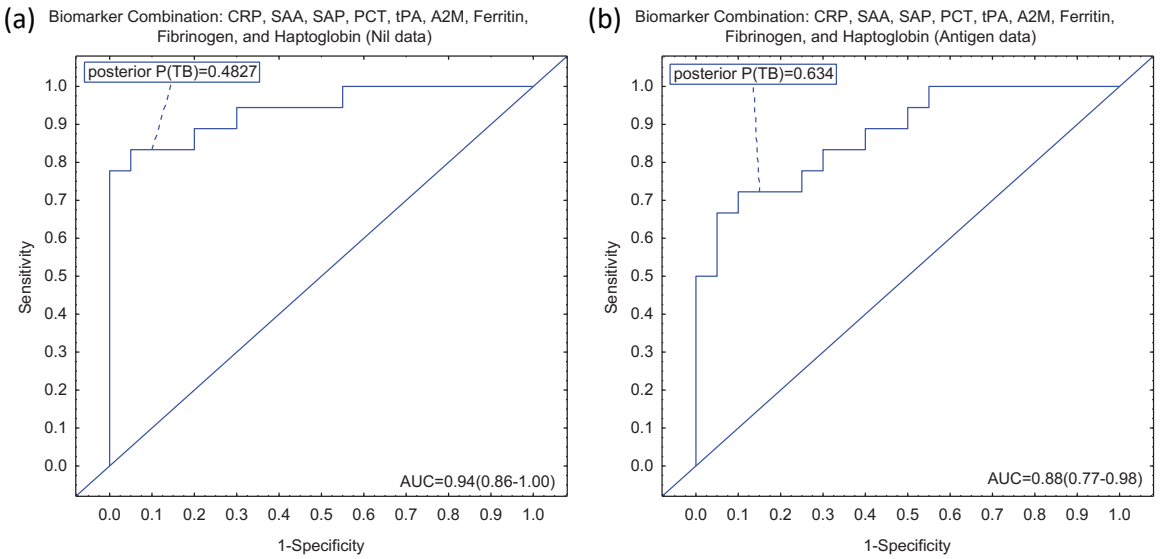

*Figure 3.10: Combination of the biomarkers CRP, SAA, SAP, PCT, tPA, A2M, Ferritin, Fibrinogen, and Haptoglobin for the diagnosis of TB from No TB in QFT Nil and QFT Antigen conditions. Area under the curve values extrapolated from the Receiver Operating Characteristics Curve analysis for the QFT Nil (**a**) and QFT Antigen (**b**) conditions when all nine biomarkers were used in combination as a biosignature for the discrimination between TB and No TB in QFT supernatant samples.*

The sensitivity and specificity achieved by this candidate when assessing the QFT Nil data alone was 83.3% and 95.0% respectively when the optimum cut-off value was chosen (Table 3.7); while for the QFT Ag data a sensitivity and specificity of 77.8% and 75.0% respectively was achieved for the optimum cut-off value (Table 3.8). Compared to Chapter 2, where the diagnostic accuracy was ~87% combining the biomarkers CRP and SAA, this finding was a great improvement. The candidate CRP/SAA biosignature, therefore, performed less effectively than when all nine biomarkers were assessed together in the QFT Nil and QFT Ag conditions, but the sensitivity and specificity of the candidate did remain stable in the *Ascaris* co-infected cohort (Table 3.8).

Table 3.7: Training/Test set statistical output of the assessed biosignature candidates for the discrimination between participants with and without active TB disease in a cohort for which Ascaris sensitization status is known. Candidate biosignature data is displayed for the unstimulated (Nil) data, as well as for the original candidate biosignature developed in Chapter 2, for ease of comparison.

Original Biosignature Candidate Developed in Chapter 2 (Serum Samples)				
CRP/SAA	**Sensitivity**	**Specificity**	**AUC**	**P(TB)**
	87.4 [78.5-93.5]	75.7 [68.8-81.8]	0.87 [0.82-0.91]	N/A
Validated and Newly Developed Biosignatures (QFT Nil Data)				
CRP/SAA	**Sensitivity**	**Specificity**	**AUC**	**P(TB)**
Training Set (n = 38)				
% (n/N)	77.8 (14/18)	75.0 (15/20)		
95% C.I. (%)	52.4-93.6	50.9-91.3		
Test Set (n = 38)				
% (n/N)	77.7 (14/18)	75.0 (15/20)	0.86	0.59
95% C.I. (%)	52.4-93.6	50.9-91.3	0.73-0.99	N/A
All 9 Biomarkers	**Sensitivity**	**Specificity**	**AUC**	**P(TB)**
Training Set (n = 38)				
% (n/N)	83.3 (15/18)	95.0 (19/20)		
95% C.I. (%)	58.6-96.4	75.1-99.9		
Test Set (n = 38)				
% (n/N)	66.7 (12/18)	75.0 (15/20)	0.94	0.4827
95% C.I. (%)	41.0-86.7	50.9-91.3	0.86-1.00	N/A
SAA/tPA/PCT	**Sensitivity**	**Specificity**	**AUC**	**P(TB)**
Training Set (n = 38)				
% (n/N)	72.2 (13/18)	80.0 (16/20)		
95% C.I. (%)	46.5-90.3	56.3-94.3		
Test Set (n = 38)				
% (n/N)	72.2 (13/18)	80.0 (16/20)	0.89	0.3079
95% C.I. (%)	46.5-90.3	56.3-94.3	0.78-1.00	N/A

Table 3.8: Training/Test set statistical output of the assessed biosignature candidates for the discrimination between participants with and without active TB disease in a cohort for which Ascaris sensitization status is known. Candidate biosignature data is displayed for the stimulated (Ag) data, as well as for the original candidate biosignature developed in Chapter 2, for ease of comparison.

Original Biosignature Candidate Developed in Chapter 2 (Serum Samples)				
CRP/SAA	**Sensitivity**	**Specificity**	**AUC**	**P(TB)**
	87.4 [78.5-93.5]	75.7 [68.8-81.8]	0.87 [0.82-0.91]	N/A
Validated and Newly Developed Biosignatures (QFT Antigen Data)				
CRP/SAA	**Sensitivity**	**Specificity**	**AUC**	**P(TB)**
Training Set (n = 38)				
% (n/N)	61.1 (11/18)	80.0 (16/20)		
95% C.I. (%)	35.7-82.7	56.3-94.3		
Test Set (n = 38)				
% (n/N)	77.7 (14/18)	75.0 (15/20)	0.72	0.4588
95% C.I. (%)	52.4-93.6	50.9-91.3	0.54-0.91	N/A
All 9 Biomarkers	**Sensitivity**	**Specificity**	**AUC**	**P(TB)**
Training Set (n = 38)				
% (n/N)	77.8 (14/18)	75.0 (15/20)		
95% C.I. (%)	52.4-93.6	50.9-91.3		
Test Set (n = 38)				
% (n/N)	72.2 (13/18)	70.0 (14/20)	0.88	0.634
95% C.I. (%)	46.5-90.3	45.7-88.1	0.77-0.98	N/A
SAA/tPA/PCT	**Sensitivity**	**Specificity**	**AUC**	**P(TB)**
Training Set (n = 38)				
% (n/N)	66.7 (12/18)	80.0 (16/20)		
95% C.I. (%)	41.0-86.7	56.3-94.3		
Test Set (n = 38)				
% (n/N)	55.6 (10/18)	80.0 (16/20)	0.79	0.4868
95% C.I. (%)	30.8-78.5	56.3-94.3	0.63-0.94	N/A

When the nine biomarkers were assessed together, it was noted that during the multivariate test for significance (Shapiro-Wilks test for normality) prior to the LOOCV, SAA and tPA were the only two that could significantly discriminate between participants with and without active disease. Here, the p-value for PCT also neared significance. For this reason, we deemed it prudent to assess SAA, tPA and PCT together using the LOOCV method as another candidate biosignature owing to the potential influence of known *Ascaris* co-infection on biosignature performance. Compared to the performance of our original candidate biosignature in this validation cohort, the combination of SAA, tPA and PCT appeared better when looking at the QFT Nil data (Table 3.7). With the combination of a sensitivity and specificity of 72.2% and 80% respectively, and a slightly higher diagnostic accuracy of 89% (AUC 0.89; 95% C.I.

0.78-1.00; Figure 3.11(a)), this candidate may be more useful for clinical application, highlighting the clear remodeling of the host immune response during known concurrent infection. It should be noted that for these markers, tPA and PCT (to a near significant extent) were only significant for their discriminatory capacity after multivariate testing and not after univariate analyses, and the differences in statistical testing methods should be taken into consideration.

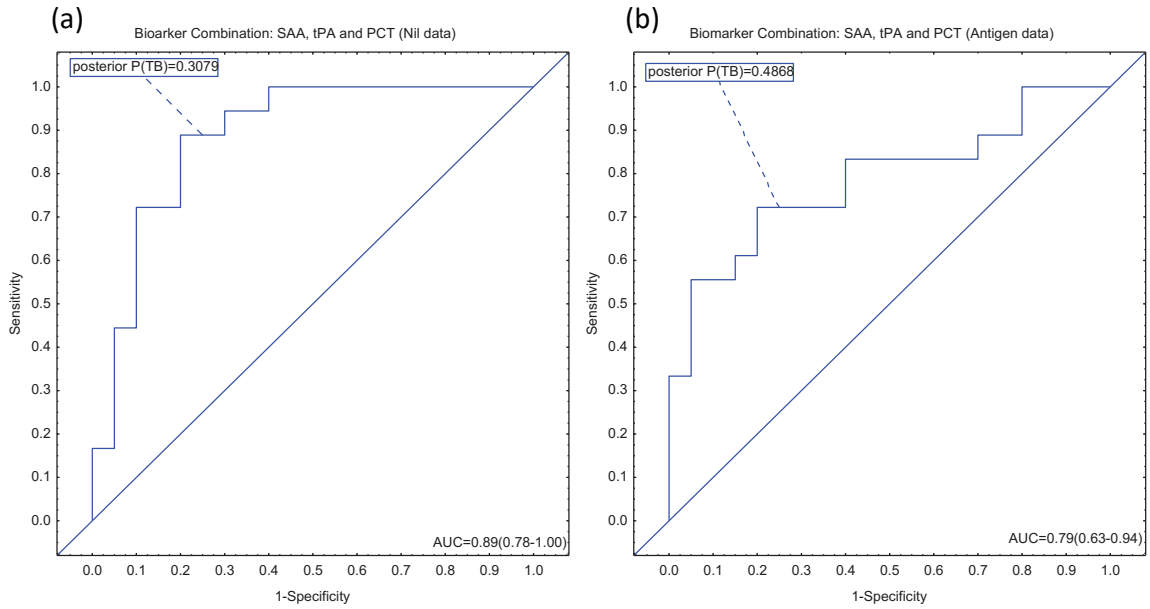

*Figure 3.11: Combination of the biomarkers SAA, tPA and PCT for the diagnosis of TB from No TB in QFT Nil and QFT Antigen conditions. Area under the curve values extrapolated from the Receiver Operating Characteristics Curve analysis for the QFT Nil (**a**) and QFT Antigen (**b**) conditions when the biomarkers SAA, tPA and PCT were used in combination as a biosignature candidate for the discrimination between TB and No TB.*

3.3.5 Influence of Ascaris co-infection on Diagnostic Accuracy

Two biomarkers, in combination, were able to distinguish between individuals with active TB disease and those without with increased diagnostic accuracy.

As previously mentioned, approximately 65% of the study population had been exposed to *Ascaris* infection. Whether or not this exposure was current or as a result of a previous infection could not be determined. It was, therefore, important to further group participants according to their state of *Ascaris* exposure. In an ideal setting with improved sample numbers, participants would have been grouped according to their level of exposure, i.e. negative or high etc. For this study, participants were grouped according to *Ascaris* sensitization status to re-assess the diagnostic accuracy of the biomarkers in an *Ascaris* co-infection setting. Participant groupings are given in Table 3.4 (*Ascaris* Classification Group). The same statistical analysis methods were employed as above in 3.3.4, and the representative diagnostic accuracies (AUC values) were compared to those identified when all participants were assessed, regardless of *Ascaris* co-infection as the mixed population would be a true representation of the clinical setting.

When the Nil stimulation condition was assessed in the *Ascaris* positive population, multivariate tests for significance identified SAA and Fibrinogen as promising candidates. The combination of these biomarkers generated a candidate biosignature that could discriminate between participants with active TB and those without active disease with a diagnostic accuracy of 96% (AUC 0.96; 95% C.I. 0.89-1.00; Figure 3.12(a)). The sensitivity and specificity results for this model were 83.3% (95% C.I. 51.5-97.7%) and 92% (95% C.I. 64.0-99.8%) respectively at the cut-off of 0.46, highlighting the improved diagnostic capabilities compared to all three biosignatures suggested above in section 3.3.4. When the Antigen stimulation condition was assessed, however, multivariate tests for significance identified SAA and tPA as promising candidates. This combination generated a candidate biosignature capable of discriminating between participants with and without active TB disease with a diagnostic accuracy of 82% (AUC 0.82; 95% C.I. 0.64-1.00; Figure 3.12(b)). Here, the sensitivity and specificities were 66.7% (95% C.I. 34.9-90.1%) and 84.6% (95% C.I. 54.6-98.1%) respectively at a cut-off of 0.52. Once again, *M.tb*-specific antigen stimulation in QFT samples proved to result in a lower diagnostic accuracy than in unstimulated samples which bodes well for clinical translation where whole blood or derivatives thereof that can be obtained within minutes without further processing or manipulation would be the ideal sample type for diagnosis.

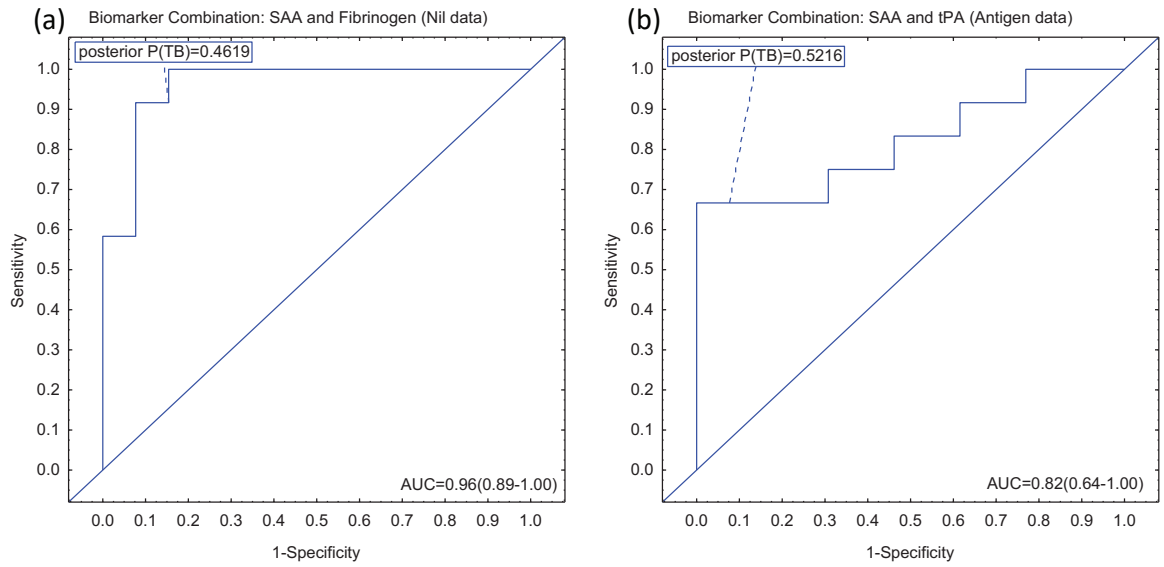

*Figure 3.12: Combinations of biomarkers assessed for the discrimination between active TB disease and No TB in Ascaris infected participants only. Displayed are area under the curve values extrapolated from the Receiver Operating Characteristics Curve analysis for the QFT Nil (**a**) and QFT Antigen (**b**) conditions. The QFT Nil condition (**a**) achieved the best diagnostic accuracy using the biomarkers SAA and Fibrinogen in combination, while the QFT Antigen condition (**b**) achieved the best accuracy using the biomarkers SAA and tPA to discriminate between TB and No TB. Posterior P(TB) is the optimum cut-off value for which the given AUC was extrapolated and for which the best performing sensitivity and specificity values corresponding to this.*

3.5 Discussion

For decades, it has been known that endemic regions of tuberculosis disease (TB) share a geographical overlap with both HIV- and intestinal helminth infection distributions[162,166–168]. The association between TB and HIV co-infections is widely researched and the consequences of concurrent infection are largely detailed. However, the association between TB and intestinal helminth infections lacks clinical research as these are difficult to conduct effectively. The importance of co-infections during disease-specific research is regularly overlooked due to obvious financial and time constraints. This highlights the potentially skewed nature of reporting research that focuses specifically on a single immunological stressor, such as TB only, without taking into consideration other confounding endemic factors. For example, a retrospective analysis of the research output on HIV, TB and STH clearly highlighted the lack of much needed research in this field, regardless of co-infection prevalence[148]. From these findings, it was observed that only 3 publications were published on PubMed between the months of July 2013 to June 2014, compared to the 74 and 447 for TB and HIV respectively. To put this data into perspective, the number of children in South Africa alone, aged 15 years or younger, who required preventative treatment for STH in the year ending 2012 was 3.2 million compared to the 39 000 and 410 000 requiring treatment for TB and HIV respectively[169–171]. While that study is limited to children, one can still appreciate the degree to which STH have been understudied not only in an endemic country such as South Africa, but also globally, underlining the importance and novelty of the work performed in this study, as well as the need to pursue this research further.

This project, therefore, aimed to build on the research performed in the first project of this thesis by considering the impact of yet another prevalent co-infection with active TB disease. Previously, the circulating levels of nine mainly pro-inflammatory acute phase proteins (APP) were investigated in serum samples from a larger clinical study that enrolled participants who presented to their primary healthcare clinic with symptoms suggestive of active TB disease. The participants used for this project were recruited in Fisantekraal, South Africa, following high infection rates found in our pilot study that used participant data from multiple South African clinical sites. In chapter 2 the aim was to identify acute phase protein signatures that could successfully discriminate between individuals with and without confirmed TB disease, with strong features as outlined by the W.H.O. Target Product Profile[127] in both HIV infected and uninfected persons. In that study we identified a biosignature combining two of the assessed APP, namely C-Reactive Protein (CRP) and Serum Amyloid A (SAA), that was able to discriminate between participants with and without active TB disease in both HIV infected and uninfected participants with a strong sensitivity (87.4%) but less than optimum specificity (75.7%). The most important outcome of that study was that the biosignature was not significantly influenced by HIV co-infection. Owing to the above-mentioned limitations, it was proposed that this biosignature be assessed for use as a point-of-care triage test at primary health care clinics as a means to highlight individuals presenting with symptoms of disease for further confirmatory tests.

While HIV is statistically and immunologically the most influential co-infection in terms of active TB disease, it is not singularly responsible for impeding efforts to control TB. Infectious diseases in resource-limited countries such as South Africa are confounded by multiple behavior and environmental factors, including poor nutrition and severe smoke exposure, such as cigarette smoke or biomass fuel smoke, as well as a variety of concurrent infections for which poor sanitation is among the top causal agent. Soil-transmitted helminth (STH) infections with *Ascaris lumbricoides (Ascaris)* are the most common STH infection among children, although accumulating evidence suggest that adult infections are severely underestimated in South Africa[151]. For this reason, the identified biosignature and the other originally assessed APP were re-assessed in the context of TB disease with *Ascaris* helminth exposure, to establish if the triage test could still be considered stable for use in helminth endemic populations, as was done for HIV infected populations. Even though the original biosignature was established from a region with known high helminth exposure rates, no information on helminth infection/exposure status was available for this cohort. This information was only available after retrospective testing in a pilot study which then lead to the initiation of this study in which participants from the same cohort were used for the validation, except their *Ascaris* infection status was now known.

The biosignature comprising of CRP and SAA displayed an overall stability in both diagnostic discriminatory capacity (AUC 0.86 compared to AUC 0.87) and specificity (75% compared to 75.7%), but not sensitivity (78% compared to 87.4%) when assessed in the unstimulated QFT plasma samples used for this study. This could be as a result of a smaller sample size compared to the original biosignature assessment in Chapter 2 where 710 participants were classified according to the harmonized classification algorithm, instead of the 48 participants assessed in this sub-study; this could also be attributed to the different sample type used in Chapter 3 compared to Chapter 2 for the cytokine analyses. Studies have demonstrated a difference in sample type stability, specifically between serum and plasma, where plasma samples display better stability in terms of reproducibility than serum; although, this finding identified a double-edged sword in that while plasma samples were more stable, serum samples displayed significantly higher concentrations of various metabolites[172].

Alternative biomarker combinations were also assessed in this study, including the combination of all nine APP as well as the combination of SAA, Procalcitonin (PCT) and Tissue Plasminogen Activator (tPA) after these three proteins were shown to be significantly different between the TB and No TB groups following multivariate tests of significance. These two biosignatures performed much better than the original biosignature in the unstimulated QFT plasma samples (AUC 0.94 and AUC 0.89 respectively) in terms of their discriminatory capacity between participants with and without active TB disease. Care should be taken to consider multiple environmental variables when developing diagnostic tools for TB such as we are trying to achieve here. For instance, in the particular community from which our participants were recruited, we expect to see an even higher infection rate particularly amongst the children as they are at higher risk of STH infections. This would be an important consideration for similar diagnostic tests in children, and the consequences thereof need to be investigated and validated properly before such a diagnostic test could be developed further for clinical use.

The previously identified two-marker biosignature developed in a population from multiple geographic sites displayed improved diagnostic accuracy in the South African sample set, but two alternative biosignatures were identified as better performing due to the alternative sample type tested.

As seen in Chapter 2, using univariate parameters for the development of robust and stable diagnostic tools are not suitable for achieving both exceptional sensitivities and specificities in combination. Multiple parameters, or biomarkers in this case, were once again the preferred option for the development of a diagnostic tool.

In order to assess the diagnostic accuracy of the nine APP in the South African samples co-infected with *Ascaris,* the general discriminant analysis Leave-One-Out Cross Validation method was employed owing to the smaller sample size compared to Chapter 2. The original biosignature made up of CRP and SAA displayed a stable diagnostic accuracy that resulted in the accurate discrimination of TB disease from No TB cases 86% of the time (AUC 0.86, 95% C.I. 0.73-0.99), as well as a stable specificity of 75% instead of 75.7% which was very promising. These improvements could have been attributed to the different sample types used between the two sample types for cytokine analysis, i.e. serum (Chapter 2) vs QFT plasma (Chapter 3), as alluded to in the introduction of this discussion. We did, however, assess other biomarker combinations which resulted in the identification of two other biosignatures that performed much better than the original. The first was a combination of three significantly different biomarkers following multivariate tests of significance using the Shapiro-Wilks test for normality: SAA, tPA and PCT. This combination achieved a diagnostic accuracy of 89% (AUC 0.89, 95% C.I. 0.79-1.00) with a sensitivity and specificity of 89% and 90% respectively. This result is already extremely close to the WHO TPP proposal for TB diagnostic tools[127]. The second biosignature was a combination of all nine APP: CRP, SAA, tPA, PCT, Ferritin, Fibrinogen, Haptoglobin, alpha-2-macroglobulin, and serum amyloid P (SAP). This combination achieved a diagnostic accuracy of 94% (AUC 0.94, 95% C.I. 0.86-1.00) with a sensitivity and specificity of 83% and 95% respectively. While the proposed specificity for the WHO TPP is 98%, a diagnostic accuracy of 94% and concurrent 95% specificity, as seen in our study, is remarkable, especially considering the assessed biomarkers are non-specific biomarkers of active TB disease. We therefore propose the incorporation of these nine biomarkers into a biosignature, along with others still currently being investigated[161,173–177], for the accurate diagnosis of active TB disease in populations with high endemic rates of both TB and intestinal helminth (*Ascaris lumbricoides*) infection in order to achieve the end goal of developing a diagnostic tool that fits the ideals of the WHO TPP in full.

As previously mentioned, Chegou *et al*.[125] developed a seven-biomarker biosignature consisting of the biomarkers CRP, SAA, inducible protein (IP)-10, interferon gamma (IFN-γ), complement factor H (CFH), apolipoprotein-A1 (Apo-A1), and transthyretin, which achieved a diagnostic accuracy of 91% (AUC 0.91, 95% C.I. 0.88-0.94) with a sensitivity of 93.8% (95% C.I. 0.84-0.98) and specificity of 73.3% (95% C.I. 0.65-0.80). This biosignature was capable of discriminating between individuals with and without active TB disease, irrespective of their HIV status, and is currently being assessed as a lateral flow test

for use as a point-of-care triage test. It should be noted that this study population was significantly larger than our own, and as such better powered for the development of a robust diagnostic tool. This does not negate the performance of our findings, however, as the scientific question for the previous study did not include the effect of STH comorbidities on the diagnostic accuracy of the biosignature. While all nine biomarkers from my study were indeed previously assessed in serum samples by Chegou *et al.*, only CRP and SAA were included in the seven-biomarker biosignature, suggesting that the remaining biomarkers assessed in my study may not be suited to a population in which *Ascaris* co-infection is not considered. It would be beneficial to validate these biomarkers in a demographically diverse and large cohort such as the AE-TBC study, specifically when *Ascaris* co-infection status is known, to further understand the impact such a co-infection has on the accuracy of TB diagnosis, since most diagnostic biomarkers are being researched and developed in countries known for high STH infection burdens. Unfortunately, this was outside of the scope of this project, but should be considered for future studies.

Antigen-stimulated samples display reduced acute phase cytokine production in comparison to unstimulated samples in both *M.tb* infected and uninfected individuals.

While not practical for clinical applications, the effects of antigen-stimulated QFT plasma compared to unstimulated plasma was still a valuable comparison to perform. From our findings, antigen-stimulated QFT plasma samples displayed reduced acute phase cytokine production compared to the unstimulated samples, suggesting a questionable use of these biomarkers in the development of diagnostic tests where co-infections with STH are concerned. *M.tb*-stimulated samples, however, would not be ideal for a point-of-care triage test as they would require longer processing. It is speculated that the antigen-stimulated condition did not discriminate as well as the unstimulated condition because the cytokine levels under unstimulated conditions were already so high that additional stimulation did not result in much more of a response. In addition to this, some cytokines suppress other cytokines present in the supernatant which we would in any case not pick up following further antigen stimulation.

The traditional 3-tube QFT-Gold TB test was used for all study samples. The antigens used to line the inner tube for stimulation are ESAT-6, CFP-10 and TB7.7, and are all *M.tb*-specific. These antigens largely stimulate $CD4^+$ T cell responses specific for *M.tb*, and while understanding the adaptive immune response to *M.tb* is still of utmost importance in the field of research, here we are mostly interested in the host's innate immune response to *M.tb*. Our findings display a downregulation of acute phase proteins related to the innate immune response (the significance of both CRP and SAA in TB disease has been discussed in Chapter 2) during challenge with the aforementioned *M.tb*-specific antigens. This downregulation we observed to be non-specific for both *M.tb* and *Ascaris* infection statuses. We also see that the concentrations of these proteins (CRP and SAA) are downregulated to the levels observed under basal conditions. We speculate that the reason for this *M.tb* suppression of acute phase proteins is possibly one, or a combination, of two options: 1) as a result of the induction of immunosuppressive immune populations; 2) as a result of an already primed immune response, either as a result of *M.tb* or *Ascaris* infection, that results in the over activation and subsequent exhaustion of immune cells that produce acute phase cytokines, albeit in *in vitro* conditions; and finally 3) due to the inhibition of some

cytokines by one or more of the cytokines induced by *M.tb* antigen stimulation, i.e. IL-1β. Unfortunately, owing to the scope of this project being largely for validation purposes, it did not include any functional investigative work for the investigation of these two options. Based on recent literature, however, we speculate that the presence of an innate immunosuppressive population during *M.tb* infection may be responsible. This cell population, known as myeloid-derived suppressor cells (MDSC), is a highly heterogeneous population of innate myeloid cells that have been shown to expand during chronic infections such *M.tb* infection, but most commonly in cancer, for which the majority of literature is based. MDSC have been shown to result in the suppression of the host response to *M.tb* specifically through the inhibition of the T cell response responsible for successful control of the pathogen[178] which may well be exacerbated by the relationship between helminths and MDSC. Literature highlights an expansion of MDSC during helminth infections (reviewed in Ginderachter *et al*.[179]) for which the different MDSC subsets appear to have opposite functions, e.g. the monocytic subset suppress antitumor immune responses while the granulocytic subset instead enhanced the clearance of helminths[180,181]. Although not the scope of this current project, this population will be discussed in the following chapters.

Our findings do, however, suggest that the use of QFT antigen stimulated samples for discriminating between individuals with and without active TB disease, using the analytes measured, may not be ideal, both logistically and performance-wise. Many studies have been conducted on the use of antigen stimulated samples, both QFT and other antigens, for TB diagnosis. However, no clear consensus can be reached for which combination of biomarkers should be used. The use of these methods have already been well reviewed by Chegou *et al*.[57,182]. The concluding remarks for the use of antigen stimulated samples for the diagnosis of TB is that it remains questionable whether or not these biomarkers will be effective enough, and obvious limitations already prevent the further development of these biomarkers. The use of antigen stimulation using antigens other than those found in QFT indeed show more promise, but still lack the effective translation into clinical management owing to the time consuming nature of performing these assays[73]. This is owing to the well-known fact that the QFT platform cannot discriminate between active disease and latent infection. Overall, our study found that the use of antigen stimulated samples did not improve the sensitivity and/or specificity of any of the biosignatures compared to the use of unstimulated samples.

Infection with *Ascaris lumbricoides* displays higher prevalence in female participants compared to men, irrespective of active TB disease.

During preliminary demographic investigations of our study sample, a skewed prevalence of *Ascaris* infection was observed in female participants compared to men. Observing a ratio of 2:1 (female to male), we speculated that sex may be a confounding factor during *Ascaris* infection, leading to an increased susceptibility in women to establish an infection upon exposure to this specie of STH. Upon further investigation using literature, we identified confounding prevalence results stratified according to sex. This was based on multiple factors, including inconsistent STH specie investigations, the lack of infection stratification according to sex, inconsistent reporting methods (i.e. infection based on one or the other STH, other than *Ascaris*), differences in geographic locations, and differences in study

population demographics such as age group, to name a few[157,183–186]. These factors are common in STH research, impeding the ability to translate findings and save on research costs. Regardless of this, further literature investigation identified a single publication that assessed the relationship between *Ascaris lumbricoides* and multiple environmental and socio-economic variables such as sex[187]. While many environmental variables and some socio-economic variables were established as being associated with *Ascaris* infection, there was no association between sex and *Ascaris* infection (Odds Ratio 1.09; p-value 0.389). It is, however, possible to suggest that women in high burden regions are more likely to come into contact with helminth sources, for example contaminated water and/or children who often play in contaminated soil, and the potential for a sex-related association for *Ascaris* infection should not be wholly disregarded.

Concurrent infection with *Ascaris* does not alter the diagnostic efficacy of the identified biosignatures on unstimulated QFT samples.

While most commonly responsible for malnourishment and impaired cognitive development in young school-going children, some helminth infections are known to be associated with reduced incidence of allergy development, especially in helminth endemic regions[188]. This phenomenon, however, appears to be species-dependent as this is frequently seen in hookworm infections, but during *Ascaris* infections allergy is rather increased, supposedly due to the cross-reactivity between *Ascaris* worm proteins and highly homologous proteins found in daily environmental allergens such as dust-mites[188,189]. Most importantly, however, helminth infections heavily modulate host protective immune responses, and the helminth-induced skewing of anti-TB T_H1 effector mechanisms to that of a predominantly T_H2 effector response has been reviewed previously[116,119,154]. This widely accepted shift in host response during co-infection threatens the outcome of multiple studies performed in highly endemic regions for both infections as the findings may be severely compromised where co-infection has not been taken into consideration. Most studies that do consider co-infection mainly focus on *Strongyloides stercoralis* (Ss), a threadworm member of the nematode class of helminths. While closely related to *Ascaris lumbricoides*, Ss infections have displayed the inverse response compared to this study, which itself is the first of our knowledge to investigate *Ascaris* in the context of TB co-infection. George *et al*.[161] measured the changes in acute phase protein concentrations in active TB individuals co-infected with Ss, and compared them to control groups. The acute phase proteins assessed here included our proteins of interest, namely CRP and SAA, along with others such as alpha-2-macroglobulin, and haptoglobin. They observed an overall downregulation of CRP and SAA in active TB individuals co-infected with Ss, whereas our study observed an increase. Literature has shown that SAA concentrations increase during active TB disease, acts as an indicator of inflammation, and resolves over the course of treatment[135]. The contrast between SAA concentrations in active TB disease and STH infection could well be explained by the different immune responses initiated to clear the two different infections. The T_H1-type response employed by the host to clear *M.tb* infection relies on the generation of an inflammatory environment to clear the bacteria, of which SAA is an important component; while the T_H2-type response employed to clear STH infections are mostly anti-inflammatory and would thus suppress the production of SAA considering its innately a pro-inflammatory function.

This increase of SAA seen in our study in the presence of STH co-infection suggests that there may still be a significant measure of host control in terms of *M.tb* infection and that host responses to STH infections don't completely suppress T_H1 responses. This inference of the data may very well not be the case. It may be that immune response types are not responsible for this finding, but rather the different STH species investigated (for example *Ascaris lumbricoides* vs *Strongyloides stercoralis*). This highlights the need to consider species-dependent mechanisms of immune modulation during studies of this nature, and also highlights the clear gap in STH research, both immunologically and physiologically.

As seen in our study, coincident helminth infection alters protein concentrations only in active TB participants following *M.tb* antigen stimulation, but not in participants without active disease who are still infected with helminths. This indicates a cumulative effect and suggest that helminth modulation of host inflammatory marker concentrations is likely dependent on concurrent active TB disease, a finding also reported elsewhere[161]. This is an important factor to consider going forward with TB research in highly endemic countries. From these preliminary results, chronic *Ascaris* infection may very well compromise host protective responses to *M.tb* infection, especially in geographically overlapping endemic countries such as South Africa. It is especially important to consider the effects of *Ascaris* co-infection may have on the efficacy of TB vaccines and vaccine development. The gold standard BCG vaccine displays wide geographic variation in terms of efficacy, with the reduced protection observed in African and Asian countries where intestinal helminth infections are highly prevalent. The high geographical overlap between infections is thought to be responsible in part for the reduced efficacy of BCG, as evidence shows TB co-infection with helminths results in significantly reduced IFN-γ production and functional impairment of T cells, which is important for the successful response to BCG vaccination[190]. Evidence has also shown that exposure to helminthic antigens in the womb and/or shortly after birth, severely impairs the efficacy of BCG and enhances neonate susceptibility to subsequent helminthic infections[191,192]. It should be noted, however, that the few studies that have indeed been performed in helminth-TB co-infection display varied, confounding results which could likely be as a result of important study design differences. This extends to the research performed on neonate responses to BCG vaccination following pre-natal exposure where current evidence is very contradictory. Such design differences may include the use of 1) different helminths, 2) the use of different helminth antigen sources, e.g. eggs, E/S products, or surface antigens, and 3) the naturally varied intensities of helminth infection found in the study sample populations[154]. This itself is a limitation for the study as no clinical data were available on the egg burden in the stool, or whether or not the participants were taking antihelminth treatment at the time of enrolment or prior to enrolment. Another important factor to consider is the lack of evidence supporting a singular helminthic infection in our study population, as polyparasitic helminth infection is not uncommon, especially in highly endemic regions, and one such example is *Ascaris lumbricoides* infection concurrently with *Trichuris trichiura*[116,119,156].

The most important finding of this study is the finding that the probability of accurately diagnosing active TB disease in an *Ascaris* sensitized population is increased when using a biosignature that combines

SAA and Fibrinogen compared to the original biosignature made up of CRP and SAA. This likely translates to *Ascaris* co-infection with active TB not detrimentally affecting the diagnosis thereof, but rather improving it somewhat. This finding does, however, deviate from our main hypothesis of validating the original CRP/SAA biosignature. Considering that the strongest performing biosignature identified (CRP, SAA, SAP, tPA, Haptoglobin, A2M, Ferritin, Fibrinogen, and PCT) in this study contains both of the biomarkers found in the above biosignature (SAA and Fibrinogen), we can deduce that these two biomarkers may well contribute to the majority of the predictive capability of the 9 biomarker biosignature. The reduced diagnostic accuracy, sensitivity and specificity observed for this biosignature compared to that of SAA and Fibrinogen may be explained by the interaction effects of the other biomarkers in the context of *Ascaris* unexposed individuals. The results of this study should therefore be validated in a larger cohort of co-infected individuals to confirm that our 9 biomarker biosignature is not detrimentally affected by the presence of *Ascaris* co-infection when attempting to accurately discriminate between individuals with and without active TB disease. While our original biosignature performance, consisting of CRP and SAA, remained stable in a helminth exposed cohort compared to the HIV stratified cohort used in Chapter 2, we are confident that the use of these two biomarkers in future TB co-infection biomarker studies with *Ascaris* will prove desirable for the development of a robust diagnostic biosignature for the discrimination between individuals with and without active TB disease in high burden, high comorbidity settings. The inclusion of Fibrinogen has also proven to be of value specifically in *Ascaris* exposed individuals.

Limitations

A major limitation was that the influence of HIV co-infection could not be assessed in the context of helminth-TB co-infection due to small participant numbers. While the influence of HIV co-infection with TB alone is well characterized, fewer publications outline the relationship between HIV and helminth co-infection in general. It is known that the geographical overlap between endemic TB, HIV and helminth regions is extensive and it is also known that individuals with HIV are more susceptible to active TB disease in high burden settings. With this knowledge, along with the emerging knowledge that soil-transmitted helminth infections impede the host response to active TB, it would be important to study these concomitant diseases and their interactions more effectively. The demographics of our sample population highlighted this need in the high occurrence of *Ascaris* and HIV infected participants compared to participants who were simply infected with *Ascaris*. Previous work has shown that *Ascaris* infection does result in increased susceptibility to HIV in high burden areas, with the T_H2 skewed response resulting in the increased expression of HIV co-receptors, increased rate of disease progression, heightened plasma viral load, and an altered immune activation profile[166,193]. however, owing to the limiting sample size we had available for the study, this relationship could not be assessed.

We believe it is important to discuss the limitation of current diagnostic tests for, not only *Ascaris lumbricoides* infection, but STH infection in general. Based on resources available for this study and the gold standard employed in South Africa, circulating levels of *Ascaris*-specific IgE using the ImmunoCAP® were determined for each participant as a measure of *Ascaris lumbricoides* sensitization.

This test is unable to distinctly discriminate between current infection and/or recent infection specifically of *Ascaris*, and thus limits this study to employing a range of circulating IgE levels for the rough diagnosis of infection. Since it is unknown at what point circulating IgE levels drop following anthelminthic treatment, we performed an interrogation into the half-life of circulating *Ascaris*-specific IgE in literature which fell short. A study performed by Cooper *et al*.[156] in 2008 on a cohort of school children assessed the effect of anthelminthic treatment on circulating IgE over a 12-month period. They identified a discrepancy between the reduction in IgE levels, since one would expect these levels to return to normal following successful anthelminthic treatment and clearance of the parasite. In some instances, IgE levels did indeed return to normal following periodic anthelminthic treatment, however, Cooper *et al*. found that in most instances IgE levels did not return to normal. They attributed these findings to a possibility of four factors, namely: (1) continued exposure in a high burden setting, (2) genetic predisposition to elevated IgE levels, (3) pre-natal exposure leading to long-term reprogramming of the immune system to a T_H2-type response – as reviewed in Chatterjee *et al*.[116], and/or (4) various other T_H2-type response skewing environmental exposures. Studies preceding the former have themselves reported elevated IgE levels 2-3 years after successful anthelminthic treatment[194,195], and others have even identified elevated IgE levels that took at least 10 years to return to normal in migrants from high burden settings that settle in low burden settings and do not experience continued exposure[196]. While these discrepancies in literature have been credited to multiple factors such as differences in study populations, effectiveness of treatment, and continued environmental exposure, more research needs to be focused on conducting reproducible studies to understand the physiological roles of circulating IgE before, during and after anthelminthic treatment.

Lastly, this study made use of QFT plasma samples instead of serum as was originally used in Chapter 2. As mentioned previously, this sample type was selected owing to the lack of complete sample sets for which serum samples were available in the *Ascaris* IgE tested participants. It is encouraging, on the one hand, that the CRP/SAA biosignature is stable in an alternative sample type like unstimulated (QFT Nil) QFT plasma, however the use of QFT plasma which has been incubated overnight at 37°C is not practical in a clinical setting. Future studies should aim to compare plasma samples with QFT plasma samples (unstimulated) in order to determine whether one could replace the other for more practical purposes. Should this prove fruitful, it would be advantageous to develop a screening tool which is stable and reliable in both serum and plasma samples as clinics would not be limited to a single specimen type and could make use of more opportunistic samples.

Concluding Remarks

This study has successfully validated the use of a previously identified TB diagnostic biosignature, combining the acute phase protein biomarkers CRP and SAA, in a region with a high *Ascaris lumbricoides* burden. This study also validated the use of an alternative sample type other than that used to develop the original biosignature, namely QFT plasma supernatants instead of serum. This is important for clinical applications should unstimulated QFT plasma prove as effective as regular plasma following further investigations. Many studies have collected QFT supernatants and stored specimens

might represent a valuable sample type for future studies. In addition, this study highlighted the high prevalence of sensitization to *Ascaris lumbricoides* antigens, likely for the first time in an adult population from South Africa. South Africa frequently experiences shortfalls in the investigation and reporting of STH infections in the adult population since children have traditionally been the most high-risk demographic group. This is evident by the lack of concise species-specific testing methods available to diagnose current infections rather than previous infections which have caused an immunological sensitization to species-specific antigens. In addition, species crossover is not taken into consideration for the tests that are currently available for commercial use. It is clear that South Africa is faced with a second co-infection that has the potential to hamper anti-TB therapeutic strategies and/or increase susceptibility to mycobacterial infection. Considering the immunological alterations both HIV and STH induce during active TB disease, more frequently on the innate immune system, more research should focus on the primary immune responses to *M.tb* infection in order to elucidate the protective mechanisms in place that we have not yet been successful in doing.

3.6 Addendum

Participant demographics for all 88 participants from both the Luminex analysis and pilot study cohort, from which the preliminary *Ascaris* sensitization data was generated.

Table A3.1: Classification of all study participants (including the pilot study participants) according to their TB and Ascaris infection statuses, as well as the general demographics for each classification group.

TB Classification Group (n = 28)				
	With *Ascaris* (n = 21) **(TBAs)**		Without *Ascaris* (n = 7) **(TB)**	
	Male:	Female:	Male:	Female:
Gender:	n = 5	n = 16	n = 3	n = 4
Median Age (Years):	35		35	
HIV Positive:	n = 0	n = 5	n = 0	n = 0
Total HIV Positive:	5		0	
Ascaris kUA/l range:	0.11 – 7.39		0.02 – 0.09	
No TB Classification Group (n = 60)				
	With *Ascaris* (n = 17) **(NoTBAs)**		Without *Ascaris* (n = 10) **(NoTB)**	
	Male:	Female:	Male:	Female:
Gender:	n = 13	n = 20	n = 11	n = 16
Median Age (Years):	35		35	
HIV Positive:	n = 3	n = 9	n = 0	n = 1
Total HIV Positive:	12		1	
Ascaris kUA/l range:	0.10 – 8.38		0.01 – 0.08	

Table A3.2: Classification of all study participants (including the pilot study participants) according to their Ascaris infection status alone, as well as the general demographics for each classification group.

***Ascaris* Classification Group (n = 88)**				
	Ascaris Positive (n = 54) **(As+)**		*Ascaris* Negative (n = 34) **(As-)**	
	Male:	Female:	Male:	Female:
Gender:	n = 18	n = 36	n = 14	n = 20
Median Age (Years):	35		35	
HIV Positive:	n = 3	n = 14	n = 0	n = 0
Total HIV Positive:	17		0	

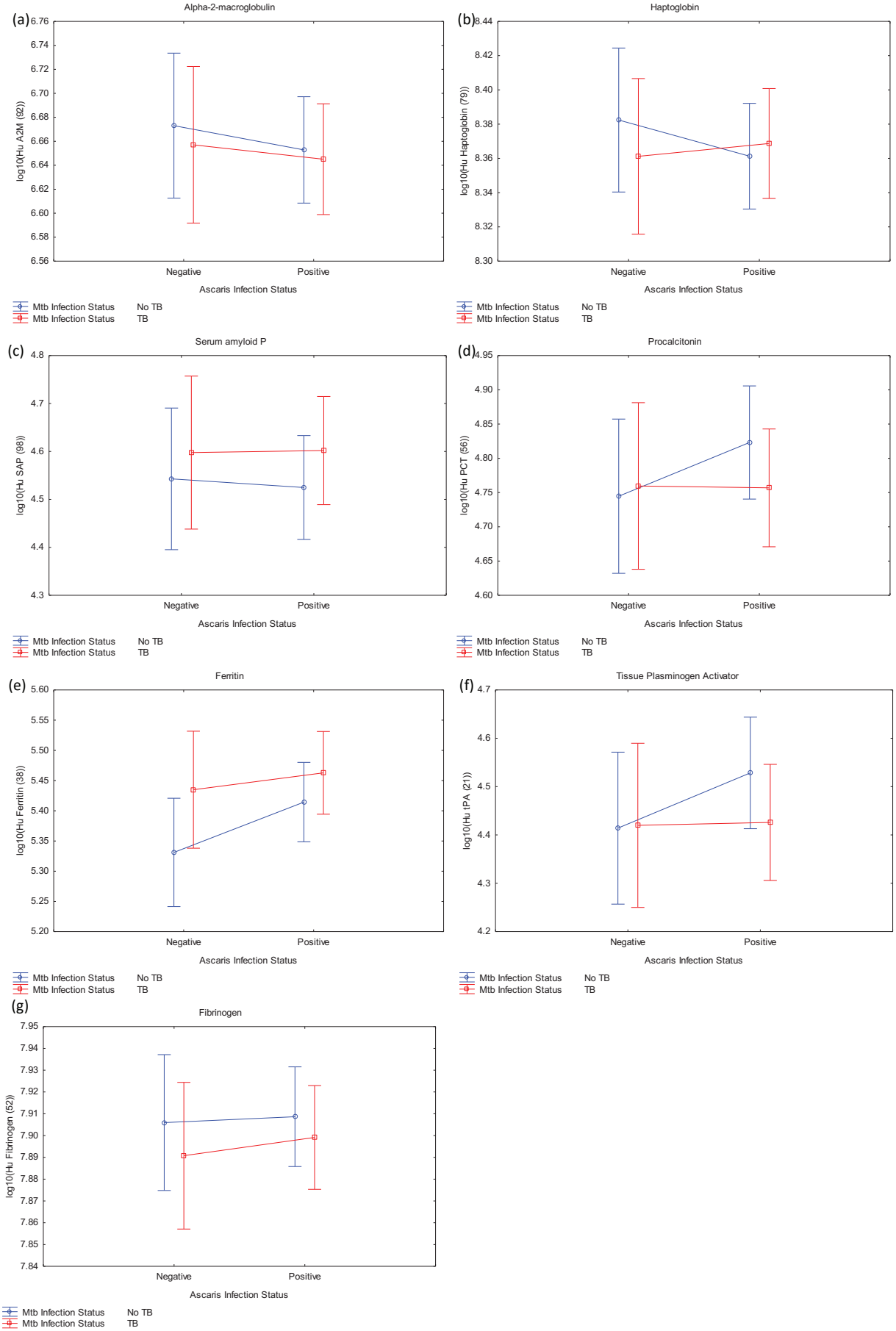

Figure A3.1: Ascaris and active TB disease coinfection influence on the remaining seven acute phase proteins. The acute phase proteins depicted include (a) alpha-2-macroglobulin, (b) haptoglobin, (c) serum amyloid P, (d) procalcitonin, (e) ferritin, (f) tissue plasminogen activator, and (g) fibrinogen. The represented data (concentrations) were log transformed and measured in ng/ml.

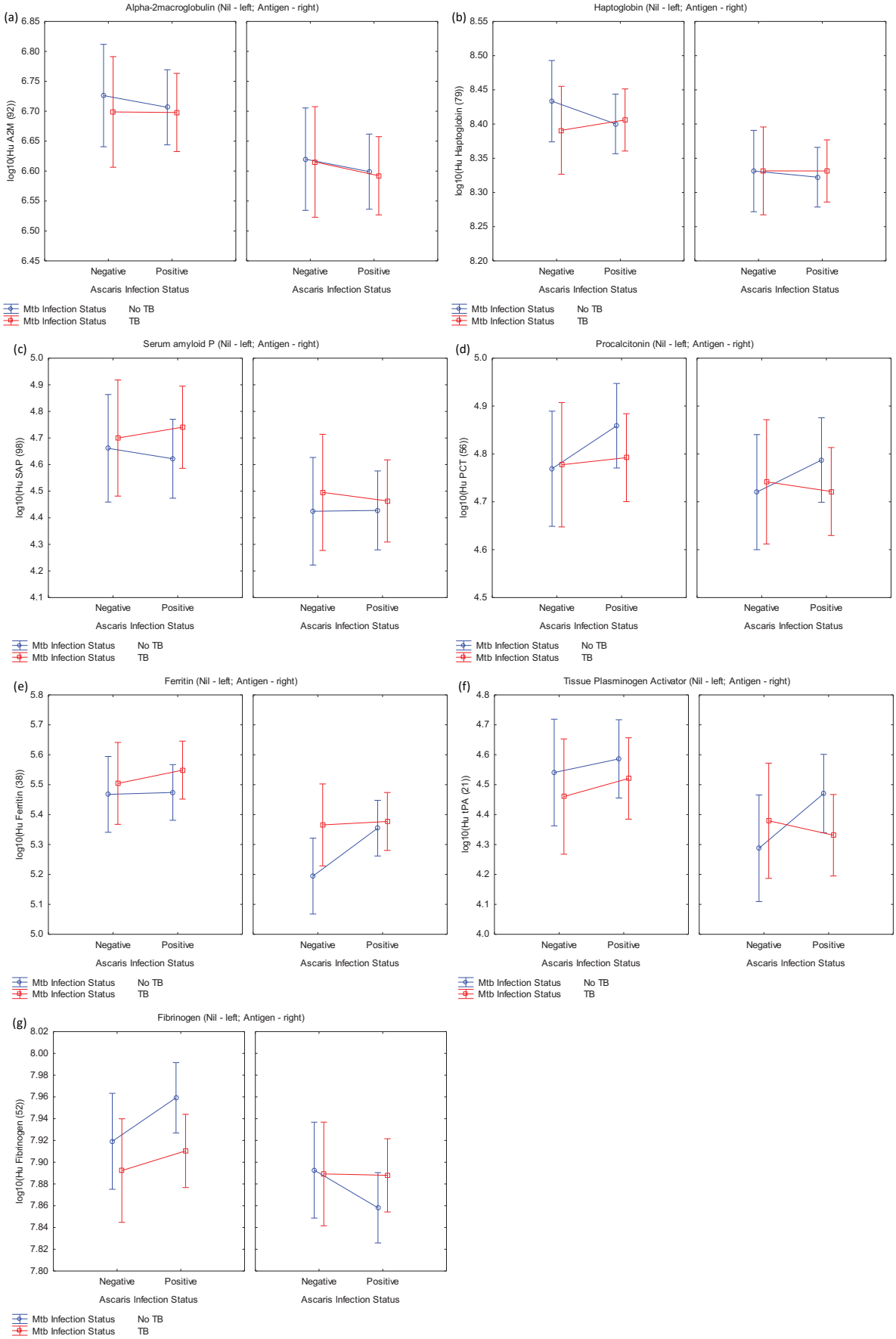

Figure A3.2: Ascaris and active TB disease coinfection influence on the remaining seven acute phase proteins under unstimulated (Nil) and antigen-stimulated (Antigen) conditions. The acute phase proteins depicted include (a) alpha-2-macroglobulin, (b) haptoglobin, (c) serum amyloid P, (d) procalcitonin, (e) ferritin, (f) tissue plasminogen activator, and (g) fibrinogen. The represented data (concentrations) were log transformed and measured in ng/ml.

CHAPTER 4

Investigation of PBMC surface marker expression as indicators of treatment response.

Identification of differentially expressed treatment-response cellular markers

Very little knowledge is available about which peripheral blood mononuclear cell (PBMC) surface markers change during TB treatment, on which cell types these changes occur, and whether such changes would constitute useful biosignatures, as the mechanism of host *M.tb* control remains poorly understood. In a recently completed Bill and Melinda Gates Foundation (BMGF)-funded TB Drug Accelerator project (PI Prof G. Walzl), in close collaboration with Becton Dickinson (BD), BD's proprietary biomarker discovery technology: FACS™ CAP (CAP: Combinatorial Antibody Profile), was evaluated on PBMCs to evaluate the technology in a more complex sample type than the cell lines on which the technology was used up to that time. The project evaluated host PBMC surface markers during TB treatment to find treatment effects (unpublished data). The data show that cellular surface molecules do change during treatment. This is not surprising as PBMCs display receptors for immune cell cytokines, chemokines and inflammatory markers and as these cells respond during inflammatory reactions. The TB Drug Accelerator project discovery looked at a panel of 252 cellular markers in a cohort of 33 active pulmonary TB cases (adult, HIV uninfected), 9 other lung disease control patients, and 11 healthy participants. Of these, a handful of biomarkers were up- or down-regulated between the point of diagnosis and the end of treatment. These markers were further analysed using Ingenuity Pathway Analysis (IPA) and the top pathways were involved in T helper cell differentiation, communication between innate and adaptive immune cells, leukocyte extravasation signalling, and caveolar-mediated endocytosis signalling (unpublished data). From the above-mentioned findings, three cellular biomarkers of interest were highlighted as the most significantly altered (in terms of expression) during treatment response, namely: CD62L (L-selectin), CD126 (Interleukin-6 Receptor) and CD120b (Tumour Necrosis Factor Receptor 2) and classified as promising targets for future investigations of biomarker candidates for the early prediction of TB treatment response. These were the only 3 markers where differences between time points on treatment remained significant after correction for multiple comparisons. The FACS™ CAP technology uses random 3-marker combinations of antibodies against surface markers without allowing for the investigation of the cells of origin of the individual markers. This limitation means that we cannot assess the cell types that are affected by anti-TB treatment and therefore has limited mechanistic potential. Furthermore, as a potential treatment response test, whole blood might be more applicable than PBMCs due to a simplification of sample processing procedures.

4.1 Study Design

Hypothesis

We hypothesize that the evaluation of the surface markers CD62L, CD126 and CD120b on individual cell types in PBMC samples from TB patients during anti-TB treatment, by flow cytometry, will allow the identification of cell-specific biomarkers of treatment response.

Aims

- The primary aim of this study was to investigate the findings of the FACS™ CAP study (that PBMC surface markers may be indicators of treatment response) in whole blood samples through the evaluation of the markers of interest at various points in relation to treatment, namely pre-treatment (baseline), week 4, and treatment end (week 24) in order to elucidate which immune subsets are responsible for the production of these markers, as well as the expression kinetics of these markers after treatment initiation.
- The secondary aim of this study was to evaluate the changes in whole blood absolute cell counts and cellular subtypes during TB treatment by using the BD Multitest™ IMK Kit (analysed using the BD FACS™ Calibur) as alternative biomarkers of treatment response indicators.

Objectives – Aim 1

- In a cohort of 19 active TB cases, investigate the FACS™ CAP study findings of five PBMC surface marker expression changes between diagnosis (BL), month 1 (M1) and end of treatment (M6) in whole blood samples by flow cytometry analyses using the BD FACS Canto™ II;
- As per the first objective, investigate these findings in an additional cohort of 12 healthy controls at the BL time point only (first visit);
- Identify the immune cell subtypes on which marker expression changes;
- Evaluate the potential of these markers as indicators of treatment response at the different stages indicated.

Objectives – Aim 2

- Using the same cohort of 19 active TB cases and 12 healthy controls, evaluate the change in various absolute immune cell counts at the following time points: at diagnosis (BL), week 2 after diagnosis (W2), month 1 (M1), and month 6 (M6, end of treatment), and compare to the BL measurements of the healthy controls;
- Evaluate the change in various absolute cell counts in approximately 50 additional healthy controls, as well as in approximately 100 additional active TB patients solely at the baseline (BL) and end of treatment (M6) time points.

4.2 Methods

4.2.1 Participant Recruitment

As part of a recently completed TB-Diabetes comorbidity investigative study known as TANDEM (P.I. Dr Katharina Ronacher; run by the Stellenbosch Immunology Research Group), 19 adult, HIV negative, confirmed active TB patients were recruited for **Aim 1 and Aim 2**. Participants were recruited from one of four field sites in the Cape Peninsula, namely: Elsiesrivier, Adriaanse, Uitsig, or Fisantekraal; and gave informed, written consent to dedicated research personnel. Peripheral blood was drawn at four follow-up time points, namely: pre-treatment (baseline), week 2 after treatment initiation, month 1 (week 4) after treatment initiation, and at end of treatment (month 6). The second month after treatment initiation is the gold standard time point at which an individual's early response to treatment is assessed. Sputum culture conversion to negative at this time point is associated with a positive treatment outcome following the full regimen[88,197]. For this reason, the month 1 time point was chosen since if we are able to predict a poor treatment outcome earlier than the gold standard month 2 time point, clinicians may be able to intervene earlier with drug susceptibility testing or checking of treatment adherence. The month 1 time point may also predict positive treatment outcomes and not necessarily only poor outcomes. **Aim 1** made use of all the major time points, with the exception of the week 2 time point which was only assessed for **Aim 2**. Additionally, a separate cohort of 112 additional active TB participants were recruited for blood draw at two follow-up time points, namely baseline and month 6 only, for the investigation of differences between the beginning and end of treatment (**Aim 2 only, includes original 19 active TB participants**).

A healthy control cohort of 52 individuals were recruited from the same four field sites, as well as the Tygerberg site, of which the data from only 12 individuals was used for **Aim 1**. **Aim 2** made use of the data from all 52 individuals recruited as controls. All gave informed consent to dedicated research personnel and were recruited for a single visit referred to as baseline. The healthy control cohort (for **Aim 1** and **Aim 2**) consisted of both household contacts (individuals who live in contact with known TB patient/s), community controls (individuals who are generally QuantiFERON (QFT)+ and live in a high burden community, but are healthy overall), and healthy individuals (individuals who are either QFT+ or QFT-, are healthy and do not live in a high burden community).

Inclusion Criteria

- Had to be between the ages of 18 and 65 years.
- Willing to give informed consent.
- Willing to have an HIV test performed and their result disclosed to a field worker, as well as consent for their result to be used for statistical purposes for the study.
- TB patients had to have a newly confirmed diagnosis of pulmonary TB infection.
- Drug susceptible TB infection (for TB cases).

- Healthy controls had to have a negative GeneXpert® (Cepheid) test on collected sputum samples, and present with no symptoms suggestive of TB disease.

Exclusion Criteria

- Participants were excluded if they had coexisting diseases such as HIV, chronic bronchitis/asthma/emphysema, or cancer.
- Participants with a haemoglobin level of <10g/l.
- Participants who weighed less than 40kg at the time of enrolment.
- Participants who were pregnant, or fell pregnant before the end of the follow-up time period.
- Steroid use within the last 6 months before enrolment.
- Previous known TB infections and/or treatment.
- Initiation of TB treatment prior to enrolment in the study.
- Any resistance to TB chemotherapeutics (mono-resistance, MDR-TB, XDR-TB).
- Alcohol abuse or the use of illegal drugs.
- Concomitant participation in a drug or vaccine trial.
- Permanent residence/residence in the study area for less than 3 months.
- Healthy controls who are known to have had TB disease previously.

For patients suspected of having TB disease, pulmonary TB infection was confirmed using GeneXpert® testing and MGIT culture. Positive MGIT cultures were further confirmed to be positive for *M.tb* complex using acid fast bacilli (AFB) staining, followed by the Capillia TB assay. Patients also had baseline and end of treatment chest x-rays (CXR) for additional diagnostic support.

Ethical Considerations

Ethics approval for this study was obtained from the Human Research Ethics Committee of Stellenbosch University under the ethics number N13/05/064. All sensitive patient information, including given names and places of work etc., were kept strictly confidential to clinical research personnel only. Participants were identified using a unique ID generated specifically for this study. This study was performed in accordance with the Helsinki Declaration.

4.2.2 Reagents and Buffers

The reagents listed in Table 4.1 were prepared and used for the completion of **Aim 1** of this study. These include FACS Lysing solution for the preparation of whole blood, FACS Buffer for Flow Cytometry, and cryomedia for the cryopreservation of cells. **Aim 2** made use of the manufacturer's kit reagents.

Table 4.1: The reagents and respective manufacturers and lot numbers used for the sample preparation of Aim 1.

	Volume:	Manufacturer:	Catalogue Number:
BD™ FACS Lysing solution			
10X FACS Lysing Solution (ml)	100	BD Biosciences	
dH_2O (ml)	900	N/A	N/A
FACS Buffer (2%)			
1X PBS	49	LONZA™	BE17-517Q
HyClone™ FCS (ml)	1	GE Healthcare Life Sciences	SV30160.03
Cryomedia (10% DMSO with 90% FBS)			
HyClone™ FCS (µl)	900	GE Healthcare Life Sciences	SV30160.03
DMSO (µl)	100	MERCK	317275-500ML

4.2.3 Laboratory Procedures for Aim 1

For each of the 19 active TB participants and 12 healthy controls, 2ml of peripheral whole blood was collected in sodium heparinized (NaHep) vacutainers at each time point (only at the baseline visit for the healthy control group). Vacutainers were inverted 10 times after venipuncture to avoid coagulation, the whole blood lysed using BD FACS™ Lysing Solution and the cells cryopreserved in 10% DMSO cryomedia. Lysis of 1ml whole blood yields a final concentration of approximately $1x10^6$ leukocytes/ml. BD FACS™ Lysing Solution was chosen as the lysing reagent for its fixation properties as it contains formaldehyde fixative which allowed for the long-term storage of samples for later batching to avoid staining and instrument variations.

Briefly, 2ml of heparinized whole blood was placed in a sterile 50ml Falcon tube and 1x BD FACS™ Lysing Solution added to fill up to 50ml (1:10 dilution). The solution was gently mixed and incubated in the dark at room temperature for 20 minutes, after which the tube was centrifuged at 400 x g for 10 minutes at room temperature. The supernatant was discarded, the pellet re-suspended in 20ml 1x PBS and the centrifugation step repeated as well as a second wash. Following the two wash steps, the pellet was re-suspended in the remaining volume of 1x PBS (roughly 100µl) and the cells cryopreserved dropwise in 2ml ice-cooled cryomedia. Finally, the cells were placed in a room temperature Nalgene Mr Frosty® which itself was then placed in a -80°C freezer overnight for step-wise freezing of the cells. The cells were then placed in liquid nitrogen storage the following day.

Antibody Panel Selection

Samples were run on the BD FACSCanto™ II (Becton Dickinson, New Jersey, USA) housed and maintained at the BD-Central Analytical Facilities (CAF) Flow Cytometry Unit at Tygerberg Medical Campus. The antibodies used for the investigation of the three markers of interest (CD62L, CD120b, CD126) are given in Table 4.2 below; all were manufactured by BD Biosciences. Two panels were

designed to assess the presence of the three markers on the different cell subsets owing to the limitation of only eight colour availability. The first panel design was aimed to investigate the three markers of interest on the surface of T and B lymphocytes, while the second panel aimed to investigate the three markers on the surface of typical innate immune cell populations, including granulocytes, monocytes and natural killer cells. Fluorochromes were assigned based first on available options from suppliers, followed by a general assignment of the brightest fluorochromes to the least expressed markers, and vice versa. For example, the fluorochrome PE was chosen for the marker CD126 as it is one of the brightest fluorochromes available and CD126 is not a highly expressed marker, whereas a more dim fluorochrome such as PerCP-Cy5.5 was chosen for markers such as CD19 (B cell marker) and CD16 (NK cell marker) as these cells are regularly expressed in a whole blood sample due to the higher frequency of these major populations in the blood.

Table 4.2: The antibodies chosen to investigate the markers of interest on the surface of immune cells, and their respective catalogue numbers and clones. The antibodies were used in two different panels, as indicated in the table, and their expected expression cell types given.

Marker:	Fluorochrome:	Clone:	Catalogue number:	Cellular Expression:
Panel 1: T and B Lymphocytes				
CD3	PE-Cy7	UCHT1	563423	T Lymphocytes
CD8	APC-H7	SK1	560179	Cytotoxic T cells
CD126	PE	M5	551850	IL-6R; Activated B and T cells, monocytes, neutrophils
CD120b	AF647	hTNFR-M1	562909	TNFR2; T cell activation co-stimulator
CD62L	V450	DREG-56	560440	L-selectin; Activated T cells, NK cells
CD58	FITC	1C3 (AICD58)	555920	LFA-3; Adhesion and activation of T cells
CD197	BV510	3D12	563449	CCR7; Activated T and B cells
CD19	PerCP-Cy5.5	HIB19	561295	B Lymphocytes
Panel 2: Natural Killer Cells, Monocytes and Granulocytes				
CD3	PE-Cy7	UCHT1	563423	T Lymphocytes
CD126	PE	M5	551850	IL-6R; Activated B and T cells, monocytes, neutrophils
CD120b	AF647	hTNFR-M1	562909	TNFR2; T cell activation co-stimulator
CD62L	V450	DREG-56	560440	L-selectin; Activated T cells, NK cells, monocytes, neutrophils
CD14	APC-H7	MφP9	560180	Monocytes
CD56	BV510	NCAM16.2 (NCAM 16)	563041	NKH-1; Natural Killer cells
CD66	FITC	B1.1/CD66	551479	Granulocytes
CD16	PerCP-Cy5.5	B73.1	565421	FcγRIII; NK cells and neutrophils

Sample Preparation for Sample Acquisition

Prior to initiation of the flow cytometry experiment, FACS Buffer was prepared and kept at 4°C until use. Following removal from liquid nitrogen, cells were immediately thawed in a 37°C waterbath, transferred to a clean 15ml Falcon tube and the volume brought up to 10ml with FACS Buffer. The cryovial was rinsed with the cell-buffer mix to remove as many of the cells from the cryovial as possible. The falcon tube was then centrifuged at 400 x g for 10 minutes, the supernatant discarded, and the cells washed twice in FACS Buffer. After the final wash, the cells were divided into the necessary 5ml Falcon tubes,

in this case (1) a negative (unstained) tube, (2) a tube for staining with Panel 1's antibodies, and (3) a tube for staining with Panel 2's antibodies. Therefore, approximately $1x10^6$ cells were stained per panel.

Staining Procedure

While the cells were being centrifuged during the wash steps, the antibody mixes were prepared for each panel. The mix was made according to the number of samples being analyzed on the day, plus an extra 10% volume to account for possible pipetting error. The total volume of antibody mix and FACS Buffer came to 50µl as the desired staining volume was 50µl. The antibody mix was then added to the pelleted cells post-wash and gently vortexed for 5 seconds. The cells and antibody were incubated in the dark for 1 hour at 4°C. Following incubation, the cells were washed in 1ml FACS Buffer to remove any unbound antibody and centrifuged at 400 x g for 5 minutes. Finally, the supernatant was discarded, and the pellet resuspended in 200µl FACS Buffer ready for acquisition. The cells were stored at 4°C in the dark until acquisition either on the same day or the following morning.

Compensation and Staining Controls

Both compensation and staining controls were performed for this study.

Compensation controls are performed as some fluorochromes are excited by more than one laser and cause spill-over to other detectors which then also detect the fluorochrome. Compensation needs to be performed to identify this and correct for it. Compensation is automatically setup using both the instrument software, mentioned previously, and is performed post-hoc using the FlowJo™ Software which is then applied to all sample files for which the particular compensation settings were used during acquisition. In order to perform compensation, BD™ Negative Control CompBeads and lysed whole blood cells from a sample set aside for optimization were incubated together for each antibody separately. This was done separately for both panels 1 and 2 prior to starting to run any samples. Cells were used for the compensation set up instead of CompBeads due to the compensation set up being more accurate if investigated using your experimental cell type of interest.

Staining controls involve the Fluorescent Minus One (FMO) technique as an additional control following compensation. FMO stain your cells of interest with all fluorochromes except the one, which is repeated for all fluorochromes until there are eight tubes of stained cells, each with a different antibody absent. This is performed so that we can determine the correct positive and negative populations which can sometimes be difficult in multi-colour experiments. For this control, the same sample type as the actual samples was used to ensure consistency in staining technique.

Sample Acquisition

BD FACSDiva™ CS&T Research Beads were used and acquired on the BD FACSCanto™ II cytometer using the BD FACSDiva™ software, version 8.0.1 (Becton Dickinson, New Jersey, USA) at the beginning of every day that samples were run. This is an automated program that sets up the cytometer for daily use and ensures proper calibration. Monthly maintenance was performed by the facility to

ensure correct upkeep of the instrument. Samples were preferably acquired on the same day, but could also be acquired after an overnight incubation in the dark at 4°C. For each sample, unlabeled (unstained) cells were first acquired to ensure that the Forward Scatter (FSC) and Side Scatter (SSC) voltages adequately distinguished between lymphocyte and granulocyte populations (Figure 4.1) and to use as a reference for the stained cells. Approximately 50 000 events were recorded for each unstained reference sample. Following the unstained acquisition, the stained samples were acquired until 1 000 000 events had been recorded or once the available volume of sample was depleted.

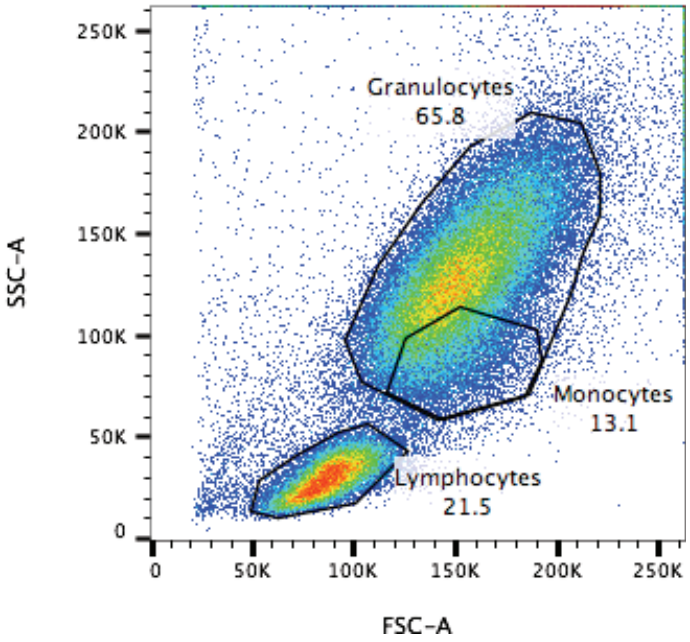

Figure 4.1: Demonstration of the FSC and SSC settings during instrument setup. The instrument settings are setup to ensure clear separation of lymphocyte and granulocyte populations as indicated.

4.2.4 Laboratory Procedures for Aim 2

For each of the 112 active TB participants and 52 healthy controls, 1ml of peripheral whole blood was collected into a 3ml vacutainer lined with the anticoagulant EDTA at each time point for investigation using the BD Multitest™ IMK (Becton Dickinson, New Jersey, USA) kit.

BD Multitest™ IMK Assay

The BD Multitest™ IMK Kit is intended for the identification and quantification of the percentages and absolute counts of various human lymphocytes, including T lymphocytes, B lymphocytes and Natural Killer cells. It follows a set protocol as indicated by BD Biosciences and employs a Lyse-No Wash technique which allows for whole blood to be stained with various cellular marker antibodies, incubated for 15 minutes, and lysed with BD FACS™ Lysis buffer without the need to wash the cells. The kit makes use of two antibody panels using BD TruCOUNT™ Tubes:

1) MultiTEST: CD3/CD8/CD45/CD4;
2) MultiTEST IMK: CD3/CD16+56/CD45/CD19

The TruCOUNT tubes are specialized tubes that contain a freeze-dried pellet of known fluorescent beads beneath a metal retainer placed at the bottom of the tube and allow for the enumeration of absolute counts of the cell populations which is beneficial for diagnostic purposes.

Sample Preparation and Acquisition

The manufacturer's instructions were followed for the procedure. Briefly, two TruCOUNT tubes were labelled for each participant with their participant ID and either "Multitest" or "Multitest IMK". For the tube labelled "Multitest", 20μl of the MultiTEST reagent was added just above the metal retainer at the bottom of the tube. For the tube labelled "Multitest IMK", 20μl of MultiTEST IMK reagent was added, again just above the metal retainer at the bottom of the tube. Following the addition of the reagents, 50μl of well-mixed, anticoagulated whole blood was added to each tube, and each gently mixed. Both tubes were then incubated in the dark for 15 minutes at room temperature, after which 450μl of test specific 1x FACS Lysing solution was added to each tube and the incubation step repeated. The samples could then be acquired on either the same day as blood collection or the following day using the FACSCalibur™ (Becton Dickinson, New Jersey, USA) Flow Cytometer, available at the BD-CAF Flow Cytometry Unit at Tygerberg Medical Campus, using the BD Biosciences MultiSET™ software v2.2.

External Quality Control

For quality control purposes, at the beginning of each week, an external quality control sample – LymphoSure (Synexa Life Sciences, South Africa) – was run to ensure correct calibration of the instrument and its lasers. Lymphosure is a quality assurance standard prepared from human peripheral blood that has an extended shelf-life of up to 69 days and considerable stability during this time period. LymphoSure reference ranges were lot-specific and indicated in a separate insert with each new batch. The LymphoSure control was replaced every three months with a new batch to ensure consistent sample viability. If a Lymphosure run failed prior to study sample acquisition, the problem was first investigated and resolved where possible and study samples not run until the quality control passed.

No compensation controls, titrations or staining controls needed to be investigated prior to running these experimental samples owing to the nature of the kit and the software used.

4.2.5 Data Analysis for Flow Cytometric Data

The third-party software FlowJo™, version 10.3 (FlowJo LLC, Oregon, USA) was used for analysis of the FCS files generated by both the BD FACSCanto™ II and FACSCalibur™ flow cytometers (Aims 1 and 2 respectively). When analyzing the data files, a plot of the cytometer run time (Time vs FSC-Height (H)) was first scrutinized to identify individual run success and instrument stability during the run (Figure 4.2(a)). The entire run for which the instrument was stable, was gated on and analyzed further in an FSC-Area (A) vs FSC-H plot used to visualize singlets (Figure 4.2(b)). This was done to select for single

cells that were detected by the lasers and not doublets as these would skew analyses. Following singlet identification, FSC and SSC voltages were set to adequately identify the lymphocyte and granulocyte populations (Figure 4.2(c)). The voltage settings to be used for each of the chosen antibodies were established using compensation and staining controls and saved – no settings were changed in order to keep acquisition consistent and reproducible.

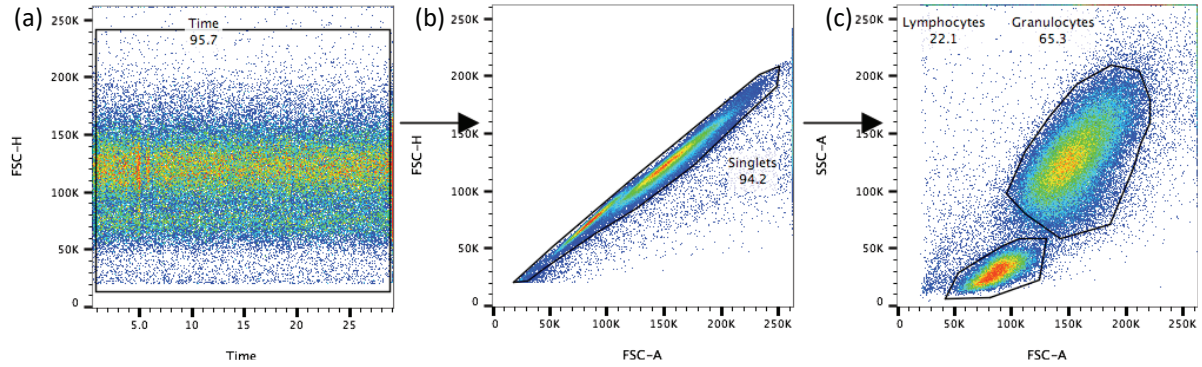

Figure 4.2: Demonstration of the gating strategy used to ensure true lymphocyte and granulocyte populations could be distinguished.

4.2.6 Statistical Analysis of Flow Cytometry Data

All data extracted from FlowJo™ were tested for normality using the D'Agostino Pearson test for normality after grouping according to individual markers. Differences between the three assessed time points over the course of standard anti-TB treatment were investigated using the repeated measures analysis of variance (RM-ANOVA) for parametric data. The RM-ANOVA is suited for data for which there is more than three groups and more than one time-point. Nonparametric data under the same conditions were assessed using Friedman's test. Friedman's test compares the medians of three or more matched groups and may be used when there is more than one time-point for each participant. When data for each marker were compared between matched time points, i.e. BL vs M6 etc., paired t-tests and the Wilcoxon signed rank test for matched pairs were used to investigate parametric and nonparametric data respectively, since the data was from the same participants at different time points. When data was compared between groups, i.e. between active TB participants and healthy controls, unpaired t-tests and the Mann-Whitney test was used to investigate parametric and nonparametric data respectively.

BD Multitest™ IMK assay data were compared across the four treatment time points using a RM-ANOVA in order to assess the variance across the four time points for each assessment criteria established by the kit, i.e. total T lymphocytes or NK cells. Tukey's post-test was also used. Data generated for the four time point assessment was normally distributed, as such a paired t-test was used to generate p-values for time points that were significantly different from each other according to Tukey's post-test (e.g. M1 vs M6). In order to assess the variance between the time of diagnosis (BL) and end of treatment (M6) time points, and healthy control data, the Wilcoxon signed rank test for matched pairs

or Mann-Whitney tests were used to investigate differences within and between groups respectively (e.g. BL vs M6 and BL/M6 vs HC respectively).

4.3 Results

4.3.1 Participant Demographics

Nineteen active TB participants were enrolled for **Aim 1** of this study and were followed up at three time points, namely at baseline, month 1 and month 6 after treatment initiation (Table 4.3). Only one of the participants did not have a follow-up at the month 6 time point due to unknown reasons for the participant's absence. Additionally, 12 healthy control participants were enrolled for **Aim 1** of this study for a single time point alone. The demographics of the participant groups is given below.

Table 4.3: Participant demographics for the active TB and healthy control participants enrolled into Aim 1 of this study.

	Active TB (n = 19)		**Healthy Controls (n = 12)**	
	Male:	Female:	Male:	Female:
Gender:	n = 11	n = 8	n = 2	n = 10
Median Age (Years):	49	44	37.5	53.5
Latently Infected:	Not Applicable		n = 1	n = 6
HIV Infection Status:	Uninfected			
Treatment Failure:	n = 1	n = 0	Not Applicable	

The previously stated participants were also enrolled for the second aim of the study looking at investigating treatment response biomarkers in absolute cell counts of patients. Not all participants were able to be followed-up at all time points. In total, 3 participants did not have data for their month 6 follow-up; one visit was missed due to unknown absence at the follow-up date, while the remaining two were as a result of difficulty obtaining the sample during phlebotomy. Two participants did not have data for their week 2 follow-up as a result of missing scheduled appointment. Potential reasons for missed follow-ups include dropping out of the study because participants "feel better" after treatment initiation, work commitments, or transportation problems to the clinic. One participant did not have any of the first three follow-up visits data as the BD Multitest™ IMK Kit had not yet arrived at the time of recruitment initiation.

An additional 112 active TB participants were recruited for **Aim 2** only. These participants only had samples taken at the baseline and month 6 (end of treatment) time points in order to assess basic differences between diagnosis and treatment completion. A cohort of 52 healthy controls were also recruited for Aim 2 and had a single sample taken at the time of recruitment (Table 4.4).

Table 4.4: Participant demographics for the active TB and healthy control participants enrolled into Aim 2 of this study.

	Active TB (n = 112)		**Healthy Controls (n = 52)**	
	Male:	Female:	Male:	Female:
Gender:	n = 68	n = 44	n = 22	n = 30
Median Age (Years):	44.5	45	38.5	30.5
Latently Infected:	Not Applicable		n = 16	n = 23
HIV Infection Status:	Uninfected			
Treatment Failure:	n = 4	n = 0	Not Applicable	

4.3.2 Gating Strategies for the Analysis of Panel 1 and Panel 2

As mentioned previously (section 4.2.5), a standard gating strategy backbone was employed for all analyses (Figure 4.2). All further gating was unique for each panel and/or cell subset, described presently. Based on the control gates identified during the compensation and staining controls (FMOs), a clearly structured gating strategy was setup to be applied to all samples acquired and used for population/marker identification and analysis for both Panel 1 and 2.

Panel 1 investigated lymphocyte subsets which included $CD4^+$ ($CD3^+CD8^-$) and $CD8^+$ ($CD3^+CD8^+$) T lymphocytes (Figure 4.3), as well as B lymphocytes ($CD3^-CD19^+$; Figure 4.4). Panel 2 investigated granulocyte and monocyte populations which included neutrophils ($CD3^-CD14^-CD66^+$; Figure 4.7), NK cells ($CD3^-CD16^+CD56^+$; Figure 4.5), NKT cells ($CD3^+CD16^+$; Figure 4.6), intermediate monocytes ($CD3^-CD14^+CD16^+$; Figure 4.8) and classical monocytes ($CD3^-CD14^+CD16^-$; Figure 4.8).

In order to determine overall marker expression in the whole blood of active TB disease participants, as well as to draw comparisons with the FACS™ CAP findings which looked at overall marker expression, a third gating strategy was developed. The standard backbone was used, after which all acquired cells were gated on in the “FSC-A vs SSC-A” plot where lymphocytes and granulocytes are normally selected for (Figure 4.9). Once all cells were gated on, the expression of each individual marker was assessed through the single gating of “Marker of interest vs SSC-A”.

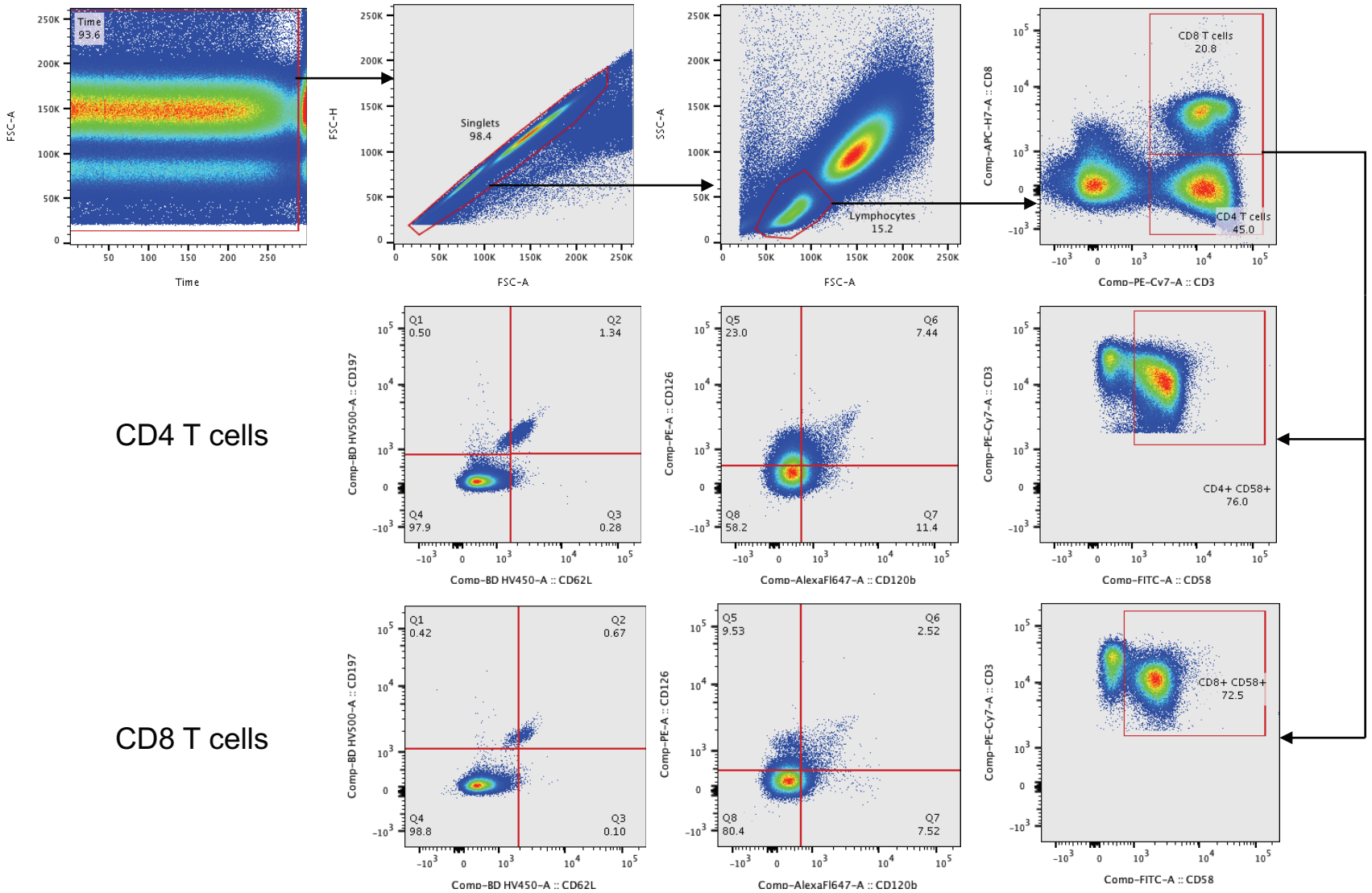

Figure 4.3: The gating strategy developed using the FMO for Panel 1 for the investigation of CD4+ and CD8+ T cell subsets. For each subset, the expression frequencies of the markers CD58, CD197, CD126, CD120b, and CD62L were assessed.

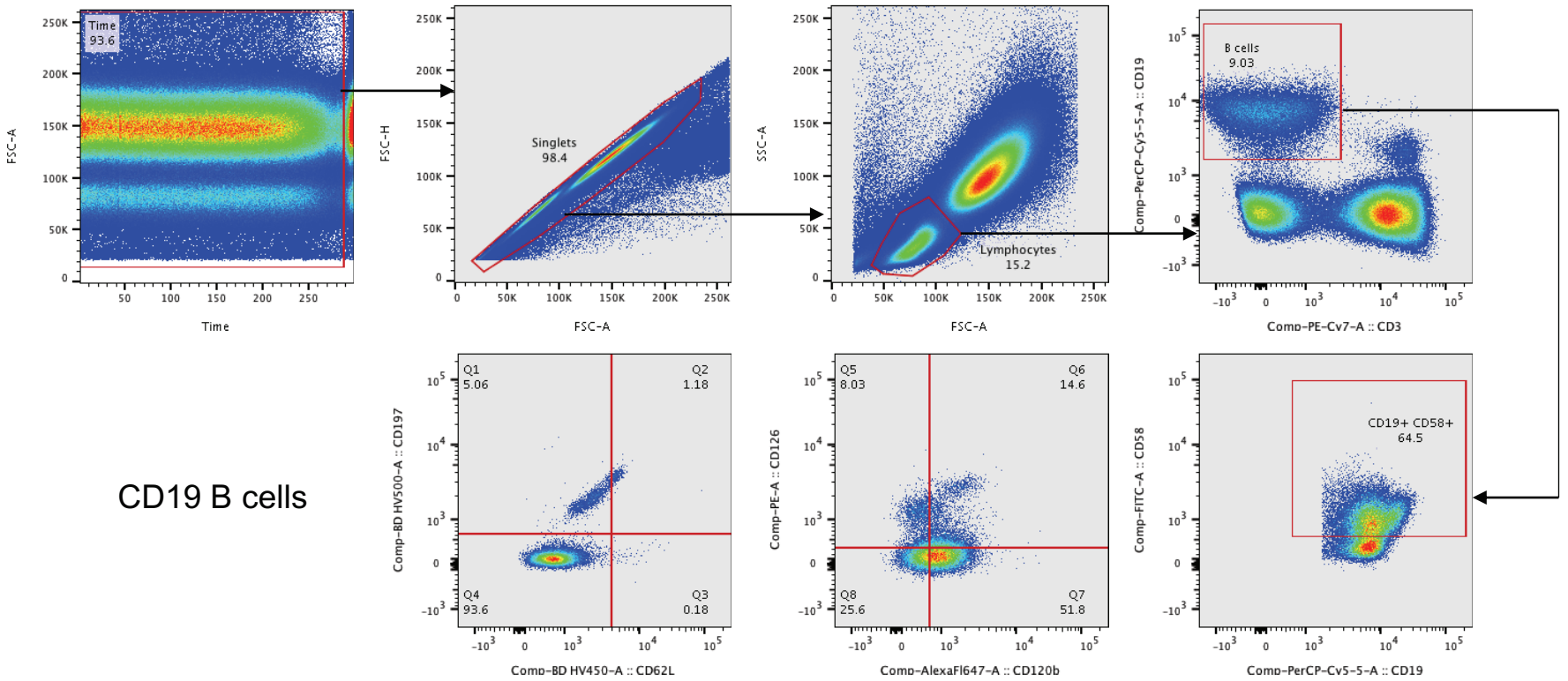

CD19 B cells

Figure 4.4: The gating strategy developed using the FMO for Panel 1 for the investigation of CD19+B cells. The expression frequencies of the markers CD58, CD197, CD126, CD120b, and CD62L were assessed.

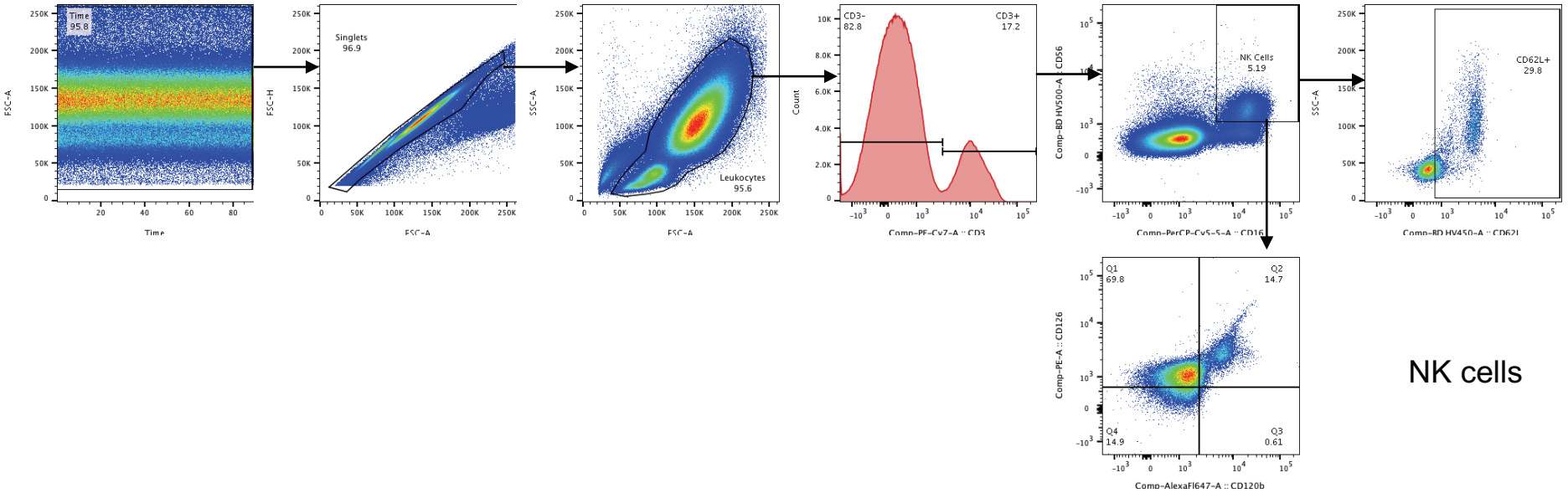

Figure 4.5: The gating strategy developed using the FMO for Panel 2 for the investigation of NK cells. The expression frequencies of the markers CD126, CD120b, and CD62L were assessed.

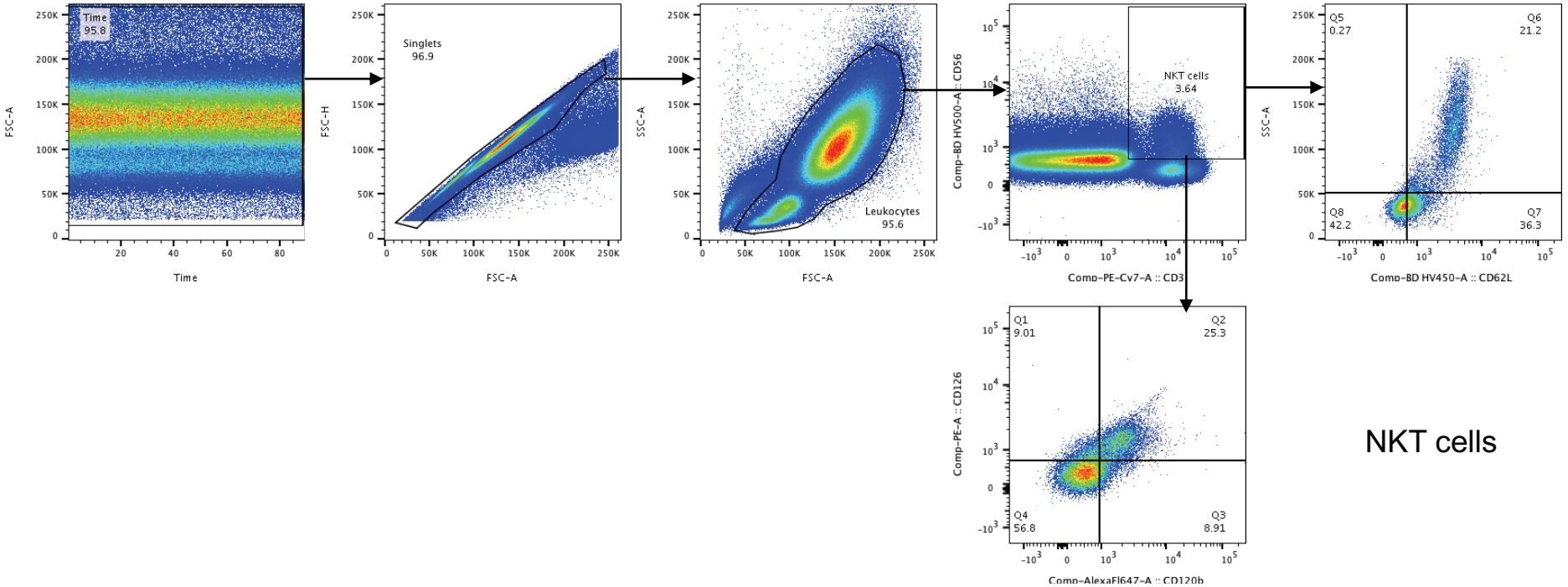

Figure 4.6: The gating strategy developed using the FMO for Panel 2 for the investigation of NKT cells. The expression frequencies of the markers CD126, CD120b, and CD62L were assessed.

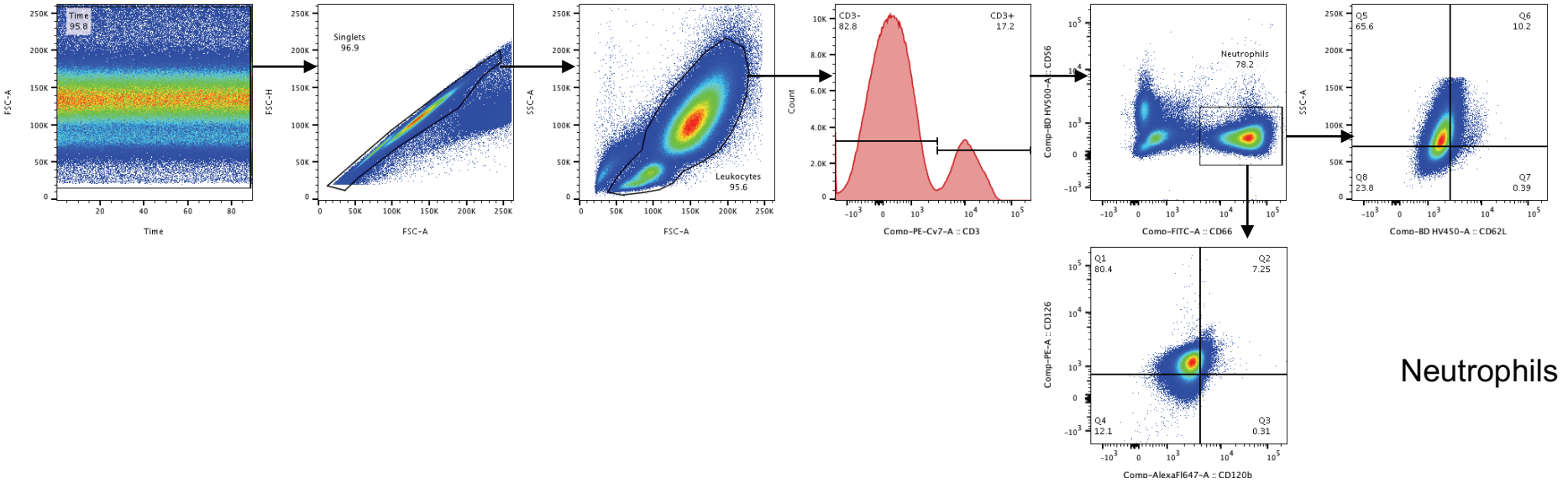

Figure 4.7: The gating strategy developed using the FMO for Panel 2 for the investigation of Neutrophils. The expression frequencies of the markers CD126, CD120b, and CD62L were assessed.

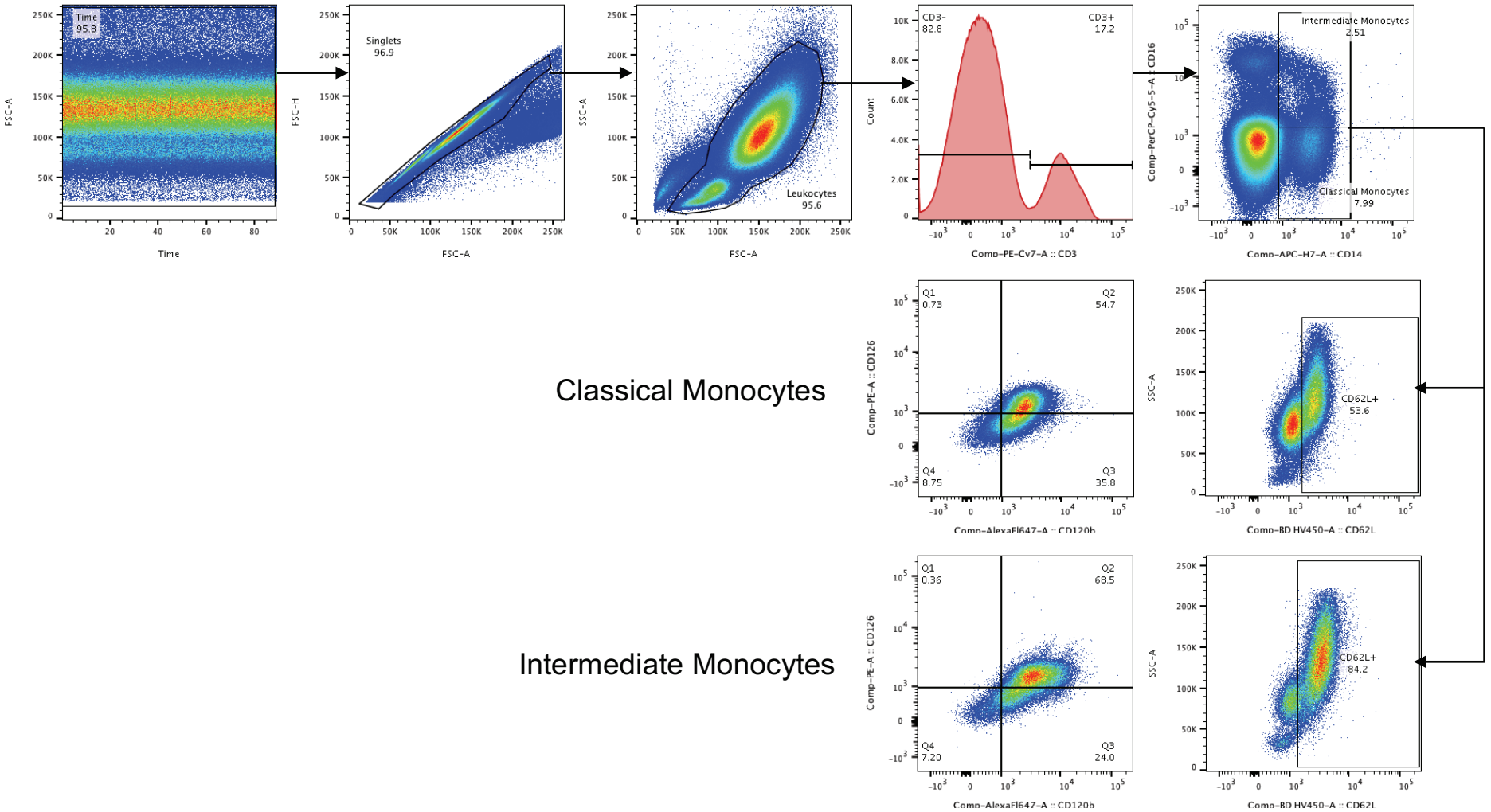

Figure 4.8: The gating strategy developed using the FMO for Panel 2 for the investigation of classical and intermediate monocyte subsets. The expression frequencies of the markers CD126, CD120b, and CD62L were assessed.

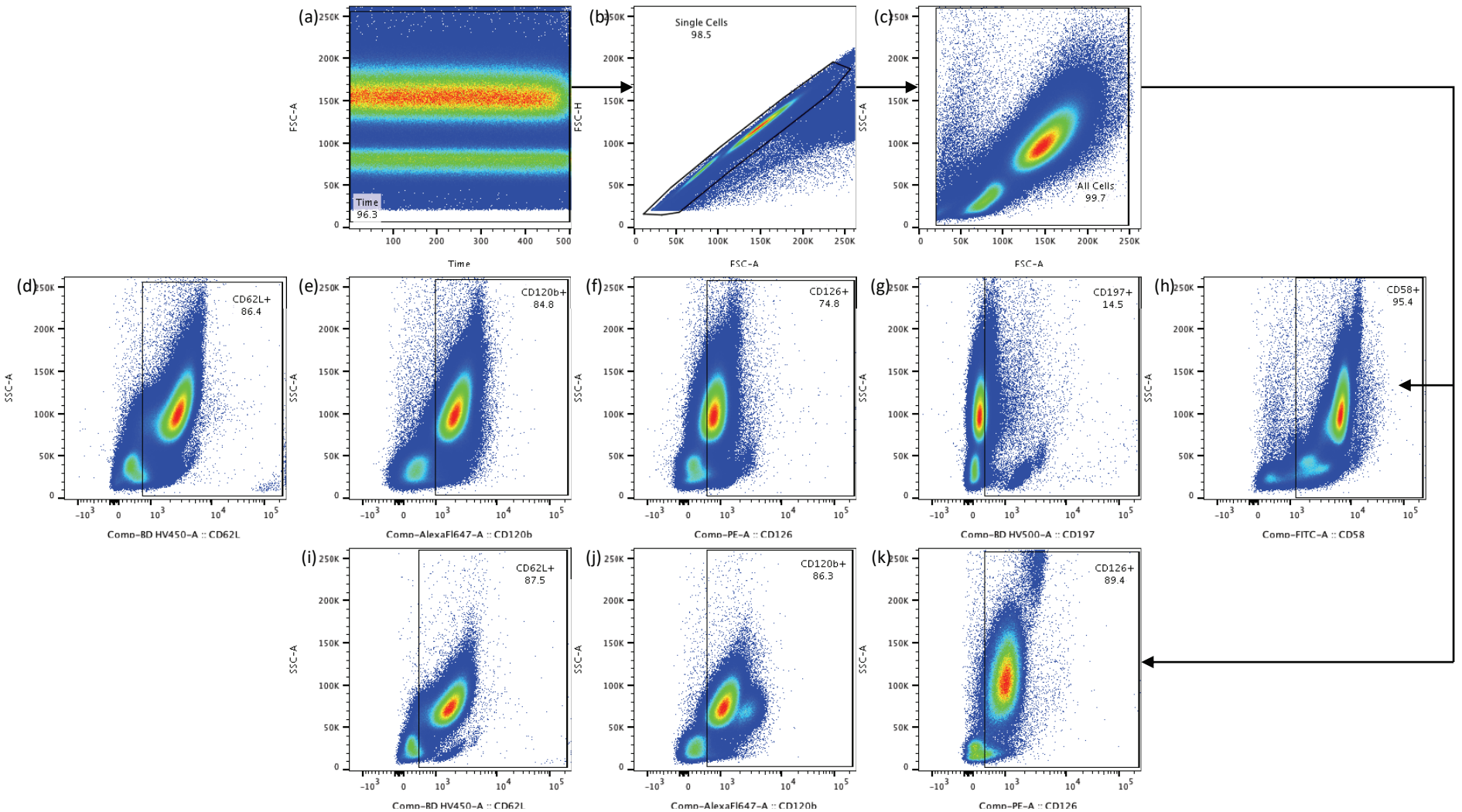

Figure 4.9: The gating strategy for the investigation of the markers of interest on all cells, developed using the FMO for Panel 1 and 2. The gating strategy backbone is given in (a) – (c). For each cellular subset, the expression frequencies of the markers (d) CD62L, (e) CD120b, (f) CD126, (g) CD197, and (h) CD58 were assessed in Panel 1; while the expression frequencies of the markers (i) CD62L, (j) CD120b, and (k) CD126 were assessed in Panel 2.

4.3.3 CD3 expression changes between Panel 1 and Panel 2

Concern was raised as to how this study would ensure consistency between the two staining panels since each participant sample was divided into two and essentially analyzed twice, even though participant samples were stained for both panels at the same time. Since both panels included the lineage marker, CD3, it was decided that the expression frequencies of this marker between panels would be compared for each timepoint and for each participant.

When plotting the frequencies of CD3 expression for Panel 1 and Panel 2 against each other, there was a significant decrease in the median frequency for Panel 2 (Figure 4.10; p = 0.015) following a Mann-Whitney test for nonparametric data. However, when the differences between the frequencies was assessed, i.e. CD3 expression in Panel 2 subtracted from CD3 expression in Panel 1, the average difference of expression between the two panels was only 3.7%, with the largest difference being 15.9% and the smallest being 0.2%. Since there is no defined threshold at which differences in marker expression should be considered significant, the fact that the average difference between Panel 1 and Panel 2 expression for the CD3 marker was only 3.7% gives us confidence that both panel results are a true representation of one another and that the differences are negligible as a result of identical gating that cannot be achieved between the 2 samples. In addition, a certain degree of variability is expected from tube to tube owing to the discrepancy in the gating strategies of the two panels.

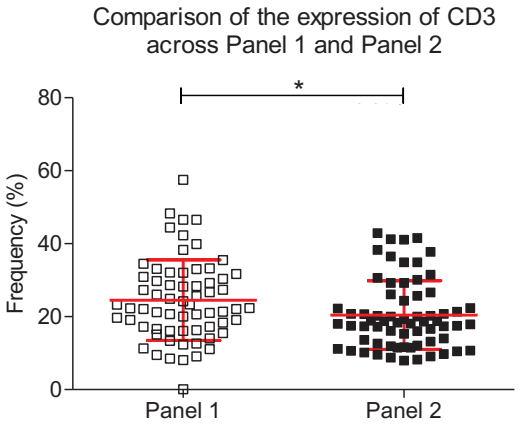

Figure 4.10: Comparison between the CD3 expression frequencies of Panels 1 and 2 for both TB patients and healthy controls (p = 0.015). The Mann-Whitney test was performed for nonparametric datasets.

4.3.4 Overall expression of the most promising FACS™ CAP markers: CD126, CD120b and CD62L, as well as CD58 and CD197.

Previous work performed by Smith in 2014 (unpublished) aimed to investigate and identify peripheral blood mononuclear cell surface markers that were differentially expressed during the course of active TB treatment using the proprietary technology, FACS™ CAP (Becton Dickinson Technologies), for potential utility in treatment monitoring. In this study, 252 surface markers were investigated on PBMCs

in a cohort of 33 active TB patients, 11 healthy community controls and 9 other lung disease controls, for which the active TB patients were followed up at diagnosis of active TB, week 4 following treatment initiation, and week 24/the end of treatment. Control sample collection only occurred at a single visit. This study identified three significantly different treatment response markers that were differentially expressed between the time of diagnosis and end of treatment (week 24). These markers included CD126, CD120b, and CD62L, and were the only markers that remained significantly different following Bonferroni correction ($p < 0.01$ in this study). Other promising markers included CD58 and CD197, but these did not retain statistical significance following the Bonferroni correction. The identification of significantly different marker expression over the course of active TB treatment spurred further investigation of the most promising biomarkers in a new cohort of active TB patients as well as in more feasible sample types for future translation into clinical settings, from which this study was designed.

This study, therefore, investigated the three most promising markers identified by the FACS™ CAP study as well as two additionally promising markers, in heparinized whole blood from a cohort of 19 active TB cases and 12 healthy controls (a mixed population of contact and community controls). This study did not use the proprietary FACS™ CAP technology, but rather employed flow cytometry using the FACS™ Canto II.

First, we assessed the overall expression of the three markers of interest (CD126, CD120b and CD62L), as well as the additional two markers (CD58 and CD197), on all cells in the peripheral blood over the course of TB treatment. Repeated Measures ANOVA (RM-ANOVA) was performed to assess the variance between marker frequencies across treatment; Bonferroni's multiple comparison post-test was used to correct for multiple comparisons. Groups of data, e.g. BL vs HC, were compared for significance using the unpaired t-test for parametric data, however the paired t-test was used to compare matched pairs (BL vs M6). The distribution of data for CD62L was nonparametric and therefore the Mann-Whitney test was used to compare cases to healthy controls, e.g. BL vs HC, and the Wilcoxon signed rank test for matched pairs of nonparametric data was used to compare the matched pairs for CD62L data. The Friedman test was used instead of a RM-ANOVA since the data was nonparametric.

The median frequency of the markers CD126 {Figure 4.11(a); BL vs HC $p = 0.0016$, M6 vs HC $p < 0.0001$} and CD120b {Figure 4.11(b); BL vs HC $p < 0.0001$, M6 vs HC $p = 0.0002$} did not change over the course of treatment (RM-ANOVA $p = 0.1463$ and 0.4345 respectively), but the BL and M6 measurements for both markers were significantly higher than the measurements in the HC group. The marker CD62L displayed a downward trend over the course of treatment, but this was not significant (Friedman $p = 0.0622$) and there was a significant difference between the frequency of CD62L at BL in cases versus the HC group (Figure 4.11(c); BL vs HC $p = 0.0081$), suggesting normalization of expression following successful anti-TB therapy.

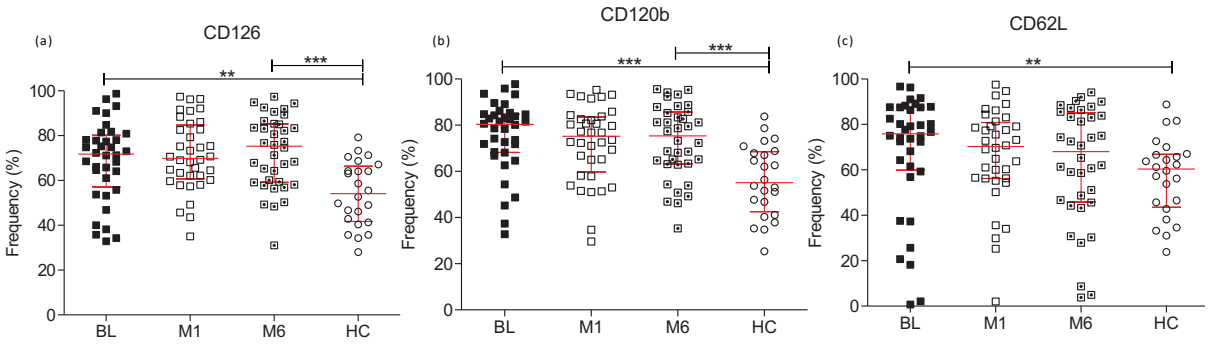

Figure 4.11: Representative dot plots of the frequency of (a) CD126, (b) CD120b and (c) CD62L on all cells acquired by flow cytometry over the course of TB treatment and in healthy controls (HC). Bars are representative of the median and interquartile range.

The frequency of CD58 (Figure 4.12(a)) and CD197 (Figure 4.12(b)) were then assessed on all cells where it was observed that CD58 expression decreased over the course of treatment towards frequencies observed in healthy controls – this was the only marker for which the change during treatment was significant (RM-ANOVA p = 0.0153). A significant change in expression was observed between the time of diagnosis and healthy control frequencies (Figure 4.12(a); p = 0.0002) as well as between the time of diagnosis and end of treatment (Figure 4.12(a); p = 0.0062). No differences in expression were observed for the marker CD197 over the course of treatment or compared to healthy controls (Figure 4.12(b)).

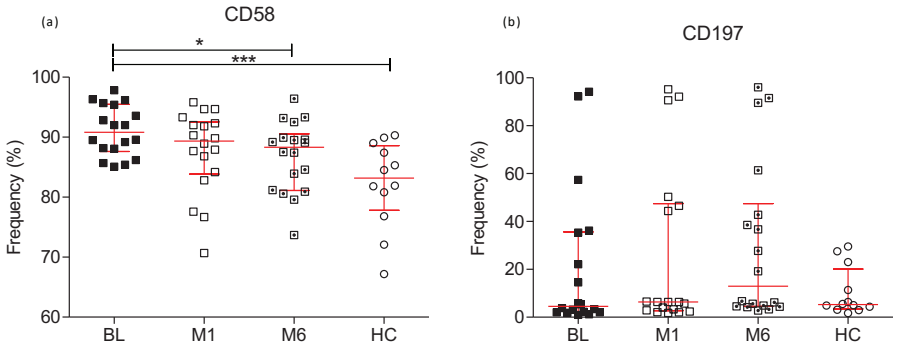

Figure 4.12: Representative dot plots of the frequency of (a) CD58 and (b) CD197 on all cells acquired by flow cytometry over the course of TB treatment and in healthy controls (HC). Bars are representative of the median and interquartile range.

Based on these findings, cell-specific expression of these markers were investigated to elucidate the possible cell subsets within peripheral blood responsible for their expression.

4.3.5 Cell subset expression of CD126, CD120b, CD62L, CD58, and CD197.

The human body contains many different types of cells. The peripheral blood compartment is no exception. Various innate and adaptive immune cells exist in circulation concurrently with cells that have immunological functions in addition to other specialized functions, like platelets (inflammatory

mediator release) and red blood cells (transportation of immune complexes to the spleen)[198]. This study investigated the expression of the markers CD126, CD120b, CD62L, CD58 and CD197 on the surface of innate (monocytes, natural killer cells, neutrophils) and adaptive (B lymphocytes, T lymphocytes) immune subsets.

A summary table of each marker in each assessed subset is given in Table 4.5. Red text represents significant results, while it should be noted that the ANOVA's performed were nonparametric for all instances except for the markers CD126 in the neutrophil subset and CD120b in the classical monocyte subset which had a parametric data. Only the $CD4^+$ and $CD8^+$ T lymphocyte subsets displayed a change in any marker's expression across treatment. Interestingly, both subsets displayed a change in the CD120b and CD58 markers, suggesting that these two markers may be promising indicators of treatment response for further assessment.

Table 4.5: Summary of the significant results observed for each marker's frequency in each cell subset assessed.

		CD4	CD8	B	NK	NKT	NP	IM	CM
CD126	BL vs M1	ns	ns	ns	ns	ns	ns	ns	ns
	BL vs M6	ns	0.0279	ns	ns	ns	ns	ns	ns
	BL vs HC	ns	ns	ns	ns	ns	ns	ns	ns
	M1 vs M6	ns	ns	ns	ns	ns	ns	ns	ns
	M1 vs HC	ns	ns	ns	ns	ns	ns	ns	ns
	M6 vs HC	ns	ns	ns	ns	ns	0.0021	ns	ns
	ANOVA	0.1195	0.0672	0.1734	0.8373	0.8213	0.4882	0.9202	0.7703
CD120b	BL vs M1	ns	ns	ns	ns	ns	ns	ns	ns
	BL vs M6	0.0109	0.0155	ns	ns	ns	ns	ns	ns
	BL vs HC	ns	ns	ns	0.0443	ns	ns	0.0263	0.0009
	M1 vs M6	ns	ns	ns	ns	ns	ns	ns	ns
	M1 vs HC	ns	ns	ns	ns	ns	ns	ns	ns
	M6 vs HC	ns	0.0360	ns	ns	ns	ns	ns	0.0396
	ANOVA	0.0263	0.0338	0.1392	0.5556	0.6902	0.7930	0.6964	0.2921
CD62L	BL vs M1	ns	ns	ns	ns	ns	ns	ns	ns
	BL vs M6	ns	ns	0.0176	ns	ns	ns	ns	ns
	BL vs HC	ns	ns	0.0067	ns	ns	ns	ns	ns
	M1 vs M6	ns	ns	ns	ns	ns	ns	ns	ns
	M1 vs HC	ns	ns	ns	ns	ns	ns	ns	ns
	M6 vs HC	ns	ns	ns	ns	ns	0.0263	ns	0.0466
	ANOVA	0.1900	0.3296	0.0667	0.4364	0.6357	0.7826	0.9631	0.4737
CD58	BL vs M1	ns	ns	ns	N/A				
	BL vs M6	0.0209	0.0184	ns	N/A				
	BL vs HC	0.0158	0.0059	ns	N/A				
	M1 vs M6	ns	ns	ns	N/A				
	M1 vs HC	ns	ns	ns	N/A				
	M6 vs HC	ns	ns	ns	N/A				
	ANOVA	0.0078	0.0178	0.2208	N/A				
CD197	BL vs M1	ns	ns	ns	N/A				
	BL vs M6	ns	ns	ns	N/A				
	BL vs HC	ns	ns	ns	N/A				
	M1 vs M6	ns	ns	ns	N/A				
	M1 vs HC	ns	ns	ns	N/A				
	M6 vs HC	ns	ns	ns	N/A				
	ANOVA	0.7944	0.4854	0.4688	N/A				

Abbreviations: BL – baseline; M6 – month 6; HC – healthy control; ns – not significant; CD4 – CD4$^+$ T lymphocyte; CD8 – CD8$^+$ T lymphocyte; B – B lymphocyte; NK – Natural Killer cell; NKT – Natural Killer T cell; NP – Neutrophil; IM – Intermediate monocyte; CM – Classical monocyte. P values are shown in red, when statistically significant.

CD4$^+$ T lymphocytes

All five markers were assessed in the CD4$^+$ T lymphocyte population. No differences in expression were seen for CD126 (Figure 4.13(a)), CD62L (Figure 4.13(b)) or CD197 (Figure 4.13(e)) across treatment or compared to healthy controls. CD120b displayed a significant **upregulation** between baseline and the end of treatment (Figure 4.13(c); p = 0.0109; ANOVA p = 0.0263), while CD58 was also significantly upregulated between baseline and the end of treatment (Figure 4.13(d); p = 0.0209; ANOVA p = 0.0078). CD58 expression was also significantly upregulated in the healthy control group (Figure 4.13(d); p = 0.0158) with expression levels returning to healthy control levels at the end of treatment.

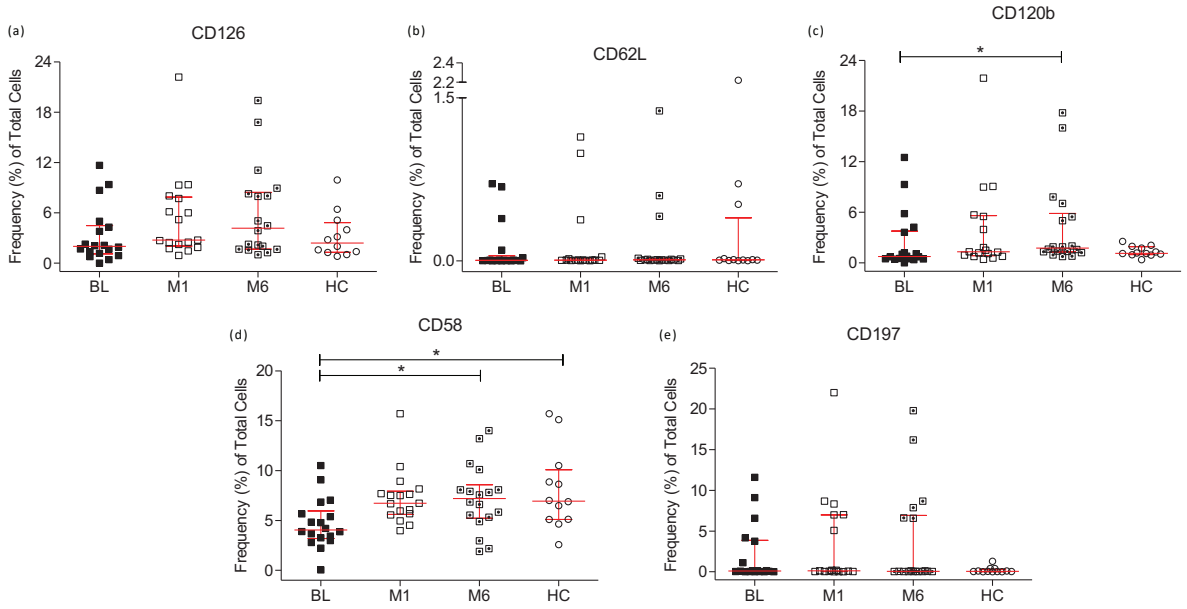

Figure 4.13: Frequency of (a) CD126, (b) CD62L, (c) CD120b, (d) CD58 and (e) CD197 expressing CD4$^+$ T lymphocytes represented as a frequency of total cells at the baseline (BL), month 1 (M1), and month 6 (M6) time points compared to healthy controls (HC). Lines represent the median and interquartile range for each time point.

CD8$^+$ T lymphocytes

All five markers were assessed in the CD8$^+$ T lymphocyte population. No differences in expression were seen for CD62L (Figure 4.14(b)) or CD197 (Figure 4.14(e)) across treatment or compared to healthy controls. The marker CD58 was upregulated between baseline and the end of treatment (Figure 4.14(d); p = 0.0184; ANOVA p = 0.0178), with levels of expression returning to healthy controls levels at the end of treatment. As such, there was a significant downregulation of CD58 at baseline compared to the healthy control group (Figure 4.14(d); p = 0.0059). The expression of CD126 was significantly upregulated over the course of treatment (Figure 4.14(a); p = 0.0279), however there were many outliers at the month 6 time point that may have skewed the outcome since this did not correspond with the ANOVA findings assessing the changes across treatment (p = 0.0672). The nonparametric tests used for comparing groups may not be as strict as the ANOVA which resulted in the significant difference between BL and M6. Lastly, the frequency of CD120b was significantly upregulated between

baseline and the end of treatment (Figure 4.14(c); p = 0.0155; ANOVA p = 0.0338), and there was a significantly greater frequency of these cells at the end of treatment compared to healthy controls (Figure 4.14(c); p = 0.036) suggesting that the expression of CD120b on $CD8^+$ T lymphocytes physiologically perform the same function in active TB cases as what they do in healthy individuals.

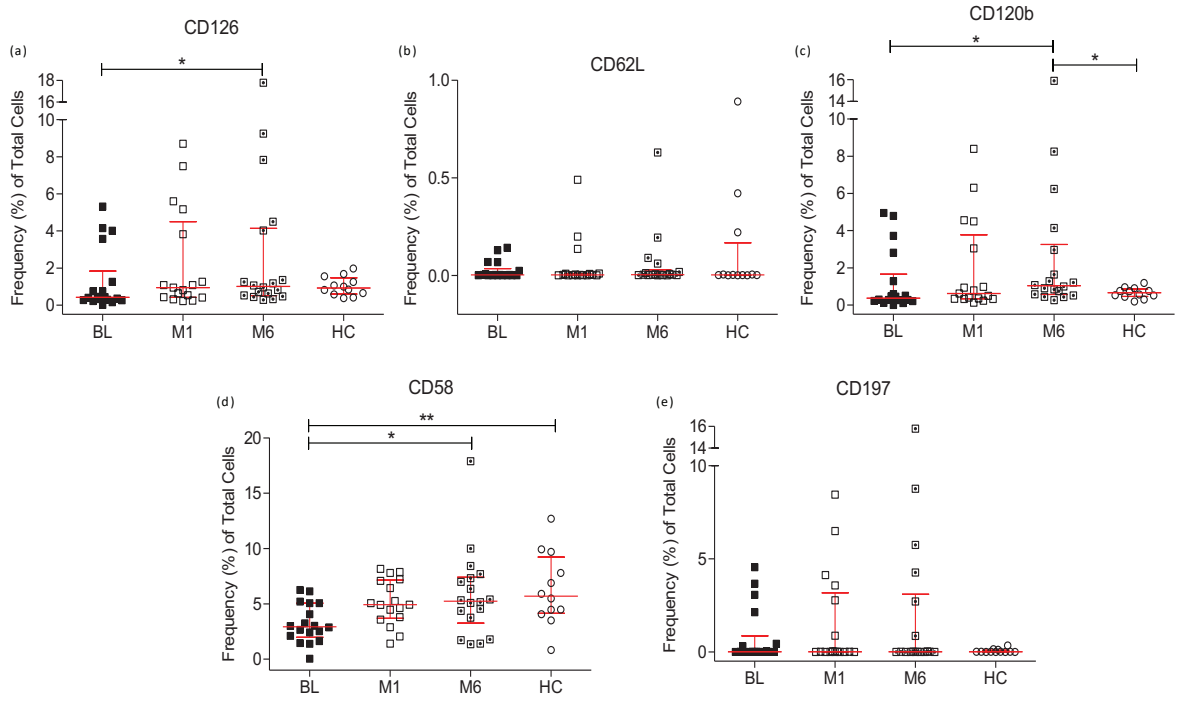

Figure 4.14: Frequency of (a) CD126, (b) CD62L, (c) CD120b, (d) CD58 and (e) CD197 expressing $CD8^+$ T lymphocytes represented as a frequency of total cells at the baseline (BL), month 1 (M1), and month 6 (M6) time points compared to healthy controls (HC). Lines represent the median and interquartile range for each time point.

B lymphocytes

All five markers were assessed in the B lymphocyte population. No differences in expression were seen for CD126 (Figure 4.15(a)), CD120b (Figure 4.15(c)), CD197 (Figure 4.15(e)) or CD58 (Figure 4.15(d)) across treatment or compared to healthy controls. The only marker that was differentially expressed across treatment was CD62L (Figure 4.15(b); p = 0.0176) which was upregulated between baseline and the end of treatment. CD62L expression was also downregulated at baseline compared to the healthy control group (Figure 4.15(b); p = 0.0067).

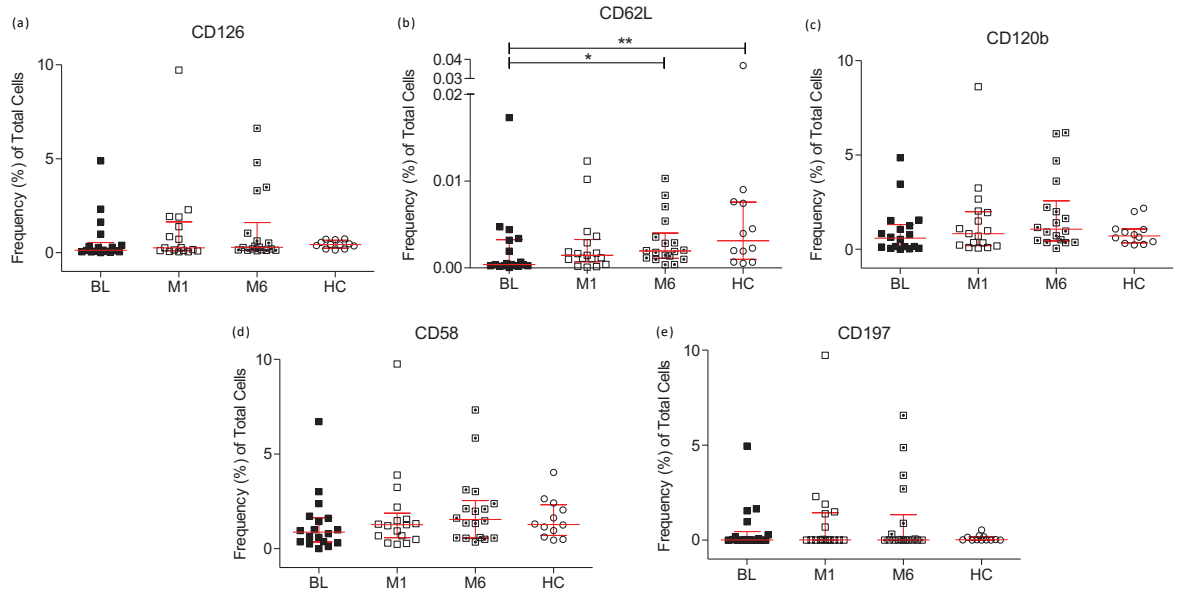

Figure 4.15: Frequency of (a) CD126, (b) CD62L, (c) CD120b, (d) CD58 and (e) CD197 expressing B lymphocytes represented as a frequency of total cells at the baseline (BL), month 1 (M1), and month 6 (M6) time points compared to healthy controls (HC). Lines represent the median and interquartile range for each time point.

Natural Killer cells

Only the three main markers of interest were investigated in the NK cell population. The frequency of CD62L (Figure 4.16(b)) and CD126 Figure 4.16(a)) were not differentially expressed across treatment or compared to healthy controls. The frequency of CD120b, however, was also not significantly different across treatment, but there was a significant downregulation of the marker at baseline compared to healthy controls (Figure 4.16(c); $p = 0.0443$).

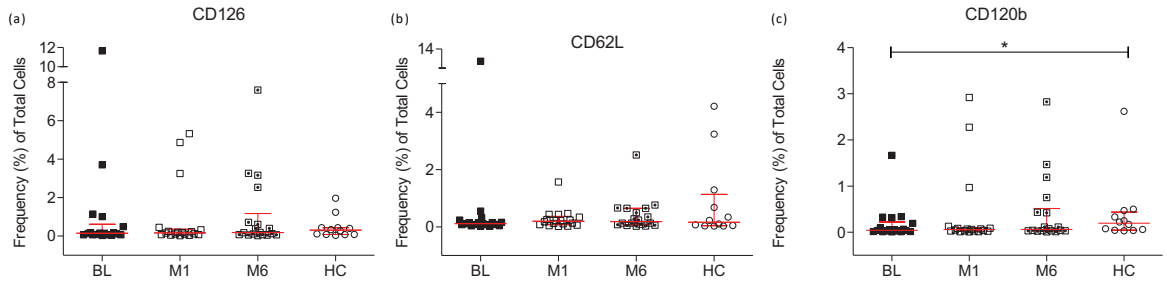

Figure 4.16: Frequency of (a) CD126, (b) CD62L, and (c) CD120b expressing NK cells represented as a frequency of total cells at the baseline (BL), month 1 (M1), and month 6 (M6) time points compared to healthy controls (HC). Lines represent the median and interquartile range for each time point.

Natural Killer T cells

Only the three main markers of interest were investigated in the NKT cell population. None of the investigated markers were differentially expressed in this population across treatment or compared to healthy controls (Figure 4.17(a)-(c)).

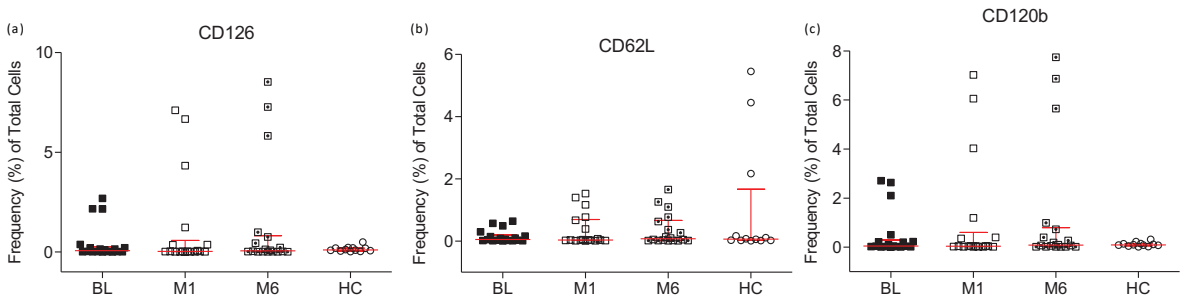

Figure 4.17: Frequency of (a) CD126, (b) CD62L, and (c) CD120b expressing NKT cells represented as a frequency of total cells at the baseline (BL), month 1 (M1), and month 6 (M6) time points compared to healthy controls (HC). Lines represent the median and interquartile range for each time point.

Neutrophils

Only the three main markers of interest were investigated in the neutrophil population. The only marker to not be differentially expressed across treatment or compared to healthy controls was CD120b (Figure 4.18(c)). CD62L and CD126 were not differentially across treatment, but their frequencies were significantly different compared to healthy controls. In the case of CD62L, the frequency was downregulated at the end of treatment compared to healthy controls (Figure 4.18(b); p = 0.0263). In terms of the frequency of CD126, it was observed to be upregulated at the end of treatment compared to healthy controls (Figure 4.18(a); p = 0.0021).

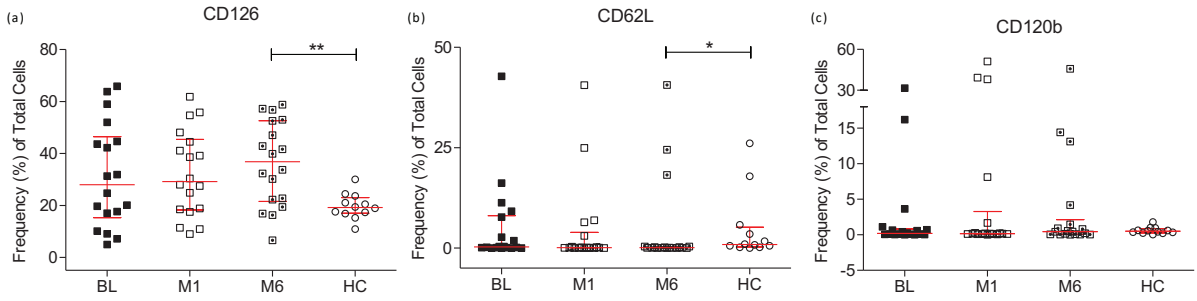

Figure 4.18: Frequency of (a) CD126, (b) CD62L, and (c) CD120b expressing Neutrophils represented as a frequency of total cells at the baseline (BL), month 1 (M1), and month 6 (M6) time points compared to healthy controls (HC). Lines represent the median and interquartile range for each time point.

Intermediate monocytes

Only the three main markers of interest were investigated in the intermediate monocyte population. Frequencies of CD62L (Figure 4.19(b)) and CD126 (Figure 4.19(a)) were not significantly different across treatment or compared to healthy controls, whereas CD120b was significantly upregulated at baseline compared to healthy controls (Figure 4.19(c); p = 0.0263).

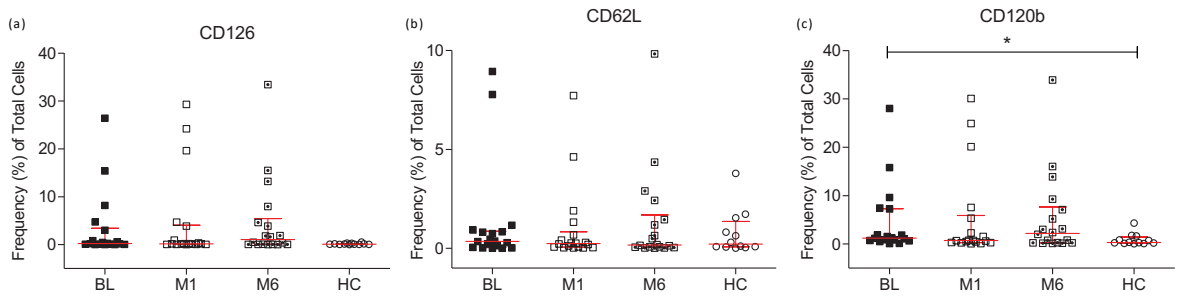

Figure 4.19: Frequency of (a) CD126, (b) CD62L, and (c) CD120b expressing intermediate monocytes represented as a frequency of total cells at the baseline (BL), month 1 (M1), and month 6 (M6) time points compared to healthy controls (HC). Lines represent the median and interquartile range for each time point.

Classical monocytes

Only the three main markers of interest were investigated in the classical monocyte population. There was no significantly different frequency of CD126 (Figure 4.20(a)) across treatment or compared to healthy controls. The frequency of CD62L was also not significantly different across treatment, however it was significantly downregulated at the end of treatment compared to healthy controls (Figure 4.20(b); $p = 0.0466$). The frequency of CD120b was significantly downregulated at baseline compared to healthy controls (Figure 4.20(c); $p = 0.0009$) and there was a visible downregulation trend across treatment, however this was not significant. There was also a significantly higher frequency of CD120b at the end of treatment compared to healthy controls (Figure 4.20(c); $p = 0.0396$).

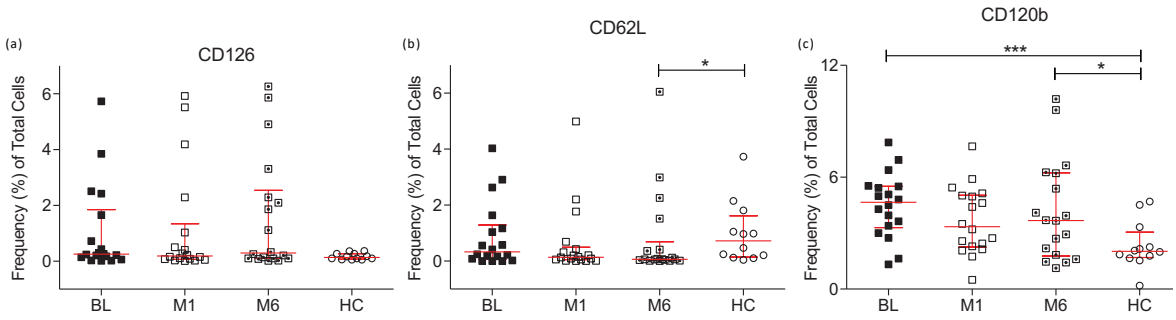

Figure 4.20: Frequency of (a) CD126, (b) CD62L, and (c) CD120b expressing classical monocytes represented as a frequency of total cells at the baseline (BL), month 1 (M1), and month 6 (M6) time points compared to healthy controls (HC). Lines represent the median and interquartile range for each time point.

4.3.6 Comparison between the expression of the markers on all cells and the individual subsets.

In order to compare the median expression frequencies of each marker on all cells and in the individual subsets, the combined median expression of each marker on each subset was calculated for each time point and the healthy controls. The mean frequency of the collective medians was then plotted together with the mean of the median expression of each marker on all cells. It should be noted that these results are for TB patients and healthy controls combined. In addition, we did not investigate all cell types present within the whole blood compartment owing to marker limitations but aimed to highlight which of

the five assessed markers were expressed most on the cell types we could indeed investigate. As a result, the combined average frequency of each marker on each of the subsets did not total the frequency of the marker on all cells. The Mann-Whitney test for nonparametric data was used to compared pairs of subsets with each other, e.g. to compare the median frequency of CD126 expression on B lymphocytes and neutrophils.

Starting with the markers CD58 and CD197, which were only assessed on the surface of $CD4^+$, $CD8^+$ T lymphocytes and B lymphocytes, the median expression frequency was compared between cell subsets and the expression of each marker on all cells. The median frequency of CD58 on all cells was particularly high at 88.83%, while T lymphocyte subsets and B lymphocytes only accounted for 13.21% of this, suggesting high frequencies of CD58 on the surface of granulocytes and monocytes which was unfortunately not assessed (Figure 4.21(a)). $CD4^+$ T lymphocytes expressed the most CD58 compared to $CD8^+$ T lymphocytes and B lymphocytes, the latter of which expressed the least. The differences between both T lymphocyte subsets and B lymphocytes was statistically significant (CD4 vs B $p = 0.0286$; CD8 vs B $p = 0.0286$). The median frequency of CD197 expression on all cells was only 5.82%, of which the assessed subsets only made up 0.09%, again suggesting high expression levels of CD197 on other leukocyte subsets (Figure 4.21(b)). $CD4^+$ T lymphocytes expressed the most compared to both $CD8^+$ T lymphocytes ($p = 0.0286$) and B lymphocytes ($p = 0.0286$), while B lymphocytes expressed significantly more CD197 than $CD8^+$ T lymphocytes ($p = 0.0286$).

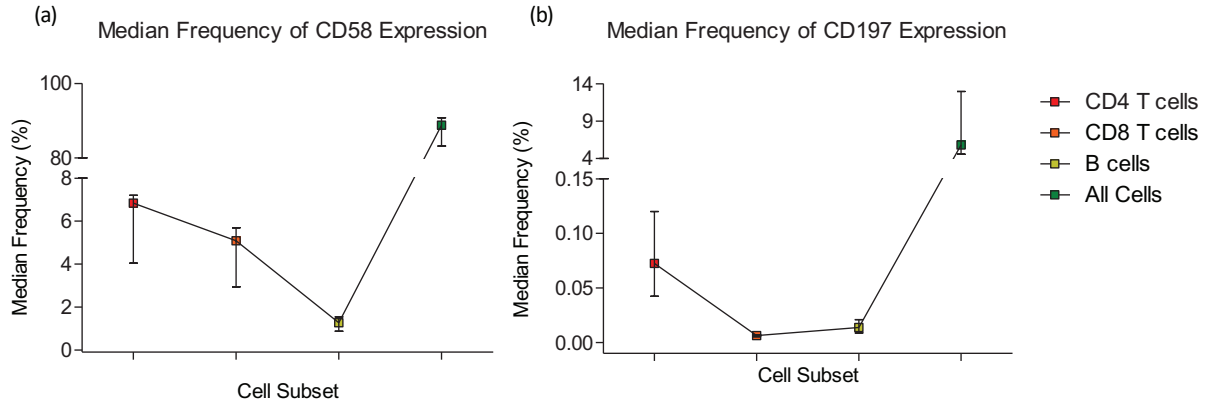

Figure 4.21: The median frequency of expression of the markers (a) CD58 and (b) CD197 which were assessed in the $CD4^+$ T lymphocyte (red data point), $CD8^+$ T lymphocyte (orange data point) and B lymphocyte (yellow data point) subsets, as well as on all cells (green data point). The plotted data points represent the mean, while the lines represent the range.

The markers CD126, CD62L and CD120b, being the markers of interest, were assessed in in the subset populations and compared to median frequency expression on all cells. The median frequency of CD126 on all cells (Figure 4.22(a)) was 70.14%, of which 32.74% was made up by the specific cell subsets investigated in this study. Of note was the significantly larger proportion of CD126 that was expressed on the neutrophil subset (median frequency of 28.29%) compared to all other subsets. The median frequency of CD62L on all cells (Figure 4.22(b)) was 67.91%, however the subsets assessed in this study only made up 0.92% of the total frequency. Lastly, the median frequency of CD120b on all

cells (Figure 4.22(c)) was 75.29%, of which only 7.48% could be accounted for by the subsets assessed in this study. The median frequency of CD120b (3.43%) was significantly higher in classical monocytes than the rest of the subsets, but an increased median frequency was also observed in the intermediate monocyte subset.

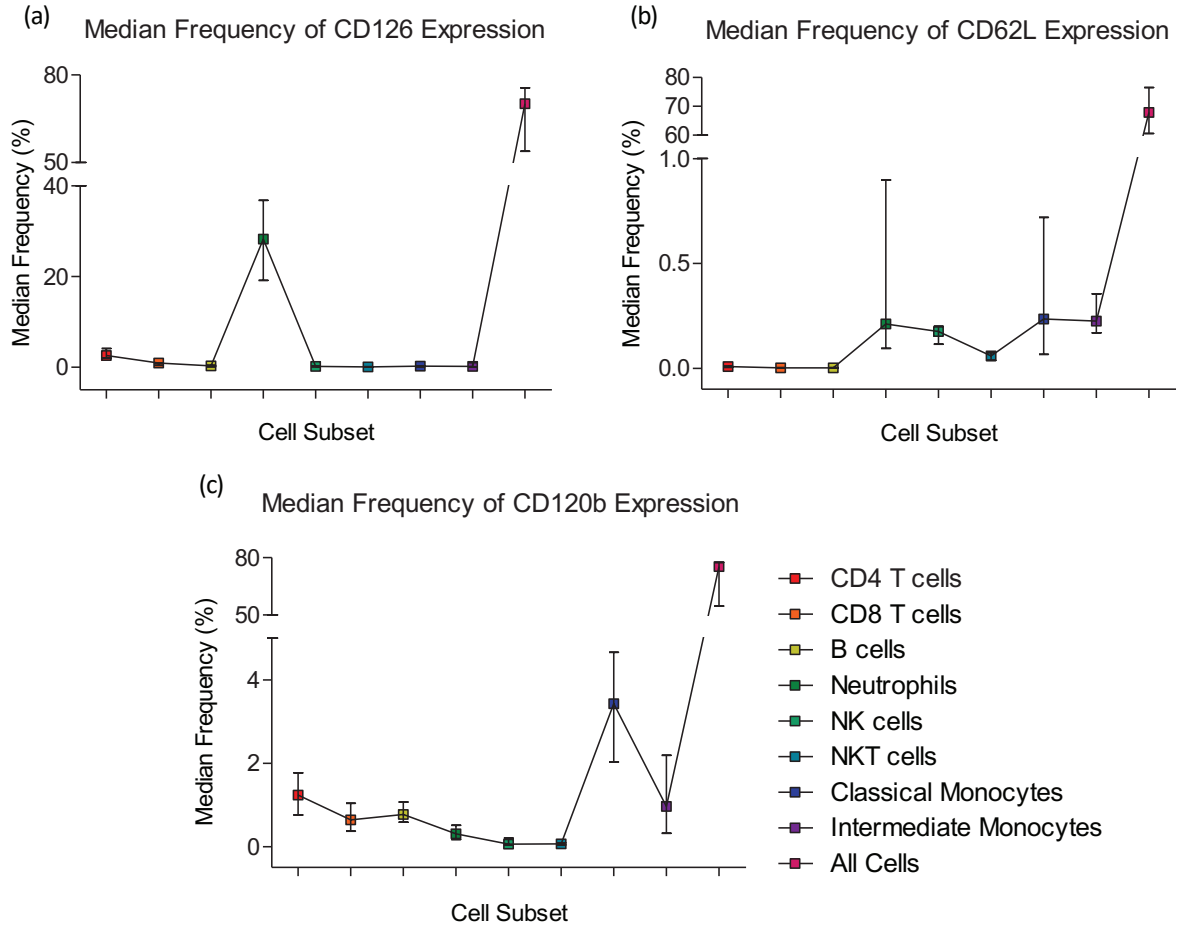

Figure 4.22: The median frequency of expression of the markers (a) CD126, (b) CD62L, and (c) CD120b which were assessed in the CD4⁺ T lymphocyte (red data point), CD8⁺ T lymphocyte (orange data point), B lymphocyte (yellow data point), neutrophil (green data point), NK cell (turquoise data point), NKT cell (light blue data point), classical monocyte (dark blue data point), and intermediate monocyte (purple data point) subsets, as well as on all cells (pink data point). The plotted data points represent the mean, while the lines represent the range.

4.3.7 BD Multitest™ IMK assay absolute counts as surrogate biomarkers for indicators of treatment response.

The same 19 participants recruited for Aim 1 of this study were recruited for Aim 2 and had an additional sample taken at week 2 after treatment initiation to make up four time points for comparison (baseline, week 2, month 1, month 6). Absolute counts were extracted from the software for each participant for the T lymphocyte ($CD3^+CD4^+$ and/or $CD8^+$), B lymphocyte ($CD19^+$) and NK cell ($CD16^+CD56^+$) populations. Both total T lymphocyte ($CD3^+$), cytotoxic T lymphocyte ($CD3^+CD8^+$) and helper T

lymphocyte ($CD3^+CD4^+$) subsets were assessed by the assay, along with immature T lymphocytes ($CD3^+CD4^+CD8^+$), a relatively uncharacterized T lymphocyte population highly upregulated during viral infections. A repeated measures ANOVA combined with Tukey's post-test assessed the variance across the four time points during treatment. Owing to missing data points (see section 4.3.1), six participants had to be excluded from the analysis. No healthy control data was included in the analysis owing to the aim being to investigate treatment-specific responses during active disease. The only subset for which a significant change was observed during treatment was the B lymphocyte subset (Figure 4.23(f); p = 0.0144; ANOVA p = 0.022). None of the other cell subsets displayed a difference in peripheral blood absolute counts during active TB disease.

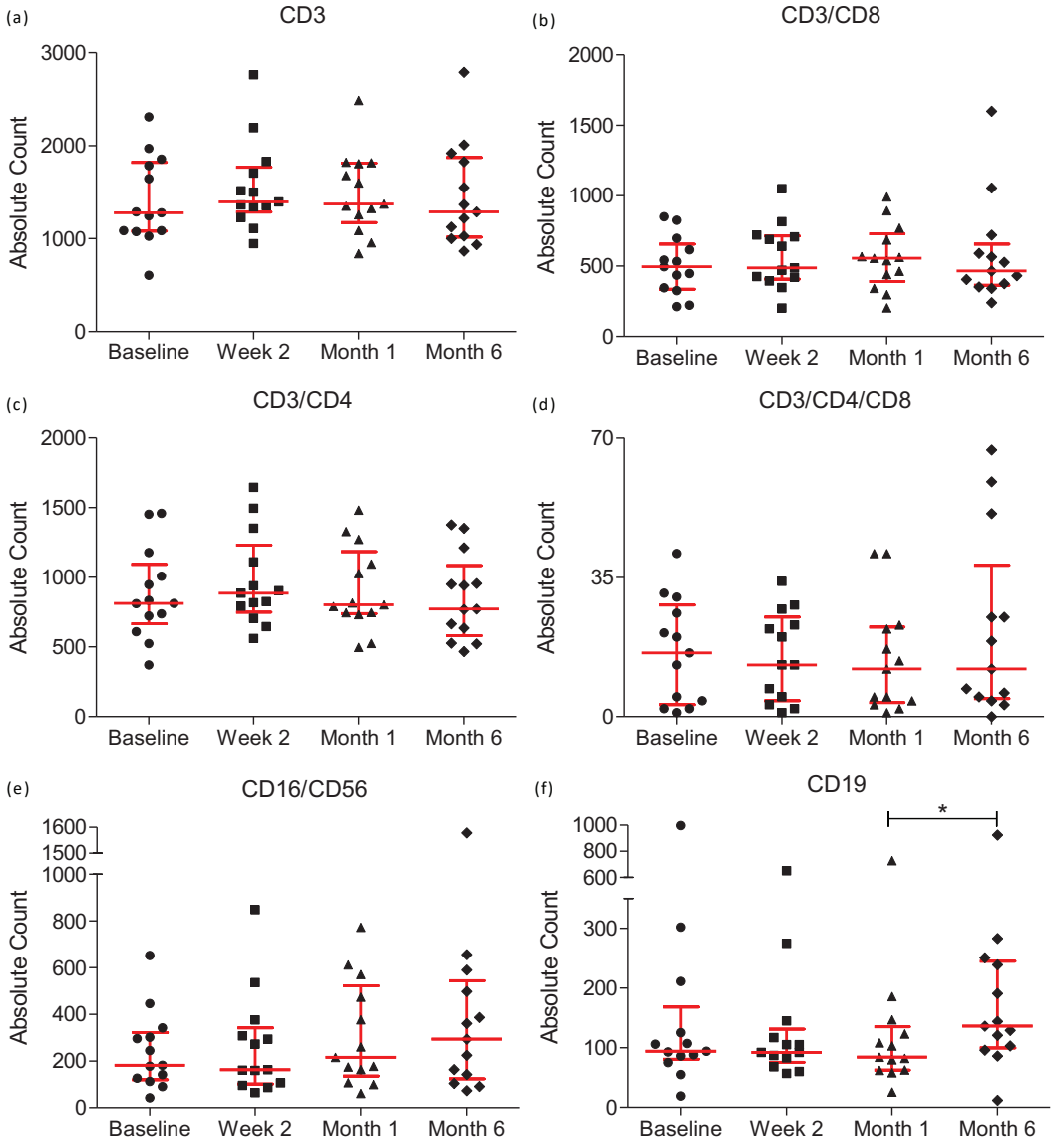

Figure 4.23: Absolute counts of innate and adaptive immune cell subsets as seen in the peripheral blood of thirteen active TB participants at four time points during TB treatment, i.e. baseline, week 2, month 1, and month 6. Assessed subsets included (a) total T lymphocytes, (b) cytotoxic T Lymphocytes, (c) helper T lymphocytes, (d) immature T lymphocytes, (e) NK cells, and (f) B lymphocytes. Lines are representative of the median and interquartile range.

An additional 112 active TB cases and 52 healthy controls were recruited separately from the above-mentioned 19 active TB cases (convenience samples). Samples were only taken at baseline and the end of treatment for these active TB cases. Differences between groups, e.g. BL vs M6, were investigated using the Wilcoxon signed rank test for matched pairs of nonparametric data, while differences between groups compared to healthy controls, e.g. BL vs HC, was assessed using the Mann-Whitney test for nonparametric data. Overall, healthy controls displayed higher median absolute counts compared to most active TB cases at baseline, and this was so for the total T lymphocyte (Figure 4.24(a); $p = 0.0037$), helper T lymphocyte (Figure 4.24(b); $p = 0.0178$), cytotoxic T lymphocyte (Figure 4.24(c); $p = 0.0088$), NK cell (Figure 4.24(e); $p = 0.0459$) and B lymphocyte (Figure 4.24(f); $p = 0.0044$) subsets. The absolute counts for B lymphocytes was significantly higher at the end of treatment compared to baseline (Figure 4.24(f); $p = 0.0017$) which corresponds with the observed response in the smaller cohort that was assessed over more time points (Figure 4.23(f)). Absolute counts of cytotoxic T lymphocyte subsets were also increased at the end of treatment compared to baseline (Figure 4.24(c); $p = 0.0089$), however this result should be interpreted with caution owing to the potentially skewing outliers observed in the Month 6 group. A similar increase in the absolute counts of immature T lymphocytes was observed at the end of treatment compared to baseline (Figure 4.24(d); $p = 0.0314$), but similar outliers could have potentially skewed the comparison outcome.

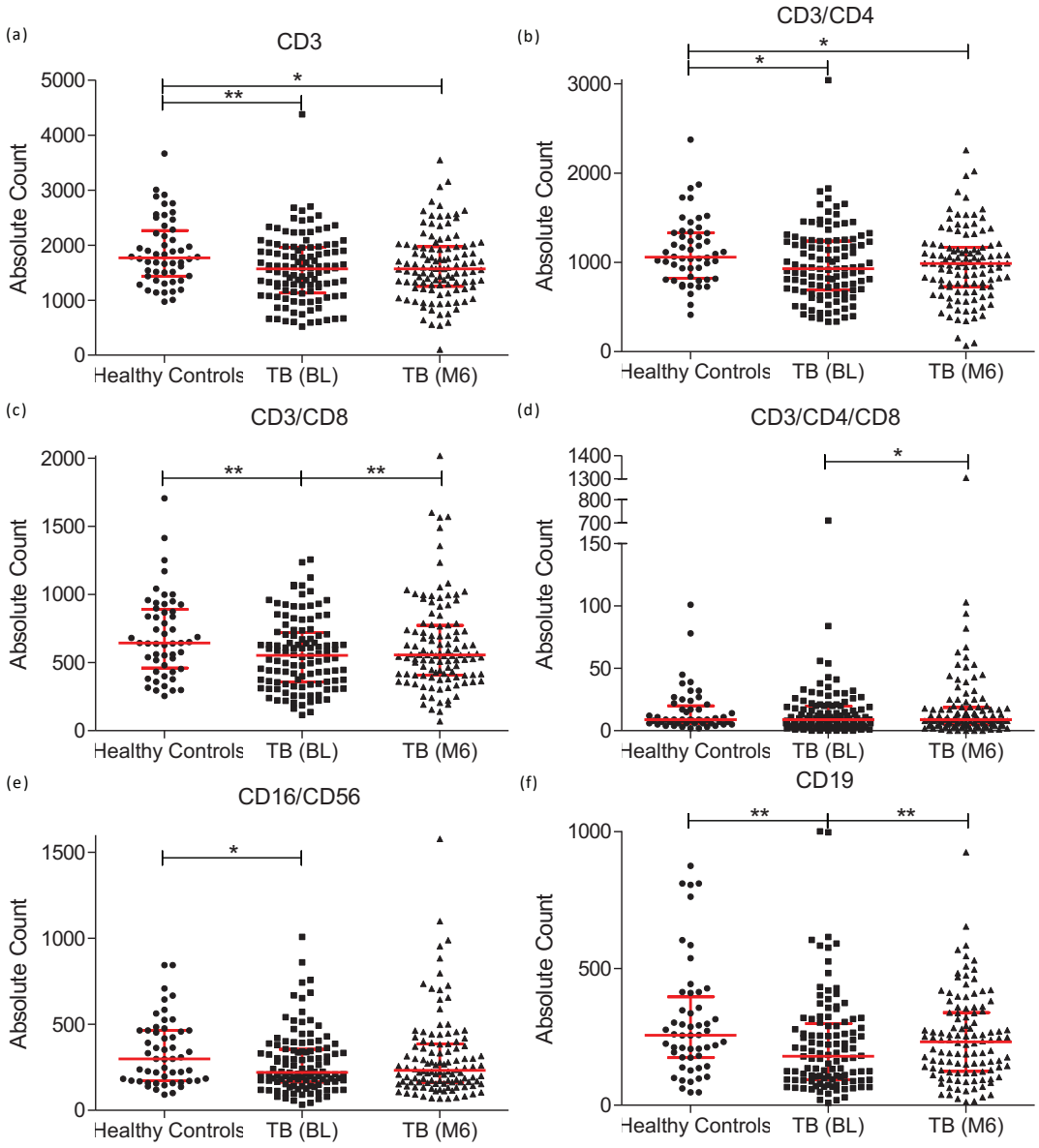

Figure 4.24: Absolute counts of innate and adaptive immune cell subsets as seen in the peripheral blood of 112 active TB participants at two time points during TB treatment, i.e. baseline (BL) and month 6 (M6), as well as 52 healthy controls. Assessed subsets included (a) total T lymphocytes, (b) helper T Lymphocytes, (c) cytotoxic T lymphocytes, (d) immature T lymphocytes, (e) NK cells, and (f) B lymphocytes. Lines are representative of the median and interquartile range.

4.4 Discussion

The outcome classification of an individual's response to treatment for active pulmonary TB disease is normally dependent on the culture status of that individual at the end of the treatment period. The gold standard tool available for the prediction of ultimate favorable or unfavorable outcomes is the conversion of sputum culture from *M.tb* positive to negative after two months of treatment. This technique falls short as a predictor of treatment outcome and treatment response, however it is currently the only available option to have been validated[94]. Sputum culture conversion as a biomarker of treatment response, however, has many shortfalls which include the well-known delay in result generation as well as its limited use in drug-susceptible samples only. In order to overcome the delay in result time, sputum smears for acid-fast bacilli have acted as a surrogate for sputum culture in recent years, but unfortunately have high false positivity rates due to the presence of dead bacteria, which limit their use in clinical settings. It is, therefore, important to investigate alternative methods for the prediction of individual responses to treatment. Blood-based tests that do not rely on the direct detection of the *M.tb* bacilli are attractive alternatives for sputum-based techniques and recent studies in viral infections have supported their use as indicators of treatment response. Such studies have demonstrated that the phenotypes and frequencies of virus-specific $CD4^+$ and $CD8^+$ T lymphocyte phenotypes correlate with viral antigen load, which may be translated into *M.tb*-specific bacterial loads upon further investigation[95,96].

Previous studies have investigated various TB-specific blood-based alternatives with varying success rates. Such alternatives include serum-based studies centered around cytokine secretion[97] and proteomic signatures[98] for the prediction of month 2 culture status and subsequent end of treatment outcome, while others have investigated plasma-based cytokine secretion for the discrimination between fast and slow responders to anti-TB treatment[99]. Interestingly, a study performed by Adekambi *et al*. identified three T cell specific biomarkers ($CD38^+IFN\text{-}\gamma^+$, $Ki\text{-}67^+IFN\text{-}\gamma^+$, and $HLA\text{-}DR^+IFN\text{-}\gamma^+$ T cells) that are capable of discriminating between active TB and latent infection cases, while two of the three ($CD38^+IFN\text{-}\gamma^+$ and $Ki\text{-}67^+IFN\text{-}\gamma^+$ T cells) were capable of monitoring treatment response with substantial decreases in frequencies at the point at which sputum culture converted to negative[37]. While these studies have all proven promising, they are limited by the need for further validation and the lack of consistent sample types being used for biomarker investigations. Additionally, it would appear that the prediction of treatment outcome is complicated by observations that individual variable readouts are not necessarily associated with month 2 culture status. As seen in a study performed by Jayakumar *et al*., combinations of both measurable variables as well as demographic factors, such as age, need to be combined as a biosignature for improved predictive accuracy[97]. The ability to predict an individual's response to treatment at an early time point would provide clinicians with the ability to potentially shorten treatment regimens for those with a favorable outcome or change the treatment regimen early on to include more intensive drugs for those with unfavorable outcomes in order to improve patient adherence and reduce the risk of developing drug resistance.

This study, therefore, aimed to investigate blood-based host biomarkers potentially associated with favorable treatment outcomes that were previously investigated in the FACS™ CAP, proprietary biomarker discovery study. The FACS™ CAP study investigated peripheral blood mononuclear cell (PBMC) surface markers that were differentially expressed during the course of active TB treatment for potential utility in treatment monitoring. In this study, 252 surface markers were investigated on PBMCs in a cohort of 33 active TB patients, 11 healthy community controls and 9 other lung disease controls. Active TB patients were followed up at diagnosis of active TB, week 4 following treatment initiation, and week 24 (end of treatment), whereas control sample collection only occurred at the enrolment visit. They identified three significantly different, PBMC-specific, treatment response markers that were differentially expressed between the time of diagnosis and end of treatment (week 24). These markers were CD126, CD120b, and CD62L, and were the only markers that remained significantly different following Bonferroni correction ($p < 0.01$ in this study). Other promising markers included CD58 and CD197, but these did not retain statistical significance following the Bonferroni correction. The identification of biologically significant markers over the course of active TB treatment spurred further investigation of the most promising biomarkers in a new cohort of active TB patients as well as in more feasible sample types for future translation into clinical settings, from which the study detailed in this chapter was designed.

The three most promising markers (described below) identified by the FACS™ CAP study were investigated, as well as the two additionally promising markers (described below), in heparinized whole blood from a cohort of 19 active TB cases and 12 healthy controls (a mixed population of contact and community controls). This study did not use the proprietary FACS™ CAP technology, but rather employed flow cytometry with customized marker panels. As an additional aim, this study also investigated the use of the commercially available BD Multitest™ IMK Assay as a predictive tool for treatment outcome, through the evaluation of absolute lymphocyte counts for various lymphocyte subsets using the BD FACSCalibur™ flow cytometer.

The five markers of interest and their respective immunological functions.

- **CD126 (IL-6R)**

CD126 is the membrane-bound, α chain of the IL-6 receptor (gp80 subunit), functionally expressed on lymphocytes and hepatocytes[199,200]. This chain of the receptor is not capable of inducing signalling alone and requires dimerization with the gp130 subunit to allow for IL-6-mediated STAT3 signalling to occur. The gp130 protein is ubiquitously expressed on all cell types and allows for IL-6 signalling to occur in cells which lack the expression of the IL-6R (CD126), since the latter subunit is limited to the surface of lymphocytes and hepatocytes, as mentioned above[199]. Alternatively, IL-6 signalling in cells lacking the gp80 subunit of the IL-6R can be mediated through a process known as "*trans*-signalling" during which membrane-bound CD126 is shed from the surface of neutrophils and macrophages by ADAM17 (a Disintegrin and Metalloproteinase; also known as TNF-α converting enzyme (TACE)), and

to a lesser extent ADAM10, to form sIL-6R (reviewed by O'Reilly *et al.*)[199,201]. In such instances, sIL-6R binds IL-6 within the cytosol, and dimerizes with gp130 on target cells for the induction of IL-6 signalling[202,203]. Traditionally, this process of IL-6R shedding is responsible, in part, for the recruitment of monocytes to the site of inflammation via the production of chemoattractants from endothelial cells which have had IL-6 signalling induced[204,205].

IL-6 is a pro-inflammatory cytokine which, along with TNF-α and IL-1β, is critical for the host defence against *M.tb* infection[206]. During the adaptive immune response, IL-12 induces the production of IFN-γ by T_H1 lymphocytes which works in synergy with IL-2 and IL-6 to activate cytotoxic ($CD8^+$) T lymphocytes. Cytotoxic T lymphocytes produce granulysin and subsequently induce the death of infected macrophages, highlighting the important role of IL-6 in the clearance of *M.tb* infection[207]. In addition, IL-6 also induces antigen presenting cells[206], mediates the differentiation of T_H17 lymphocytes and suppresses the development of T_{Reg} lymphocytes[200]. While IL-6 is important for host control of *M.tb* infection, it has been shown to be dispensable for the control of *M.tb* growth; TNF-α is the indispensable cytokine for antimycobacterial effector mechanisms[208,209].

IL-6 is produced by multiple cell types, however, it's receptor is limited to only a few to ensure that IL-6 signalling is tightly controlled to avoid inappropriate immune responses[199,210]. Murine studies have shown that while IL-6R blockade does indeed promote the progression of *M.tb* infection compared to wild-type counterparts, it is far less pronounced or severe than in mice where TNF-α is blocked[207]. These results demonstrate the superior importance of TNF-α over IL-6 in the host defence against *M.tb* infection and suggest that while the IL-6R is important for host control of infection, it does not play as important a role as the TNFR2-TNF-α axis described below.

IL-6R blockers like Tocilizumab (TCZ) are frequently used in inflammatory conditions and autoimmune diseases like rheumatoid arthritis and Crohn's disease since anti-IL-6 monoclonal antibodies (mAb) are ineffective. A study performed by Nish *et al*. clearly demonstrated the T lymphocyte-specific responses to direct deletion of CD126[211]. Mice deficient in the α chain of the IL-6R had significantly impaired T_H1 and T_H17 responses following stimulation with LPS *in vivo*. In addition, these IL-6Rα deficient mice successfully mounted a T_H1 response in the absence of T_{Reg}, however they were unable to develop functional memory subsets which demonstrates the importance of IL-6 signalling in memory T lymphocyte differentiation[211–213]. As such, treatment with IL-6R blockers is strongly discouraged in individuals with previous active TB disease or latent infection owing to the risk of reactivation or progression to active disease. However, in contrast, the knowledge that TNF-α is more important than IL-6 in the defence against TB infection, as well as the evidence that the risk of TB reactivation in rheumatoid arthritis patients is very low in the low-TB prevalence settings where this expensive type of therapy can be used, has prompted many to reintroduce the clinical use of IL-6R blockers irrespective of a patients history with TB disease[207].

- **CD120b (TNFR2)**

Tumour Necrosis Factor Receptor 2 (TNFR2) is expressed exclusively on immune cells and is the second receptor for the pro-inflammatory cytokine, TNF-α; the first is TNFR2's counterpart, TNFR1 (CD120a) which is expressed on all cell types[214]. TNF-α is produced by a variety of immune cells during *M.tb* infection, some of which include alveolar macrophages, dendritic cells, T lymphocytes and B lymphocytes. As a largely pro-inflammatory cytokine, TNF-α is known to be responsible, in part, for the successful isolation of mycobacteria into central organised structures within the lung, i.e. the granuloma. Contrastingly, TNF-α may also act as an anti-inflammatory mediator of immune pathology when over expressed during chronic inflammation/infection. While the pro-inflammatory properties of TNF-α have experimentally been proven to be indispensable for the control of *M.tb* infection and the formation of robust granulomas in the host, the mechanisms behind its anti-inflammatory properties are unknown and many speculate that they may be linked to the membrane-bound form of TNF-α to which CD120b binds[215,216]. As such, CD120b is unable to bind to soluble forms of TNF-α, a function which is exclusive to TNFR1, and can thus not induce macrophage apoptosis which is a key mechanism for host control of *M.tb* infection[215]. TNFR2 does, however, function to activate NF-κβ signalling within host cells for the transcription of protective host factor genes in order to induce pro-inflammatory cellular proliferation[217].

The importance of TNF-α cannot be taken for granted. *M.tb*-infected macrophages are known to release TNF-α in conjunction with IL-12 whereby TNF-α binds to TNF receptors on helper T lymphocytes ($CD4^+$) to induce the production of more TNF-α in addition to IFN-γ. These cytokines then activate infected monocytes/macrophages in tandem to induce the production of antimicrobial products like reactive oxygen intermediates (ROI) and reactive nitrogen intermediates (RNI). These antimicrobial products then aid in the formation of the granuloma[215]. TNF-α has also been shown to induce the activation and differentiation of cytotoxic T lymphocytes ($CD8^+$) for added mycobacterial killing[217]. Mice deficient in TNF-α or its receptors are known to succumb to infection swiftly owing to poor control and highly disorganised granulomatous structures. In contrast, the suppressive activity of TNF-α has also been demonstrated through the blockade of TNFR2 on CD4+ T cells which inhibits the production of IL-2, and instead promotes T_H17 differentiation[218–220]. Like with IL-6R blockers, anti-TNFR therapy is known to reactivate latent TB infection, further highlighting the importance of the TNFR2-TNF-α signalling axis in the host control of *M.tb* infection.

- **CD62L (L-selectin)**

L-selectin is cell adhesion molecule found on the surface of neutrophils, lymphocytes, monocytes, eosinophils and hematopoietic progenitor cells. It is primarily responsible for the homing of naïve T lymphocytes from circulation, through the epithelium to secondary lymphoid organs where antigen presentation occurs[221]. Activation of naïve T lymphocytes results in the loss of L-selectin from its surface via the ADAM17 molecule which cleaves the receptor and allows the activated T lymphocytes to return to circulation and carry out their effector functions[221–223]. L-selectin is also a marker of T lymphocyte

memory; the expression or lack thereof discriminates between two distinct memory T lymphocyte subsets, namely central memory T lymphocytes (T_{CM}; $CD62L^+CD197^+$) and effector memory T lymphocytes (T_{EM}; $CD62L^-CD197^-$)[221,224,225]. As is evident, memory subset phenotypes are also dependent on the expression of the marker CD197 (CCR7) which is described below. In terms of myeloid cell expression, L-selectin is known to be involved in the migration of neutrophils to the site of *M.tb* infection in the same way activated T lymphocytes return to circulation to carry out effector functions. In order for neutrophils to migrate to the site of infection, L-selectin is cleaved from the surface which allows for the rapid production of reactive oxygen species (ROS)[226]. Studies have shown that neutrophils of human origin that are exposed to *M.tb* have reduced L-selectin expression on their surface; this is proposed to be indicative of activated neutrophil degranulation[227].

- **CD197 (CCR7)**

CD197, also known as CCR7 (C-C chemokine receptor type 7), is characteristically a marker expressed on the surface of T lymphocytes, specifically on the memory subsets. As mentioned previously for L-selectin, CD197 expression is investigated in conjunction with L-selectin to define the central memory (T_{CM}; $CD62L^+CD197^+$) and effector memory (T_{EM}; $CD62L^-CD197^-$) T lymphocyte subsets, and functions in the migration of naïve T lymphocytes to secondary lymphoid organs[221,224]. $CD4^+$ and $CD8^+$ T lymphocytes that express CD197 are known to produce large amounts of IL-2 in order to drive antigen-specific T lymphocyte differentiation which is consistent with literature definitions of T_{CM} effector functions[223]. The T_{EM} subset is known to produce cytokines like IFN-γ, while the T_{CM} subset is known to produce mostly IL-2, and TNF-α to a lesser extent[228–230]. CD197 has also been found to be expressed on the surface of dendritic cells and appears to be responsible for their migration during infection[231]. Knockout studies in mice have described scenarios in which CD197 deficient mice are fully capable of controlling *M.tb* infection irrespective of the increased inflammatory environment this induced[232]. Many human studies involving memory markers have focused on antigen-specific $CD8^+$ T lymphocyte responses. Recent findings have characterized active TB disease by the expansion of T_{CM} and T_{EM} phenotypes, while latent infection has been characterized by terminally differentiated ($CD45RA^+CD197^-$) memory phenotypes[48]. Other studies have observed a reduction of CD197 expressing cells at the site of infection, which reflects the findings for L-selectin and suggests a successful migration and activation of naïve T lymphocytes to secondary lymphoid tissues[233].

- **CD58**

CD58 is the marker for lymphocyte function associated antigen 3 (LFA-3), a costimulatory molecule expressed on the surface of antigen presenting cells, including macrophages and mature dendritic cells, and responsible for strengthening adhesion between cells. CD58 is the ligand for the surface marker CD2 (LFA-2) which is expressed on the surface of T lymphocytes and NK cells. Binding of CD58 to CD2 initiates strong adhesion between professional antigen presenting cells and T lymphocytes, in an antigen-independent manner. This induces the expansion of naïve T lymphocytes and the production of large amounts of IFN-γ from memory T lymphocytes[234]. It is suggested that this large release of IFN-

γ may upregulate the expression of additional costimulatory and cell adhesion molecules like B7 and intercellular adhesion molecule 1 (ICAM-1) respectively, allowing for the magnification of the immune response due to simultaneous activation of multiple adhesion pathways[235]. To support this, studies have shown that the co-expression of B7 and CD58, and their respective ligands, on the surface of antigen presenting cells and T lymphocytes enables optimal antigen presenting functions and a more potent immune response to smaller amounts of available antigen[235,236].

Studies on the expression of CD58 during *M.tb* infection have observed a more dominant function for this marker in dendritic cells. Hanekom *et al*. observed an upregulation of CD58 on the surface of dendritic cells following infection of human monocyte-derived dendritic cells with virulent strains of *M.tb*, as did Henderson *et al*.[237,238]. This upregulation was accompanied by the upregulation of other costimulatory and cell adhesion markers like MHC I and II, CD40, CD54, and CD80, as well as the increased production of proinflammatory cytokines (IL-12, IL-6, IL-1, and TNF-α). Interestingly, the expression of CD58 has been identified on the surface of type II pneumocytes during *M.tb* infection, cells which are known to be invaded by *M.tb* bacilli and support their replication and growth[239–242]. This suggests that type II pneumocytes are capable of binding to CD2-expressing NK cells or T lymphocytes present in the lung at the site of infection to either support or suppress immune responses. However, it is more reasonable to speculate a more immunosuppressive function of CD58-expressing pneumocytes owing to the evidence that type II pneumocytes harbor and promote *M.tb* replication, and can induce cytokine patterns suggestive of T_{Reg} expansion[243].

Comparison between the FACS™ CAP findings and those from this study.

As mentioned previously, the FACS™ CAP study identified three biomarkers, CD126, CD120b and CD62L, that were significantly downregulated at the end of treatment compared to the time of diagnosis after the Bonferroni correction. Two additional markers, CD58 and CD197, were also significantly up- and down-regulated at the end of treatment compared to the time of diagnosis, respectively. Since this study investigated the expression of markers on the surface of PBMC, we compared the findings to the expression of the five markers on all cells acquired by the flow cytometer, i.e. all immune cells present in peripheral whole blood that survived the cryopreservation process.

Where the markers CD126, CD120b, CD62L, and CD197 were observed to be downregulated at the end of treatment compared to at the time of diagnosis in the FACS™ CAP study, the study performed for this thesis observed no change in marker frequencies over the course of treatment. If one had to disregard the large outliers within the data for CD197, there was in fact an observed upregulation of the marker after the initiation of treatment compared to the time of diagnosis, contrary to previous findings. CD62L expression was lower after the initiation of treatment compared to the time of diagnosis but was not significantly so ($p = 0.06$). Considering this, CD62L should not be excluded from future studies since the smaller sample size in this study likely limited a fair representation of this marker in terms of significance. CD58 was the only investigated marker that displayed a significant change during the course of treatment. Whereas the only promising marker in the FACS™ CAP study that was

upregulated between diagnosis and the end of treatment, our study showed significant downregulation of CD58 at the end of treatment compared to baseline levels (Figure 4.12(a); p = 0.0153). Based on the literature summarized above for CD58, the downregulation of this marker over the course of standard anti-TB treatment may be representative of immune reconstitution following successful treatment.

The contrasting findings between the two studies could be explained by one of the following reasons:

- The difference in sample preparation methods and sample types. The FACS™ CAP study made use of BD's proprietary combinatorial antibody profile technology for the investigation of isolated PBMC, whereas our study simply made use of lysed whole blood, which would contain more immune cells that isolated PBMCs since the Ficoll-Hypaque isolation technique would exclude granular immune cell populations.
- Sample size variation. Our study did not have the same number of active TB participants (19) compared to the FACS™ CAP study which recruited 33. While the differences in sample size would not explain the contrasting results seen for the markers CD58 and CD197, it could explain the statistically not significant differences observed for the markers CD62L, CD126 and CD120b.

In order to successfully translate laboratory methods and findings into simple, readily available clinical tools one first needs to simplify the sample to be used so as to prevent long turnaround times and the need for skilled laboratory staff and equipment on site. Using whole blood instead of PBMC is, therefore, a much more applicable sample type on which to optimize future tests for clinical translation which is why this study investigated the differences in findings between the two sample types. We suggest that results generated from enriched cellular fractions, such as PBMC, would not be suited for screening studies aimed at identifying potential treatment response markers as these studies should ideally be performed using the sample intended for use in the clinical setting. Although the aim of this study was not to validate the FACS™ CAP findings, but to evaluate the cells of origin of the markers of interest, the results shown here conclude that the expression of the five evaluated markers do not change during treatment at the three assessed time points (diagnosis, month 1 and month 6). Future studies might investigate the use of a combination of these markers as indicators of early treatment response (indication of treatment response at the month 1 time point) but the value of these markers as treatment response indicators is questionable. What our study did aim to investigate was which subsets of immune cells these five markers of interest were being expressed on and at what frequency compared to overall expression of the markers on all cells.

Identification of immune cell subsets responsible for the expression of the five markers of interest during active TB disease and in healthy controls.

We investigated the expression of the markers CD126, CD120b, CD62L, CD58 and CD197 on the most well-defined immune cell subsets found in whole blood over the standard treatment regimen period. These included both $CD4^+$ and $CD8^+$ T lymphocytes, B lymphocytes, NK cells, NKT cells, neutrophils,

classical monocytes and intermediate monocytes, and their frequencies were assessed at the time of diagnosis (BL), one month following treatment initiation (M1) and the end of treatment (M6). Frequencies of each marker expressed on each subset in active TB participants were compared over treatment, as well as between the time of diagnosis and healthy control frequencies (BL vs HC). Healthy control frequencies for each marker on each subset were also compared to frequencies observed during active TB disease at the end of treatment (M6 vs HC). The expression of CD58 and CD197 was only investigated on the surface of T lymphocytes and B lymphocytes owing to fluorochrome restrictions in the flow cytometer available for use, i.e. the BD FACS Canto II is only able to assess eight markers at a time which limits the number of markers of interest that can be included after lineage markers have been decided upon.

The most surprising finding of this study is the fact that none of the five markers assessed were differentially expressed between the time of diagnosis (BL) and the month 1 time point which was the original hope. This is likely as a result of the small sample size, especially compared to the parent study which recruited 33 participants compared to the 19 recruited in this study. The difference in marker expression could be small enough that the cohort used for this study was not large enough to pick up on and this is a limitation. The most important finding of this study is that of the five markers assessed, the median expression frequencies of CD58 and CD120b were the only two to change significantly over the course of treatment, and only on the surface of $CD4^+$ and $CD8^+$ T lymphocytes.

The finding that CD58 is expressed on the surface of cells that traditionally are supposed to express its ligand, CD2, was interesting. Literature suggests that CD58 is a costimulatory molecule expressed only on the surface of antigen presenting cells in order to enhance cellular adhesion between antigen presenting cells and effector cells[234–236,244]. Contrasting findings from studies in chronic inflammatory diseases, like rheumatoid arthritis, have highlighted a function for CD58 as a memory marker on a recently identified subset of adaptive immune memory T lymphocytes called stem cell-like memory T lymphocytes (T_{SCM})[245–247]. These naïve-appearing T_{CM} lymphocytes ($CD62L^+CD197^+CD45RA^+CD45RO^-$) express activation markers like CD95, CD122 as well as CD58, and develop as a result of mammalian target of rapamycin (mTOR) inhibition which induces a change in T lymphocyte metabolic state to that of fatty acid oxidation[245,248]. Unfortunately, we were unable to report on this population frequency since neither of the panels included the CD45RA or CD45RO markers which are essential for distinguishing this population from T_{CM} populations. The large proportion of unexplained CD58 expression, as seen in the frequency of CD58 expression on all cells, is likely explained by the antibody panel design. In hindsight, CD58 should have been included in the second panel investigating innate immune cells but was excluded on the basis of too little space owing to the number of lineage markers required for this panel. The finding that the frequency of CD58 expression only changes over the course of TB treatment in $CD4^+$ and $CD8^+$ T lymphocytes supports the recent literature finding that CD58 is indeed expressed on T lymphocytes. Since our findings display an upregulation of CD58 over the course of treatment on both subsets, this suggests that both $CD4^+$- and $CD8^+$-specific T_{SCM} lymphocyte populations are being produced following successful anti-TB

treatment. Unfortunately, this study was unable to investigate the frequency of these cells owing to the lack of the CD45RA and CD45RO memory markers which are necessary for their classification. Should future studies investigate this population further, this phenotype would be a novel finding for the monitoring of treatment response, and it would be a novel target for vaccine development, especially because this phenotype has been shown to persist in circulation for decades, as seen by Fuertes Marraco and colleagues studying a yellow fever vaccine[248].

The significant change in CD120b expression over the course of TB treatment identified in the FACS™ CAP study was inversely represented in this study in that where the FACS™ CAP study reported a downregulation of the marker over treatment, we identified an upregulation of CD120b expression on both $CD4^+$ and $CD8^+$ T lymphocyte subsets over standard treatment. We were successfully able to identify the cell subsets which were responsible for the significant change, i.e. $CD4^+$ and $CD8^+$ T lymphocytes. However, while the frequency of CD120b expression was significantly different over the course of treatment for these subsets, the majority of CD120b expression was in fact accounted for by the classical monocyte subset. Classical monocytes are a subset of monocytes that express the traditional CD14 monocyte lineage marker, but not the marker CD16, the expression of which differentiates intermediate ($CD14^+CD16^+$) and non-classical ($CD14^-CD16^+$) monocytes from classical monocytes ($CD14^+CD16^-$)[249,250]. Classical monocytes perform primarily phagocytic functions compared to intermediate and non-classical monocytes which function primarily to produce inflammatory mediators and patrol the vascular system, respectively. Classical monocytes are also characterised by their potent antimicrobial capabilities and their production of antimicrobial agents such as ROS and IL-10[250,251]. It is, therefore, easy to state that classical monocytes are the effector monocyte subset during *M.tb* infection and elicit the defensive mechanisms of the innate immune system. During the early stages of infection, monocytes are the main producers of TNF-α, and subsequently express both TNFR1 and TNFR2 on their surface[252]. While the function of TNFR2 expression has been contested, a recent study by Gane *et al*. has supported the hypothesis that TNFR2 expression on the surface of classical monocytes is responsible for the upregulation of anti-inflammatory cytokines, like IL-10, while the TNFR1 is responsible for the upregulation of pro-inflammatory cytokines[249,252,253]. They also noted the ability of TNFR2 to bind soluble TNF-α in addition to membrane-bound TNF-α, contrary to all previous literature we investigated. This suggests that, while the median frequencies of CD120b expression on classical monocytes is not significantly different over the course of anti-TB treatment, the inflammatory environment of an individual with active TB disease is strongly characterised by phagocytes polarised towards an M2 phenotype, likely to control immediate tissue damage resulting from chronic *M.tb* infection. It is interesting that this classical monocyte subset should be polarised towards an M2 macrophage phenotype since current literature supports the hypothesis that non-classical monocytes are responsible for differentiation to the M2 phenotype. Literature does suggest, however, that there may be a mechanism by which classical monocytes may also differentiate into M2 macrophages, but this has yet to be elucidated[251,254].

In terms of the comparisons between healthy controls and active TB patients at the BL and M6 time points, CD197 did not display any significant change between the groups and there were no observable

differences in expression frequencies between active TB patients and healthy controls. Based on the median frequency of CD197 expression, as identified in Figure 4.21(b), the expression of CD197 is very low in the lymphocyte population of peripheral blood. These findings are supported in literature, as T_{CM} lymphocytes responsible for CD197 expression are known to be restricted to the lymphoid organs of the immune system which would prevent us from identifying them within whole blood[255–258]. Expression differences between healthy controls and active TB patients at diagnosis were observed for both the $CD4^+$ and $CD8^+$ T lymphocyte subsets, and in both instances the healthy control participants had significantly higher levels of CD58 expression compared to active TB patients. This suggests that healthy, uninfected individuals have a larger proportion of T_{SCM} lymphocytes than cases of active TB disease that have not yet started treatment. Based on these and previously mentioned findings, monitoring the expression of CD58 on the surface of $CD4^+$ and $CD8^+$ T lymphocyte subsets could be very useful for the monitoring of response to treatment. Coincidentally, CD58 was the only marker for which there was a significant difference between healthy controls and active TB participants at baseline for the $CD4^+$ and $CD8^+$ T lymphocyte subsets. Only the marker CD120b on the surface of $CD8^+$ T lymphocytes was significantly different between healthy controls and active TB cases at the end of treatment where healthy controls had significantly less CD120b expression. This supports our previous findings and literature that CD120b (TNFR2) may be predominantly responsible for anti-inflammatory functions. A steep increase in the expression of CD120b at the end of treatment suggests that $CD8^+$ T lymphocytes are performing tissue repair functions following the clearance of chronic *M.tb* infection. The B lymphocyte subset was the only lymphocyte subset to significantly display a difference in CD62L expression between active TB patients at diagnosis and the end of treatment, as well as between active TB patients at diagnosis and healthy controls. While the difference between active TB patients at diagnosis and the end of treatment was comparatively significantly different ($p = 0.0176$), the change in expression of CD62L across treatment time points was not significant ($p = 0.0667$). Future treatment monitoring studies should not exclude the expression of CD62L on the surface of B lymphocytes, as the low sample size of this study may have resulted in a near-significant result, which warrants its further investigation, as discussed previously. Considering the observation that the expression of CD62L on the surface of B lymphocytes increases at the end of treatment, reflecting healthy control levels of CD62L-expressing B lymphocytes, further supports this further investigation as the return of marker expression levels to those seen in uninfected cases provides an indication of the restoration of adaptive immunity. Additionally, the increased expression of CD62L on B lymphocytes indicates the restoration of memory B lymphocyte populations[259,260].

Innate immune cell subsets investigated in this study also included NKT cells which were the only subset to **not** display any significant change in any of the markers. NKT cells are a population of CD1d-restricted, unconventional T cells that respond to antigen presented by the CD1d major histocompatibility complex class I (MHC I) receptor. The antigens presented by this receptor are specifically lipids, glycolipids or highly hydrophobic peptides which induce the production of immunoregulatory cytokines[25–27]. Upon further investigation of the literature, NKT cells do not express the CD120b, CD126 or CD58 surface markers, but do express CD197 and CD62L to a lesser extent.

Unfortunately, CD197 was not able to be investigated on this subset during flow cytometric analyses due to our marker panel design, however we were able to assess CD62L expression. The available research on the NKT cell population is very limited owing to its relatively recent discovery. Data that is available has identified the presence of these cells predominantly within the thymus, as well as its scarcity within draining lymph nodes, which supports our finding that CD62L expression is very low since CD62L controls homing to the lymph nodes[28]. Other studies have also demonstrated a significantly low presence of NKT cells during active TB disease specifically which would further support this study's inability to properly characterise their phenotype[25].

NK cells only displayed one significantly different comparison between healthy controls and active TB patients at the time of diagnosis. Here, the frequency of CD120b-expressing NK cells was higher in the healthy control group. While NK cells are known to express CD120b, literature suggests that its expression is upregulated on NK cells during chronic inflammatory conditions, such as HIV infection[261]. However, a recent study published by Chowdhury *et al.* reported that NK cell frequencies are upregulated during latency only, and decrease during active disease, disputing the expansion of NK cells during chronic inflammatory conditions[24]. Other studies have indicated that CD120b is an important signal transducer involved in TNF-α and IL-2 induced NK cell differentiation[262]. Our observation that active TB patients have lower CD120b-expressing NK cells is, therefore, supported by Chowdhury *et al.*'s findings, considering that approximately 58% of our healthy control cohort was documented as being latently infected. The neutrophil subset displayed significant differences in the frequency of both CD126 and CD62L between active TB patients at the end of treatment and healthy controls. In this instance, healthy controls had fewer CD126-expressing neutrophils, but more CD62L-expressing neutrophils than active TB patients at the end of treatment. This can be explained by the function of CD62L in neutrophils. Healthy controls would have more CD62L-expressing neutrophils since they have not yet been activated by exposure to *M.tb* in the lungs and attracted to the lymph nodes where CD62L would be shed prior to neutrophils returning to circulation.

When considering the phenotypes predominantly responsible for the five markers assessed (Figure 4.21(a) and (b), Figure 4.22(a), (b) and (c)), both CD58 and CD197 expression is highest on the surface of $CD4^+$ T lymphocytes, however they do not account for the total CD58- and CD197-expressing cells found within whole blood as was identified when all cells were assessed. Possible cell types which could alternatively be expressing CD58 have already been discussed. Since T lymphocytes are the cellular population responsible for the majority of memory phenotypes within the immune system, alternative subsets that could be responsible for the expression of CD197 in peripheral blood may include dendritic cells and neutrophils, even though the former is present at very low numbers in peripheral blood. Following dendritic cell activation at the site of infection, the expression of CD197 is significantly upregulated, allowing for their migration to the T cell area of draining lymph nodes. Likewise, the migration of antigen-stimulated neutrophils to draining lymph nodes is strictly dependent on the expression of CD197, allowing neutrophils to traffic to the T cell zones of the lymph node[263–266].

The neutrophil subset is responsible for the majority of CD126 expression, while classical monocytes are responsible for the majority of CD120b expression (discussed previously). Neutrophils are known to express high levels of the IL-6R on their membrane surface, primarily so that ADAM17-mediated shedding of the receptor can occur for the production of sIL-6R. The sIL-6R form of CD126 is then able to bind IL-6 within the cytosol and subsequently interact with a variety of different cell types that express gp130, thereby inducing IL-6 signalling in cells that do not express CD126 via the process of *trans*-signalling. IL-6 *trans*-signalling is firstly activated via the apoptosis of *M.tb*-infected neutrophils, which subsequently activates ADAM17 and the signal transducer and activator of transcription (STAT)3 molecule, an essential regulator of antiapoptotic genes[203,205]. Monocyte recruitment then ensues, which suggests that the high expression of CD126 on neutrophils circulating in the peripheral blood of active TB patients is a precursor for the monocyte recruitment that is to follow once the circulating neutrophils finally reach the lung. Our findings, therefore, are supported by literature. Neutrophil subsets should, according to literature, not exist in circulation without the expression of CD126, since neutrophil apoptosis is the trigger for CD126 shedding. Lastly, the neutrophil and classical monocyte subsets are responsible for the expression of CD62L. This finding is not unexpected, since both subsets are known to express CD62L in order to home from circulation to the site of disease in order to encounter the invading pathogen. At this point, neutrophils and classical monocytes are activated and CD62L is cleaved via ADAM17, allowing the activated cells to carry out their effector functions.

Despite efforts to identify novel alternatives for biomarkers of treatment response, it would appear that the assessment of biomarkers on the surface of $CD4^+$ and $CD8^+$ T lymphocyte subsets still hold the most promise. Since these subsets are the most important for a successful host response to TB, this is not surprising. Efforts should, therefore, be made to investigate novel biomarkers on these subsets during the course of anti-TB treatment. Alternatively, the genes associated with CD58- and CD120b-specific immunological pathways could be investigated in the context of *M.tb*-specific $CD4^+$ and $CD8^+$ T lymphocytes. Recent advances in the prediction of treatment outcome have arisen largely from host blood RNA signatures such as those developed by Thompson *et al*. in which a five-gene host biosignature based on host responses to anti-TB therapy was developed[267]. This biosignature was capable of accurately assessing pulmonary inflammation, as measured by PET-CT, as well as near perfect discrimination of patients in whom treatment failed from patients who were cured. Thompson and colleagues subsequently demonstrated significant improvements in GeneXpert treatment failure prediction when used in conjunction with the five-gene biosignature, supporting the feasibility of treatment outcome prediction tools at the point-of-care level. We, therefore, suggest further investigation of the markers that displayed the most promise in this study on a surface marker level, as well as the genes involved with these markers and their immunological signalling pathways during active TB disease. With data available from such large consortia, assessing potential future gene signatures in large, multi-site cohorts would be very feasible and resource friendly.

Investigation of commercially available diagnostic reference tools for the enumeration of immune subset counts as a measure of response to treatment.

The enumeration of lymphocyte percentages and absolute counts are common practice in the characterization and monitoring of some autoimmune disease and immunodeficiencies like severe-combined immunodeficiency (SCID) syndrome and HIV/AIDS, respectively. These enumerations are frequently performed using the BD Multitest^{TM} IMK assay, which is intended for the identification and quantification of the percentages and absolute counts of various human lymphocytes, including T lymphocytes, B lymphocytes and Natural Killer cells. Since both innate and adaptive cell subsets are known to be reduced and/or impaired during active TB disease, it was hypothesized that the absolute counts generated from a readily available and well validated commercial product could provide a means of monitoring treatment response during active TB disease.

Absolute counts of T lymphocyte ($CD3^+CD4^+$ and/or $CD8^+$), B lymphocyte ($CD19^+$) and NK cell ($CD16^+CD56^+$) populations were investigated for nineteen participants at the baseline, week 2 (W2) after treatment initiation, month 1 (M1) after treatment initiation, and month 6 (M6, end of treatment) time points. For the T lymphocyte populations, total T lymphocyte ($CD3^+$), cytotoxic T lymphocyte ($CD3^+CD8^+$) and helper T lymphocyte ($CD3^+CD4^+$) subsets were assessed by the assay, along with immature T lymphocytes ($CD3^+CD4^+CD8^+$), a relatively uncharacterized T lymphocyte population known to be highly upregulated during viral infections[268,269]. An additional 112 active TB participants and 52 healthy controls were assessed at the BL and M6 (end of treatment) time points only.

None of the assessed populations displayed any change in absolute counts over the course of standard anti-TB treatment when four time points were assessed. Median absolute counts appeared to trend upwards in the NK cell ($CD16^+CD56^+$) subset over the course of treatment, however this did not reach significance (Figure 4.23(e)). The B lymphocyte subset did, however, display a significant difference in median absolute counts between the M1 and M6 time points (Figure 4.23(f)), suggesting a significant rise in the number of circulating B lymphocytes following successful treatment completion.

We had the opportunity to assess the assay in a larger cohort of active TB disease patients at diagnosis (BL) and end of treatment (M6) only and compared absolute counts to those identified in healthy control populations. Due to the substantially larger sample size, we were better able to identify differences between the start and end of anti-TB treatment. We previously mentioned an upward trend in the NK cell subset across the four time points during anti-TB treatment, however with the larger sample size there was no significant difference between the time of active TB diagnosis and the end of treatment for this subset. Consistent with our findings across the four time points, there was a significant increase in the absolute number of B lymphocytes at the end of treatment, which was comparable to healthy control levels as supported by the significant decrease in absolute B lymphocyte counts at the time of diagnosis compared to healthy controls (Figure 4.24(f)). Recent studies have identified such an increase of B lymphocytes at the end of anti-TB treatment, specifically activated memory phenotypes expressing FasL[259,260,270]. These B lymphocytes were shown to perform regulatory functions, possibly

for the control of tissue damage following chronic inflammation, and while FasL was not assessed in this study, it is possible that the increase of activated memory B lymphocyte frequencies is driving the increase in absolute counts seen in this study[259].

Comparisons of the absolute counts of total T lymphocytes and the $CD4^+$ and $CD8^+$ subsets identified in active TB disease cases between those identified in healthy controls highlighted an overall reduction of these subsets during active TB disease at the time of diagnosis, which did not return to healthy control levels at the end of treatment. Based on previous work by Malherbe and colleagues using PET-CT imaging techniques, the inflammatory environment within the lungs of active disease patients is not always resolved following successful treatment, indicating that although adherent patients may successfully complete the standard treatment regimen, there may remain a population of bacilli within lung lesions that continue to induce inflammatory responses[271]. While these lesions have shown to resolve after prolonged follow up in most cases, the evidence that metabolically active lesions persist in the lung even after successful treatment would support our findings of reduced circulatory T lymphocyte subsets following treatment completion due to continued T lymphocyte activation. Owing to the nature of this study, investigation of PET-CT scans was not within the scope.

Based on the findings from this study, the use of the BD Multitest™ IMK assay would not be a feasible option for the monitoring of response to anti-TB treatment. We propose that a larger cohort, as was available for the diagnosis and end of treatment comparisons, may have provided stronger evidence for possible relationships between the four time points assessed. This, however, was outside the scope of the larger study for which the BL and M6 only samples were collected. B cells do appear to have an important function in TB and this was also highlighted in gene expression studies during TB treatment, where B cell pathways feature strongly during the later stages of treatment[86,267].

Limitations

In order to truly identify treatment response biomarkers, relapse needs to be taken into consideration. Our study only reported 1 treatment failure which prevents the determination of the original objective. This is a limitation of this study as there was not sufficient time to conduct a large-scale study with many more participants and a lengthy follow-up time period required to pick-up relapse cases. Most studies employ a minimum 2-year follow-up period to identify enough relapse cases to ensure a well-powered study. In addition to this, approximately 7% of all active disease cases relapse, and in the case of this study, no relapse cases would not be identified.

Lastly, since the markers investigated in this study did not display the same pattern of expression change over the course of treatment as the FACS™ CAP study, this study could not successfully achieve the original aim as none of the markers changed in expression by the month 1 time point.

Concluding Remarks

This study did not observe significant changes between any of the five markers investigated over the course of anti-TB treatment, except for the marker CD58 which significantly decreased between diagnosis and the end of treatment. Additionally, there were no significant changes for any of the markers assessed between diagnosis and month 1 following treatment initiation or between month 1 and the end of treatment when investigating the various immune subsets, suggesting that the month 1 time point in this instance was not useful as an early indicator of response to treatment. When investigating the subsets, however, this study did observe a significant change in the markers CD58 and CD120b in both the $CD4^+$ and $CD8^+$ T lymphocyte subsets over the course of treatment. These findings elude to the close relationship between the innate and adaptive arms of the immune system, particularly the role of TNF-α bridging the gap between the two. The innate immune response to active TB disease has been relatively under-researched compared to the adaptive counterpart. This is understandable since active TB disease control and clearance requires the robust effects of the adaptive response. We, therefore, propose further research into the innate immune response against *M.tb,* as this arm of the immune system clearly plays an important role in determining the adaptive immune response and the eventual outcome of infection. The following chapter will attempt to separate the assessment of responses of the innate and adaptive immune systems in addition to investigating their combined effect.

CHAPTER 5

Evaluation of the Contribution of Individual Leukocyte Subsets Towards the Overall Immune Response.

Chapter 3 and 4 of this dissertation have illustrated differential expression of both acute phase/innate cytokines and surface markers on innate immune cell subsets. Specifically, Chapter 3 validated the performance of an innate, two-biomarker biosignature in an adult population with active TB disease and concurrent infection with *Ascaris lumbricoides (Ascaris),* an intestinal parasite. Previous work in children has illustrated the differential expression of several acute phase/innate cytokines and chemokines between *Ascaris* infected and uninfected, as well as cytokines and chemokines from the adaptive immune response, after overnight antigenic stimulation with *M.tb* antigens. The differential expression profile was found to be able to discriminate between *Ascaris* infected vs *Ascaris* uninfected individuals (unpublished data). Likewise, Chapter 4 identified the differential expression of various surface receptors, involved primarily in innate immunity, on the surface of innate immune subsets between participants with active TB disease and healthy controls. These subsets included neutrophils, NK cells, intermediate monocytes, and classical monocytes. Additionally, only the $CD4^+$ and $CD8^+$ T lymphocyte subsets displayed any significant change in surface marker expression over the course of anti-TB treatment, highlighting the long-term importance of the adaptive immune response, yet still maintaining the importance of the innate system in the mechanism of adaptive immune activation. This was accomplished through the markers differentially expressed on these two subsets over the course of treatment, namely CD58 and CD120b. The upregulation of both markers on the surface of adaptive immune cells during the course of treatment, we speculate, could be representative of inadequate bacterial clearance, leading to the upregulation of receptors responsible for lymphocyte migration and pro-inflammatory-mediated signalling, respectively.

Considering the predominance of the innate immune system in our findings and the support from previous studies, the cytokine contribution of the subsets identified in Chapter 4 need to be further investigated in order to investigate the mechanism behind the differential cytokine production observed in innate immune cells. We propose that this could be done by examining peripheral white blood cells from healthy, yet latently infected individuals to evaluate whether this differential expression is due to direct activation of innate cell subsets by *M.tb* antigen, or if it can be attributed to innate immune cells responding to antigen-specific T cells that have been sensitized to *M.tb* antigen.

5.1 Study Design

Hypothesis

We hypothesise that the differential expression of innate immune response proteins in an antigen-specific manner in reaction to *M.tb* antigens is dependent on the presence of both innate and adaptive leukocyte subsets.

Aims

The aim of this study is to evaluate and compare the differential expression profiles of various innate cytokines in culture conditions with single white blood cell subsets and combinations of such subsets, in order to determine the contribution of each leukocyte subset to the cytokine signature. This work did not focus on *Ascaris* worm exposure but merely evaluated the ability of different cell populations to produce specific cytokines.

Objectives

- Isolate innate cell subsets (monocytes and neutrophils) and T cells from the peripheral blood of 3 QFT positive and 3 QFT negative individuals.
- Perform a QuantiFERON-TB Gold In-Tube test (only the Nil and Antigen tubes) using the gold standard 1ml heparinised peripheral blood (representative of all subsets and their respective ratios), as well as 1ml of each individually isolated cell subset and/or combination of cells.
- Perform a Luminex immunoassay using the supernatants from the whole blood and the various isolated cell cultures following overnight QFT stimulation to determine the cytokine expression profile of each condition and compare the individual cell results and cell combinations.

5.2 Methods

5.2.1 Participant Recruitment

In order to perform this pilot study, healthy adult volunteers from the laboratory who were between the ages of 18 and 65 were recruited after giving written, informed consent. Three volunteers who tested QFT positive, and three who tested QFT negative were recruited; all were from Stellenbosch University, Faculty of Medicine and Health Sciences, Tygerberg, Cape Town, and assigned a unique participant identifier.

Ethical Considerations

Ethical approval was obtained from the Human Research Ethics Committee of Stellenbosch University under the ethics number: N13/05/064. This study was performed in accordance with the Helsinki Declaration.

5.2.2 Reagents and Buffers

The reagents listed in Table 5.1 were prepared and used for the completion of this study. These include MACS Buffer for MACS® isolation, 4% paraformaldehyde for the fixation of cells, 2% FACS buffer for flow cytometry, and cryomedia for the cryopreservation of live and fixed cells.

Table 5.1: General reagents prepared for use during this study, their manufacturers and catalogue numbers.

	Volume:	Manufacturer:	Catalogue Number:
MACS Buffer (Filter Sterilised)			
1X PBS (ml)	4000	LONZA™	BE17-517Q
2mM EDTA (g)	2.98	Sigma-Aldrich	
0.5% BSA (g)	20	Sigma-Aldrich	A7030
4% Paraformaldehyde (PFA)			
1X PBS (ml)	30	LONZA™	BE17-517Q
16% PFA (ml)	10	Thermo Scientific	28908
FACS Buffer (2%)			
1X PBS (ml)	49	LONZA™	BE17-517Q
HyClone™ FCS (ml)	1	GE Healthcare Life Sciences	SV30160.03
FACS Buffer with 4% PFA			
1X FACS Buffer (2%) (ml)	7.5	N/A	N/A
16% PFA (ml)	2.5	Thermo Scientific	28908
Cryomedia (10% DMSO with 90% FBS)			
HyClone™ FCS (µl)	900	GE Healthcare Life Sciences	SV30160.03
DMSO (µl)	100	MERCK	317275-500ML
Red Blood Cell (RBC) Lysis Buffer			
dH_2O (ml)	450	N/A	N/A
10X RBC lysis buffer (ml)	50	BioLegend	420301

Supplemented RPMI

Supplemented RPMI was prepared from normal RPMI-1640 media (Sigma-Aldrich, Catalogue number: R8758-500ML) to which 1% L-glutamine and 2% FCS was added.

Purity Determination Antibodies

Details of the antibodies used for the determination of the isolated cell subset purities are given in Table 5.2. Owing to single stains being used for each participant and condition (each FACS tube would only have **one** single antibody added to it for the purpose of purity checks), it was not necessary to select fluorochromes which had the same emission spectrum, i.e. using a PE-labelled antibody for both CD3 and CD14.

Table 5.2: Details of the Antibodies used for the Determination of Cell Subset Purities.

Antibody	Manufacturer	Clone	Catalogue Number	Lot Number
CD3-PE	BD Biosciences	UCHT1	300408	B137334
CD14-PE	BD Biosciences	MϕP9	345785	71304
CD15-FITC	BD Biosciences	HI98	301904	B138473

5.2.3 Laboratory Procedures

From each participant, approximately 20ml of whole blood was collected into sodium heparinised vacutainers and processed using the QuantiFERON-TB Gold In-Tube assay (Qiagen®, Maryland, USA) within two hours of blood draw. Each sample was then divided for experimental purposes as follows:

- 2mL of whole blood were kept aside in one of the heparinised vacutainers for later distribution into a QuantiFERON (QFT) Nil and QFT Antigen (Ag) tube (1ml whole blood into each), and
- The remaining 18mL of whole blood was used for a Peripheral Blood Mononuclear Cell (PBMC) isolation.

Peripheral Blood Mononuclear Cell (PBMC) Isolation

PBMC's were isolated from the collected peripheral whole blood using the Ficoll-Paque PLUS Density Centrifugation technique (GE Healthcare Life Sciences, United States). Briefly, NaHep vacutainers were inverted five times and whole blood diluted in a sterile 50ml Falcon tube at a ratio of approximately 1:1 with sterile 1X PBS, not exceeding 35ml in total. The diluted blood was then slowly pipetted over 15ml of Ficoll without disturbing the Ficoll layer, and centrifuged at room temperature (RT) for 25 minutes at 400 x g with brake and acceleration off. Following centrifugation, the plasma was aspirated and discarded, while the PBMC layer was aspirated into a separate 50ml Falcon tube and washed once with 50ml sterile 1X PBS at 400 x g for 10 minutes. The remaining red blood cell pellet was **not** discarded, but put aside for further processing, as explained later. The supernatant was discarded and the pellet re-suspended in the remaining liquid, after which it was washed for a second time in 10ml filter sterilized MACS® buffer (1X PBS, FCS, 0.5M EDTA). The pellet was re-suspended in 10ml MACS® buffer and the cells counted using a haemocytometer and ZEISS microscope (ZEISS, Germany). To prepare the cells for counting, 10µl of the cell suspension was added to 40µl Trypan Blue (Thermo Fisher Scientific, United States) to obtain a 1 in 5 dilution.

Before proceeding, approximately 50µl of the PBMC fraction and 50µl FACS buffer with 4% PFA was set aside in a 5ml FACS tube for later purity checks using flow cytometric analysis. The PBMC fraction was then used to isolate $CD14^+$ monocytes and $CD3^+$ T cells using the MACS® MicroBead isolation technique (Miltenyi Biotec, Cologne, Germany).

MACS® MicroBead Isolation

The principle of MACS® isolation is to magnetically label target cells with antibodies, referred to as MicroBeads, specific to cell populations and to load this suspension into a MACS® column which is placed in a magnetic field created by a MACS® Separator. The magnetically labelled cells are retained within the column and the unlabelled cells pass through unhindered and this fraction is depleted of the target cell. The column is then removed from the MACS® Separator so that the retained cells can be

eluted into separate tubes as the positively selected, pure fraction. This technique can be used for positive selection or depletion (negative selection – where the cells of interest are unlabelled).
The MACS® isolation technique required that all reagents be pre-cooled to 4°C, all equipment pre-cooled to -20°C and the cells kept cold (on ice during processing or incubated at 4°C) to prevent non-specific capping of the antibodies and non-specific binding of the antibodies to the cell surface. The manufacturer's instructions for the technique were followed.

Column Specifications:
As mentioned above, the MACS® isolation technique uses MACS® columns to separate the cell suspension via magnetic fields. Each column has a different capacity for both input and output of cells and as such the column choice should be event-specific owing to the varied number of cells obtained per isolation. For this study either an MS or LS column was used depending on the total number of cells isolated after the PBMC isolation (Table 5.3).

Table 5.3: MACS® Column specifications for the MS and LS column types used for positive selection.

	MS Columns		**LS Columns**	
	Max No. Labelled Cells	Max No. Total Cells	Max No. Labelled Cells	Max No. Total Cells
Manual Use	1 x 10^7 cells	2 x 10^8 cells	1 x 10^8 cells	2 x 10^9 cells
Prime	500µl		3ml	
Wash	3 x 500µl		3 x 3ml	
Rinse	1ml MACS® Buffer		5ml MACS® Buffer	

Where necessary, i.e. where there were too many cells for the LS column even, the samples were split into two and run in two separate columns to ensure the highest possible number of cells were retrieved.

Isolation 1 – CD14 positive cells
CD14 positive cells were isolated using the PBMC fraction and CD14 microbeads. The protocol is given in brief below. The isolated cells were counted after isolation, purity check fractions taken and processed, and the remainder kept on ice before continuing with the experiment. At least 2.5 x 10^6 $CD14^+$ monocytes needed to be isolated in total for the experiment.

Staining Procedure:
The manufacturer's instructions in the product insert were followed for each microbead type, e.g. CD14 microbeads, as well as for the columns.
Briefly, following the centrifugation step at the end of the PBMC isolation, the entire supernatant was aspirated using a P200 pipette without unsettling the pellet and leaving no residual volume. If a residual volume of MACS® buffer remained behind, it was estimated and taken into account for the following addition of MACS® buffer up to 60µl. If no residual volume remained behind, 60µl MACS® buffer was added to resuspend the pellet, followed by 20µl CD14 microbeads per 7 x 10^6 cells. This was incubated

in the fridge (4°C) for 20 minutes, after which 2ml MACS® buffer was added per 7 x 10^6 cells and centrifuged at 445 x g for 10 minutes at RT without the brake. The supernatant was again carefully aspirated but leaving behind approximately 1-2mm of residual volume to avoid cells loss. The pellet was re-suspended in 500µl MACS® buffer and briefly kept on ice while the magnetic separation was set up.

Magnetic Separation:

A new column (chosen according to the cell count of each individual isolation as described above) was placed in the magnetic field of the MACS® Separator and primed according to the column specifications in Table 3. The cell suspension was added to the column and the unlabelled cells collected in a 15ml Falcon tube. The column was then washed according to Table 3, each time adding the MACS® buffer only when the column reservoir was empty. These cells were the CD14 negative fraction and kept on ice to be used for the isolation of CD3 positive cells. The column was removed from the MACS® Separator, inserted into a clean 15ml Falcon tube and rinsed according to Table 3 using the plunger and MACS® buffer to elute the positively labelled CD14 cells. A cell count was performed, as before, and purity fractions taken, before continuing with the experiment. For the purity check, approximately 50µl of the fraction was removed into a FACS tube along with 50µl FACS buffer (2% Fetal Calf Serum (FCS) in 1X PBS) containing 4% Paraformaldehyde (PFA) fixative for later purity checks by fluorescent antibody staining and flow cytometric analysis using the FACS™Canto II instrument (Becton Dickinson, New Jersey, USA).

Isolation 2 – CD3 positive cells

CD3 positive T cells were isolated from the CD14 negative cell fraction that remained following isolation 1 using the exact same procedures with the exception of the use of CD3 microbeads. These cells were counted after being isolated, had purity check fractions taken and processed, and the remainder kept on ice before continuing with the experiment. At least 5.5 x 10^6 $CD3^+$ T cells needed to be isolated in total for the experiment.

<u>Red Blood Cell Lysis and Neutrophil Isolation</u>

Using the red blood cell (RBC) fraction kept aside during the PBMC isolation, 4ml of the top layer of the red blood cell pellet was carefully aspirated through the remaining Ficoll-Paque layer into **four** clean 50ml Falcon tubes (1ml red blood cells into each) for the isolation of neutrophils. To this, 50ml of RBC lysis buffer was added and mixed with the red blood cells by inverting the tubes. The dilutions were incubated on ice for 10 minutes, then centrifuged at 300 x g for a further 10 minutes at 10°C. The supernatant was carefully aspirated from each tube with a 25ml pipette as the red blood cell pellet is very sensitive to decanting, followed by the addition of 1ml 1X PBS to each tube to resuspend the pellets. The contents of the four tubes were then combined into one and washed twice with 50ml 1X PBS, centrifuging at 300 x g for 10 minutes at 10°C, carefully removing the supernatant after each wash. After the second wash, the pellet was resuspended in 1ml MACS® buffer, 50µl removed for

purity checks (as described previously), the cells counted and kept on ice briefly until further use. At least 8 x 10^6 neutrophils needed to be isolated in total for the experiment.

5.2.4 QuantiFERON-TB Gold In-Tube Stimulations

In order to assess the contribution of each leukocyte subset to the overall cytokine release observed in whole blood, the whole blood and isolated cell subsets were stimulated using the QuantiFERON-TB Gold In-Tube assay (Qiagen®, Maryland, USA) for the comparison of their *M.tb*-specific cytokine profiles.

The QuantiFERON-TB Gold In-Tube (QFT) assay, simply put, is an overnight stimulation whole blood assay used to asses *M.tb* infection status through the measurement of *M.tb* antigen-specific responses, and employs the use of three primary tubes: the "Nil" (unstimulated), "Antigen" (Ag) and "Mitogen" (Mit) tubes. A pre-determined manufacturer cut-off value is used to determine positive or negative infection classifications. The Nil tube provides an unstimulated sample so as to act as the negative control – the tube lining remains free of any *M.tb*-specific antigens. The Ag tube is lined with a cocktail of *M.tb*-specific antigens, namely ESAT-6, CFP10 and TB7.7. The cocktail lining concentration is specific for the stimulation of exactly 1ml of whole blood, and represents the *M.tb*-specific response mounted by the host. Alternatively, the Mit tube is lined with phytohaemagglutinin (PHA) and provides a positive control for the assay, indicating whether or not the assay was successful. QFT tubes are generally incubated for 18-24 hours at 37°C and 5% CO_2, after which they are centrifuged at 2500 x g for 15 minutes (room temperature), and the supernatants harvested.

This technique was adjusted for this study to accommodate the use of single cell subsets, and is described below.

<u>QuantiFERON Stimulation of Whole Blood, Monocytes, Neutrophils, and Lymphocytes</u>

As described above, the QFT assay employs three different tubes. However, for this study, only the Nil and Ag tubes were used since the assay was not being used for clinical diagnostics, and the participants were already cognizant of their current QFT status. As 1ml of whole blood is added to standard QFT tubes, this study aimed to use the expected number of specific cell subsets that are found in 1ml of whole blood for each stimulation. For instance, literature estimates that for every 1ml of peripheral blood, approximately 1.25 x 10^6 lymphocytes ($CD3^+$ T cells) are present, therefore, in order to investigate the contribution of lymphocytes to the overall cytokine production observed in whole blood, 1.25 x 10^6 lymphocytes were used per QFT tube. The total number of each cell subset required per isolation, as well as the target number of each cell subset per stimulation, are given in Table 5.4. The number of cells required per isolation was increased to accommodate the loss of cells for purity checks and cytospin.

Table 5.4: The number of cells required per stimulation and in total for each isolated cell subset.

	Number of Stimulations*:	**Number of Cells per Stimulation:**	**Total Number of Cells Required:**
Whole Blood	2	N/A	N/A
Monocytes ($CD14^+$)	4	5 x 10^5 cells	2.5 x 10^6 cells
Lymphocytes ($CD3^+$)	4	1.25 x 10^6 cells	5.5 x 10^6 cells
Neutrophils	2	3 x 10^6 cells	8 x 10^6 cells

*Number of stimulations includes both unstimulated and stimulated tubes (Nil and Ag respectively).

Each cell subset had both an unstimulated (Nil) and stimulated (Ag) condition, for which 1ml of either whole blood or cell suspension was required. In order to make up the required number of cells for each QFT tube, the volume to be removed was calculated for each subset based on the haemocytometer cell counts, and this volume transferred into a fresh 15ml Falcon tube. The cells were then centrifuged at 400 x g for 10 minutes, the pellet resuspended in 2ml of supplemented RPMI. Other than the individual cell subset stimulations, the study included a condition that combined monocytes and lymphocytes, again using the estimated cell numbers reported in the literature. Once all of the cell subsets were isolated, 1ml of whole blood was transferred into a QFT tube, while the isolated subsets were resuspended in 1ml RPMI per stimulation and added to the respective QFT tubes. The tubes were then incubated overnight for 20 hours at 37°C (5% CO_2), not centrifuged, and the supernatants harvested into 2 x 150µl aliquots which were stored at -80°C until use.

The remaining cells were gently resuspended in fresh supplemented RPMI and transferred into fresh 15ml Falcon tubes labelled accordingly.

<u>For the whole blood:</u>

The cells transferred from the whole blood QFT tubes were first lysed to remove the red blood cells by adding 10ml of FACS Lysing solution (contains a fixative). The cells were gently mixed and incubated in the dark for 10 minutes. The cells were washed twice with 1X PBS, centrifuging at 400 x g for 10 minutes after every wash.

<u>For the cells resuspended in RPMI:</u>

PFA fixative (4%) was added in a 1:1 ratio to the cells transferred from the cell subset QFT tubes gently mixed and incubated in the dark for 10 minutes. The cells were also washed twice with 1X PBS, centrifuging at 400 x g for 10 minutes after every wash.

1ml of cryomedia was then added to all cells in a dropwise fashion, the cells transferred to a cryovial and stored in a Mr Frosty at -80°C overnight.

5.2.5 Cytospin Imaging for Assessment of Isolated Population Morphology

In order to visualize the isolated cell subsets, the cytospin technique was used to concentrate cells on to a fixed point on a glass microscope slide before being stained with the RapiDiff staining method. The RapiDiff method is a simple, fast method by which to visualize basic cell morphology under a light microscope. Briefly, approximately 20µl of isolated cells (these included monocytes, $CD3^+$ T cells and neutrophils), that remained after the correct number of cells were removed for stimulation in the QFT tubes, was added to 980µl 1X PBS in a 2ml Eppendorf. A cytocentrifuge was used in which microscope slides were placed in at an angle, after being placed in a slide holder together with filter paper and a plastic funnel through which the cell suspension was added. The 1ml of cells were added to the funnel and the cytocentrifuge spun at 95 rpm for 7 minutes with slow acceleration. The slides were left to air-dry for 15 minutes before staining.

The dry cytospin slides were stained using the Rapi-Diff (Clinical Sciences Diagnostics, Johannesburg, South Africa) staining technique. Each slide was first placed in the fixative solution for 30 seconds, and allowed to air-dry. Slides were then placed in the eosinophilic stain for 25 seconds and allowed to air-dry. Lastly, each slide was placed in the basophilic stain for another 25 seconds, followed by a wash step in 1X PBS. Each slide was allowed to air-dry overnight before 1 drop of VectaMount™ mounting medium (Vector Laboratories, California, USA) was placed on the cells and a cover slip placed on top. This allowed for oil-immersion magnification at 1000X on a ZEISS microscope (ZEISS©, Germany) fitted with an Axiocam MRc 195 microscope camera (ZEISS©, Germany); images were taken using the ZEN lite 2012 (blue edition, version 1.1.1.0) imaging software (ZEISS©, Germany).

5.2.6 Purity Determination using Flow Cytometry

Sample Staining

Following the PBMC isolation and the MACS® isolation of the $CD14^+$ and $CD3^+$ cells, and the neutrophils, 50µl of each cell fraction was placed in separate 5ml FACS tube, as mentioned previously, along with 50µl FACS buffer containing 4% PFA. Each tube was incubated for 10 minutes in the dark at room temperature (RT), the cells washed once with 1ml FACS buffer and centrifuged at 300 x g for 10 minutes (RT). The supernatant of the isolated cell subsets was discarded and the cells resuspended in 50µl FACS buffer. For the PBMC fraction, however, the cells were resuspended in 400µl FACS buffer and 100µl distributed into four separate FACS tubes (Table 5.5), after which the cells were centrifuged at 400 x g for 5 minutes, the supernatant discarded, and the pellet resuspended in 50µl FACS buffer. Each Falcon tube was stained according to the strategy given in Table 4 below. The cells were stained for 30 minutes at 4°C in the dark, and washed once with 1ml FACS buffer after incubation. The cells were then centrifuged at 400 x g for 10 minutes, the supernatant discarded and the pellet re-suspended in 200µl FACS buffer, and stored in the fridge until acquisition on the same or following day.

Table 5.5: Staining conditions and single stain specifications for the purity check samples.

Staining Condition:	Volume:
PBMC Unstained	N/A
PBMC Stained with CD3 PE	2µl
PBMC Stained with CD14 PE	
PBMC Stained with CD15 FITC	
Isolated CD3 Cells Stained with CD3 PE	
Isolated CD14 Cells Stained with CD14 PE	
Isolated Neutrophils Stained with CD15 FITC	

Sample Acquisition and Data Analysis

Samples were acquired on the BD FACSCanto™ II using the FACSDiva™ software (Becton Dickinson, New Jersey, USA), version 8.0.1, and the FCS data files for each sample saved for further analysis. The third-party software, FlowJo® (FlowJo LLC, Oregon, USA) version 10.3, was used for the analysis of the FCS files generated by the BD FACSCanto™ II. When analyzing the data files, a plot of the cytometer run time (Time vs FSC-Height (H)) was first scrutinized to identify individual run success and instrument stability during the run (Figure 5.1(a)). The entire run for which the instrument was stable, was gated on and analysed further in a FSC-Area (A) vs FSC-H plot used to visualize singlets (Figure 5.1(b)). This was done to select for single cells that were detected by the lasers and not doublets as these would skew analyses. Following singlet identification, FSC and SSC voltages were set to adequately identify the lymphocyte and granulocyte populations (Figure 5.1(c)).

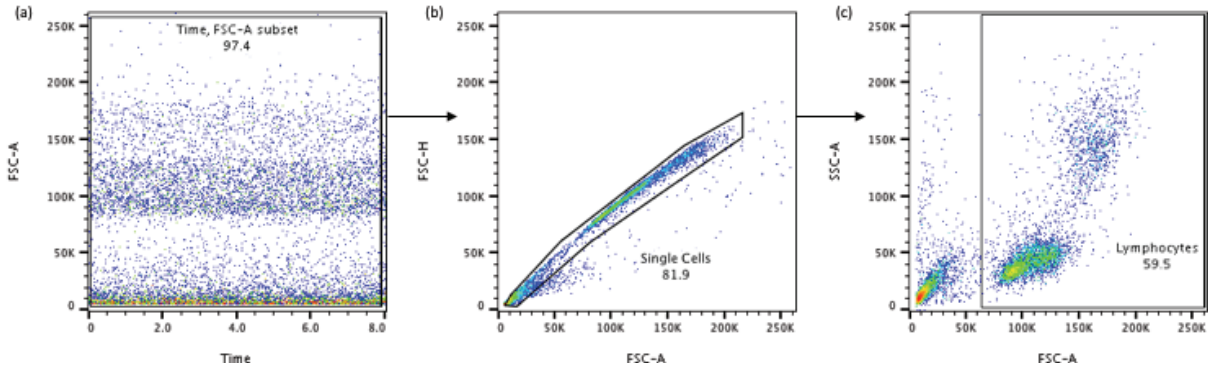

Figure 5.1: An example of the general gating strategy used for all samples prior to fluorochrome-specific gating. (a) Time gating was done to ensure instrument stability, (b) singlets were then identified to exclude doublets, and (c) lymphocytes were the final gate set prior to fluorochrome-specific gating.

5.2.7 Luminex Immunoassay for Subset Cytokine Profile Investigation

The concentrations of 27 cytokines were assessed in the QFT supernatants of all stimulation conditions using the Luminex immunoassay platform (Luminex, Bio-Rad Laboratories, Hercules, CA, USA). The cytokines were evaluated using the Bio-Plex Pro Human Cytokine Grp I Panel (27-Plex) supplied by Bio-Rad (catalogue number: M50-0KCAF0Y; Bio-Rad Laboratories, Hercules, CA, USA). The kit was

run in singlets, but with two standard curves: one for the plasma QFT supernatant samples, and one for the RPMI QFT supernatant samples. The assessed cytokines included: Interleukin (IL)-1β, IL-2, IL-4, IL-5, IL-6, IL-7, IL-8, IL-9, IL-10, IL-12(p70), IL-13, IL-15, IL-17A, IL-1R antagonist (a), Granulocyte colony-stimulating factor (G-CSF), Granulocyte-macrophage (GM)-CSF, Interferon (IFN)-γ, IFN-γ-inducible protein (IP)-10, Monocyte chemoattractant protein (MCP)-1, Macrophage inflammatory protein (MIP)-1α, MIP-1β, Eotaxin, Regulated on activation, normal T cell expressed and secreted (RANTES; also known as chemokine (C-C motif) ligand (CCL) 5), Tumour necrosis factor (TNF)-α, Vascular endothelial growth factor (VEGF), Platelet-derived growth factor (PDGF)-bb, and Basic Fibroblast Growth Factor (FGF basic). Data for IL-1β were later excluded from further analysis owing to an irregular standard curve.

Assay Preparation and Procedure

The samples, standards and controls were prepared as mentioned in Chapter 2 for the 4- and 5-Plex Bio-Rad kits. Please refer to Chapter 2 “Methods”.

Sample Acquisition

Acquisition was performed on the MAGPIX® Luminex platform (Luminex, Bio Rad Laboratories, Hercules, CA, USA). The beads from each sample were acquired individually and analysed using the Bio-Plex Manager™ Software version 6.1 according to recommended settings. Instrument settings were adjusted to ensure 50 bead events per region, with sample size set to 50μl for both multiplex kits.

Statistical Analysis

Statistical data analysis was performed using Statistica version 12.0 (Statsoft, Ohio, USA). A p-value of < 0.05 was considered statistically significant. Mixed model analysis was used to evaluate the differences between cytokine levels within the different subjects since the same cytokines were evaluated twice for each participant, i.e. in the Nil (unstimulated) and Antigen (stimulated) conditions, as well as for each subset. Mixed models generally have a combination of both fixed and random effects which influence the variance between samples; in this study the fixed effect was the participant identification, which also existed as the main effect, while the random effects were the sample type (whole blood vs neutrophils vs monocytes vs lymphocytes vs combined), stimulation conditions (unstimulated vs stimulated), and the QFT status (positive or negative). Interaction effects were evaluated between these criteria, with the participant identification being nested within the QFT status since one participant cannot be both QFT positive **and** negative. The random effects were evaluated as a full factorial, i.e. all possible combinations of the three random effect variables were evaluated. In order to assess the variance of these effects, an ANOVA using the type III sum of squares was run. The type III sum of squares (marginal) was chosen due to the small sample size since this type is not sample size dependent. Since no missing data was present, the least squares (LS) means could be derived during a pairwise comparison for the selected effects in selected cytokines, for example a pairwise comparison using the LS means with confidence interval was performed for each cytokine

assessed. The least squares means in the best linear-unbiased estimate of the marginal means of the design.

Visual comparison for cytokine data was created using two third-party software packages, namely Pestle[272] version 1.8 and SPICE (Simplified Presentation of Incredibly Complex Evaluations) version 5.3033 (National Institute of Allergy and Infectious Diseases, Maryland, USA). Pestle is a software that formats ".csv" files containing exported FlowJo data into ".spd" files which are compatible for import into the SPICE software (freely available at http://exon.niaid.nih.gov/spice/).

5.3 Results

5.3.1 Participant Demographics

Six healthy volunteer participants, three who tested positive for QFT and three who tested negative for QFT, were recruited from laboratories located on the Faculty of Medicine and Health Sciences, Stellenbosch University, Cape Town. Participants were all uninfected with HIV and their demographics given in Table 5.6.

Table 5.6: Demographics of the six healthy volunteer participants.

	QuantiFERON Negative (n = 3)		**QuantiFERON Positive (n = 3)**	
	Male	Female	Male	Female
Gender:	n = 0	n = 3	n = 1	n = 2
Median Age (Years):	24		37	
Latently Infected:	No		Yes	
HIV Infection Status:	Uninfected			

5.3.2 Morphology of Isolated Cell Subsets

The cytospin technique was used to concentrate cells from the isolated cell subsets onto microscope slides. The partially dried slides were subjected to the Rapi-Diff staining technique for visualization of the cell morphology under 1000X magnification (oil immersion) on a ZEISS microscope fitted with and Axiocam microscope camera. $CD3^+$ T lymphocytes (Figure 5.2(a)) and $CD14^+$ monocytes (Figure 5.2(b)) isolated from the PBMC fraction of whole blood, as well as banded (Figure 5.2(c)), mature (Figure 5.2(d)) and hyper-segmented (Figure 5.2(e)) neutrophils isolated from the red blood cell fraction of whole blood were visualized this way. Neutrophil morphologies (Figure 5.2(c)-(e)) were visualised from a single neutrophil population.

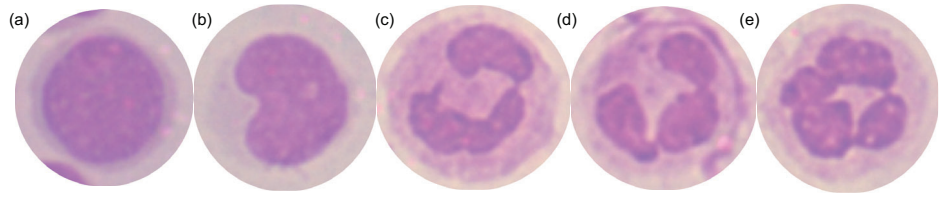

Figure 5.2: Morphological characteristics of the isolated cellular fractions. (a) Isolated $CD3^+$ T lymphocytes and (b) $CD14^+$ monocytes from the lymphocytic cellular fraction were visualized, as well as (c) banded neutrophils, (d) mature neutrophils, and (e) hyper-segmented neutrophils from the red blood cell fraction, under 1000X magnification using a ZEISS microscope following cytospin and RapiDiff staining.

All three isolated cellular fractions were relatively pure and confirmed by Flow Cytometric purity checks, given below. Lymphocyte nuclei are characteristically round in shape and large, taking up the majority of the cytosol which is clear, while monocyte nuclei are characteristically "kidney" or "U"-shaped with a clear cytosol. The cytosol of the neutrophil population is granular which gives the cell a more "purple" overall appearance owing to the cytosolic granules taking on some of the RapiDiff stain. The nuclei of the neutrophils vary depending on the cellular stage of maturation, but may include a "banded" appearance which represents a relatively immature neutrophil, or "segmented" appearance which represents a mature neutrophil, for which extensive segmentation succeeds that of a segmented neutrophil and represents a neutrophil that has entered the late stage of maturation ("hyper-segmented"; Figure 5.2(e)).

5.3.3 Cell Subset Yield and Purity

PBMC were isolated from healthy volunteers who tested either positive (QFT+) or negative (QFT-) during diagnostic QFT tests. Approximately 18ml of peripheral blood were used for the isolation which was performed following a standard PBMC isolation method using Ficoll-Paque density gradient media. $CD14^+$ monocytes were then isolated from the PBMC fraction, and the $CD14^-$ fraction used to isolate $CD3^+$ T lymphocytes. Neutrophils, which express the CD15 surface marker, were also isolated from the RBC fraction that remained beneath the Ficoll-Paque media. Literature estimates of the expected yields are given in Table 5.7.

Table 5.7: Expected cell frequencies and yields from a standard Ficoll-Paque density media gradient centrifugation experiment (based on literature estimates) for total PBMC, lymphocytes and monocytes alike.

	PBMC	**Lymphocytes**	**Monocytes**	**Neutrophils**
Expected Frequency (%)*	N/A	40 – 60	10 – 35	45 – 75
Expected Yield (cells/ml)	1-2 x 10^6	6-9 x 10^5	1.5-5.3 x 10^5	6.8-11 x 10^5
Expected Total Yield (cells)⁺	3 x 10^7	1.2-1.8 x 10^7	3-11 x 10^6	1.4-2.3 x 10^7

Abbreviations: PBMC – peripheral blood mononuclear cells; % - percentage

*Expected Frequency refers to the expected frequency of lymphocytes and monocytes within the **PBMC** fraction, but the expected frequency of neutrophils within **1ml of whole blood**.

⁺Expected total yield (total number of cells) for approximately 20ml of whole blood, the amount stipulated in the methods section.

During these experiments, on average, approximately 5.4 x 10^6 $CD14^+$ monocytes, 8.5 x 10^6 $CD3^+$ T lymphocytes, and 2.3 x 10^7 $CD15^+$ Neutrophils were isolated from the healthy participants (Table 8). While the monocyte yield was within the standard range, the lymphocyte yield was lower than expected by almost half. Even though a lower yield was observed for lymphocytes, when the data was translated into the proportion of PBMC this data was indeed within the normal range. It is possible that the $CD3^+$ cell-specific isolation resulted in some cell loss, which is known to occur with isolation techniques that stress the cells, and account for the less-than-normal yield. There were, however, enough lymphocytes isolated for the purposes of this investigation. Additionally, it was observed that the frequency of the

isolated cellular fractions conformed to the standard ranges as per flow cytometric analyses (Table 5.8). Each participant's isolated cell numbers and proportions are given in Table 5.8, which highlights the ever increasing awareness of individual heterogeneity.

The purity of each isolated population was determined by single stain flow cytometry. The frequency of each population as part of the PBMC population, prior to individual isolations, was also assessed via the staining of a fraction of PBMC kept aside before continuing with further cell-specific isolations. The average frequency of $CD14^+$ monocytes and $CD3^+$ T lymphocytes in the PBMC fraction was 14.0% and 55.7%, respectively, while the average frequency of neutrophils was 0.55% (Table 5.8). While it is generally accepted that the PBMC fraction of whole blood should not contain any neutrophils, there has been literature published in recent years that describes a population of low-density neutrophils (LDN) which frequently fractionate along with the PBMC. These LDN are hypothesized to represent the granulocytic myeloid-derived suppressor cell (MDSC) population owing to their both neutrophil- and MDSC-like appearance, as well as considerable potential to suppress T cells which is characteristic only of the granulocytic MDSC and not common neutrophils[273,274]. Therefore, the frequency of $CD15^+$ cells in the PBMC fraction was assessed to determine whether or not these LDN were present in the study sample population – little to no LDN were identified in the PBMC of the study's healthy volunteers.

Following cell-specific isolations, the purity of the fraction was determined. A population of cells with a purity of above 75% was considered adequate for the intended downstream use. The average purity of the $CD14^+$ monocytes and $CD3^+$ T lymphocytes was 94.3% and 98.6%, respectively, while the average purity of the $CD15^+$ Neutrophil fraction was 82.4%. All of the sample purities were above the accepted threshold and were considered appropriate for use in the downstream analyses. An example is given in Figure 5.3 of the expected frequencies of $CD14^+$ monocytes within the PBMC fraction (Figure 5.3(a) and (b)), as well as the purity of the enriched/isolated fraction of $CD14^+$ monocytes (Figure 5.3(c) and (d)).

The antibody staining for Donor 2 was not successful (Table 5.8). Because the purities of the remaining 5 samples were of a high quality, it can confidently be suggested that the protocol and technique was successful and that purities of the same standard could be expected. The frequency of Donor 5's $CD14^+$ monocytes in the PBMC fraction was uncharacteristically low. Literature estimates suggest that $CD14^+$ monocyte frequencies range from 10-35% in healthy adults[275], concurrent with the frequencies observed in the rest of the samples, however a frequency of 0.82% is very low. Upon further investigation, the staining of the PBMC fraction may have been unsuccessful since comparisons with the enriched monocyte population successfully displayed a sizeable $CD14^+$ population of cells.

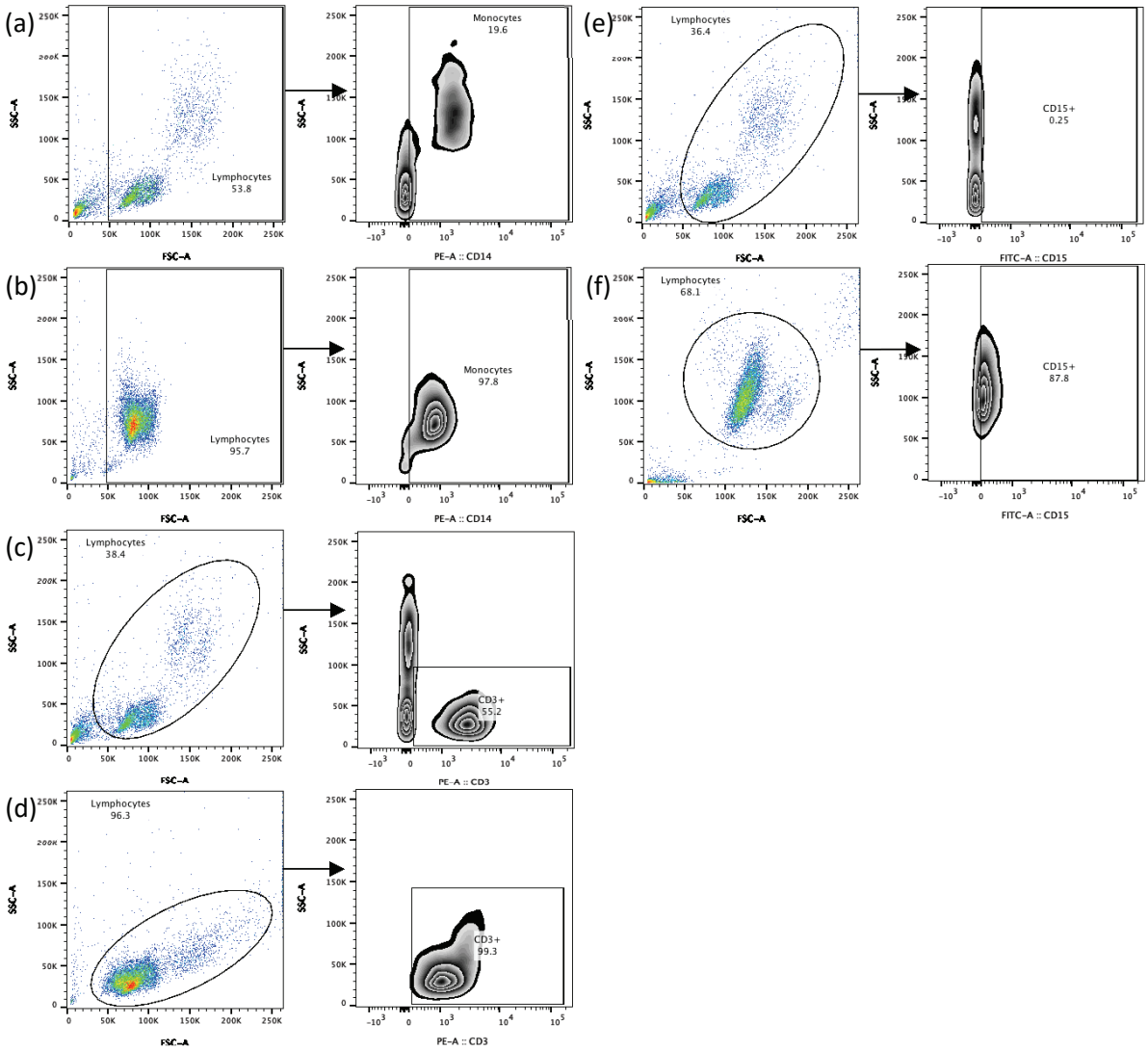

Figure 5.3: Comparison between the flow cytometry data for PBMC and isolated cell fractions. Depicted is (a) the dot plot of the PBMC gate, labelled "Lymphocytes", from which CD14⁺ stained monocytes were investigated. Likewise, (b) is the dot plot of the isolated population of cells from which CD14⁺ stained monocytes were investigated; (c) the PBMC dot plot from which CD3⁺ stained T cells were investigated, while (d) is the isolated T cell dot plot from which CD3⁺ T cells were investigated; (e) the PBMC dot plot from which CD15⁺ stained neutrophils were investigated, while (f) is the isolated neutrophil dot plot from which CD15⁺ neutrophils were investigated. The gates were kept the same to ensure consistent parameters.

Table 5.8: Fraction purities (given as a percentage) obtained for each isolated cell subset, as well as the frequency (given as a percentage) of PBMC that these cells make up.

Sample ID:	**QFT Status:**	**Monocytes**			**Lymphocytes**			**Neutrophils**		
		Number Isolated:	Freq. of PBMC:	Isolated Purity:	Number Isolated:	Freq. of PBMC:	Isolated Purity:	Number Isolated:	Freq. of PBMC:	Isolated Purity:
Donor 1	Positive	4.5×10^6	17.3	91.3	5.2×10^6	56.5	98.9	1.9×10^7	0.04	71.7
Donor 2*	Negative	2.8×10^6	-	-	9.5×10^6	-	-	7.5×10^6	-	-
Donor 3	Positive	5.6×10^6	14.6	94.8	5.0×10^6	56.1	97.7	1.4×10^6	1.42	83.4
Donor 4	Negative	6.0×10^6	19.6	97.8	7.1×10^6	58.0	99.2	1.5×10^7	0.42	93.0
Donor 5	Positive	3.6×10^6	0.82	89.9	1.2×10^7	55.3	98.3	2.8×10^7	0.09	77.0
Donor 6	Negative	9.9×10^6	17.7	97.7	1.2×10^7	52.6	98.9	6.6×10^7	0.78	86.7
Average:		**5.4×10^6**	**14.0**	**94.3**	**8.5×10^6**	**55.7**	**98.6**	**2.3×10^7**	**0.55**	**82.4**

Abbreviations: ID – identification; QFT – QuantiFERON; Freq – Frequency; PBMC – peripheral blood mononuclear cells.

* Unsuccessful purity check.

5.3.4 Cytokine Profile of Individual Subsets and Combinations

A Luminex 27-Plex immunoassay was performed in order to investigate the expression concentrations (pg/ml) of 27 different soluble innate and adaptive immune response cytokines. This was done for both the Nil (unstimulated) and Ag (stimulated) samples of each isolated cell subset. The immunoassay was successful, however owing to an irregular standard curve and difficulty in normalizing the data, one cytokine was removed from further analysis. It should be noted that both the plasma- and RPMI-based standard curves that were run in tandem to be applied to the two different sample types (QFT plasma supernatant and QFT RPMI supernatant), were both of good quality and acceptable for use. These were then applied to their respective wells via the Bio-Plex Manager™ Software version 6.1. In order to investigate the true antigen-specific cytokine production for each condition, the Antigen tube results were corrected for the background through the subtraction of the Nil tube results from the Antigen tube results (TBAg-Nil) so as to remove the influence of background cytokine production.

Statistical Considerations

Statistical analyses for this study were performed in Statistica version 12.0 (Statsoft, Ohio, USA), as stated previously in the methods section. Prior to statistical analysis, the data was “cleaned” in order for the most accurate results to be obtained. As such, negative values in the Antigen stimulated samples (background corrected) were substituted for zero. This was done for two reasons: (1) one cannot have a “negative expression” of a biological molecule, a negative value ultimately translates into the molecule or, in this case cytokine, not being produced by the sample and thus the motivation to substitute these values for zero; (2) any data transformation that needed to be performed to correct irregularly distributed data would not be successful with negative values. With that said, the most common transformation method used in Statistica is generally log transformation, which is also problematic with zero values. Fortunately, the software is capable of circumventing this scenario through the addition of “1” to each and every variable value so that when log transformation is performed, the outcome of log10(1) is in actual fact “0” and negates the original problem.

For this study, the above mentioned negative value substitutions were made for all antigen stimulated sample (background corrected) values. Following this, the distribution of each cytokine’s data was assessed using frequency distribution histograms. All of the cytokines contained outlier data, so the data was log transformed and the distribution re-assessed. From this, 26 out of the 27 cytokines assessed achieved normally distributed data which could be used for further analyses. However, the data for IL-1β measurements required additional formatting steps. The winzorise correction method was used in this case, but unfortunately the data remained irregular and was excluded from further analysis. The remaining 26 cytokines were assessed further using the methods outlined in section 5.2.7 of the methods section, while IL-1β measurements were not included in further evaluations. The graphs for all 26 cytokines can be found in the Addendum (Addendum A5.1 – Responses to Non-Specific Stimulation; Addendum A5.2 – Responses to Antigen Stimulation).

Overall Cytokine Profile – Subset-Specific Production

To answer the research question, the overall production of the 26 assessed cytokines were evaluated in all 5 cell subsets assessed, namely whole blood, neutrophils, monocytes, lymphocytes and combined culture of monocytes and lymphocytes. In order to discriminate between production of a cytokine and no production, an arbitrary cut-off value was calculated for each cytokine based on both plasma (cytokine cut-offs in whole blood) and RPMI supernatant (cytokine cut-offs in isolated cell subsets that were cultured in RPMI) standard curve data. The standard deviation was calculated for each cytokine using the lowest standard curve value, representative of the lowest possible readout for the cytokine in that specific kit. Cut-offs were then calculated as 2 standard deviations above the mean. A median cytokine concentration (pg/ml) above this cut-off was considered positive for production. Those cytokines that were produced by the specific cell subsets were also ranked according to median concentrations so as to visualise which cytokines were produced in greater quantities. The ranking system used was a simple "highest to lowest" ranking in which the highest value was shaded dark green and transitioned lighter until the lowest value which was shaded dark red (Microsoft Excel conditional formatting tool).

When unstimulated samples were investigated as such (Table 5.9), the whole blood compartment produced all of the 26 cytokines assessed in this study, with RANTES and IL-13 being produced at the highest and lowest concentrations, respectively. The neutrophil subset produced very few cytokines, but MIP-1β and IL-13 were produced at the highest and lowest concentrations, respectively. The monocyte subset only lacked the production of IL-15, and produced IL-8 at the highest concentrations, and IL-13 at the lowest once again. The lymphocyte subset lacked the production of four cytokines, and produced MIP-1β and IL-7 at the highest and lowest concentrations, respectively. Lastly, the combined culture of monocytes and lymphocytes resulted in high levels of IL-8 and IP-10 production, with IL-15 being the cytokine produced at the lowest concentration.

When stimulated samples were investigated (Table 5.10), the whole blood compartment did not produce 5 of the cytokines assessed in this study, with IL-8 and IL-7 being produced at the highest and lowest concentrations, respectively, in contrast to the unstimulated condition. The neutrophil subset only produced 2 cytokines out of the total 26. These were IL-8 and MIP-1β at the highest and lowest concentrations, respectively. The monocyte subset produced even fewer cytokines compared to unstimulated conditions, with IL-8 remaining the highest produced cytokine, but IL-7 the lowest. The stimulated lymphocyte subset only produced 2 cytokines, namely TNF-α and IL-8 at the highest and lowest concentrations, respectively, which was also in contrast to the unstimulated condition. Lastly, the combined culture of monocytes and lymphocytes resulted in the production of only 3 cytokines, namely IL-8, MIP-1β and IP-10 in order of highest to lowest concentrations.

For ease of reference, a visualization of the tabulated results (Table 5.9 and 5.10) was also constructed using a combination of two third party software programs, Pestle and SPICE version 5.3033 (NIAID,

USA), and can be found in the Addendum (Addendum Figure A5.3 and Figure A5.4). It should be mentioned that the pie charts represent the proportion each cytokine contributed to the overall profile based on their median concentrations.

Table 5.9: Cytokines produced in the whole blood compartment and by the isolated subsets investigated in this study in the unstimulated condition. Values given represent the median cytokine concentration (pg/ml) for the specific cell type, while cytokines that were not produced above the cut-off value are indicated as "Not Produced". The median cytokine concentrations were ranked per cell subset according to the amount of cytokine produced, i.e. the median cytokine concentrations were scaled from highest to lowest using a colour scale ranging from dark green to dark red, with dark green being the highest concentration and dark red the lowest for that cell type.

Cytokine	Whole Blood	Neutrophil	Monocyte	Lymphocyte	Combined
IL-1ra	419.7	17.4	58.1	25.5	322.4
IL-2	27.2	Not Produced	1.9	3.0	21.9
IL-4	5.8	Not Produced	2.0	1.6	4.7
IL-5	18.9	Not Produced	3.0	3.1	8.9
IL-6	27.0	Not Produced	73.5	12.0	338.1
IL-7	11.2	1.8	2.9	1.5	4.1
IL-8	384.8	46.1	2829.9	86.7	5180.0
IL-9	48.7	2.2	12.7	11.3	30.3
IL-10	35.3	4.9	2.9	Not Produced	45.9
IL-12(p70)	51.7	14.3	4.9	3.0	6.1
IL-13	4.0	1.2	1.1	2.1	18.2
IL-15	23.6	Not Produced	Not Produced	Not Produced	3.8
IL-17A	173.8	3.0	19.0	22.0	93.2
Eotaxin	77.8	Not Produced	8.9	6.6	18.3
FGF-basic	111.2	Not Produced	7.0	Not Produced	11.1
G-CSF	93.6	2.8	16.4	8.1	41.8
GM-CSF	78.1	Not Produced	4.9	6.9	11.8
IFN-γ	171.7	Not Produced	13.7	16.2	51.7
IP-10	399.3	Not Produced	90.0	273.3	5056.4
MCP-1	199.3	Not Produced	16.5	Not Produced	116.3
MIP-1α	7.7	2.6	12.9	20.4	71.0
PDGF-bb	876.6	Not Produced	70.3	13.3	48.0
MIP-1β	397.0	104.7	881.1	1060.6	3782.1
RANTES	3621.6	12.4	172.7	270.8	462.7
TNF-α	96.7	Not Produced	46.8	56.5	402.9
VEGF	79.4	76.1	10.9	2.5	15.8

Table 5.10: Cytokines produced in the whole blood compartment and by the isolated subsets investigated in this study in the stimulated condition. Values given represent the median cytokine concentration (pg/ml) for the specific cell type, while cytokines that were not produced above the cut-off value are indicated as "Not Produced". The median cytokine concentrations were ranked per cell subset according to the amount of cytokine produced, i.e. the median cytokine concentrations were scaled from highest to lowest using a colour scale ranging from dark green to dark red, with dark green being the highest concentration and dark red the lowest for that cell type.

Cytokine	Whole Blood	Neutrophil	Monocyte	Lymphocyte	Combined
IL-1ra	43.840	Not Produced	63.9	Not Produced	Not Produced
IL-2	8.580	Not Produced	1.57	Not Produced	Not Produced
IL-4	Not Produced	Not Produced	Not Produced	Not Produced	Not Produced
IL-5	Not Produced	Not Produced	Not Produced	Not Produced	Not Produced
IL-6	5.420	Not Produced	Not Produced	Not Produced	Not Produced
IL-7	1.970	Not Produced	1.465	Not Produced	Not Produced
IL-8	375.230	139.45	2606.315	3.155	807.995
IL-9	5.620	Not Produced	1.7	Not Produced	Not Produced
IL-10	Not Produced	Not Produced	Not Produced	Not Produced	Not Produced
IL-12(p70)	2.870	Not Produced	Not Produced	Not Produced	Not Produced
IL-13	Not Produced	Not Produced	Not Produced	Not Produced	Not Produced
IL-15	Not Produced	Not Produced	Not Produced	Not Produced	Not Produced
IL-17A	47.210	Not Produced	Not Produced	Not Produced	Not Produced
Eotaxin	11.490	Not Produced	2.26	Not Produced	Not Produced
FGF-basic	5.730	Not Produced	Not Produced	Not Produced	Not Produced
G-CSF	5.910	Not Produced	3.35	Not Produced	Not Produced
GM-CSF	11.040	Not Produced	Not Produced	Not Produced	Not Produced
IFN-γ	21.970	Not Produced	8.055	Not Produced	Not Produced
IP-10	116.900	Not Produced	33.565	Not Produced	584.145
MCP-1	132.920	Not Produced	Not Produced	Not Produced	Not Produced
MIP-1α	4.270	Not Produced	8.535	Not Produced	Not Produced
PDGF-bb	106.690	Not Produced	Not Produced	Not Produced	Not Produced
MIP-1β	149.720	14.865	231.505	Not Produced	694.05
RANTES	243.990	Not Produced	Not Produced	Not Produced	Not Produced
TNF-α	6.600	Not Produced	7.955	5.295	Not Produced
VEGF	10.440	Not Produced	Not Produced	Not Produced	Not Produced

Differential Responses Between Isolated Cell Types and Whole Blood

We assessed the *ex vivo* and *M.tb*-specific production of 26 cytokines/chemokines within plasma supernatants of whole blood cultures and RPMI supernatants of individual cell cultures, to assess individual cell subset cytokine profiles and how they differ to those seen in a complete cellular environment context (i.e. in whole blood). The cytokine responses were compared between the assessed cell types, namely between whole blood, neutrophils, monocytes, lymphocytes and the combined culture condition. Upon first investigation of the unstimulated samples, it was observed that seven cytokines/chemokines were produced in significantly larger amounts when monocytes and T lymphocytes were cultured in combination, compared to the amount produced in whole blood. These cytokines included IL-6 (Figure 5.4(a)), IL-8 (Figure 5.4(b)), IL-13 (Figure 5.4(c)), IP-10 (Figure 5.4(d)), MIP-1α (Figure 5.4(e)), TNF-α (Figure 5.4(f)), and MIP-1β (Figure 5.4(g)). The significance values are given in Table 5.11, along with the differences in cytokine expression between whole blood and the other cell types investigated, namely neutrophils (NP), monocytes (Mo) and Lymphocytes (Ly). It should be mentioned that these differences were not limited by *M.tb* infection, and were thus observed in both QFT+ and QFT- participants. A full table containing all of the comparisons, as well as the graphs for all 26 cytokines can be found in the Addendum (Addendum Table A5.1, and Addendum Figure A5.1).

Table 5.11: Significance values for each of the cytokines that were downregulated in whole blood compared to the combined culture of monocytes and T lymphocytes after non-specific stimulation. The values for both latently infected (QFT+) and uninfected (QFT-) participants are given for each cytokine, and differences that were not significant are represented by red text. Downward-facing arrows in parentheses given after significant differences indicate whether the cytokine production was up-(↑) or down-(↓) regulated in the cell type compared to whole blood.

Cytokine	QFT Status	WB vs NP	WB vs Mo	WB vs Ly	WB vs Co
IL-6	QFT+	0.000014 (↓)	0.0097 (↑)	0.35	0.00003 (↑)
	QFT-	0.000021 (↓)	0.63	0.0075 (↓)	0.00056 (↑)
IL-8	QFT+	0.00024 (↓)	0.0015 (↑)	0.031 (↓)	0.000028 (↑)
	QFT-	0.00064 (↓)	0.0033 (↑)	0.0057 (↓)	0.000015 (↑)
IL-13	QFT+	0.061	0.057	0.53	0.00038 (↑)
	QFT-	0.044 (↓)	0.0197 (↓)	0.29	0.00095 (↑)
IP-10	QFT+	0.0000000000026 (↓)	0.00037 (↓)	0.53	0.000004 (↑)
	QFT-	0.0000000000024 (↓)	0.0056 (↓)	0.01 (↓)	0.000011 (↑)
MIP-1α	QFT+	0.18	0.63	0.028 (↑)	0.00037 (↑)
	QFT-	0.21	0.8	0.42	0.037 (↑)
MIP-1β	QFT+	0.014 (↓)	0.023 (↑)	0.023 (↑)	0.0083 (↑)
	QFT-	0.11	0.16	0.24	0.012 (↑)
TNF-α	QFT+	0.000011 (↓)	0.51	0.95	0.0037 (↑)
	QFT-	0.000015 (↓)	0.11	0.061	0.086

Abbreviations: WB – Whole Blood; NP – Neutrophil; Mo – Monocyte; Ly – Lymphocyte; Co – Combined.

None of the assessed cytokines/chemokines were produced in significantly greater amounts in the combined culture of monocytes and T lymphocytes compared to whole blood after stimulation with *M.tb*-specific antigens (See Addendum Figure A5.2 for reference).

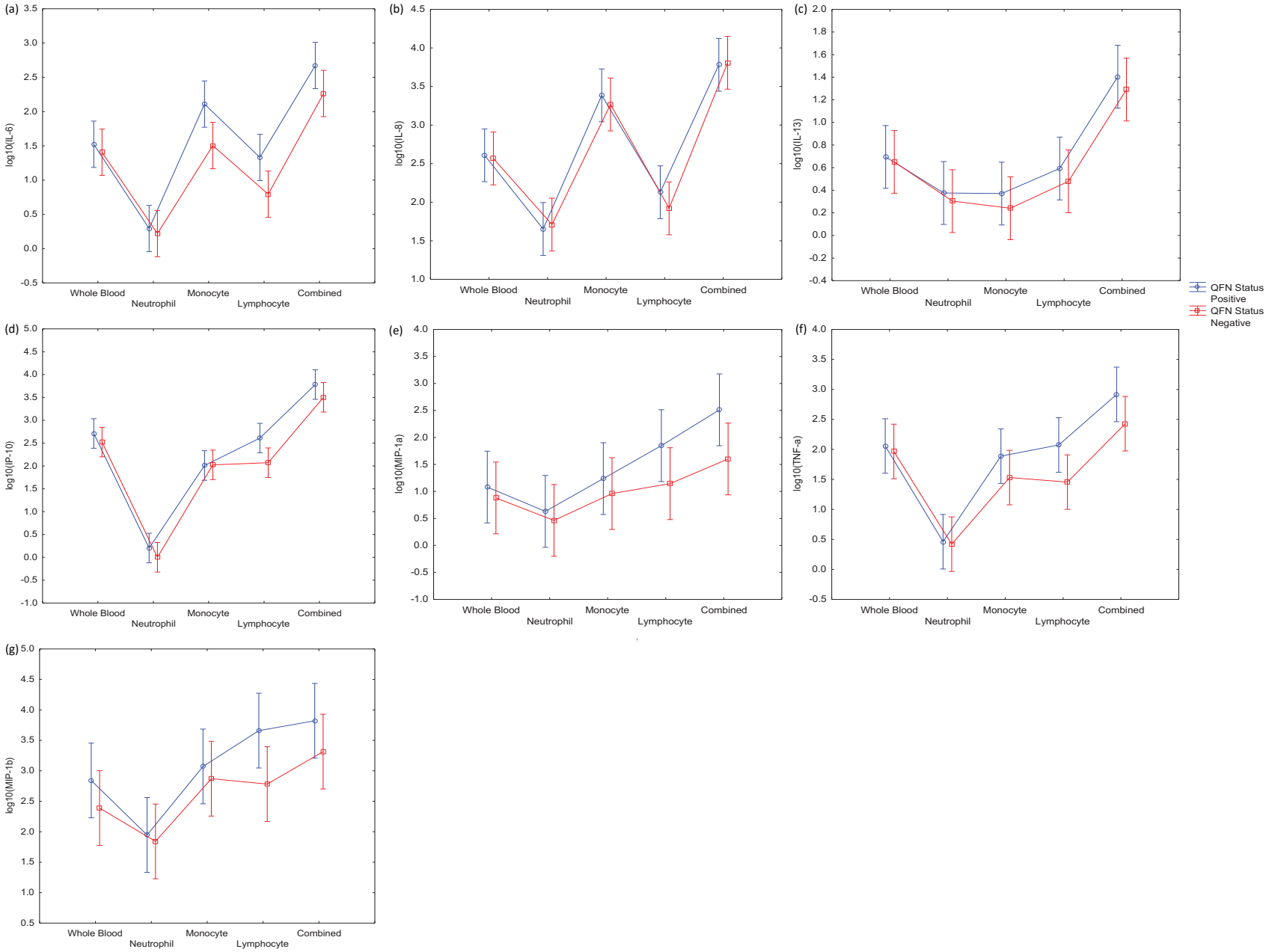

Figure 5.4: The seven cytokines that had a significantly lower production in whole blood compared to when monocytes and T lymphocytes were co-cultured in response to non-specific stimulation. These cytokines included (a) IL-6, (b) IL-8, (c) IL-13, (d) IP-10, (e) MIP-1α, (f) TNF-α, and (g) MIP-1β; blue and red data points represent data for QFT+ and QFT- participants respectively.

5.4 Discussion

The development of a swift and strong innate response to *Mycobacterium tuberculosis* infection is of paramount importance for the clearance and/or containment of the bacteria from/within the lungs. Activation of *M.tb*-specific pro-inflammatory cytokines and their signalling cascades are necessary for the development of structurally organised granulomas, as well as for the successful recruitment of effector cells from the adaptive response to the site of infection to further strengthen granuloma structure[276]. It is, therefore, incredibly important for a suitable inflammatory response to be initiated by resident myeloid subsets at the site of disease. Owing to the broad spectrum of mycobacterial infection outcomes observed in human populations, there are many inflammatory response checkpoints at which the response may not be adequate enough to clear and/or contain mycobacterial bacilli[277]. Latent infection arises from this tenuous form of bacterial control. Since approximately 23% of the world's population has latent *M.tb* infection[278], these individuals present a large reservoir for potential bacterial transmission should the individual progress to active TB disease. This highlights the importance of investigating the mechanics of latent infection for the prevention of a rise in global incidence cases and, ultimately, transmission. Latent infection can be assessed using the QuantiFERON-TB Gold In-Tube test assay which measures IFN-γ release in response to challenge with *M.tb*-specific antigens. Prior exposure to the pathogen elicits a large IFN-γ response owing to the large number of *M.tb*-specific memory T lymphocytes in circulation. Recently it has been suggested that the repertoire of innate myeloid cells may well be able to develop their own form of immunological memory, termed "Trained Immunity" which delivers a paradox in immunological understandings[279,280].

As mentioned earlier, previous work has illustrated the differential expression of several acute phase/innate cytokines in both QFT positive and negative children after antigen stimulation. As part of a pilot study in our research group focussed on intestinal helminth burdens and immunological responses in children, this differential expression profile identified in QuantiFERON supernatants stimulated overnight with *M.tb* antigens could discriminate between uninfected children and those infected with *Ascaris lumbricoides* (unpublished data). Work performed in Chapter 3 of this thesis supported the increase of innate subset cytokines in an adult *Ascaris*-exposed population, however these data were not from *M.tb*-specific antigen responses, but rather from naturally circulating mediators within the periphery of active TB participants, i.e. from serum. These findings sparked speculation into the development of innate 'memory' and prompted the further investigation of myeloid subsets as to their ability to differentially produce cytokines. This has previously not been investigated in healthy human populations.

This study, therefore, examined and compared the *M.tb*-antigen specific and non-specific responses of peripheral myeloid and lymphoid cells from the blood of latently infected, yet healthy individuals to uninfected healthy individuals. We specifically aimed to evaluate whether the differential expression of innate cytokines was due to direct activation of innate cell subsets by *M.tb*-specific antigens, or if it

could be attributed to innate immune cells responding to antigen-specific T lymphocytes that have been sensitized to *M.tb*-specific antigens.

In this study, both innate (monocytes and neutrophils) and adaptive (T lymphocytes) cell subsets were isolated from the peripheral blood of three QFT positive and three QFT negative, but otherwise healthy, individuals. Cells were incubated overnight (20 hours) in QuantiFERON-TB Gold In-Tube Nil (unstimulated) and Antigen (stimulated) tubes in 1ml suspensions with supplemented RPMI media, at a frequency representative of *in vivo* cellular frequencies. Whole blood samples were also incubated in the same manner as a representation of the *ex vivo* cytokine response when all cellular subsets are present; a combination condition of both innate and adaptive cell subsets were also evaluated in order to determine whether differential cytokine expression is as a result of innate immune cells responding to antigen-specific, previously sensitized T lymphocytes. The cytokine profiles of the QFT culture supernatants were then investigated using the Luminex immunoassay platform which measured the expression of 27 various cytokines, of which one was excluded from analysis owing to a faulty standard curve. The production of pro- and anti-inflammatory cytokines by innate and adaptive immune subsets as well as their contributions to that of the whole blood inflammatory profile, the *ex vivo* representation of the *in vivo* environment, was then compared between groups.

The cytokine responses to non-specific stimulation demonstrated that the whole blood compartment produced all 26 cytokines, with the predominant cytokine produced being RANTES (CCL5). RANTES is a chemoattractant responsible for the homing and migration of effector and memory T lymphocytes during acute infections. The receptor for RANTES is CCR5, which is also the receptor for the chemokines MIP-1α and MIP-1β which have unknown, overlapping functions with RANTES. RANTES performs an early, protective role during *M.tb* infection, limiting bacterial growth by recruiting IFN-γ-producing, antigen-specific T cells as well as macrophages and monocytes through the expression of its receptor CCR5[281]. Data suggests RANTES modulates $CD8^+$ T lymphocytes specifically[282,283], and its levels are known to be elevated in BAL of TB patients[284]. This suggests that the whole blood compartment in our participants may have been challenged with other pathogens that resulted in the upregulation of this cytokine. The neutrophil subset did not produce 13 of the 26 cytokines assessed in this study. Those that were produced by neutrophils were predominantly MIP-1β and VEGF. MIP-1β is a chemoattractant for monocytes, Natural Killer cells, and $CD4^+CD25^+$ T_{Regs}[285], is known to be secreted by neutrophils[286], and performs an immunoregulatory role through the promotion of T_H2 differentiation from naïve T_H0 cells. This is accomplished by the cytokine, IL-4, which has been shown to specifically elevate the expression of MIP-1β resulting in the reduction of local cytotoxic T cell responses[287,288]. Evidence shows elevated levels of IL-4, MIP-1β and regulatory SOCS1&3 proteins in the lungs of active disease patients correlate with concurrent reductions of IFN-γ, IL-17 and CCL5, typical T_H1 response cytokines[289]. Meanwhile, VEGF is known to be produced by human neutrophil subsets, is upregulated in patients with active TB disease and downregulates following the successful completion of treatment, highlighting the disadvantageous nature of angiogenesis in active TB disease[290,291]. These cytokines are known to facilitate T_H2 directed responses suggesting a protective function for neutrophils in

preventing tissue damage during the homeostatic state. The neutrophil data should, however be interpreted cautiously owing to the lower population purities achieved during the isolation process.

The monocyte subset did not produce any IL-15, but this result was expected since the production of IL-15 monocytes is mainly surface-bound. Monocytes did, however, produced large concentrations of IL-8 (CXCL8). IL-15 is responsible for the stimulation of IFN-γ producing cells, both innate and adaptive, including Natural Killer cells and $CD8^+$ T lymphocytes. It is particularly important for the control of the proliferation and survival of naïve and memory $CD8^+$ T lymphocytes during *M.tb* infection[292,293]. Meanwhile, IL-8 is a chemokine produced primarily by macrophages upon *M.tb* infection for the recruitment of T lymphocytes to the site of infection, thereby enhancing innate immune responses and acting as an important bridge between the innate and adaptive immune responses to *M.tb* infection[294–296]. It is also known to be released by neutrophils in conjunction with TNF-α, MIP-1α and MCP-1 specifically during active TB disease, supposedly for the enhanced recruitment of innate and adaptive effector populations, but this was not observed in our study[297]. The high production of IL-8 following non-specific stimulation, again, suggests that the participants enrolled for this study may have been infected with other pathogens eliciting an adaptive immune response, but these data were not available. Additionally, the lymphocyte subset did not produce IL-10, IL-15, FGF-basic or MCP-1. The production of IL-10 is generally associated with the activation of T_{Reg} cells, while MCP-1 is responsible for the recruitment of monocytes to the site of infection. Coincidentally, both are known to be involved in the expansion and recruitment of a suppressive myeloid cell type known as myeloid-derived suppressor cells (MDSC) which suppress T cell-specific responses to cancer and bacteria[181,298]. With the absence of the production of these cytokines, it is plausible to suggest that these cells remain in a T_H1 phenotype, however the predominance of MIP-1β production suggests otherwise. The predominance of MIP-1β could likely be as a result of alternate infections resulting in the recruitment of monocytes for innate immune clearance.

Lastly, the combined culture of monocytes and T lymphocytes displayed the production of all 26 cytokines, as observed in the whole blood condition. The combined culture produced large amounts of IL-8, IP-10 and MIP-1β. The production of IL-8 could be accounted for by the large monocyte production of this cytokine, while MIP-1β production could likewise be accounted for by the lymphocyte subset. IP-10 is a cytokine expressed in large quantities during active TB disease, is a driver of the proinflammatory immune responses and correlates with the extent of systemic inflammation. The primary function of IP-10 is IFN-γ driven chemoattraction of activated T_H1 cells[299,300]. This suggests that the combined culture of monocytes and T lymphocytes results in the successful activation of both T_H1 and T_H2 responses for the maintenance of a balanced immune system.

In addition to these subset specific differences, the identification of seven cytokines that were produced in significantly greater amounts in the combined culture of monocytes and T lymphocytes compared to whole blood (Figure 5.4) elude to a suppressive mechanism that results in the downregulation of key pro-inflammatory cytokines in the whole blood compartment. It is speculated that the reason behind this

is the naturally found suppression of cytokine production in the whole blood compartment. This is expected because of the various interactions between different immune cells and soluble factors, for example, which interact with each other to maintain a state of homeostasis. An example would include the cytokine TGF-β which inhibits T cell proliferation and effector functions, as well as monocyte/macrophage phagocytic and effector functions to naturally suppress the immune response and prevent tissue damage[301–303]. When monocytes and T cells were cultured together, macrophages (the main producer of TGF-β) are removed from the environment thereby eliminating the suppressive effects observed in the whole blood compartment. There are many other cells and cytokines which perform similar functions within the immune system, TGF-β is simply one such example. These interactions between related soluble products and cells would explain the lower cytokine production observed in the whole blood compartment compared to the co-culture of monocytes and T cells. Most notably, the downregulation of the cytokines IL-6, IP-10 and TNF-α in the whole blood responses are cause for concern owing to the important role these proinflammatory cytokines play in the control of *M.tb* infection. As mentioned previously, IP-10 is an important driver of the recruitment of IFN-γ-producing T_H1 lymphocytes during *M.tb* infection, while TNF-α is crucial for the development of robust granulomas for the containment of *M.tb* bacilli. Should such cytokines be suppressed in the whole blood during active TB disease (not assessed in this chapter), infection control would very likely be unsuccessful. Considering this and previously highlighted data from specific cell subsets, the possibility of MDSC carrying out this suppressive function is highly likely and warrants further investigation.

MDSC are a heterogeneous population of innate myeloid cells which, during chronic inflammation, have potent immunosuppressive properties, particularly towards T lymphocytes. These cells may also mediate protective roles as regulatory myeloid cells during acute inflammation since the hallmark of their immunosuppressive activities arises as a result of chronic inflammation. Since the mediators of MDSC expansion and activation (MIP-1β in both the monocyte and neutrophil subsets, VEGF in the neutrophil subset, and IL-10 in whole blood) are upregulated in this study without antigen-specific stimulation, it supports the less well known literature that these regulatory myeloid cells perform a protective role during early *M.tb* infection to facilitate the reduction of immunopathology[304]. Previous literature has identified elevated production of these cytokines in the peripheral blood of active TB cases that was not antigen-specific, and supports the current study's findings[178]. To the best of our knowledge, antigen-specific responses have not yet been assessed.

In terms of the antigen-specific responses observed in this study, very few cytokines were observed to be produced in response to *M.tb*-antigen stimulation. Interestingly, however, all cell subsets produced IL-8 suggesting a strong and successful drive for the recruitment of *M.tb*-specific T lymphocytes. Briefly, the whole blood compartment did not produce IL-4, IL-5, IL-10, IL-13, or IL-15, but still produced large concentrations of RANTES as observed during unstimulated conditions. This suggests that the whole blood response to *M.tb*-specific antigens was directed towards the recruitment of antigen-specific T lymphocytes for pathogen clearance. The neutrophil subset only produced MIP-1β in addition to IL-8, with IL-8 becoming the predominant cytokine produced by antigen-stimulated neutrophils, instead of

MIP-1β. This eludes to a T_H1-dominant immune response elicited by neutrophils. The monocyte subset, as mentioned previously, produced mostly IL-8 in an antigen-specific manner, along with 11 other assessed cytokines. The predominance of TNF-α production in the lymphocyte subset, the only other cytokine produced other than IL-8 by this subset, suggests that the adaptive response to *M.tb* antigens is largely protective and that the T_H1 immune response is active. Lastly, the combined culture condition only produced three cytokines, including IL-8. The other two included IP-10 and MIP-1β. These results mimicked the unstimulated combined cytokine response and suggested that these three cytokines are the predominant cytokines involved in bridging the gap between *M.tb*-specific innate and adaptive immune responses.

The work performed in this chapter has highlighted the development of non-specific innate immune suppression through the apparent suppression of protective host responses in the whole blood of participants compared to responses observed in the combined culture of monocytes and lymphocytes.

In light of the results generated in this study, the objectives were successfully achieved. It was hypothesized that the differential expression of innate immune response proteins is dependent on the presence of both innate and adaptive leukocyte subsets. During this study, it was observed that the presence of both innate and adaptive leukocyte subsets may **not** be necessary for the differential expression of *M.tb*-antigen specific cytokines, at least in the monocytic compartment of peripheral blood. The differential expression of cytokines characteristically involved in the development of T_H2 adaptive responses in the monocyte compartment of participants suggests that regulatory myeloid cells perform a more prominent role during *M.tb* infection than traditionally thought and may be an indication of recent exposure to *M.tb* infection as is supported by literature[178]. Also, it would be wise to consider that these regulatory myeloid cells may be a strong biomarker for progression to active TB disease should the balance between regulatory myeloid cells and effector myeloid cells be disrupted.

Future studies should investigate the role of regulatory myeloid cells between latently infected participants and individuals with active TB disease so as to elucidate their function in each case, i.e. do regulatory myeloid cells act as immune suppressors and result in the progression from latent to active disease because of poor infection control? Future studies should also address which other myeloid and/or lymphoid cells are being influenced by regulatory myeloid cells, specifically in the context of active TB disease. One such possibility could be the investigation of myeloid-derived suppressor cell function during active TB disease and latent infection following *M.tb*-specific antigen stimulation since it is known that this population of cells is expanded during active disease, and since the differentially expressed monocytic cytokines observed in this study are largely responsible for the expansion and recruitment of MDSC.

5.5 Addendum

Table A5.1: Significance values for each of the cytokines that were downregulated in whole blood compared to the combined culture of monocytes and T lymphocytes after non-specific stimulation. The values for both latently infected (QFT+) and uninfected (QFT-) participants are given for each cytokine, and differences that were not significant are represented by red text. The significance values for each of the cytokines are also given for the comparisons between the subsets.

Cytokine	QFT Status	WB vs NP	WB vs Mo	WB vs Ly	WB vs Co	NP vs Mo	NP vs Ly	NP vs Co	Mo vs Ly	Mo vs Co	Ly vs Co
IL-6	QFT+	1.4E-05	0.0097	0.35	3.0E-05	1.0E-07	8.9E-05	2.3E-09	0.0013	0.012	5.0E-06
	QFT-	2.1E-05	0.63	0.0075	0.00056	8.0E-06	0.011	2.0E-08	0.0027	0.0016	2.0E-06
IL-8	QFT+	0.00024	0.0015	0.031	2.8E-05	2.3E-07	0.032	1.4E-08	1.3E-05	0.069	4.4E-07
	QFT-	0.00064	0.0033	0.0057	1.5E-05	1.0E-06	0.31	1.7E-08	6.0E-06	0.017	7.4E-08
IL-13	QFT+	0.061	0.057	0.53	0.00038	0.98	0.19	7.0E-06	0.18	7.0E-06	0.0001
	QFT-	0.044	0.0197	0.29	0.00095	0.695	0.29	1.2E-05	0.15	6.0E-06	0.0001
IP-10	QFT+	2.6E-11	0.00037	0.53	4.0E-06	3.4E-09	4.9E-11	1.1E-13	0.0014	4.5E-09	1.0E-06
	QFT-	2.4E-11	0.0056	0.01	1.1E-05	6.4E-10	4.6E-10	1.6E-13	0.77	5.7E-08	8.8E-08
MIP-1a	QFT+	0.18	0.63	0.028	0.00037	0.075	0.0015	2.2E-05	0.073	0.001	0.053
	QFT-	0.21	0.8	0.42	0.037	0.14	0.048	0.0025	0.57	0.061	0.17
MIP-1b	QFT+	0.014	0.023	0.023	0.0083	0.0033	7.8E-05	2.9E-05	0.0898	0.035	0.63
	QFT-	0.11	0.16	0.24	0.012	0.006	0.012	0.00035	0.79	0.19	0.12
TNF-a	QFT+	1.1E-05	0.51	0.95	0.0037	3.8E-05	9.0E-06	4.3E-08	0.47	0.00091	0.0043
	QFT-	1.5E-05	0.11	0.061	0.086	0.00047	0.00087	1.0E-06	0.77	0.0027	0.0015

Abbreviations: WB – Whole Blood; NP – Neutrophil; Mo – Monocyte; Ly – Lymphocyte; Co – Combined.

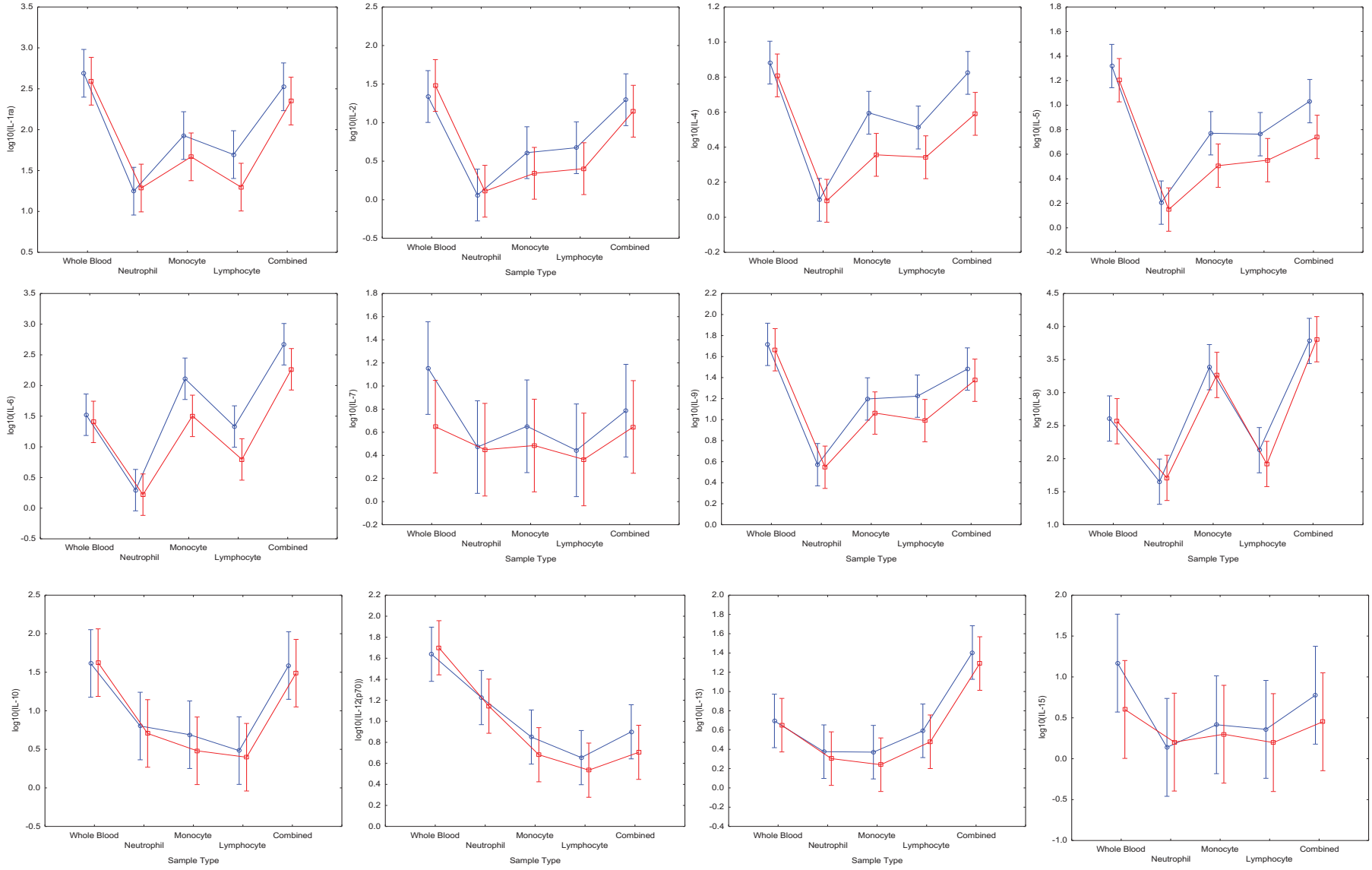

Figure A5.1: The 26 cytokines assessed during this study, under unstimulated conditions.

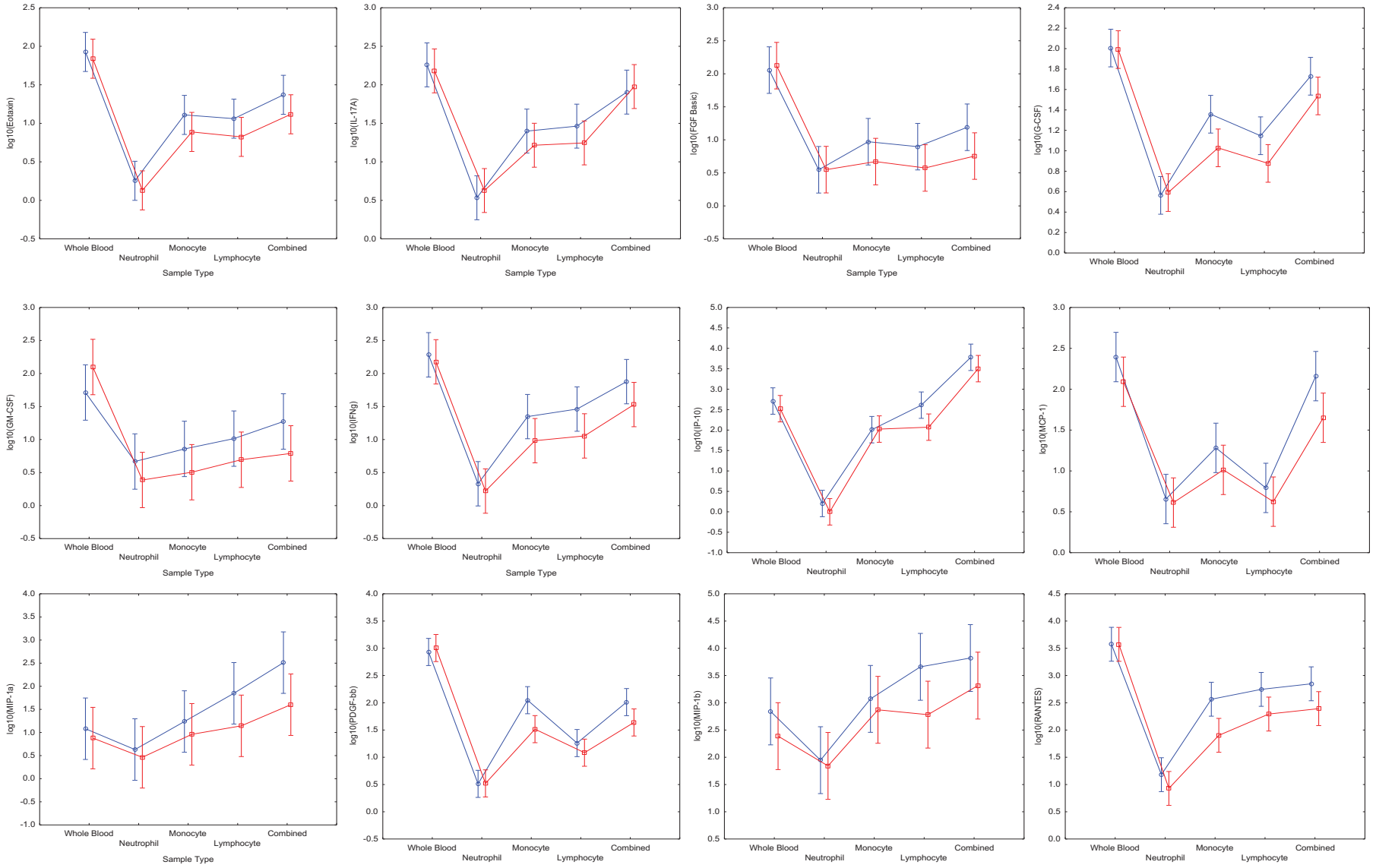

Figure A5.1: Continued…The 26 cytokines assessed during this study, under unstimulated conditions.

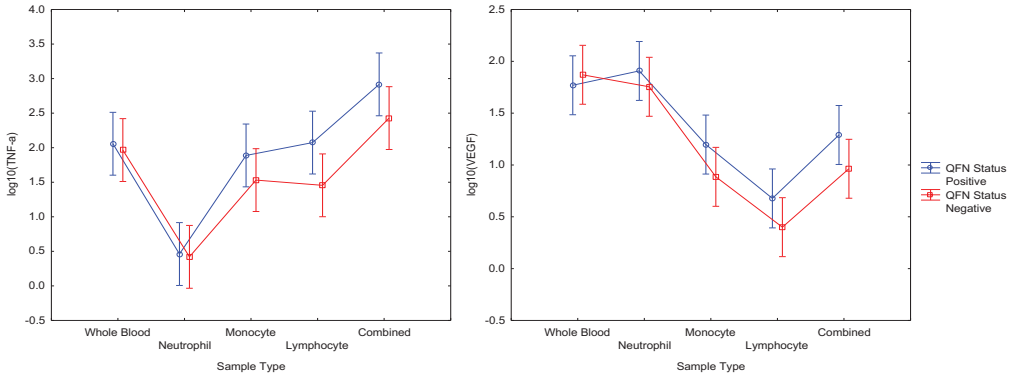

Figure A5.1: Continued…The 26 cytokines assessed during this study, under unstimulated conditions. Blue and red data points represent data for QFT+ and QFT- participants respectively.

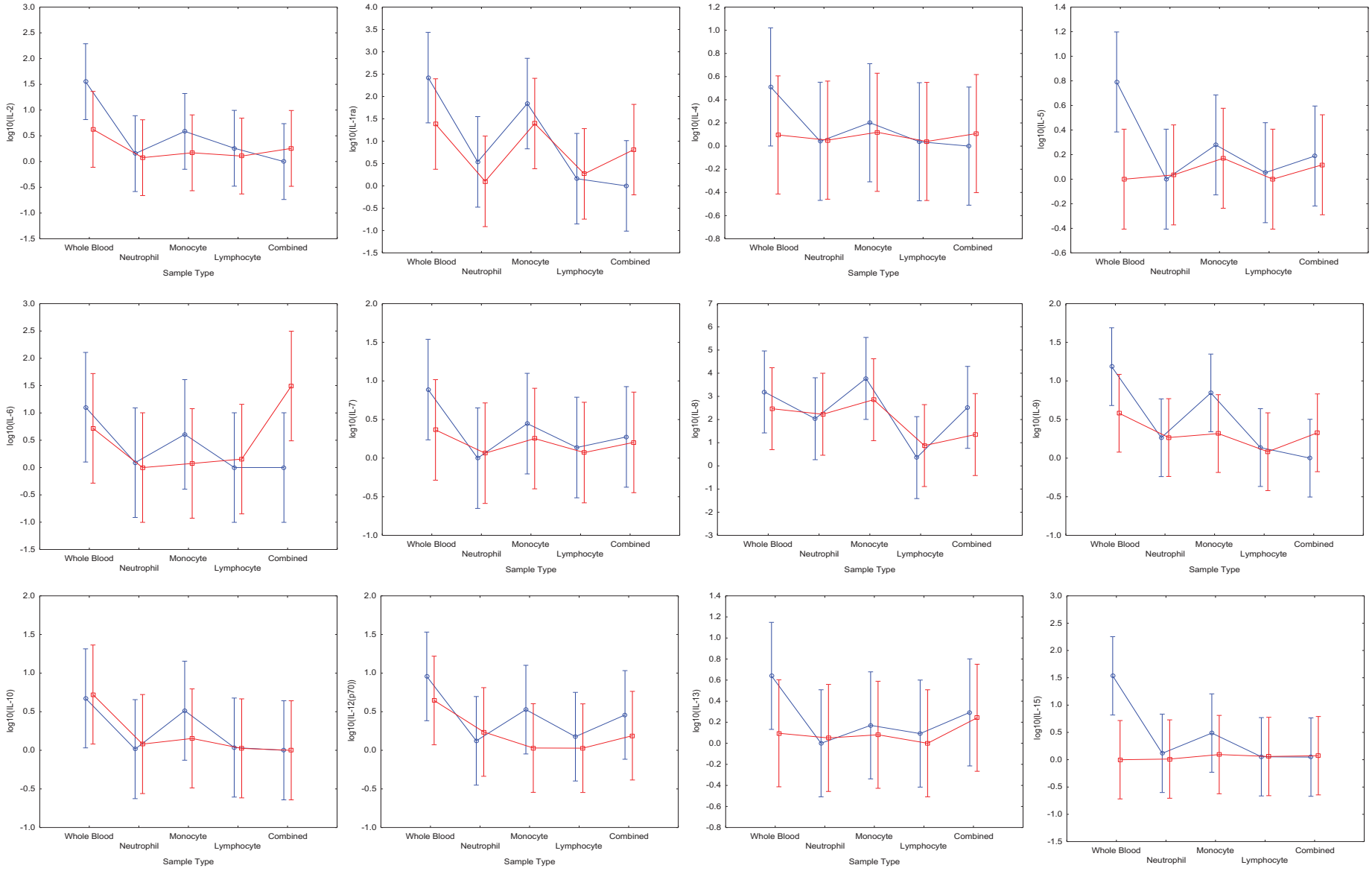

Figure A5.2: The 26 cytokines assessed during this study, under stimulated conditions.

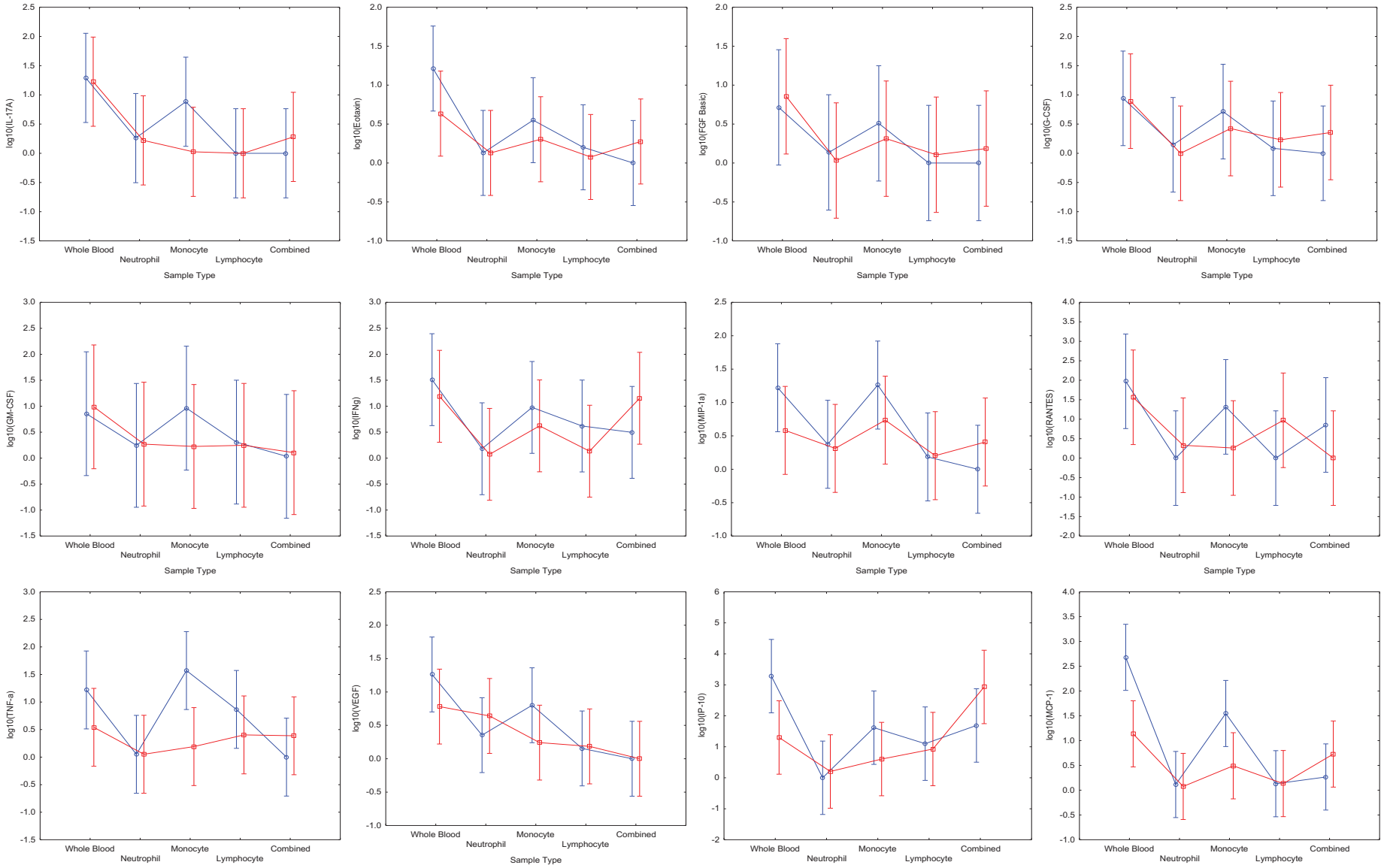

Figure A5.2: Continued…The 26 cytokines assessed during this study, under stimulated conditions.

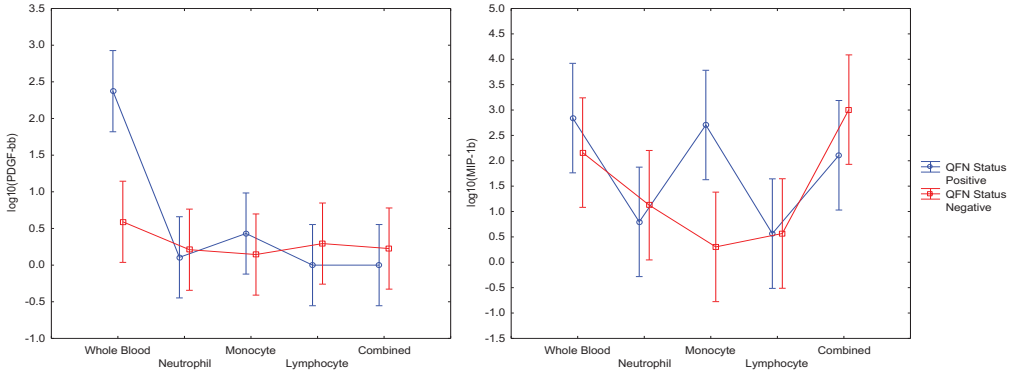

Figure A5.2: Continued…The 26 cytokines assessed during this study, under stimulated conditions. Blue and red data points represent data for QFT+ and QFT- participants respectively.

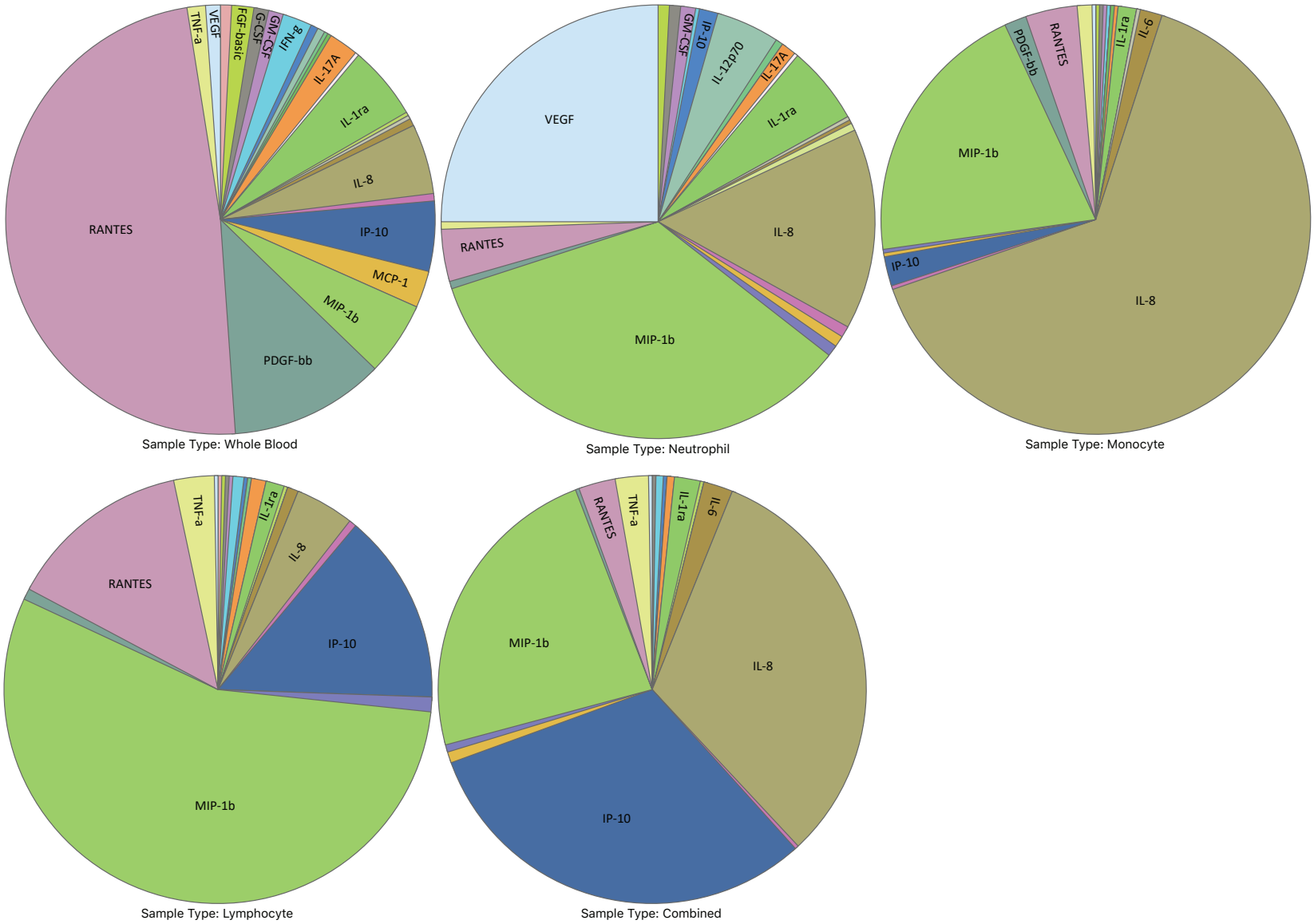

*Figure A5.3: SPICE pie charts representing the relative contributions of each cytokine to the overall individual cell subset cytokine profile of **unstimulated** samples, expressed as a proportion.*

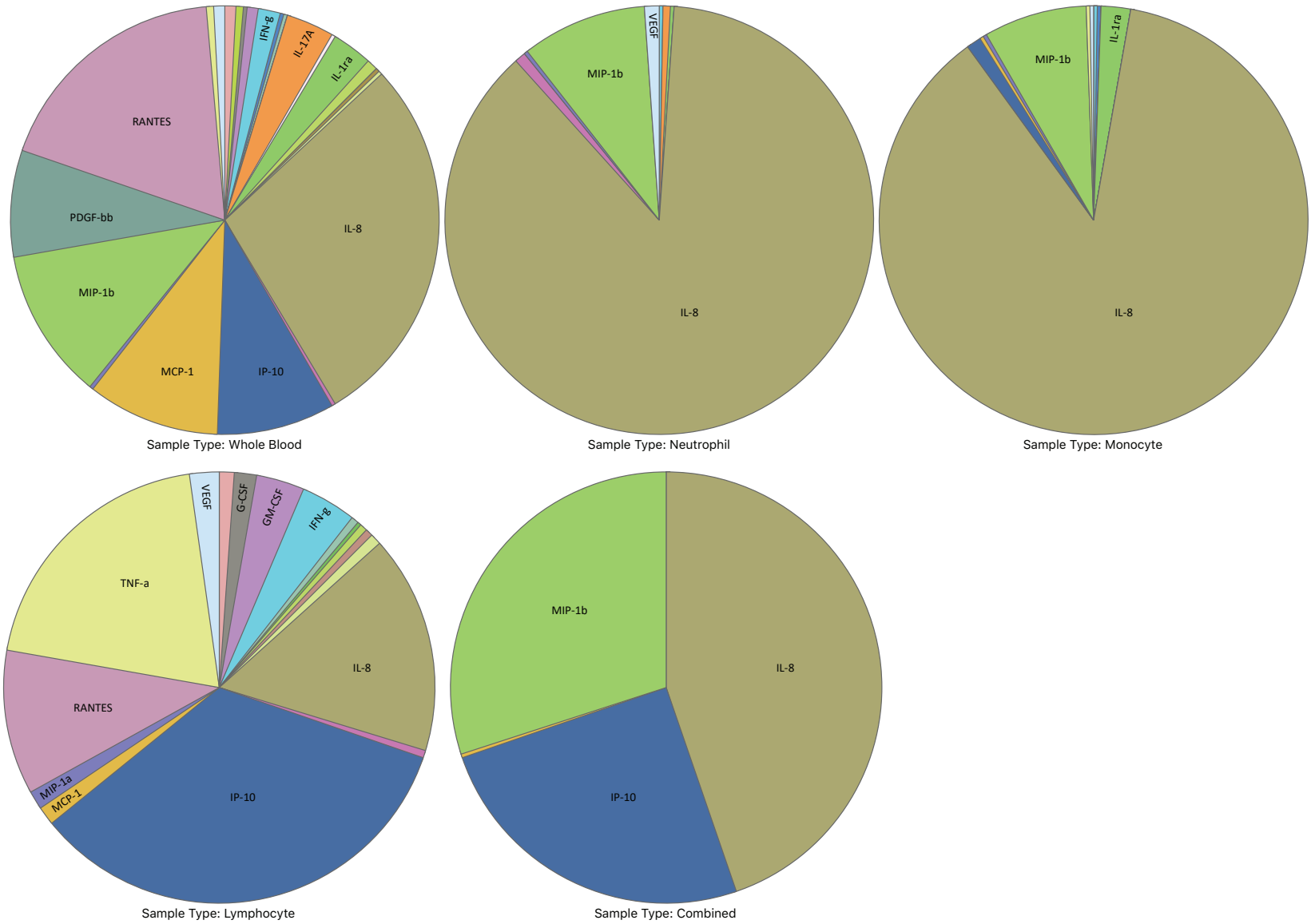

*Figure A5.4: SPICE pie charts representing the relative contributions of each cytokine to the overall individual cell subset cytokine profile of **antigen stimulated** samples, expressed as a proportion.*

Chapter 6

Investigation into the role of Myeloid-Derived Suppressor Cells in peripheral blood during the immune response to TB disease.

The complexity and current limited understanding of the innate immune system is not lost on the scientific community. Paradoxes like the development of innate immune memory in response to certain pathogen-associated molecular patterns have confounded traditional beliefs and created more questions than answers. Such is the case with the findings generated in Chapter 5 of this thesis where it was observed that *M.tb*-specific antigens are capable of independently and directly activating innate myeloid subsets without the need for antigen-specific adaptive subset counterparts being present. More specifically, Chapter 5 identified what could be considered the "trained immunity" of the peripheral blood monocyte compartment, which has previously not been identified. Currently, trained immunity is defined as "a heightened response to a secondary infection that can be exerted both toward the same pathogen and a different one (cross-protection)" (as defined by Netea *et al*.)[279]. Trained immunity in mammals confers a degree of non-specific protection against infections through induction via either (1) the proinflammatory cytokines IL-1 and TNF[305,306], or via (2) pathogen-associated molecular pattern (PAMP) recognition by pathogen-recognition receptors (PRRs), like the Toll-like receptor (TLR) family. Previous research has shown trained immunity-type responses develop in monocytes, macrophages and NK cells in response to whole microorganisms, like H37RV, following exposure to LPS and/or BCG vaccination (reviewed in Netea *et al*.[280]). However, no previous work has identified such a response in the context of *M.tb*-specific peptides like those found in commercial interferon-gamma release assays.

Chapter 5 also demonstrated the significantly upregulated expression of cytokines like IL-6, IL-8, IL-13, IP-10, MIP-1α, MIP-1β, and TNF-α under experimental conditions in which monocytes were co-cultured with $CD3^+$ T lymphocytes, compared to whole blood responses. $CD3^+$ T lymphocyte responses were concurrently dampened under these conditions, suggesting a suppressive mechanism may be active. A heterogeneous population of innate, immature myeloid cells has the potential to elicit the observed suppressive responses. Known as myeloid-derived suppressor cells (MDSC), these cells are known to expand during states of chronic inflammation such as during cancer, and bacterial and viral infections, but most importantly are known for their potent suppression of T lymphocytes, among other functions[181]. Two distinct effector subsets of MDSC exist, namely monocytic MDSC (M-MDSC) and polymorphonuclear MDSC (PMN-MDSC) which characteristically resemble monocytes and neutrophils, respectively, through their expression of known monocyte and neutrophil phenotypic markers, i.e. CD14 and CD15, respectively[307]. A third, less well known subset also exists as "early" MDSC (eMDSC) which are thought to be the precursors of the effector subsets, but little knowledge is available on this subset both in cancer and other inflammatory diseases[307].

A number of the cytokines mentioned above are frequently associated with the mechanisms driving the expansion and recruitment of MDSC, therefore, their significant upregulation during culture of

monocytes with enriched $CD3^+$ T lymphocytes suggests that MDSC may be eliciting the suppressive effect. The reason behind this hypothesis is that there is a large possibility of isolating M-MDSC during a $CD14^+$ monocyte isolation using MACS® microbeads. M-MDSC and monocytes share the CD14 marker, and the MACS® isolation technique does not discriminate labelled cells based on size, allowing M-MDSC present in the PBMC fraction to be isolated simultaneously with non-suppressive monocyte subsets. Since Chapter 5 identified the upregulation of these cytokines in latently infected and uninfected healthy controls, it is possible that this data is representative of a previous study in our research group that demonstrated an increase in the MDSC population in recently infected participants, but a reduction of MDSC in those who are remotely exposed[308]. It is therefore suggested that MDSC, particularly the M-MDSC subset, are expanded in the periphery during latent *M.tb* infection and may play a role in the containment of dormant bacilli[35]. It would be important to investigate the degree with which the MDSC population is expanded in healthy, recently exposed controls compared to during active TB disease. More recent work from our research group has successfully identified the MDSC population within whole blood of active TB disease patients, however, as the field of MDSC research developed, it became clear that the determination of the frequency of this population should occur in PBMC rather than in whole blood. This leads to one of the aims of this chapter, in which the frequency of circulating MDSC, and their respective subsets, were investigated in participants with active TB disease as well as participants with latent *M.tb* infection.

Since our understanding of the physiological characteristics of MDSC are relatively uncertain, investigations need to be carried out to further elucidate the phenotypic profile of these cells in order to better understand (1) the immunological functions associated with MDSC, as well as (2) the interactions MDSC are capable of eliciting with other cell types. This was the basis for the secondary aim of this chapter in which a specific protein of interest previously not investigated in active TB disease in any cell type, was investigated for either its presence or absence on the surface of MDSC. This protein, caveolin, is responsible for an alternative endocytic pathway capable of providing an alternative mechanism of entry into host cells that bypasses the phagolysosome and, therefore, pathogen elimination. Caveolin, a membrane lipid scaffold protein, has been found to be highly expressed on MDSC cell surfaces in a murine TB model, when compared to other myeloid subsets such as dendritic cells (Prof. Manfred Lutz, personal communication, unpublished findings). Furthermore, caveolar-mediated endocytosis signaling was highlighted in previous work as significantly upregulated during the TB treatment period by bioinformatics pathway analyses (B. Smith; unpublished Master's work and the precursor study for the FACS Select study in Chapter 4 of this thesis, 2014). Through the expression of caveolin-1 (the predominant form of the caveolin protein) at the plasma membrane of various phagocytes, invaginations or caveolae of the plasma membrane are formed, rich in cholesterol and other lipids[309]. These membrane-bound vesicles are capable of endocytosing various molecules, including live bacteria, and travel through to the cell interior where they may fuse to form pH neutral, endosome-like structures called caveosomes. Here, endocytosed bacteria are likely capable of evading the host immune system as well as be nourished by the abundance of lipids found in these vesicles[309–311]. Data on MDSC from a murine *M.tb* infection model has elegantly shown the presence of live *M.tb* bacilli within MDSC[35], but

no proof of this concept exists in human TB studies. It is understood that MDSC are poor antigen-presenting cells, so considering the evidence that live *M.tb* bacilli may be readily internalized, suggests that MDSC are utilizing an alternative entry mechanism, for which the caveolar-mediated endocytosis pathway is the most likely. We, therefore, planned to investigate the presence or absence of this protein on the surface of MDSC as part of a proof-of-concept study to supplement current MDSC phenotype literature.

6.1 Study Design

Hypothesis

We hypothesise that MDSC alter immune responses during *M.tb* infection and disease.

Aims

The primary aim of this study is to investigate the immunomodulatory role of MDSC in peripheral blood mononuclear cells (PBMC) on the immune response during active TB disease compared to latent *M.tb* infection. The secondary aim of this study is to investigate the presence or absence of caveolin and TLR4 on MDSC as a theoretical proof-of-concept for future studies, using classical monocytes as the control population.

Objectives

- Characterise the frequency of MDSC and MDSC subsets in PBMC from participants with active TB disease and latent *M.tb* infection, using classical monocytes isolated from PBMC as the control population.
- Investigate the surface expression of caveolin-1 and TLR4 on MDSC using flow cytometry, comparing results to the classical monocyte control population.
- Investigate the potential of MDSC to suppress *M.tb*-specific immune responses during active TB disease in PBMC using the cytokine profile seen by the leukocyte subset stimulations.

6.2 Methods

6.2.1 Participant Recruitment

Participants were recruited from two field sites, Adriaanse and Dunoon, in the Cape Peninsula. From these two sites, eighteen participants with confirmed active TB were recruited at time of diagnosis before initiation of treatment by dedicated professionals. Each participant agreed to give approximately 20ml of peripheral blood from venipuncture into sodium heparin-coated vacutainers to prevent clotting.

Ten healthy, QFT+ participants were recruited from Tygerberg as healthy controls without known recent TB contacts, and also consented to giving approximately 20ml of peripheral blood into sodium heparin-coated vacutainers.

Inclusion Criteria

- Had to be between the ages of 18 and 65 years.
- Willing to give informed consent.
- Willing to have an HIV test performed and their result disclosed to a field worker, as well as consent for their result to be used for statistical purposes for the study.
- TB patients had to have a newly confirmed diagnosis of pulmonary TB infection.
- Susceptible TB infection.
- TB patients had to have an HbA1c level of <42mmol/mol (6%) (non-diabetic).
- Healthy controls had to have a negative GeneXpert® MTB/RIF (Cepheid) test on collected sputum samples, and present with no symptoms suggestive of TB disease.

Exclusion Criteria

- Participants were excluded if they had coexisting diseases such as HIV, chronic bronchitis/asthma/emphysema, or cancer.
- Participants with a haemoglobin level of <10g/l.
- Participants who weighed less than 40kg at the time of enrolment.
- Participants who were pregnant at the time of enrolment.
- Steroid use within the last 6 months before enrolment.
- Previous known TB infections and/or treatment.
- Any resistance to TB chemotherapeutics, including GeneXpert® detected rifampicin resistance (monoresistance, MDR-TB, XDR-TB).
- Alcohol abuse or the use of illegal drugs.
- Concomitant participation in a drug or vaccine trial.
- Permanent residence/residence in the study area for less than 3 months.
- Healthy controls who are known to have had TB disease previously.
- Healthy controls who had a negative QFT status.

Ethical Considerations

Ethics approval for this study was obtained from the Human Research Ethics Committee of Stellenbosch University under the ethics number S16/10/212. Participant recruitment formed part of the ScreenTB study which obtained from the Human Research Ethics Committee of Stellenbosch University under the ethics number N16/05/070. All sensitive patient information, including given names and places of work etc., were kept strictly confidential to clinical research personnel only. Participants were identified using a unique ID generated specifically for this study. This study was performed in accordance with the Helsinki Declaration.

6.2.2 Reagents and Buffers

The reagents listed in Table 6.1 were prepared and used for the completion of this study. These include MACS Buffer for MACS® isolation, 4% paraformaldehyde for the fixation of cells, 2% FACS buffer for flow cytometry, and cryomedia for the cryopreservation of live and fixed cells.

Table 6.1: General reagents prepared for use during this study.

	Volume:	**Manufacturer:**	**Catalogue Number:**
MACS Buffer (Filter Sterilized)			
1X PBS (ml)	4000	LONZA™	BE17-517Q
2mM EDTA (g)	2.98	Sigma-Aldrich	
0.5% BSA (g)	20	Sigma-Aldrich	A7030
4% Paraformaldehyde (PFA)			
1X PBS (ml)	30	LONZA™	BE17-517Q
16% PFA (ml)	10	Thermo Scientific	28908
FACS Buffer (2%)			
1X PBS (ml)	49	LONZA™	BE17-517Q
HyClone™ FCS (ml)	1	GE Healthcare Life Sciences	SV30160.03
Cryomedia (10% DMSO with 90% FBS)			
HyClone™ FCS (µl)	900	GE Healthcare Life Sciences	SV30160.03
DMSO (µl)	100	MERCK	317275-500ML

Co-stimulatory Antibody Working Solution

The co-stimulatory antibodies anti-CD28 and anti-CD49d (Becton Dickinson, New Jersey, USA) were used during the cell stimulations, and were prepared according to Table 6.2.

Table 6.2: Co-stimulatory antibody working solution preparation details.

Reagent:	Concentration:	Volume:
Anti-CD28 (Clone: L293)	1000µg/ml	2.5µl
Anti-CD49 (Clone: L25)	1000µg/ml	2.5µl
PBS	1 X	45µl
		50µl

Purified Protein Derivative (PPD) Working Solution

PPD was prepared for use as the primary stimulatory agent during this study. From a stock solution (concentration 1mg/ml) of 1ml, a working solution was prepared using non-supplemented RPMI to obtain a concentration of 200µg/ml. Following addition of the working solution to 1ml of the cell suspension (described in the methods section below), the final PPD concentration used for stimulations was 10µg/ml.

Supplemented RPMI

Supplemented RPMI was prepared from normal RPMI to which 1% L-glutamine and 2% FBS was added.

6.2.3 Laboratory Procedures

The collected peripheral blood was processed within two hours after blood draw. In order to investigate MDSC's they had to be isolated from peripheral whole blood, and for this the MACS® Microbead Isolation (Miltenyi Biotec, Cologne, Germany) technique was used. MDSC's are phenotypically considered to have an HLA-DR negative, CD33 positive lineage as they are a regulatory subset of immature myeloid cells.

Peripheral Blood Mononuclear Cell (PBMC) Isolation

PBMC's were isolated from the collected peripheral whole blood using the Ficoll-Paque PLUS Density Centrifugation technique (GE Healthcare Life Sciences, United States). Briefly, NaHep vacutainers were inverted five times and whole blood diluted in a sterile 50ml Falcon tube at a ratio of approximately 1:1 with sterile 1X PBS, not exceeding 35ml in total. The diluted blood was then slowly pipetted over 15ml of Ficoll without disturbing the Ficoll layer and centrifuged at room temperature (RT) for 25 minutes at 400 x g with brake and acceleration off. Following centrifugation, the plasma was aspirated and discarded, while the PBMC layer was aspirated into a separate 50ml Falcon tube and washed once with 50ml sterile 1X PBS at 400 x g for 10 minutes. The supernatant was discarded, and the pellet re-suspended in the remaining liquid, after which it was washed for a second time in 10ml filter sterilized MACS® buffer (1X PBS, FBS, 0.5M EDTA). The pellet was re-suspended in 10ml MACS® buffer and the cells counted using a haemocytometer and ZEISS microscope (ZEISS, Germany). A portion of the

cells were diluted in a 1 in 5 dilution using Trypan Blue (Thermo Fisher Scientific, United States) and the cell count determined.

After determining the cell count, approximately 2 x 10^6 PBMC's were transferred into a clean 15ml Falcon tube, centrifuged at 300 x g for 8 minutes, the supernatant removed, and the pellet re-suspended in 2ml supplemented RPMI. These cells were then set aside on ice for later use in the Purified Protein Derivative (PPD) stimulations as a control fraction.
Another fraction of approximately 2 x 10^6 PBMC's were transferred to a clean 15ml Falcon tube for use in a CD14 positive monocyte isolation, described below, as a second control fraction.
The remaining cells and the CD14 isolation fraction were then centrifuged at 300 x g for 10 minutes at 8°C in preparation for the magnetically activated cell sorting (MACS®) microbead technique explained below.

MACS® MicroBead Isolation

For more details on the principle and column specifications of MACS® isolation, see Chapter 5, section 5.2.3.

Isolation 1 – CD33 positive cells

A MACS® Whole Blood CD33 isolation kit was modified to isolate CD33 positive cells from isolated PBMC's so as to reduce the overall number of isolations that needed to be performed on one day. The protocol is given in brief.

Staining Procedure:

The manufacturer's instructions in the product insert were followed for each microbead type, e.g. CD3 microbeads or whole blood CD33 microbeads as in this instance, as well as for the columns.
Briefly, following the centrifugation step at the end of the PBMC isolation, the entire supernatant was aspirated using a P200 pipette without unsettling the pellet and leaving no residual volume. 50µl whole blood CD33 microbeads per 7 x 10^6 cells was then added to the pellet. This was incubated in the fridge (4°C) for 20 minutes, after which 2ml MACS® buffer was added and centrifuged at 445 x g for 10 minutes at RT **without the brake**. The supernatant was again carefully aspirated but leaving behind approximately 1-2mm of residual volume to avoid cells loss. The pellet was re-suspended in 4ml MACS® buffer and kept on ice while the magnetic separation was being set up.

Magnetic Separation:

A new column (chosen according to the cell count of each individual isolation as described above) was placed in the magnetic field of the MACS® Separator and primed according to the column specifications in Chapter 5, Table 3. The cell suspension was added to the column and the unlabeled cells collected in a 15ml Falcon tube. The column was then washed according to Table 5.3 (Chapter 5), each time adding the MACS® buffer only when the column reservoir was empty. The flow through contained the CD33 negative cellular fraction which was kept on ice for use in a CD3 positive isolation. The column

was removed from the MACS® Separator and inserted into a clean 15ml Falcon tube and rinsed according to Table 5.3 (Chapter 5) using the plunger and elution buffer to elute the positively labeled cells. A cell count was performed, as before, before continuing with the stimulations.

Those cells that were left over after the stimulations were cryopreserved in 1ml cryomedia and step-frozen in a Nalgene Mr Frosty™ at -80°C after which it was stored in liquid nitrogen until use in flow cytometry.

Isolation 2 – CD3 positive cells

CD3 positive T cells were isolated from the CD33 negative cell fraction that remained following isolation 1 using the exact same procedures with the exception of the use of CD3 microbeads instead of whole blood microbeads. These cells were counted after being isolated, had purity check fractions taken and processed, and the remainder kept on ice until the PPD stimulations.

Isolation 3 – CD14 positive cells

The CD14 positive isolation was performed in tandem with the CD33 isolation using the 2 x 10^6 PBMC's kept aside after determining the PBMC cell count. The isolation followed the same procedure as the CD33 isolation, with the exception of the use of CD14 microbeads. These cells were counted after isolation, purity check fractions taken and processed, and the remainder cryopreserved in 1ml cryomedia as a positive control for the flow cytometry analysis.

Cell Stimulations

Each of the isolated cell fractions were stimulated with PPD, proteins derived from *M.tb,* after having anti-CD28 and anti-CD49d co-stimulatory antibodies added to ensure proper cellular activation and to assess the antigen-specific response elicited by these cells. Each cell fraction had an unstimulated condition and a stimulated condition for comparative reasons, and specific cell numbers used in each stimulation to mimic host internal cellular concentrations (outlined in Table 6.3).

Table 6.3: Outline of the stimulation conditions used, and the cell numbers used for each.

	Unstimulated	**Stimulated**	**Cell Number per Tube**	
PBMC	Yes	Yes	~1 x 10^6	
CD33	Yes	Yes	~5 x 10^5	
CD3	No	Yes	~1.25 x 10^6	
Co-Culture Experiment			**CD33**	**CD3**
CD33 + CD3*	No	Yes	~5 x 10^5	~1.25 x 10^6
CD33 + CD3 (1:1)*	No	Yes	~5 x 10^5	~5 x 10^5

*Two co-culture conditions were included, one to assess the response seen when in vivo cell numbers are used, and one to assess the response seen when equal numbers of each cell type are used.

For each stimulation condition, the required number of cells were re-suspended in 1ml RPMI and transferred to a sterile 2ml Eppendorf tube. 5µl of co-stimulatory antibodies were then added to each tube (both "Unstimulated" and "Stimulated" where applicable)

In the "Stimulated" tubes, 20µl of the PPD working solution was added and mixed thoroughly by pipetting up and down. All of the tubes were then placed in the incubator at 37°C, 5% CO_2 for 16 hours. Following the first incubation, 8µl of Brefeldin A was added to all of the tubes (Stimulated and Unstimulated), mixed thoroughly and placed back into the incubator for another 4 hours for a total incubation time of 20 hours. The supernatant was harvested into 3 x 150µl aliquots which were stored at -80°C until further use. The remaining cells were then fixed with 4% PFA as previously described and cryopreserved in 1ml cryomedia for later use in flow cytometry.

6.2.4 Cytospin Imaging for Assessment of Isolated Population Morphology

In order to visualize the cells that made up the isolated populations, the cytospin technique was used to concentrate cells on to a fixed point on a glass microscope slide before being stained with the RapiDiff staining method. Consult Chapter 5 (section 5.2.5) for the methodology.

6.2.5 Flow Cytometric Analyses for the Phenotyping of MDSC's

Purity Checks

After the PBMC isolation and the MACS® isolation of the CD3+, CD14+ and CD33+ cells, 100µl cell fractions were placed in separate 5ml Falcon tubes for each cell type and fixed with 1:1 volume 4% PFA for 10 minutes in the dark at RT. After the incubation, the cells were washed once with 1ml MACS® buffer and centrifuged at 300 x g for 10 minutes (RT). The supernatant was discarded, and the cells re-suspended in 50µl MACS® buffer. Each Falcon tube was stained according to the strategy given in Table 6.4 below. The cells were stained for 30 minutes at 4°C in the dark and washed once with 1ml MACS® buffer after incubation. The cells were then centrifuged at 400 x g for 10 minutes, the supernatant discarded, and the pellet re-suspended in 200µl MACS® buffer, ready for acquisition on the same or following day. The cells were kept in the fridge until acquired on the BD FACSCanto™ II (Becton Dickinson, New Jersey, USA).

Table 6.4: Staining conditions and single stain specifications for the purity check samples.

Staining Condition:	Antibody:	Volume:
PBMC Unstained	None	N/A
PBMC Stained with CD3	PE	2µl
PBMC Stained with CD14	FITC	
PBMC Stained with HLA-DR and CD33	HLA-DR: APC-Cy7 CD33: PE	
Isolated CD3 Cells Stained with CD3	PE	
Isolated CD14 Cells Stained with CD14	FITC	
Isolated CD33 Cells Stained with HLA-DR and CD33	HLA-DR: APC-Cy7 CD33: PE	

Antibody Panel

Using the BD FACSCanto™ II, an eight colour panel was set up to investigate the phenotype of the MDSC in terms of caveolin and TLR4 expression. Three lineage markers were selected to accurately identify the immature myeloid cell population, namely CD11b, HLA-DR, and CD33. The marker CD3 was included to exclude any possible T cells in the isolated fraction, while CD14 and CD15 were used to identify between the two MDSC subpopulations, namely monocyte-like MDSC's (CD14) and granulocyte-like MDSC's (CD15). The antibodies chosen for this study are given in Table 6.5 along with the concentrations to be used as determined by the single stain antibody titrations, the method described previously in Chapter 4.

Table 6.5: The antibodies chosen to investigate the phenotype of MDSC's in terms of their TLR4 and potential Cav-1 expression. Their clones and volumes to be used per test are also given.

Marker:	Fluorochrome:	Clone:	Isotype:	Catalogue no:	Volume*:
CD3	APC-Cy7	SK7	Mouse	557832	1.25µl
CD14	PE	MφP9	Mouse	347497	2.5µl
CD15	BV510	W6D3	Mouse	563141	0.3µl
CD11b	PerCP-Cy5.5	M1/70	Rat	101228	0.6µl
CD33	PE-Cy7	P67.7	Mouse	333946	0.3µl
HLA-DR	APC	L243	Mouse	307610	2.5µl
TLR4	BV421	TF901	Mouse	564401	1.25µl
Cav-1	FITC	7C8	Mouse	Sc-53564	5µl

*A 50µl staining volume was used throughout.

Compensation and staining controls (Fluorescence Minus One) were also performed to complete the optimization of this panel using the techniques described in Chapter 4. These controls allowed for the bench-marking of sample background and signal spillover.

Sample Staining, Acquisition and Analysis

As outlined in Chapter 4, 2% FBS in PBS was prepared and kept at 4°C prior to sample staining. Following removal from liquid nitrogen, cells were immediately thawed in a 37°C waterbath, transferred to a clean 15ml Falcon tube and the volume brought up to 10ml with 2% FBS in PBS. The cryovial was rinsed with the cell-buffer mix to remove as many of the cells from the cryovial as possible. The falcon tube was then spun at 400 x g for 10 minutes, the supernatant discarded and the cells washed twice in 2% FBS in PBS. After the final wash, the cells were divided into the necessary tubes.

While the cells were being centrifuged during the wash steps, the antibody mixes were prepared for each panel. The mix was made according to the number of samples being analysed on the day, plus an extra 10% volume to account for possible pipetting error. The total volume of antibody mix and 2% FBS in PBS added up to 50µl, as the desired staining volume was 50µl. The antibody mix was then added to the pelleted cells post-wash and gently vortexed for 5 seconds. The cells and antibody were then incubated in the dark for 1 hour at 4°C. Following incubation, the cells were washed in 1ml 2% FBS in PBS to remove any unbound antibody and centrifuged at 400 x g for 5 minutes. Finally, the supernatant was discarded and the pellet resuspended in 200µl 2% FBS in PBS ready for acquisition. The cells were stored at 4°C in the dark until acquisition either on the day or the following morning.

Samples were acquired on the BD FACSCanto™ II using the FACSDiva™ software (Becton Dickinson, New Jersey, USA), version 8.0.1, using the saved settings established during the setup experiments to ensure consistency and reproducibility, and the FCS data files for each sample saved for further analysis. In terms of which samples were acquired, all of the HLA-DR negative CD33 positive cells cryopreserved following magnetic separation (not used for co-culture experiments) were stained and acquired to investigate their phenotype (MDSC phenotyping). The cells from the co-culture experiments were also stained and acquired to assess the change in their phenotypes after stimulation, both the MDSC's and the T cells.

6.2.6 Co-culture Cytokine Profile Investigation

Luminex Immunoassay

The concentrations of 22 cytokines and chemokines were assessed in the culture supernatants from all study participants and their culture conditions using the Luminex immunoassay platform (Luminex, Bio Rad Laboratories, Hercules, CA, USA). The cytokines assessed are given in Table 6.6. Four of the cytokines/chemokines were evaluated using a MILLIPLEX® multiplex kit (MERCK MILLIPORE, Darmstadt, Germany), while the remaining 18 cytokines were evaluated using an R&D Systems® multiplex kit (R&D Systems®, Minnesota, USA). Each manufacturer employs sometimes vastly different reagents, for which there are many, and as such the preparation of all reagents shall not be outlined in detail. However, the principle of the technique remains constant. Please refer to the manufacturer's instructions for further details.

Table 6.6: The two multiplex kit details for the assessment of human cytokines and chemokines.

Multiplex Kit:	**MILLIPLEX® MAP Human Cytokine/Chemokine Kit**	
Catalogue Number:	HCYTOMAG-60K	
Manufacturer:	MERCK MILLIPORE	
Cytokines Assessed:	Interferon (IFN)-α2	Interleukin (IL)-4
	Macrophage inflammatory protein (MIP)-1α	IL-6
Multiplex Kit:	**Human Cytokine Kit**	
Catalogue Number:	LXSAHM-20	
Manufacturer:	R&D Systems®	
Cytokines Assessed:	ADAMTS13	CD40 Ligand (CD40L)
	C-C motif chemokine ligand (CCL) 1	CCL2/monocyte chemoattractant protein (MCP)-1
	C-X-C motif chemokine ligand (CXCL) 11	Fas cell surface death receptor (Fas)
	IFN-γ	IL-1β
	IL-13	IL-2
	IL-33	MIP-1β
	IFN-γ-inducible protein (IP)-10	Tumour necrosis factor (TNF)-α
	Granulocyte-macrophage colony-stimulating factor (GM-CSF)	IL-1α
	IL-10	IL-22

MILLIPLEX® MAP Assay Preparation and Procedure

The standards, controls and samples were prepared according to the manufacturer's instructions. All prepared reagents and samples were allowed to reach room temperature before use. Briefly, the 96-well plate was pre-wet with 200µl of the prepared 1X assay-specific wash buffer. The plate was placed on a plate-shaker (800 ± 50 rpm) for 10 minutes at room temperature, and the wash buffer decanted. 25µl of each standard and/or control was added according to the plate template, with 1X wash buffer being used for the background (0 pg/ml) standard. The appropriate matrix solution was then added to each sample and control well, which in this instance was supplemented RPMI owing to the manufacturer's instructions indicating that the tissue-culture culture medium be used. 25µl assay-specific assay buffer was added to each sample well, as well as the background wells, followed by 25µl of sample culture supernatant into the appropriate wells (according to the plate template). The prepared antibody-immobilized beads were vortexed, and 25µl added to each well. The plate was then sealed, wrapped in foil to protect from light, and incubated overnight at 4°C. The following day, the plate was

washed twice with 200µl wash buffer, followed by the addition of 25µl of the prepared detection antibodies. The plate was incubated on a plate-shaker for 1 hour at room temperature, 25µl of prepared streptavidin-PE added to each well and incubated for a further 30 minutes on a plate-shaker at room temperature. The well contents were then decanted and washed twice with 200µl wash buffer. If read immediately, 150µl sheath/drive fluid was added to each well and the plate incubated for 5 minutes on a plate-shaker, followed by immediate acquisition. If not, the plate was sealed, wrapped in foil, and incubated at 4°C until ready for acquisition.

R&D Systems® Assay Preparation and Procedure

The standards and samples were prepared according to the manufacturer's instructions. All prepared reagents and samples were allowed to reach room temperature before use. Samples were diluted by adding 40µl assay-specific calibrator diluent to 20µl sample supernatant. Briefly, 50µl of the microparticle cocktail was added to each well of the 96-well plate after vortexing. Standards and samples were added in 50µl volumes to the appropriate wells, as per the plate template – no controls are used in the R&D Systems® multiplex kits. The plate was incubated at room temperature for 2 hours on a plate-shaker (800 ± 50 rpm), after which it was washed three times by adding 100µl of prepared, assay-specific wash buffer to each well. 50µl of the prepared diluted biotin antibody cocktail was then added to each well, and the plate incubated again for 1 hour at room temperature on a plate-shaker. The plate was again washed three times using 100µl wash buffer, and 50µl of diluted streptavidin-PE was added to each well following this. The plate was incubated for 30 minutes at room temperature on a plate-shaker and washed three times using 100µl wash buffer. If read immediately, 100µl wash buffer was added to each well one final time before being incubated for 2 minutes on a plate-shaker at room temperature and acquire immediately. If not, the plate was sealed, wrapped in foil, and incubated at 4°C until ready for acquisition.

Sample Acquisition

Acquisition was performed on the Bio-Plex 200 suspension array system, using the dual-laser, flow-based microplate reader system (Bio Rad). The beads from each sample were acquired individually and analysed using the Bio-Plex Manager™ Software version 6.1 according to recommended settings. Instrument settings were adjusted to ensure 50 bead events per region, with sample size set to 50µl for both multiplex kits.

6.2.7 Data and Statistical Analyses

All data were statistically analysed using GraphPad Prism version 5.0 (GraphPad Software, San Diego, CA, USA) and Statistica version 12.0 (Statsoft, Ohio, USA). A p-value of < 0.05 was considered statistically significant.

Flow Cytometry Data

FCS files generated during acquisition on the flow cytometer were analysed using the third party software FlowJo® (FlowJo LLC, Oregon, USA), version 10.3. Gating strategies were applied (section 6.3.4) and the relevant data, such as median fluorescent intensities of marker expression and frequencies, were extracted. Using GraphPad Prism, data were compared between groups (between TB patients and healthy controls) using the Mann-Whitney test for nonparametric data. This test was also used to compare data within groups, for example the comparison between monocyte and MDSC cell types within the healthy control group. Briefly, (1) total MDSC and monocyte frequencies, (2) MDSC subset frequencies, (3) expression of TLR4 and Cav-1 on the surface of these subsets and total cells, as well as (4) the MFI of each of these markers were compared between groups. The expression levels and MFI of TLR4 and Cav-1 were also compared within groups between MDSC and monocytes.

Luminex Data

Cytokine data generated using the Luminex platform were analyzed using Statistica version 12.0 (Statsoft, Ohio, USA). Data were first assessed for the distribution of the data for each cytokine individually. Thereafter, raw data was either kept as it was, log transformed, or winsorized depending on the distribution. Raw data was only kept as it was if the distribution of cytokine/chemokine's data was normal. Raw data was log transformed when the normality of the errors did not fit a normal distribution curve and was, therefore, skewed; raw data was winsorized when extreme and spurious outliers were evident in frequency distribution plots of cytokines. As was done previously in Chapter 5, mixed model analysis was used to evaluate the differences in cytokine levels between culture conditions. In order to assess the variance of the analyses, an ANOVA using the type III sum of squares was run for the same reasons outlined in Chapter 5. However, unlike in Chapter 5, pairwise comparisons were not performed for the least squares (LS) means owing to there not being paired data. Graphs were generated using GraphPad Prism 5.0 in order to create uniform figures.

6.3 Results

6.3.1 Participant Demographics

As stated previously, eighteen participants with active TB were recruited at diagnosis from the Adriaanse and Dunoon regions of the Cape Peninsula. Ten healthy donors with positive QFT test results from the Tygerberg region were also recruited (Table 6.7). Participants were assessed for treatment outcome following the standard six-month treatment regimen and as such were classified as "Cured", "Probable Cure" and "Failure". Participants with a "Probable Cure" outcome were classified as such mainly when their final sputum culture at month 6 (end of treatment) was positive owing to contaminant growth, but Capillia TB assays and/or GeneXpert® results were negative for *M.tb*.

Table 6.7: Active TB and Healthy Control Participant Demographics.

	Active TB (n = 18)		**Healthy Controls (n = 10)**	
	Male:	Female:	Male:	Female:
Gender:	n = 13	n = 5	n = 4	n = 6
Median Age (Years):	35	31	30	26
QuantiFERON Status:	Positive (n = 18)		Positive (n = 2)	Positive (n = 5)
HIV Infection Status:	Uninfected			
Treatment Failure: (Unknown)*:	n = 2 (n = 3)	n = 0	Not Applicable	

* Participants with unknown treatment outcomes were as a result of the participants missing their end of treatment visit with clinicians.

6.3.2 Isolated Population Yields and Purities

HLA-DR$^-$CD33$^+$ MDSC's, as well as CD14$^+$ monocytes were isolated from approximately 18ml of peripheral blood from active TB and healthy control participants, following a standard PBMC isolation using density gradient media. On average, approximately 4.02x10^6 and 2.99x10^6 HLA-DR$^-$CD33$^+$ MDSC's were isolated from the active TB participants and healthy controls respectively. Approximately 2.04x10^6 and 8.3x10^5 CD14$^+$ monocytes were likewise isolated from the active TB participants and healthy controls respectively (Table 6.8). MDSC and monocytes made up approximately 28% and 19% of the PBMC fraction, respectively, in active TB cases, while they only made up approximately 15% and 9% of the PBMC fraction, respectively, in healthy controls (Table 6.8). CD3$^+$ T cells were also isolated from 7 active TB participants and 5 healthy controls for use during co-culture experiments, and the average isolated CD3$^+$ T cell purity was approximately 79%, while the proportion of PBMC these cells made up was approximately 47% (Table 6.8). Purities for each isolated population was determined by single stain flow cytometry. Upon further investigation, the proportions, as well as the cell numbers of monocytes and MDSC's, were not correlated to each other, or to age, or time to sputum culture

conversion. Unfortunately, demographic data for each participant on other inflammatory conditions present at the time of sample collection was not available. Such conditions ideally would have included intestinal helminth infections and a recent minor bacterial or viral infection (a cold or the flu) as these conditions would surely have influenced the yield of each cell type.

Once each cell type was isolated individually, the enriched cell purities were determined and considered adequate for our intended use. The average purity of isolated HLA-DR^{-}CD33^{+} MDSC's was 77.5%, while the average purity for CD14^{+} monocytes was 73.4% and 78.78% for CD3^{+} T cells.

Table 6.8: Individual participant data on the yield and purity for each cell subset isolated during this study, namely MDSC, monocytes and T cells. The number of cells isolated, the purity of the fraction and proportion that each subset makes up of the PBMC fraction were reported.

Sample ID:	Sample Group:	QFT Status:	MDSC			Monocytes			T Cells		
			Number Isolated:	Isolated Purity:	Freq. of PBMC:	Number Isolated:	Isolated Purity:	Freq. of PBMC:	Number Isolated:	Isolated Purity:	Freq. of PBMC:
SCRN060	ATB	Positive	4.40E+06	87.00%	-	-	-	-	7.90E+06	70.90%	-
SCRN062	ATB	Positive	2.50E+06	76.30%	15.50%	-	-	-	7.60E+06	85.20%	22.80%
SCRN078	ATB	Positive	4.10E+06	-	-	2.90E+06	95.20%	34.80%	2.90E+06	-	-
SCRN079	ATB	Positive	1.90E+06	-	-	1.00E+06	44.60%	11.10%	4.80E+06	65.60%	56.60%
SCRN094	ATB	Positive	1.60E+07	51.50%	17.10%	6.10E+06	87.00%	19.80%	-	-	-
SCRN104	ATB	Positive	2.10E+06	-	-	-	-	-	6.60E+06	91.60%	64.60%
SCRN395	ATB	Positive	6.60E+06	65.50%	24.60%	2.00E+06	60.20%	11.90%	-	-	-
SCRN424	ATB	Positive	8.50E+06	54.60%	26.70%	2.30E+06	71.90%	15.20%	2.20E+06	75.20%	46.50%
SCRN426	ATB	Positive	3.80E+06	78.90%	38.20%	2.30E+06	76.50%	28.20%	3.20E+06	84.20%	46.60%
SCRN428	ATB	Positive	6.60E+05	-	-	3.40E+06	78.00%	19.20%	-	-	-
SCRN593	ATB	Positive	1.63E+06	-	-	-	-	-	-	-	-
SCRN594	ATB	Positive	1.00E+06	-	-	-	-	-	-	-	-
SCRN622	ATB	Positive	2.69E+06	89.30%	26.50%	-	-	-	-	-	-
SCRN624	ATB	Positive	5.88E+06	84.60%	66.60%	1.13E+06	-	-	-	-	-
SCRN626	ATB	Positive	3.44E+06	64.20%	11.10%	6.88E+05	-	-	-	-	-
SCRN627	ATB	Positive	2.56E+06	75.30%	24.10%	8.75E+05	-	-	-	-	-
SCRN628	ATB	Positive	3.25E+06	71.50%	25.00%	1.31E+06	78.10%	13.10%	-	-	-
SCRN629	ATB	Positive	1.43E+06	-	-	4.37E+05	-	-	-	-	-
Control 1	HC	Positive	3.06E+06	96.20%	21.20%	-	-	-	6.60E+06	-	-
Control 2	HC	Positive	4.94E+06	63.60%	15.00%	-	-	-	5.66E+06	-	-
Control 3	HC	Positive	1.37E+06	94.90%	25.10%	-	-	-	7.66E+06	-	-
Control 4	HC	Positive	2.80E+06	68.50%	5.47%	-	-	-	6.60E+06	-	-

Control 5	HC	Positive	2.75E+06	-	-	-	-	-	1.05E+07	-	-
Control 6	HC	Positive	8.75E+05	-	-	9.99E+04	-	-	-	-	-
Control 7	HC	Negative	3.88E+06	89.10%	8.10%	6.25E+05	-	-	-	-	-
Control 8	HC	Negative	3.06E+06	83.20%	11.10%	1.13E+06	79.80%	10.00%	-	-	-
Control 9	HC	Positive	4.75E+06	84.40%	24.20%	8.75E+05	-	-	-	-	-
Control 10	HC	Negative	2.38E+06	79.20%	9.89%	1.44E+06	65.90%	8.67%	-	-	-
Average:	**ATB**		**4.02E+06**	**72.61%**	**27.54%**	**2.04E+06**	**73.94%**	**19.16%**	**5.03E+06**	**78.78%**	**47.42%**
	HC		**2.99E+06**	**82.39%**	**15.01%**	**8.33E+05**	**72.85%**	**9.34%**	**7.40E+06**	**N/A**	**N/A**

Abbreviations: ATB – active TB disease; HC – healthy control; QFT – QuantiFERON; Freq. – Frequency; N/A – not applicable

6.3.3 Phenotyping Analysis – Morphology

The cytospin technique was used to concentrate cells from our isolated populations onto glass microscope slides. The partially dried slides were subjected to the Rapi-Diff staining technique for visualization of the cell morphology under 1000X magnification (oil immersion) on a ZEISS microscope fitted with and Axiocam microscope camera. Cellular fractions from isolated monocytes (Figure 6.1(a)), isolated $CD3^+$ T cells (Figure 6.1(b)), as well as isolated PBMC's (Figure 6.1(c-g)) were visualized this way.

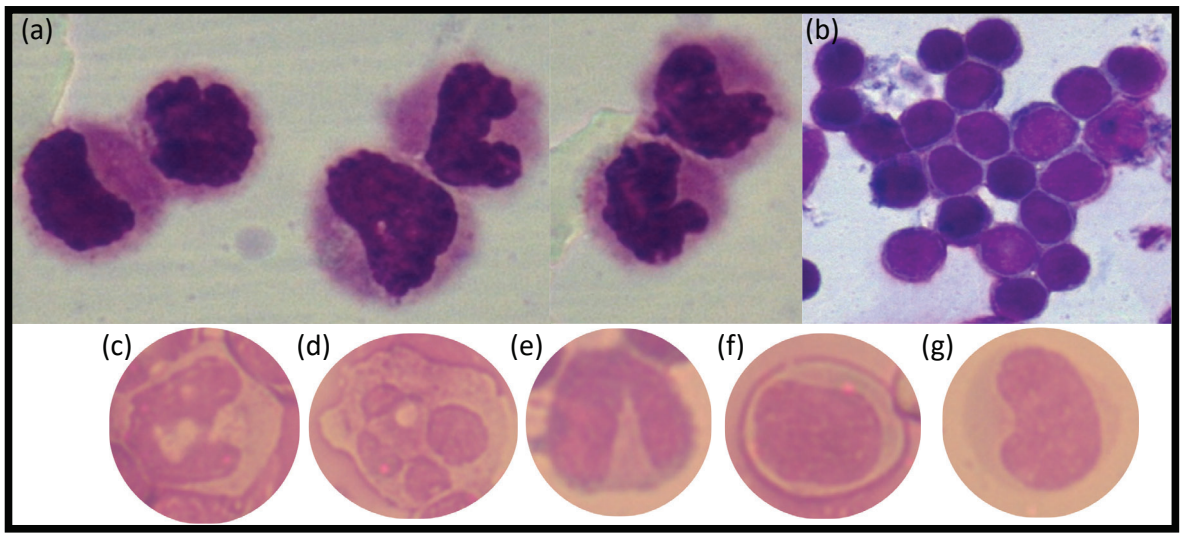

Figure 6.1: Morphological characteristics of the isolated immune cell populations. Isolated monocytes (a), isolated $CD3^+$ T cells (b), and cells present in the total isolated PBMC fraction (c-g) were visualized under 1000X magnification using a ZEISS microscope following cytospin and RapiDiff staining. From the PBMC fraction banded neutrophils (c), mature neutrophils (d), eosinophils (e), lymphocytes (f), and monocytes (g) were observed. Sizes are not indicated owing to this study wanting to identify the different cellular structures rather than size.

The isolated monocyte fraction (Figure 6.1(a)) was approximately 73% pure as confirmed by flow cytometric purity checks (Table 6.8). Monocyte nuclei are characteristically "kidney" or "U"-shaped with a clear cytosol, while the nuclei of lymphocytes (Figure 6.1(b)) are characteristically round in shape and large, taking up the majority of the cytosol which itself is also clear. The lymphocyte fraction, which was made up of mostly $CD3^+$ T cells, was also relatively pure, correlating with the purity data from Flow Cytometry.

In terms of the composition of the PBMC fraction as a whole, we identified a large number of low-density (LD)-neutrophils (Figure 6.1(c and d)). Neutrophils themselves are generally accepted as being absent in the PBMC fraction, as these cells are too dense to remain in the layer above the density gradient media and are meant to pellet with the red blood cells. Previous studies, however, have demonstrated the isolation of these cells with the lymphocyte populations during density gradient isolation, contrary to accepted dogma, and have identified them to be a collection of both immature and mature neutrophils. The immature LD neutrophil fraction was identified as having an MDSC appearance in that

they display suppressive T cell functions, display myeloid and neutrophil markers, and indeed morphologically have a neutrophil-like appearance, of which the suppressive potential is limited to only neutrophils resembling MDSC, i.e. PMN-MDSC[273,274]. Both banded (Figure 6.1(c)) and mature (Figure 6.1(d)) LD neutrophils cells could be seen in our PBMC fraction, but not the hyper-segmented late stage of neutrophil maturation, consistent with referenced studies, supporting the hypothesis that high-density neutrophils are not capable of carrying out suppressive effector functions.

A small number of eosinophils (Figure 6.1(e)) were also observed, along with the expected lymphocytes (Figure 6.1(f)) and monocytes (Figure 6.1(g)) which were observed in high frequencies.

6.3.4 Phenotyping Analysis – Extracellular Markers

HLA-DR$^-$CD33$^+$CD11b$^+$ MDSC and CD14$^+$ Monocyte gating strategies developed from the Fluorescence Minus One staining control.

Isolated PBMC underwent negative HLA-DR MACS® bead isolation, followed by positive CD33 MACS® bead isolation in order to achieve an enriched population of HLA-DR$^-$CD33$^+$CD11b$^+$ MDSC-like cells on which we investigated extracellular phenotypic marker expression via flow cytometry on a BD FACSCanto™ II (Becton Dickinson, New Jersey, USA). Since these cells are unique and their phenotypic markers still largely disputed, we built a gating strategy for the identification of MDSC from the enriched population using markers that are most widely accepted as being representative of MDSC. HLA-DR$^-$CD33$^+$CD11b$^+$ MDSC are accepted as having at least two distinct subsets: monocytic MDSC (M-MDSC) which morphologically resemble monocytes and express the monocyte-specific CD14 surface marker; and polymorphonuclear MDSC (PMN-MDSC) which morphologically resemble granulocytic myeloid cells, such as neutrophils, and express the characteristic granulocyte surface marker CD15[29,31,181,298,307,312]. Recently, a third subset has been identified and is known as “early” MDSC (eMDSC) which are proposed to be the precursors of m- and PMN-MDSC owing to their lack of CD14 or CD15 expression, but expression of other characteristic MDSC surface markers[307]. Taking into consideration these three different subsets, we followed the gating strategies outlined in Figures 6.3 (eMDSC), 6.4 (M-MDSC) and 6.5 (PMN-MDSC). Briefly, each gating strategy began with a standard protocol – a “Time vs FSC-A” gate was first made to ensure that the instrument was stable throughout the acquisition of that specific sample (Figure 6.2(a)), i.e. only those events that were captured during the most stable part of the acquisition were included for further analysis. Possible reasons for a break in instrument stability could include a short blockage which was then resolved, manual operator changes in sample acquisition flow rate, or incorrect laser alignment, but the latter should never occur if the correct pre-acquisition setup and maintenance were performed.

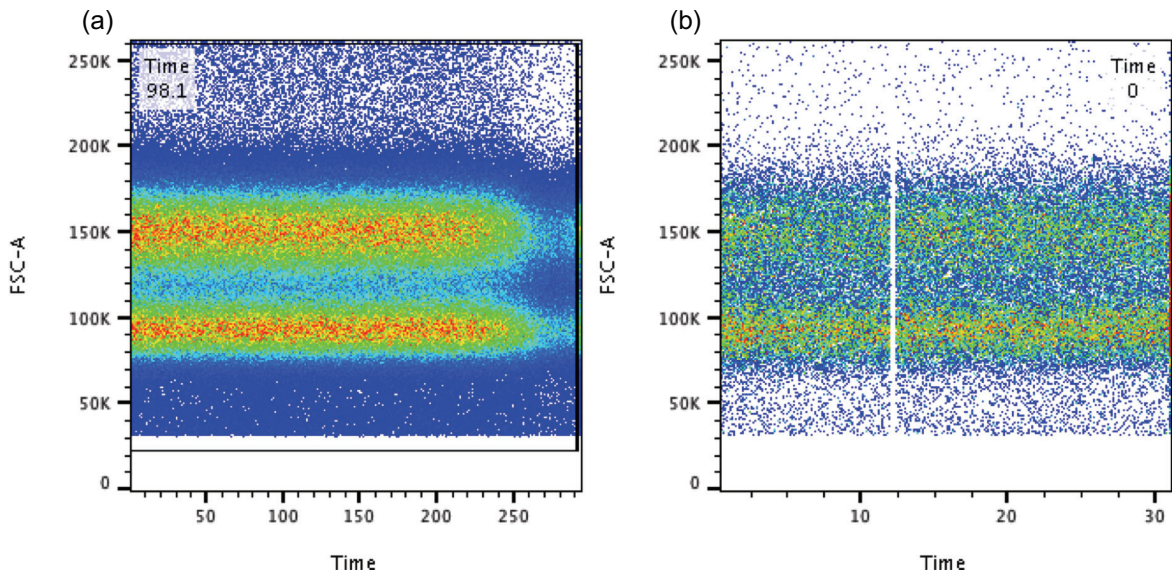

Figure 6.2: A visual comparison between a (a) stable and (b) unstable sample acquisition where an interruption in the sample flow (b) may be observed around 12.5 on the Time axis. In instances where the run was unstable, the time gate was set on the largest stable proportion of acquired events, for example all events to the right of the acquisition break in (b). The examples given were taken from an optimization run.

Next, we gated “FSC-A vs FSC-H” for the exclusion of doublet events, followed by a “FSC-A vs SSC-A” gate for the selection of the isolated cell population (this population has been labelled as “Lymphocytes” for ease of analysis). The isolated populations were then gated according to their respective lineage markers. It should be highlighted here that in some instances of the gating strategy representations a “Contour Plot” was used instead of the generally used “Pseudocolour Plot” when population separations were being assessed for markers that are expressed at low frequencies, or when the markers expressed are on a low frequency cell population as is the case for eMDSC and PMN-MDSC.

Myeloid-derived suppressor cells are proposed to present a basic $CD3^{-}HLA\text{-}DR^{-/low}CD33^{+}CD11b^{+}$ phenotype in humans. While the phenotype characteristics for m- and PMN-MDSC have been described above, the eMDSC subset phenotype is still largely under debate. The gating strategy below (Figure 6.3) represents our proposed phenotype based on an extensive literature search. Briefly, following the standard gating protocol, we plotted the phenotypic marker “CD3 vs SSC-A” and selected for the $CD3^{-}$ population only. We then plotted “CD14 vs CD15” and selected the double negative population (Lin-), as eMDSC are believed to be precursors and not express either of these lineage markers. Next, we plotted “HLA-DR vs SSC-A” and excluded the $HLA\text{-}DR^{+}$ population (Q3), followed by “CD33 vs SSC-A” for the selection of the $CD33^{+}$ eMDSC population. No consensus has been reached regarding the expression of the marker CD11b in this subset. Lastly, the expression of the markers of interest, Cav-1 and TLR-4, were assessed in the eMDSC population by plotting “Cav-1 vs SSC-A” and “TLR-4 vs SSC-A” for individual expression and “TLR-4 vs Cav-1” for possible co-expression.

M- and PMN-MDSC were gated slightly differently to the eMDSC subset owing to more literature being available (Adapted from Bronte *et al.*[307]). Briefly, following the standard gating protocol, we plotted "CD3 vs HLA-DR" and selected the $CD3^{-}HLA\text{-}DR^{-/low}$ population, followed by "CD33 vs CD11b" for the selection of $CD33^{+}CD11b^{+}$ myeloid cells, referred to as total MDSC. Total MDSC were then plotted "CD14 vs CD15" to distinguish between the monocytic ($CD14^{+}CD15^{-}$; Figure 6.4) and granulocytic ($CD14^{-}CD15^{+}$; Figure 6.5) fractions, followed by the investigation of the expression of the markers of interest as done for the eMDSC strategy (Figure 6.3).

As described in the Methods section of this study, a fraction of isolated PBMC underwent a separate positive CD14 MACS® bead isolation in order to achieve an enriched population of $CD14^{+}$ Monocytes on which we investigated extracellular phenotypic marker expression via flow cytometry on a BD FACSCanto™ II (Becton Dickinson, New Jersey, USA) as a control population. Since monocytes are a mature myeloid cell population, the surface expression of HLA-DR is upregulated. We built a gating strategy for the identification of Monocytes from the enriched population using markers to achieve a $CD3^{-}HLA\text{-}DR^{+}CD14^{+}$ phenotype (Figure 6.6). Briefly, following the standard gating protocol, lymphocytes were plotted "CD3 vs CD14" for the selection of $CD3^{-}CD14^{+}$ cells, followed by an "HLA-DR vs SSC-A" plot for the selection of $HLA\text{-}DR^{+}$ cells. This $CD3^{-}HLA\text{-}DR^{+}CD14^{+}$ population was then investigated for the expression of the Cav-1 and TLR4 markers of interest, as described previously.

Each gating strategy was applied to the acquired samples in separate workspaces, and none of the gates altered other than the "Time", "Singlets" and "Lymphocyte" gates, where necessary. This was because of sample variation that cannot be corrected for as each individual participant is different and responds differently to mycobacterial challenge. The "Time" gates were also adjusted for each individual sample because of variation introduced when sample batches are run on consecutive days, and possible instrument blockage between sample acquisition (wash steps were included between participant batches during acquisition, however, blockages may occur sporadically in the event the sample was not entirely re-suspended prior to acquisition).

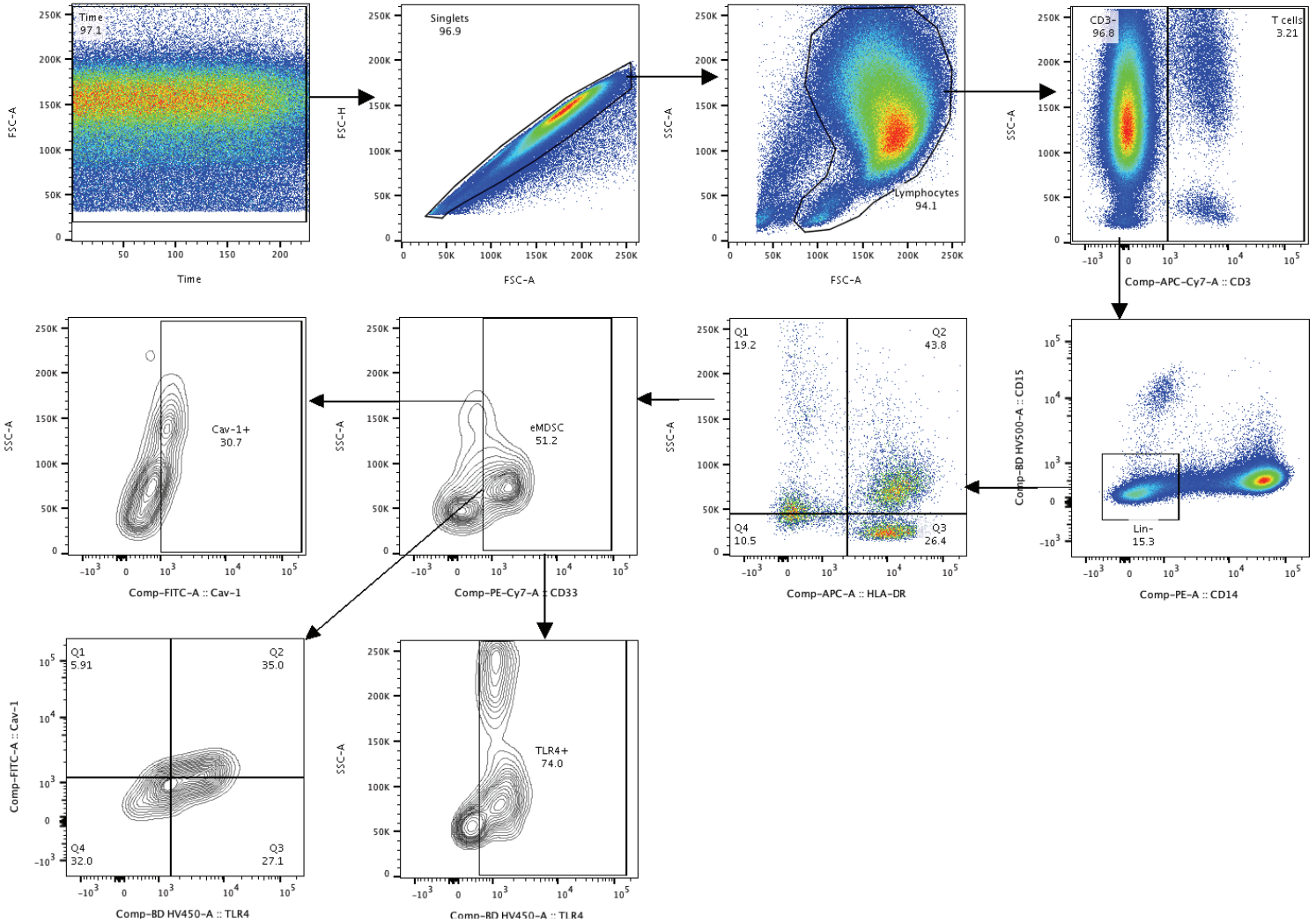

Figure 6.3: Gating strategy employed for the identification of eMDSC from enriched HLA-DR-CD33+ MDSC isolated from PBMC. The expression of the markers of interest, Cav-1 and TLR4, was investigated on the surface of eMDSC. Contour plots were used as alternatives to dot plots for a more clear distinction between populations owing to the small proportion of eMDSC in the total MDSC population (Gating based on the recommendations published by Bronte et al.[307] in Nature Communications).

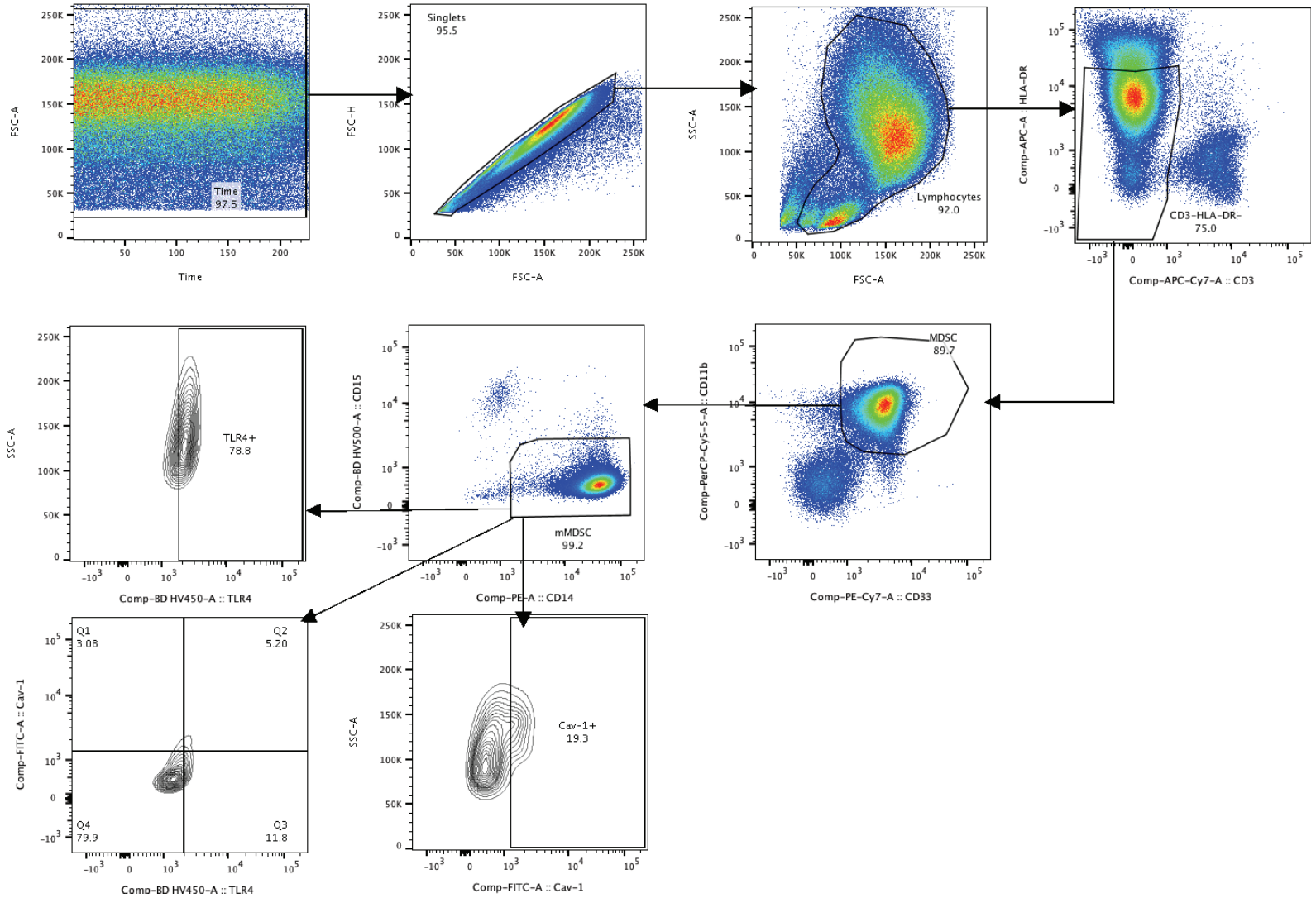

Figure 6.4: Gating strategy employed for the identification of M-MDSC from enriched HLA-DR^{-}CD33^{+} MDSC isolated from PBMC. The expression of the markers of interest, Cav-1 and TLR4, was investigated on the surface of M-MDSC (Gating based on the recommendations published by Bronte et al.[307] in Nature Communications).

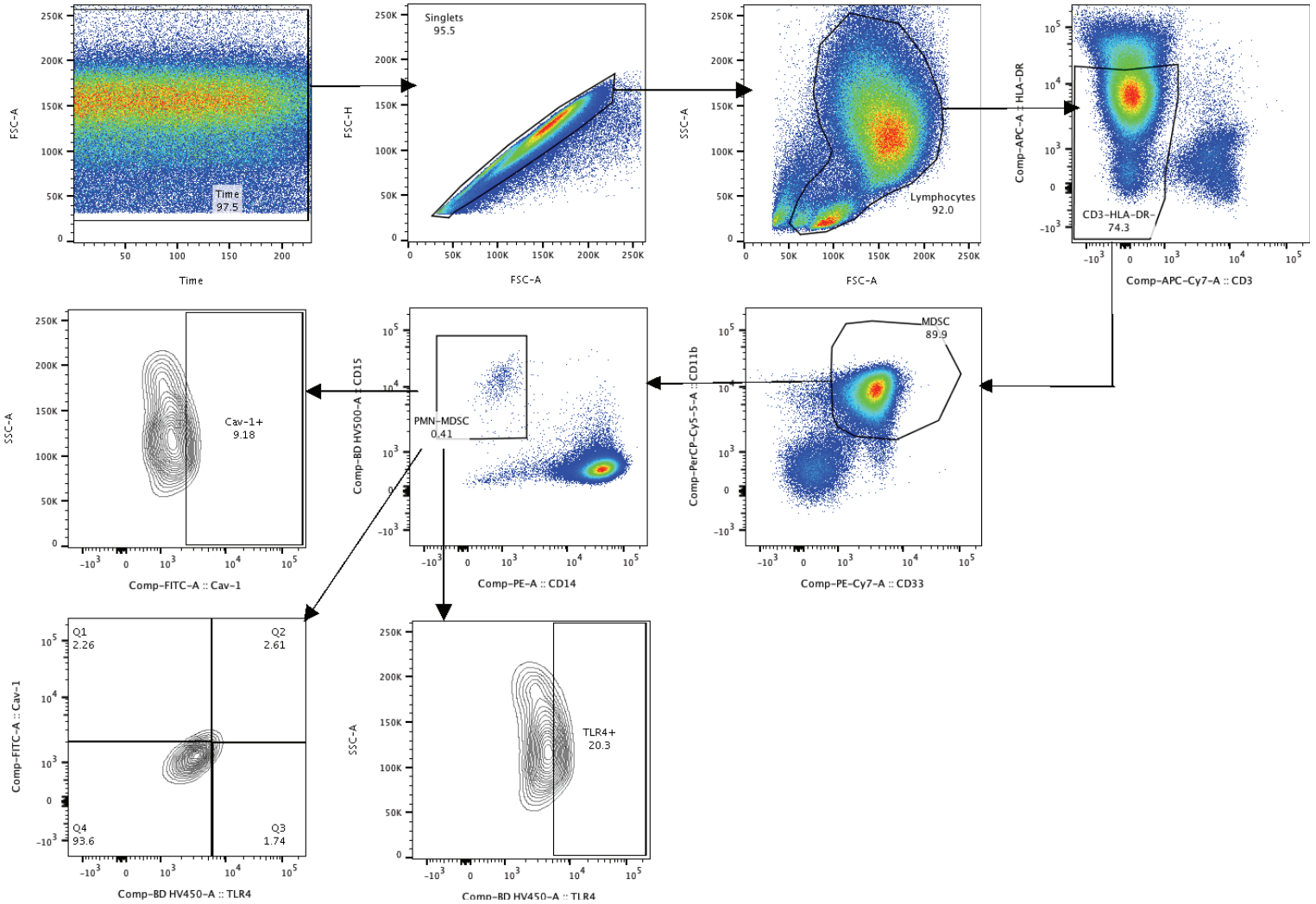

Figure 6.5: Gating strategy employed for the identification of PMN-MDSC from enriched HLA-DR$^-$CD33$^+$ MDSC isolated from PBMC. The expression of the markers of interest, Cav-1 and TLR4, was investigated on the surface of PMN-MDSC. Contour plots were used as alternatives to dot plots for a more clear distinction between populations owing to the small proportion of PMN-MDSC in the total MDSC population (Gating based on the recommendations published by Bronte et al.[307] in Nature Communications).

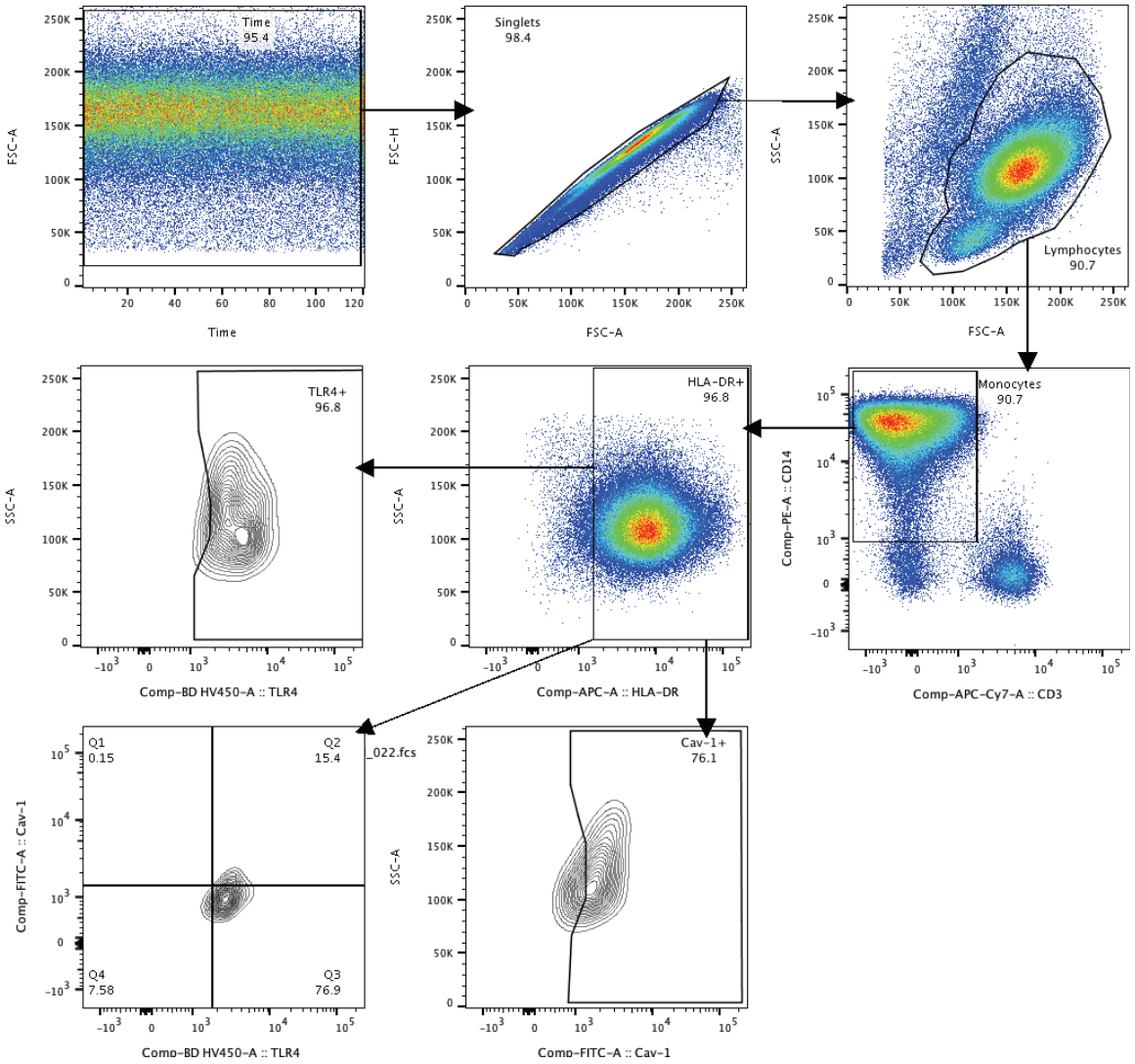

Figure 6.6: Gating strategy employed for the identification of CD14⁺ Monocytes from the enriched CD14⁺ Monocyte population isolated from PBMC. The expression of the markers of interest, Cav-1 and TLR4, was investigated on the surface of Monocytes.

HLA-DR$^-$CD33$^+$CD11b$^+$ MDSC are expanded in active TB participants compared to healthy, QFT positive and negative controls.

In this study we identified a significant increase in the median frequency of total MDSC, as a percentage of total isolated PBMC, in the periphery of active TB patients compared to healthy, QFT positive and negative controls (Figure 6.7(a); p = 0.0078). It was observed that approximately 4.5% of the isolated PBMC fraction was made up of total MDSC (Figure 6.7(a)) in the TB patients, and that this percentage is mostly as a result of the M-MDSC subset's contribution (Figure 6.7(b)). Approximately 88% of the total TB patient MDSC population was made up of the M-MDSC subset, for which there was a significant increase in the frequency of total M-MDSC during active disease compared to healthy controls (Figure 6.7(b); p = 0.012). We observed no significant differences in the frequencies of total eMDSC between TB patients and healthy controls (Figure 6.7(c); p = 0.79), but we did observe a significant increase in the frequency of total PMN-MDSC (Figure 6.7(d); p = 0.01). Here we observed a median frequency of approximately 0.3% and 0.05% of total PBMC for eMDSC and PMN-MDSC respectively during active disease, and approximately 0.35% and 0.001% of total PBMC for eMDSC and PMN-MDSC respectively in healthy controls. This suggests that peripheral circulating M-MDSC play the biggest role in immune modulation during active TB disease.

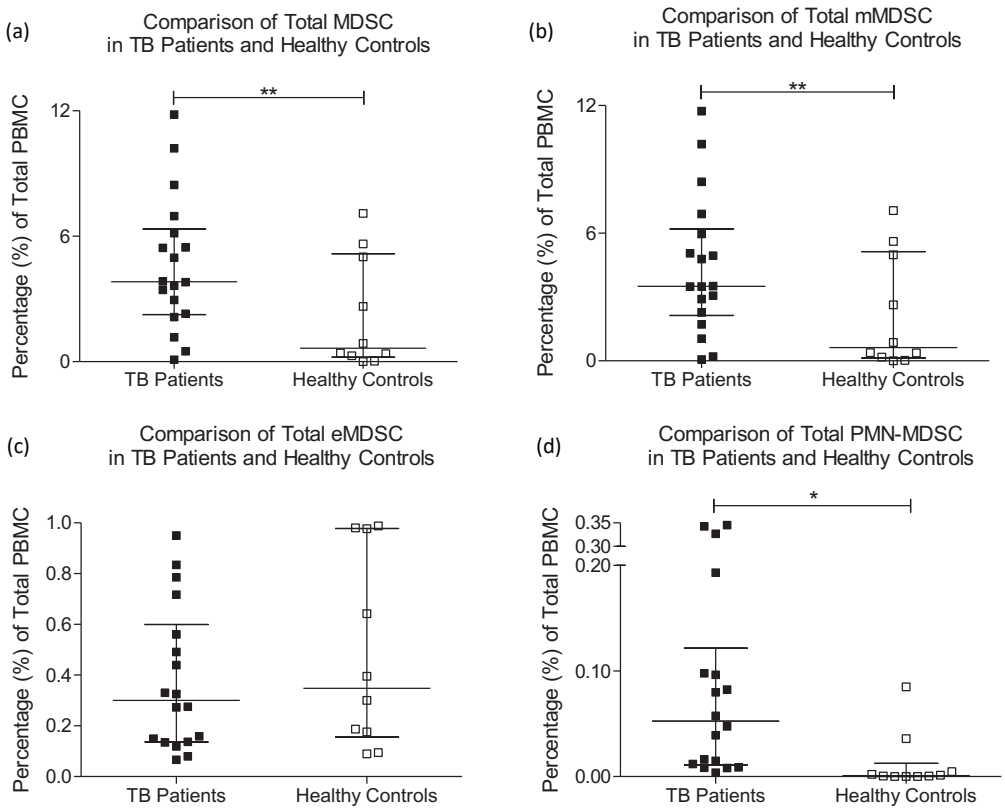

Figure 6.7: Frequencies of MDSC subsets as a percentage of the total number of isolated PBMC in TB patients compared to QFT positive and negative healthy controls. (a) Total MDSC (p = 0.0078) frequencies increased during active disease, (b) total M-MDSC (p = 0.012) frequencies increased during active disease, (c) total eMDSC (p = 0.79) frequencies did not change, and (d) total PMN-MDSC (p = 0.01) frequencies increased during active disease in HLA-DR$^-$CD33$^+$ cells isolated from PBMC (Error bars represent the median and interquartile range (IQR)).

Subsequent comparison of the frequency of the different MDSC subsets in TB patients (Figure 6.8(a)) and healthy controls (Figure 6.8(b)) separately, was performed. In both TB patients and healthy controls, the predominant MDSC subset was the M-MDSC subset which was significantly upregulated compared to both e- and PMN-MDSC during active disease (Figure 6.8(a); $p < 0.0001$ in both cases), but not compared to eMDSC in healthy controls (Figure 6.8(b); $p = 0.03$). This suggests that the precursor MDSC (eMDSC) are indeed present in a healthy state, but potentially differentiate into mature myeloid cells like monocytes and neutrophils, until mycobacterial challenge where they appear to differentiate mainly into the monocytic MDSC fraction, thereby switching their differentiation from pro-inflammatory to suppressive cell types. This observation is corroborated by the observation that healthy control populations may have higher frequencies of eMDSC compared to active TB patients (Figure 6.7(c)), suggesting a reduction in subset size upon infection with *M.tb*. This is also supported by the observation that CD14 median fluorescent intensity (MFI) is significantly upregulated in both TB patients (Figure 6.9(a); $p < 0.0001$) and healthy controls (Figure 6.9(b); $p < 0.0001$) compared to CD15 expression when using the median fluorescent intensity of the marker as a measure of the degree of expression. The eMDSC subset was upregulated in both TB patients (Figure 6.8(a); $p = 0.0006$) and healthy controls (Figure 6.8(b); $p = 0.0035$) compared to PMN-MDSC. When assessing total frequencies of the MDSC effector phenotypes, i.e. M- and PMN-MDSC, as a percentage of total HLA-$DR^{-}CD33^{+}CD11b^{+}$ MDSC, we validated the predominance of the M-MDSC fraction as the main subset isolated from whole blood during both active TB disease and in healthy controls (Figure 6.8(c)).

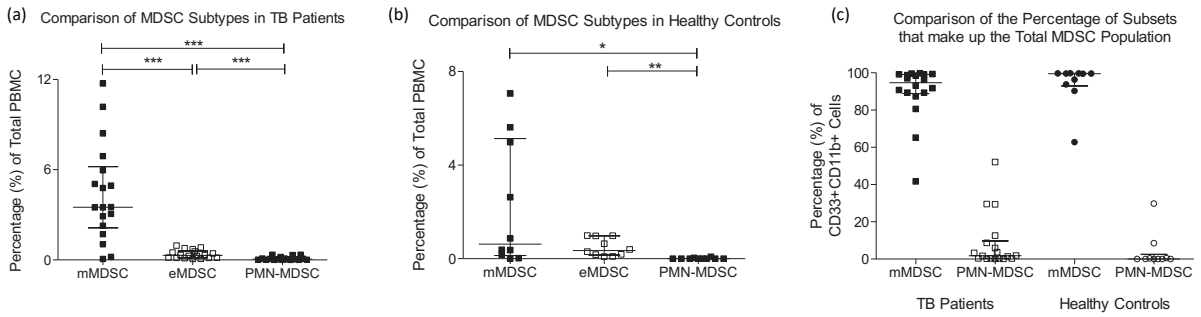

Figure 6.8: Comparison between the frequencies of the different MDSC subsets (as a percentage of the total number of isolated PBMC) in (a) TB patients and (b) healthy controls. M-MDSC were upregulated in TB patients compared to both eMDSC ($p < 0.0001$) and PMN-MDSC ($p < 0.0001$), and eMDSC were upregulated compared to PMN-MDSC ($p = 0.0006$). In healthy controls, M-MDSC were upregulated compared to PMN-MDSC only ($p = 0.03$), and eMDSC were upregulated compared to PMN-MDSC ($p = 0.0035$). (c) A comparison between the percentage of the m- and PMN-MDSC subsets (effector subsets) that make up the total MDSC population was also made in TB patients and healthy controls, as a percentage of total MDSC, rather than total PBMC (Error bars represent the median and IQR).

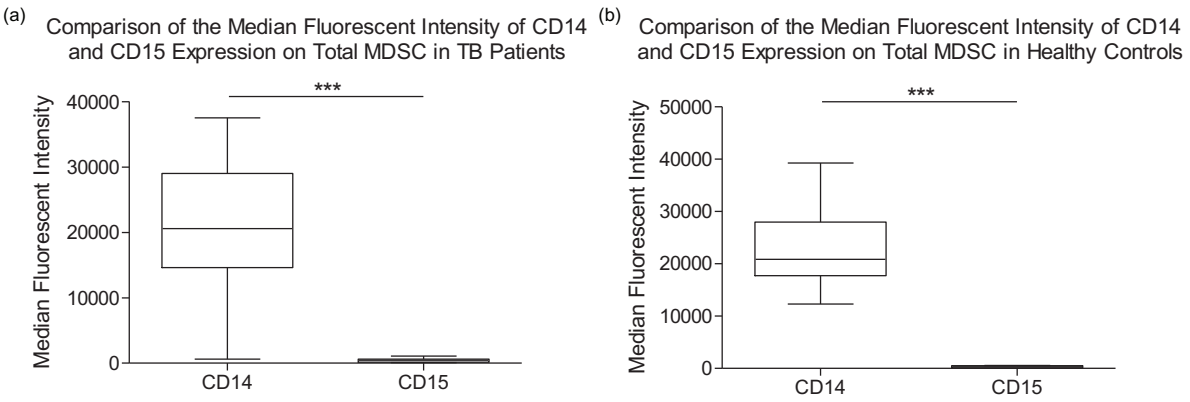

Figure 6.9: Median fluorescent intensities of the surface markers CD14 and CD15, comparing their expression in (a) TB patients ($p < 0.0001$), and (b) healthy controls ($p < 0.0001$). Lower and upper whiskers of the box and whisker plots represent the 5th and 95th percentile respectively, while the horizontal line within the box represents the median.

CD3$^-$HLA-DR$^+$CD14$^+$ Monocytes are not differentially expanded in active TB participants or healthy controls or compared to total HLA-DR$^-$CD33$^+$ MDSC.

Autologous monocytes (CD3$^-$HLA-DR$^+$CD14$^+$) were isolated from participants where PBMC cell numbers were permitting to act as a positive control for the M-MDSC subset. M-MDSC are capable of maturing into monocyte-derived macrophages through the action or inaction of various soluble mediators within the inflammatory environment, resulting in the phenotypic maturation of the HLA-DR marker[181]. Monocytes isolated from the PBMC fraction would, therefore, contain mostly monocytes but could also have contained some M-MDSC since selection was not based on maturation state. CD14$^+$ monocytes were isolated using a positive MACS® isolation technique and CD14$^+$ microbeads, and their frequencies compared between TB patients and healthy controls. As a frequency of total isolated PBMC, no statistically significant difference was observed between the frequencies of isolated monocytes between TB patients and healthy controls (Figure 6.10(a); $p = 0.26$), however the low number of healthy control samples makes this result difficult to interpret. When monocyte frequencies were then compared to the frequency of MDSC in TB patients (Figure 6.10(b); $p = 0.80$) and healthy controls (Figure 6.10(c); $p = 0.19$), no statistically significant differences were observed. It should be mentioned that these frequencies were derived from the stored samples and not from the purity check samples. We believe that a larger monocyte sample size may have allowed for a better comparison.

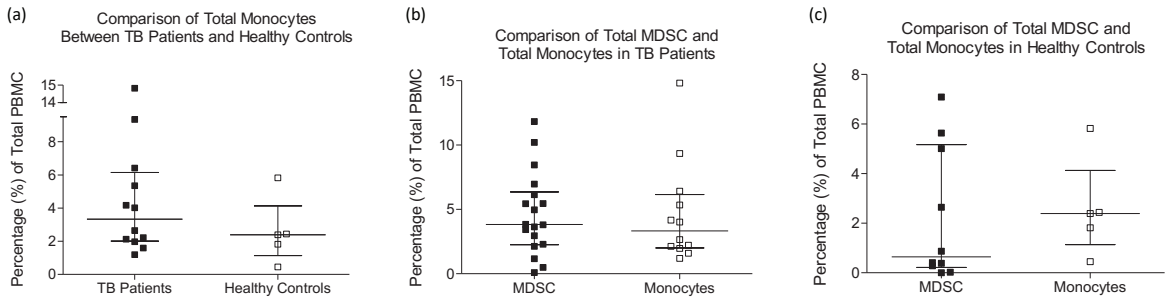

Figure 6.10: Comparison of the frequency of isolated autologous HLA-DR$^+$CD14$^+$ monocytes, as a percentage of the total number of isolated PBMC, (a) between TB patients and healthy controls (p = 0.26). Monocyte frequencies were also compared to isolated MDSC frequencies in (b) TB patients (p = 0.80) and (c) healthy controls (p = 0.19) (Error bars represent the median and IQR).

We observed a statistically significant upregulation in the expression of the surface marker CD14 on the MDSC of healthy controls compared to monocytes (Figure 6.11(b); p = 0.0013), but not on those of TB patients (Figure 6.11(a); p = 0.09). The median MFI of CD14-expressing MDSC between TB patients and Healthy Controls was not significantly different (data not shown), suggesting the need for the constitutive expression of this marker on MDSC regardless of infection status. The observation that MDSC express CD14 so highly could be indicative of the mechanism by which these cells are able to recognize antigens, specifically bacterial LPS. While not significantly different to monocytes during *M.tb* infection (Figure 6.10(b)), the median fluorescent intensity of CD14 on the surface of MDSC appears to be consistent with or without infection, further suggesting a need for the constitutive expression of this surface marker, regardless of infection status. MDSC are known to be poorly phagocytic, but we are aware that they are capable of internalizing bacteria. We, therefore, hypothesized that MDSC are capable of internalizing *M.tb* through a mechanism which is dependent on the surface receptor CD14. Literature has shown that CD14 may act as a co-receptor for the detection of bacterial LPS when complexed with TLR4 and the LPS binding protein (LBP) to activate the MyD88-dependent NF-κβ signaling pathway. The expression of TLR4 was subsequently assessed on the surface of MDSC and monocytes, as given below.

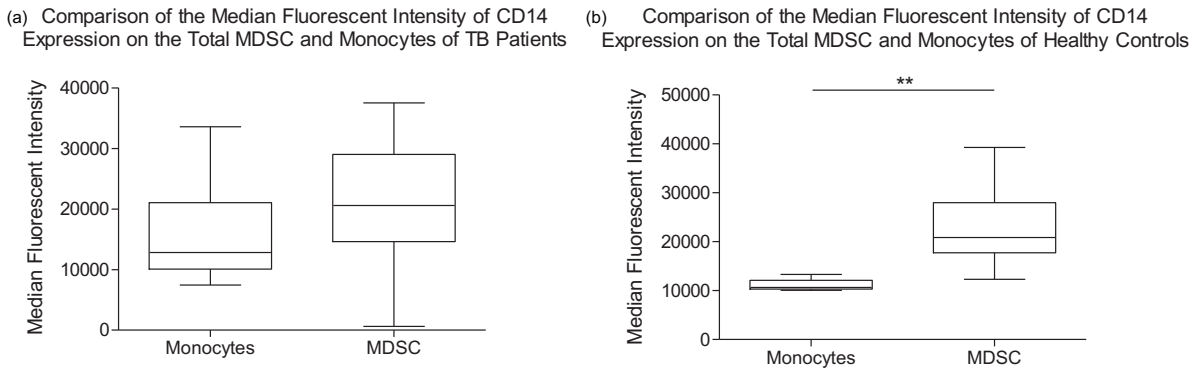

Figure 6.11: Median fluorescent intensity of the surface marker CD14, comparing its expression between total MDSC and Monocytes in (a) TB patients (p = 0.09), and (b) healthy controls (p = 0.0013). Lower and upper whiskers of the box and whisker plots represent the 5th and 95th percentile respectively, while the horizontal line within the box represents the median.

The Caveolin-1 protein can be observed on the surface of MDSC and monocytes, and, along with TLR4, is differentially expressed in the Monocytes of TB patients but not MDSC.

Based on the observations and hypothesis given above, we investigated the expression of TLR4 as well as that of Caveolin-1 (Cav-1) on the surface of MDSC and monocytes as a control population. We observed no significant differences in the number of Cav-1- (Figure 6.12(a), p = 0.719) or TLR4-expressing (Figure 6.12(b); p = 0.581) MDSC between TB patients and healthy controls. We did, however, observe a significant upregulation of both Cav-1- (Figure 6.12(c); p = 0.012) and TLR4-expressing (Figure 6.12(d); p = 0.011) monocytes during active infection. This suggests that the naturally occurring monocytes of a healthy individual do not express the surface markers Cav-1 or TLR4 when one investigates cellular frequencies as a percentage of total isolated PBMC.

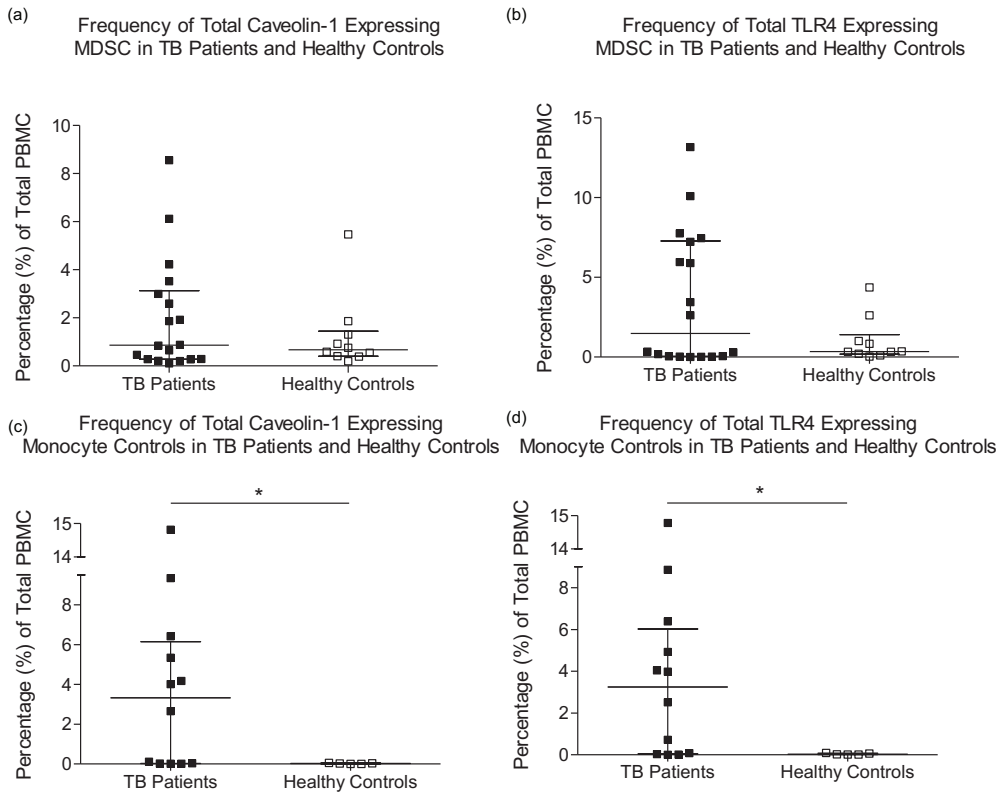

Figure 6.12: Comparison of the frequency of cells, both MDSC and monocyte, expressing the surface markers Caveolin-1 and TLR4 between TB patients and healthy controls. Represented are the differences in the frequency of MDSC expressing (a) Caveolin-1 (p = 0.719) and (b) TLR4 (p = 0.581), as well as the differences in the frequency of Monocytes expressing (c) Caveolin-1 (p = 0.012) and (d) TLR4 (p = 0.011) as a percentage of total isolated PBMC (Error bars represent the median and IQR).

While a large percentage of MDSC isolated from healthy controls expressed Caveolin-1 and TLR4 (Figure 6.12(a) and (b) respectively), the expression was not high as was observed when the median fluorescent intensities of both markers were assessed (Figure 6.13(a) and (b), respectively; p = 0.051 and p = 0.102, respectively). This again suggests an *M.tb*-specific upregulation of both markers, even though the differences were not statistically significant.

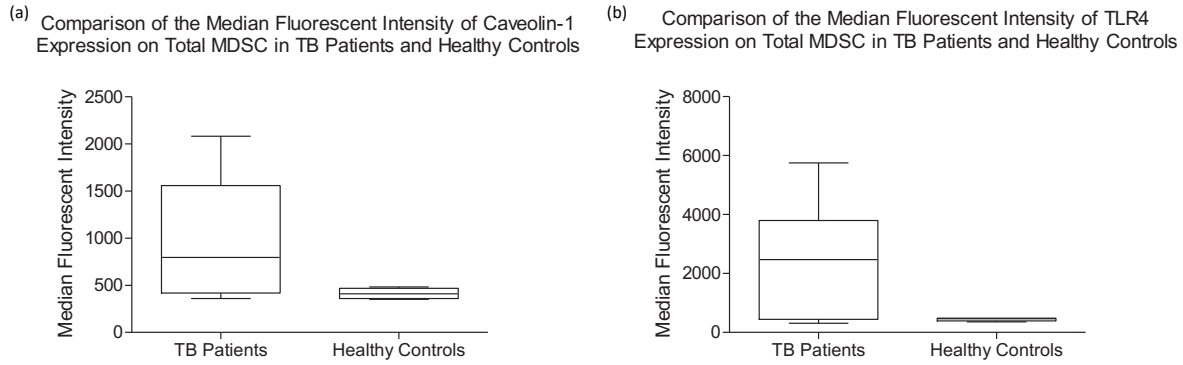

Figure 6.13: Median fluorescent intensities of the surface markers (a) Cav-1 (p = 0.051) and (b) TLR4 (p = 0.102), measuring their expression on the surface of MDSC TB patients and healthy controls. Lower and upper whiskers of the box and whisker plots represent the 5th and 95th percentile respectively, while the horizontal line within the box represents the median.

The differences in expression were then assessed between MDSC and monocytes in individuals with active disease, and those without. Monocytes were observed to express significantly more Caveolin-1 than MDSC in TB patients (Figure 6.14(a); p = 0.012), however, no significant difference was observed between the number of Caveolin-1 expressing monocytes and MDSC in healthy controls (Figure 6.14(b); p = 0.1). The number of TLR4-expressing MDSC and monocytes was observed to not be significantly different in TB patients (Figure 6.14(c); p = 0.983), while there was a significant downregulation in the number of TLR4-expressing monocytes in the healthy controls compared to MDSC (Figure 6.14(d); p = 0.008).

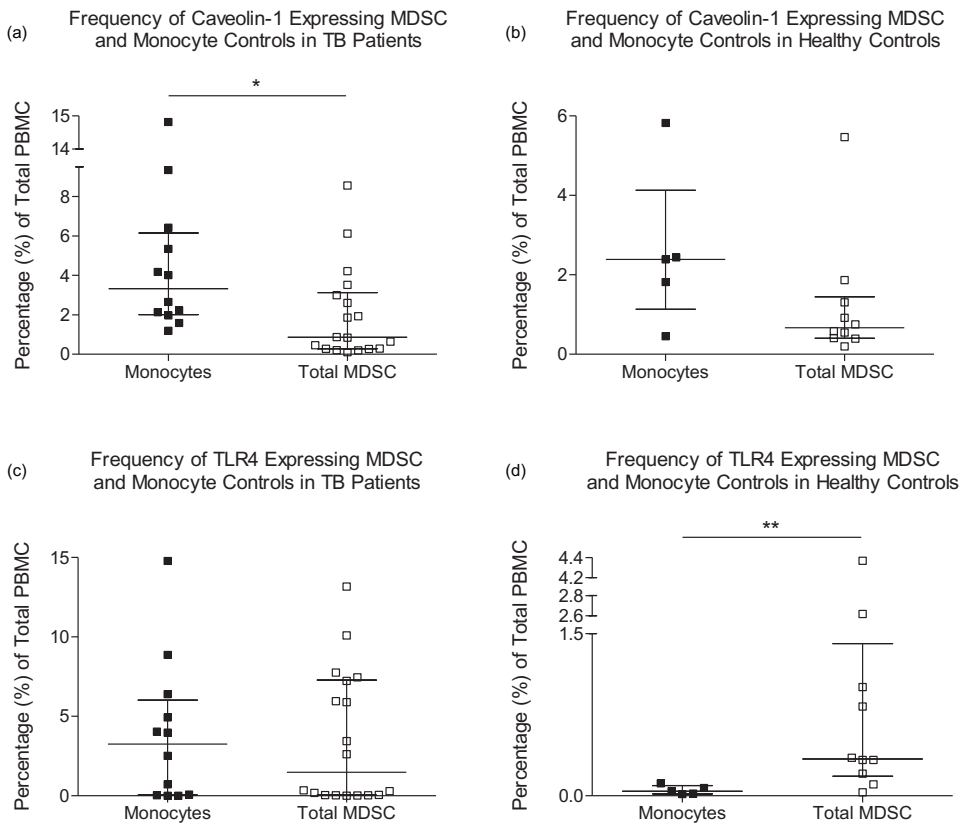

Figure 6.14: Comparison between the frequency of MDSC and monocytes expressing the surface markers Caveolin-1 and TLR4 in TB patients and healthy controls. Represented is the comparison between in the frequency of Caveolin-1-expressing MDSC and Monocytes in (a) TB Patients (p = 0.012) and (b) healthy controls (p = 0.1), as well as the comparison between the frequency of TLR4-expressing MDSC and Monocytes in (c) TB Patients (p = 0.983) and (d) healthy controls (p = 0.008) as a percentage of total isolated PBMC (Error bars represent the median and IQR).

6.3.5 Cytokine Profile Analysis

PPD-specific stimulation of HLA-DR$^-$CD33$^+$ MDSC alone results in the upregulation of cytokines associated with MDSC induction, recruitment and regulation.

HLA-DR$^-$CD33$^+$ MDSC's were isolated from only seven of the active TB participants owing to the limited space available on the Luminex multiplex plates and the desire to retain as many control stimulations as possible for each participant. The concentrations of 22 cytokines were assessed in culture supernatants from the 7 participants with active TB disease using the multiplex Luminex immunoassay platform. For each participant, culture supernatants were assessed from each of the stimulation conditions, as outlined in Table 4. Differences in cytokine concentrations were assessed between PPD-stimulated and unstimulated HLA-DR$^-$CD33$^+$ MDSC conditions, as well as between PPD-stimulated MDSC/T cell co-culture and PPD-stimulated CD3$^+$ T cell culture conditions in order to investigate the PPD-specific effects of MDSC on CD3$^+$ T cells. During statistical analysis, raw data was either kept as it was, log transformed, or winsorized depending on the distribution of the data. Raw data was only kept as it was, if the distribution of cytokine/chemokine's data was normal. Raw data was log transformed when the normality of the errors did not fit a normal distribution curve and was, therefore, skewed; raw

data was winsorized when extreme and spurious outliers were evident in frequency distribution plots of cytokines. Table 6.9 outlines which data were adjusted, and how. It is not made mention which individual cytokines were analyzed with their original raw data or not further on in the text but is implied from Table 6.9.

Table 6.9: Normalization methods employed to ensure the normal distribution of raw data for each cytokine, prior to statistical analyses.

Cytokine:	Normalization Method Used (if any):
CD40L	None (Raw Data Used)
CXCL11	None (Raw Data Used)
Fas	None (Raw Data Used)
IL-33	None (Raw Data Used)
IFN-α2	None (Raw Data Used)
CCL2/MCP-1	Log Transformed
IFN-γ	Winsorized
MIP-1β	Winsorized
IL-22	Winsorized
ADAMTS13	Log Transformed and Winsorized
IL-1β	Log Transformed
IL-13	Log Transformed
IL-2	Log Transformed
CCL1	Log Transformed
IP-10	Log Transformed
GM-CSF	Log Transformed
IL-1α	Log Transformed
IL-10	Log Transformed
TNF-α	Log Transformed
IL-6	Log Transformed
MIP-1α	Log Transformed
IL-4	Log Transformed

The stimulation of HLA-DR$^-$CD33$^+$ MDSC with PPD resulted in the significant upregulation of multiple cytokines well known to be involved in the induction of MDSC in the tumor microenvironment, as well as during active TB disease, but also as effector function molecules. These cytokines included IL-6 (Figure 6.15(a); $p = 0.0006$), IL-10 (Figure 6.15(b); $p = 0.0023$), IL-13 (Figure 6.15(c); $p = 0.0059$), IL-1β (Figure 6.15(d); $p = 0.0175$), IFN-γ (Figure 6.15(e); $p = 0.0209$), and TNF-α (Figure 6.15(f); $p = 0.0262$).

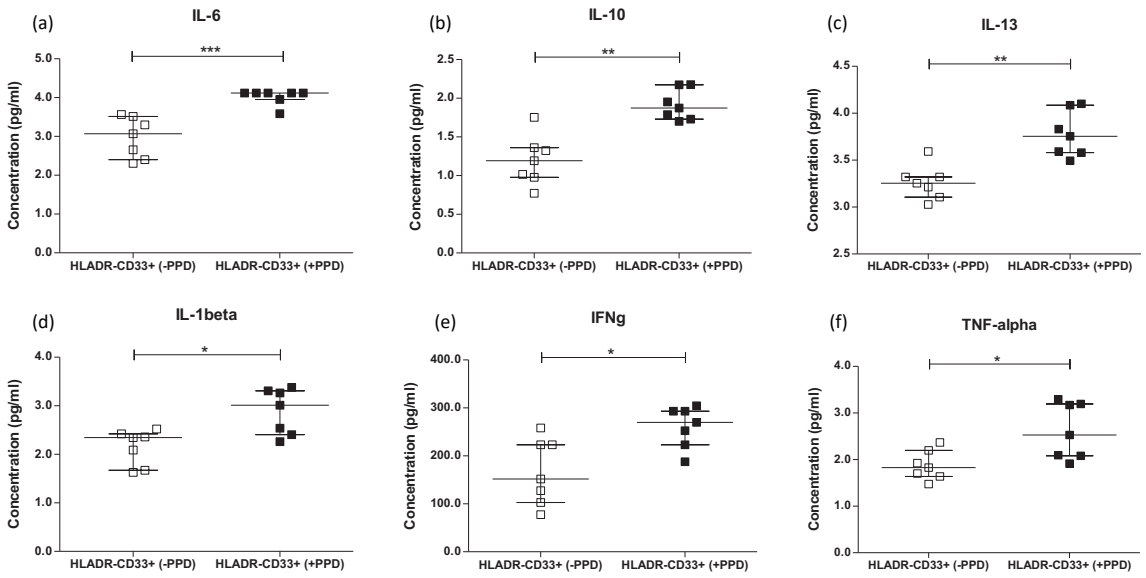

Figure 6.15: Cytokines involved primarily in the induction of HLA-DR$^-$CD33$^+$ MDSC were upregulated following stimulation of MDSC with PPD, compared to unstimulated HLA-DR$^-$CD33$^+$ MDSC. The secretion of the cytokines (a) IL-6 (p = 0.0006), (b) IL-10 (p = 0.0023), (c) IL-13 (p = 0.0059), (d) IL-1β (p = 0.0175), (e) IFN-γ (p = 0.0209), and (f) TNF-α (p = 0.0262) were all upregulated following stimulation with PPD (error bars represent the median and interquartile range).

Stimulation of HLA-DR$^-$CD33$^+$ MDSC with PPD also resulted in the significant upregulation of MIP-1α (Figure 6.16(a); p = 0.0064) and MIP-1β (Figure 6.16(b); p = 0.0023) concentrations compared to unstimulated samples.

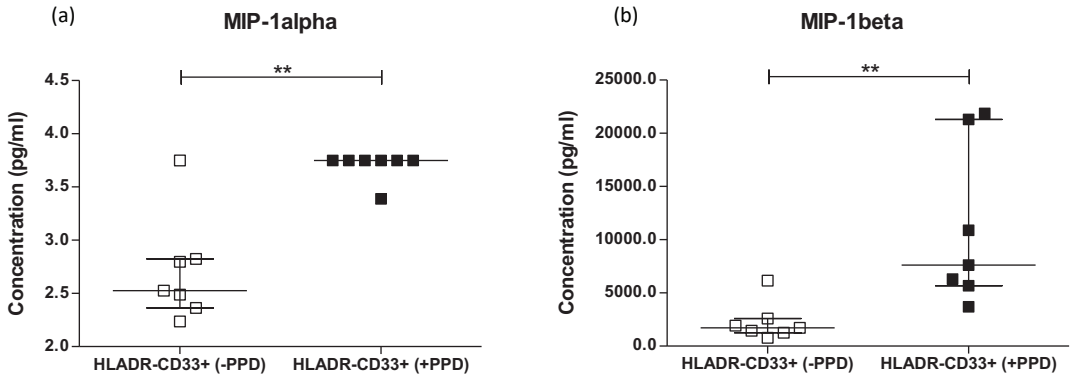

Figure 6.16: Upregulated cytokines involved in the recruitment and regulation of HLA-DR$^-$CD33$^+$ MDSC following stimulation with PPD, compared to unstimulated HLA-DR$^-$CD33$^+$ MDSC. The secretion of the cytokines (a) MIP-1α (p = 0.0064), and (b) MIP-1β (p = 0.0023) were upregulated by these cells following PPD stimulation in the absence of any other cell populations (error bars represent the median and interquartile range).

HLA-DR$^-$CD33$^+$ MDSC display an upregulation of cytokines involved in MDSC induction and function in the tumor microenvironment, but that have previously not been assessed in the context of active TB disease, following PPD-specific stimulation.

Cytokines involved in MDSC induction and function in the known tumor microenvironment were also observed to be upregulated during PPD-specific stimulation of HLA-DR$^-$CD33$^+$ MDSC in the absence of other cell types compared to the unstimulated condition. These cytokines included soluble Fas (Figure 6.17(a); p = 0.0469), IL-22 (Figure 6.17(b); p = 0.0244) and IL-33 (Figure 6.17(c); p = 0.0125) and have been shown to be largely involved with MDSC induction as well as effector functions. Interestingly, the cytokines IL-1α (Figure 6.17(d); p = 0.0175) and ADAMTS13 (Figure 6.17(e); p = 0.0282) were also observed to be upregulated in PPD-stimulated HLA-DR$^-$CD33$^+$ MDSC in the absence of any other enriched cell populations. These two cytokines were of particular interest as they have no clear function in the context of MDSC.

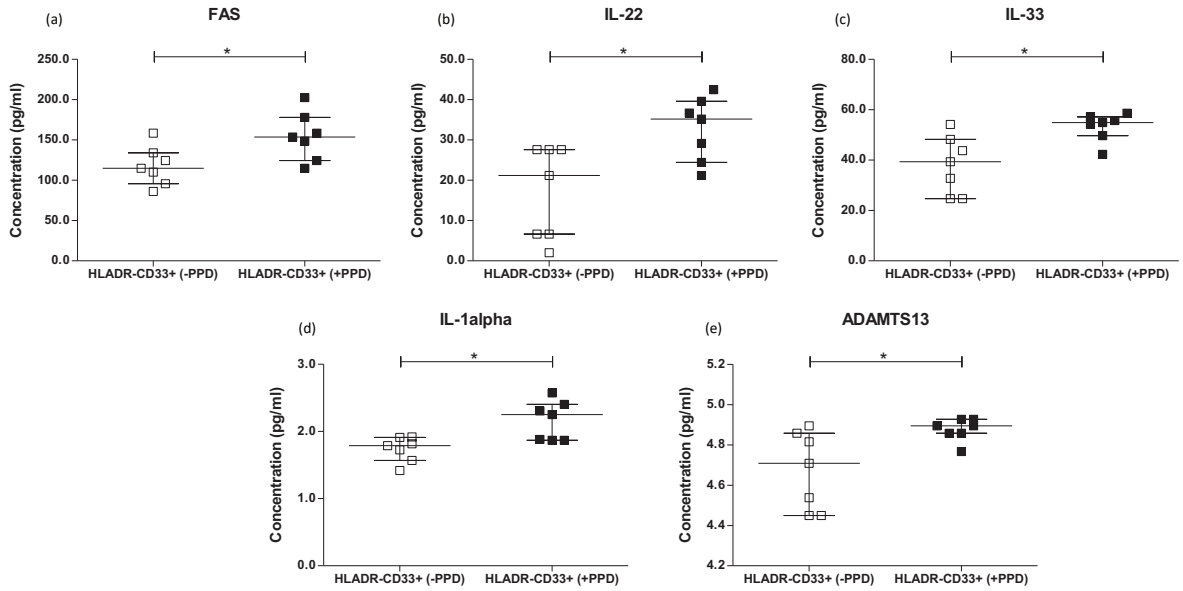

Figure 6.17: Upregulated cytokines involved in unconventional induction and immunosuppressive functions of HLA-DR$^-$CD33$^+$ MDSC following stimulation with PPD, compared to unstimulated HLA-DR$^-$CD33$^+$ MDSC. The secretion of the cytokines (a) soluble Fas (p = 0.0469), (b) IL-22 (p = 0.0244), (c) IL-33 (p = 0.0125), (d) IL-1α (p = 0.0175) and (e) ADAMTS13 (p = 0.0282) were upregulated by these cells following PPD stimulation in the absence of any other cell populations (error bars represent the median and interquartile range).

PPD-specific stimulation of CD3$^+$ T cells co-cultured in the presence of HLA-DR$^-$CD33$^+$ MDSC results in CD3$^+$ T cell suppression.

Following the culture of HLA-DR$^-$CD33$^+$ MDSC with PPD alone, these cells were also co-cultured in the presence of CD3$^+$ T cells at a 1:2.5 ratio (5x10^5 MDSC were co-cultured with 1.25x10^6 T cells) and stimulated with PPD to mimic *in vivo* cellular composition conditions. The concentrations of two cytokines were upregulated when PPD stimulated CD3$^+$ T cells were co-cultured together with HLA-DR$^-$CD33$^+$ MDSC compared to PPD stimulated CD3$^+$ T cells cultured alone, namely soluble Fas (Figure 6.18(a); p = 0.0454), and IL-1β (Figure 6.18(b); p = 0.0223). IL-1β was previously observed to be upregulated (Figure 6.15(d)) in the supernatant of HLA-DR$^-$CD33$^+$ MDSC stimulated with PPD alone.

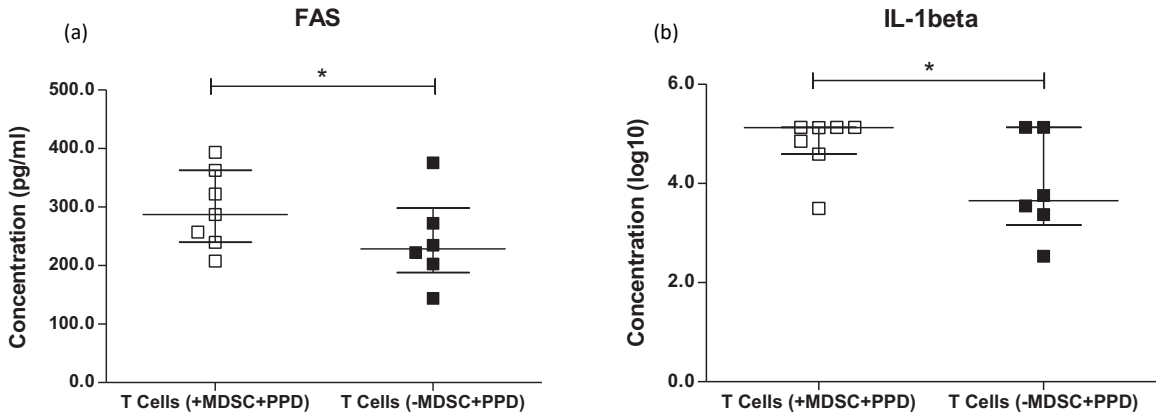

Figure 6.18: Co-culture of PPD stimulated CD3⁺ T cells with (+MDSC) and without (-MDSC) HLA-DR⁻CD33⁺ MDSC resulted in the significant (a) upregulation of soluble Fas (p = 0.0454), and (b) upregulation of IL-1β (p = 0.0223) concentrations in the presence of MDSC, when co-cultured in a ratio of 1:2.5 (error bars represent the median and interquartile range).

HLA-DR⁻CD33⁺ MDSC were also co-cultured in the presence of CD3⁺ T cells at a 1:1 ratio (5x10ˆ5 MDSC were co-cultured with 5x10ˆ5 T cells) and stimulated with PPD to assess possible dose-dependent responses in *ex vivo* experiments. When HLA-DR⁻CD33⁺ MDSC were co-cultured with CD3⁺ T cells at a 1:1 ratio, only two cytokine concentrations were found to be significantly altered, namely IFN-γ (Figure 6.19(a); p = 0.0334) and CCL2/MCP-1 (Figure 6.19(b); p = 0.0129), compared to those observed when CD3⁺ T cells were stimulated with PPD and cultured alone. The concentration of IFN-γ observed when CD3⁺ T cells were co-cultured in the presence of HLA-DR⁻CD33⁺ MDSC and stimulated with PPD was downregulated compared to when CD3⁺ T cells were cultured and stimulated with PPD in the absence of HLA-DR⁻CD33⁺ MDSC (Figure 6.19(a)). Conversely, PPD-specific concentrations of CCL2 were upregulated during co-culture of CD3⁺ T cells in the presence of HLA-DR⁻CD33⁺ MDSC (Figure 6.19(b)).

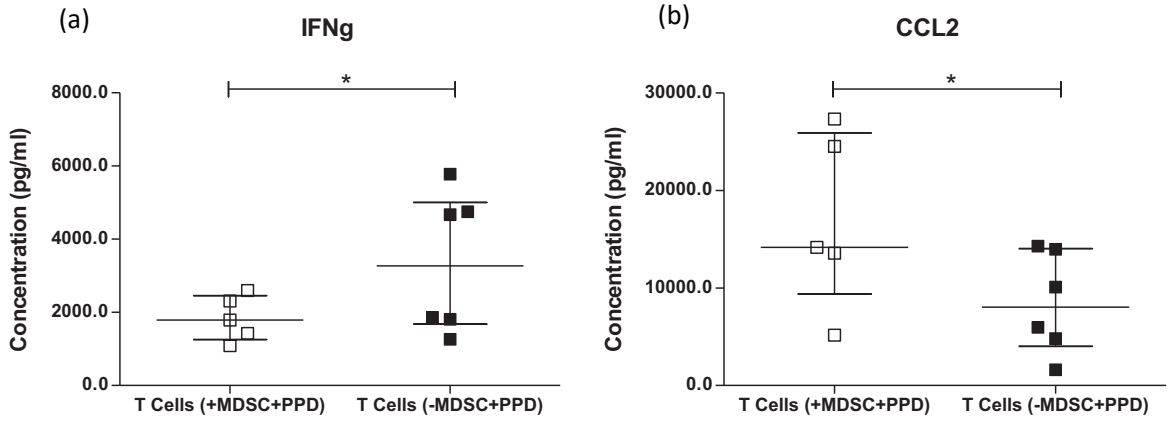

Figure 6.19: Co-culture of PPD stimulated CD3⁺ T cells with (+MDSC) and without (-MDSC) HLA-DR⁻CD33⁺ MDSC resulted in the significant (a) downregulation of T cell-specific IFN-γ (p = 0.0334), and (b) upregulation of C-C Motif Chemokine Ligand 2 (CCL2) (p = 0.0129) concentrations in the presence of MDSC, when co-cultured in a ratio of 1:1 (error bars represent the median and interquartile range).

PPD-specific stimulation of HLA-DR$^-$CD33$^+$ MDSC both alone and during co-culture with CD3$^+$ T cells did not up- or down-regulate 8 of the 22 cytokines/chemokines evaluated in this study, some of which are known to be involved in MDSC expansion.

The final findings of the cytokine/chemokine profile analysis identified eight evaluated cytokines/chemokines that were neither significantly up- nor down-regulated in any of the above mentioned culture conditions. These included IL-4, GM-CSF, IP-10, CCL1, IL-2, CD40L, CXCL11, and IFN-α2 (data not shown).

6.4 Discussion

Mycobacterium tuberculosis (*M.tb*) infection results in a spectrum of outcomes, ranging from immediate innate-mediated bacterial clearance, controlled chronic infection, subclinical disease to extensive active TB in humans. Pai[8] and colleagues have comprehensively outlined these infection profiles, although our understanding of the mechanisms behind progression and control of infection are poorly understood. It is known that during *M.tb* infection, inadequate or defective T cell responses contribute to TB disease progression, as is seen in immunocompromised individuals with HIV infection for example. However, in cases where individuals with active TB disease are otherwise healthy, the cause of such defective responses remains unknown. Additionally, defective innate responses also contribute to adverse outcomes of infection and myeloid-derived suppressor cells are one example of a cell type that might contribute in this regard. The expansion of myeloid-derived suppressor cells has been documented largely in cancer, but also in bacterial and viral infections, including HIV. In both active TB disease and HIV, MDSC frequencies have been observed to be down-regulated following curative treatment, supporting the notion that these cells may exacerbate disease states [313]. With this in mind, the point at which MDSC frequencies decline during treatment is unknown, and investigations into this in the context of anti-TB treatment may provide an alternative cellular marker of treatment response, as the down-regulation of MDSC may be indicative of the restoration of protective immunity.

In this study we aimed to investigate the frequency of MDSCs and their subsets within the PBMC compartment of whole blood from participants with active TB disease and those without, as well as investigate the potential for these cells to suppress adaptive immune responses. Previous studies of MDSC in active TB disease have identified their expansion at the site of disease and in the peripheral blood of diseased individuals, however, their frequency has not been documented within PBMC[30,308]. Recent advances in MDSC biology in the field of oncology have demonstrated that MDSC are more accurately measured in PBMC rather than whole blood, and that phenotypic characterization within the whole blood compartment may lead to a gross overestimation of the PMN-MDSC subset in particular due to the presence of neutrophils which share the CD15 marker. Findings identified in Chapter 5 of this thesis drew attention to potential suppressive mechanisms in whole blood. During the co-culture of monocytes and $CD3^+$ T lymphocytes the concentrations of the cytokines IL-6, IL-8, IL-13 IP-10, MIP-1α, MIP-1β, and TNF-α were observed to be higher during co-culture than in whole blood. Owing to their known importance during *M.tb* infection control, suggests that there may be a suppressive cell population, like MDSC, within whole blood that is contributing to the downregulation of these important pro-inflammatory cytokines. Considering this apparent suppression and the limited data available on the role of MDSC in active TB disease, this study focused on the further investigation of MDSC phenotype and function in PBMC in the context of active TB disease.

Acknowledgement of Limitations.

Before discussing the results of this study, it was important to acknowledge the primary limitation of this study – the MACS® bead isolation technique. Considering that purities were less than 100%, the

isolated cells can, at best, be classified as an enriched MDSC population. Alternative platforms such as fluorescently activated cell sorting using instruments like the BD FACSJazz™ (Becton Dickinson, New Jersey, USA) is likely to yield higher cell purities. As a result, inferences made from the data presented, may not be wholly representative of the population, as other immune cells may have been present in the enriched population contributing to the response. I also acknowledge that in order to claim true $CD3^+$ T cell suppression by MDSC, more stringent suppression assays would need to be performed, but could not during this project owing to time constraints and the scope of the aims. Future studies using improved isolation methods are planned to validate significant findings.

In addition to these limitations, we acknowledge that the enriched MDSC and CD3+ T cell populations may contain other cell types, other than MDSC, which may account for any observed suppressive effects in co-culture. Such cells may include T_{Regs} which express the CD3 surface receptor and suppress conventional $CD4^+$ and $CD8^+$ T cells, or even dying cells which may release factors that induce immunosuppressive effects.

MDSC enriched from PBMC are significantly upregulated in participants with active TB disease, compared to participants with latent *M.tb* infection.

The phenotyping of eighteen active TB participants and ten healthy controls in this study confirmed the upregulation of the MDSC population in the PBMC compartment of whole blood during active TB disease. Current literature reports on the expansion of the $CD3^-HLA\text{-}DR^{-/low}CD33^+CD11b^+$ (total MDSC) phenotype in peripheral blood and at the site of active TB disease, with the latter being reported in murine TB models and human pleural TB studies[31,35,178,307]. Many of these studies have investigated MDSC in the context of whole blood, but more recent literature demonstrate that both the PMN-MDSC and M-MDSC subsets, are retained in the buffy coat or the mononuclear fraction following density centrifugation. Consequently, this study has provided the first such estimate of MDSC frequencies as a percentage of total PBMC. As observed, approximately 4.5% of PBMC from active TB participants displayed a MDSC-specific phenotype, of which the majority were M-MDSC. Likewise, healthy control PBMC also displayed a majority M-MDSC phenotype, even though the median frequency was significantly lower than that found in active TB participants. This presents as the first such finding in the context of active TB disease and could point to a less important role for the PMN-MDSC subset in the whole blood compartment of active TB patients and healthy controls. In contrast, previous studies investigating the expansion of MDSC subsets at the site of disease identified the PMN-MDSC subset as being predominant[30,35]. Whether or not these findings specifically reflect the cellular compartment of the lungs is beyond the scope of this study, however it is likely that they do not – it is known that only a very small fraction of neutrophils (activated, low-density neutrophils specifically) remain in the PBMC layer following Ficoll-Hypaque isolation methods. PBMC would, therefore, not constitute a reliable source for the investigation of PMN-MDSC frequencies in whole blood and the comparisons thereof to the lung. In terms of marker specificity. CD15 is a good marker for the identification of PMN-MDSC within the PBMC compartment, but not in whole blood since the PBMC compartment does not contain high density neutrophils, which constitute the traditional granulocytic, non-suppressive population of

neutrophils. Alternatively, future studies should consider the use of the LOX-1 marker, which discriminates between PMN-MDSC and neutrophils in whole blood, unlike CD15[314]. Neutrophils with suppressive functions express the marker LOX-1, while neutrophils without suppressive activities do not, which provides a definitive PMN-MDSC-specific marker for use in future studies since this subset is essentially a neutrophil with suppressive abilities[314]. Unfortunately, LOX-1 was described in literature after the experimental design of this study was planned. Based on this limitation, we are still confident that the PMN-MDSC subset frequency would not be the predominant subset in *in vivo* PBMC from active TB participants or healthy controls as each sample was fixed prior to cryopreservation and it has been shown that PMN-MDSC that are **not** fixed do not survive the cryopreservation process[315].

With the limitations of the PMN-MDSC marker in mind, this study did also observe a significant difference in the frequency of PMN-MDSC and the precursor, eMDSC subset in both active TB participants and healthy controls, for which there was significantly higher levels of the latter. There was, however, no significant difference in the frequency of eMDSC between active TB participants and healthy controls, suggesting that hematopoiesis produces a consistent number of these precursor cells regardless of whether or not infection is controlled, i.e. whether *M.tb* infection has remained latent or has progressed to active disease. Since the discovery of eMDSC is relatively recent, previous studies would have researched these populations, but not reported on their frequencies as the eMDSC phenotype is negative for any lineage markers like CD14 or CD15. These results are therefore the first reported frequencies of the eMDSC subset and could suggest that eMDSC produced during latent infection differentiate into effector MDSC subsets, particularly M-MDSC, but at a lower rate than during active disease, resulting in lower levels of immune modulation and perhaps immune protective functions owing to the native function of MDSC which includes tissue repair, as does a homeostatic T_H2 response.

As mentioned previously, MDSC were able to be enriched from the healthy control population. It is generally accepted in literature that MDSC are not able to be isolated from healthy controls, and this is due to them not having a chronic inflammatory condition[181]. Previous studies have observed an increase in MDSC frequencies in healthy controls recently exposed to *M.tb* (tuberculin skin test (TST) positive household contacts) which could support our findings in QFT positive healthy controls, although TST positivity was not assessed in this study[178]. Alternatively, since this study's healthy control population consisted of mostly latently infected participants (QFT+), the expansion of MDSC could be speculated to be as a result of a state of low-grade chronic inflammation observed during latency, and is supported by literature[316]. Both hypotheses could explain this study's observations, however, future MDSC studies should assess the T cell-specific suppression of QFT+ healthy controls compared to TST+ healthy controls as the aforementioned study found that TST+ MDSC suppressed T cell function to a lesser extent than MDSC from active TB participantsd[178].

Control monocyte population frequencies are similar in both participants with and without active TB disease.

Traditional monocytes are frequently used as the control population specifically for the M-MDSC subset owing to the shared morphological characteristics but contrasting functional characteristics. In this study, monocytes were isolated from a fraction of PBMC kept separate prior to the MDSC isolation. CD14 microbeads were then used to isolate traditional monocytes from PBMC and it is important to keep in mind that some M-MDSC may have been isolated in addition to the monocytes since both cell types express the surface marker CD14. Phenotyping of the enriched monocyte population allowed for the discrimination between $CD14^+$ cells that were either HLA-DR positive or negative, of which the HLA-DR positive cells were considered traditional monocytes since MDSC are an immature population of cells and would thus not express the HLA-DR receptor. This study investigated the differences in enriched monocyte frequencies, as a frequency of total PBMC, between active TB participants and healthy controls. No significant difference for the monocyte frequencies was observed between the two participant groups, and no significant difference was observed when comparing the frequencies of enriched monocytes with total MDSC in both participant groups. There was, however, a significant difference in the median fluorescent intensity (MFI) of CD14 expression in healthy controls when comparing CD14 expression by enriched monocytes and total MDSC. In this instance, enriched MDSC from healthy controls expressed significantly more CD14 on their surface compared to enriched monocytes. A similar increase was observed in active TB disease participants; however, the difference did not reach significance ($p = 0.09$).

Functionally, CD14 is known to act as a co-receptor that works in conjunction with TLR4 and the MD-2 protein to form a multi-receptor complex for the recognition of bacterial lipopolysaccharide (LPS)[317,318]. While *M.tb* is not a Gram negative bacteria and does not contain LPS as a cell wall component, Lipoarabinomannan (LAM) is an *M.tb*-specific lipid glycoprotein cell wall component that physiochemically resembles LPS and induces the same CD14/TLR4/MD-2 multi-receptor complex in the human host[319]. The significant increase in CD14 expression on the surface of enriched MDSC compared to enriched monocytes could, therefore, be indicative of a heightened ability of these cells to respond to bacterial lipid-based cell wall components.

In a study performed by He *et al*. investigating the function of CD14 in murine monocytes, it was found that the S100A9 protein was capable of binding to CD14 and that CD14 was an essential co-receptor for S100A9-mediated TLR4 stimulation and subsequent NF-$\kappa\beta$ signaling[320]. The S100A9 protein is of particular importance owing to its known involvement in MDSC. S100A9 is a calcium-binding protein expressed primarily in neutrophil granulocytes and some monocyte subsets, but, more importantly, is expressed on the surface of immature monocytes[321,322]. For this reason, the S100A9 protein is growing in popularity as a marker of M-MDSC, along with its S100A8 counterpart with which S100A9 is normally expressed in the form of a heterodimer[32,323]. MDSC are well known to express S100A8/9 and, as stated previously, is most likely expressed on the M-MDSC subset, however there is insufficient literature available on the expression of S100A8/9 on the PMN-MDSC subset. The possibility of this marker being

expressed on PMN-MDSC as well can, therefore, not be excluded. Levels of the S100A8/9 heterodimer are known to be elevated during inflammatory diseases including metastatic cancer, and biological functions of this heterodimer include the induction of inducible nitric oxide synthase (iNOS)[320,324]. iNOS, apart from arginase-1 (Arg-1), is the enzyme responsible for the suppressive properties of the MDSC population, resulting in the suppression of T cell migration and the induction of T cell anergy[181,325,326]. S100A9 is also known to be a ligand for the TLR4 and RAGE (Receptor for Advanced Glycation End-Products) receptors, the latter also being documented in cancer and associated with MDSC expansion[324,327,328]. Considering the literature above, the findings observed by He *et al.* highlight the importance of CD14 expression in MDSC function, in conjunction with other receptors like TLR4. Most importantly, He *et al.* identified the focal binding of S100A9 proteins to subdomains of monocyte membranes that also contained TLR4 and the protein membrane-lipid protein caveolin-1. Further evidence displays the internalization of S100A9 proteins into early endosomes[320]. We therefore, hypothesize that S100A9-expressing M-MDSC are capable of internalizing molecules or compounds into endosomal structures via CD14/TLR4/Caveolin-1-mediated endocytosis (when expressed/bound in the same membrane subdomains), thereby mediating not only immune suppression during *M.tb* infection, but also immune evasion of bacteria from phagosomal degradation. Additionally, the elevated expression of CD14 on the surface of MDSC compared to monocytes in this study supports this hypothesis.

MDSC and control monocyte populations enriched from both participants with active TB disease and healthy controls express the markers Caveolin-1 and TLR4 on their surfaces, as confirmed by flow cytometry.

Based on the above-mentioned literature, the phenotypic investigation of Caveolin-1 and TLR4 on the surface of MDSC was warranted. The surface expression of both TLR4 and Cav-1 via flow cytometry has never before been investigated in MDSC in the context of active TB disease, or any other disease. Unpublished data from confocal microscopy experiments have identified caveolin protein expression on MDSC, and while this study could confirm the presence of the Cav-1 protein through flow cytometric analyses, further investigations would need to be done in order to identify the internalized caveosome structure. This objective was not designed to be answered in this study and was therefore not investigated further.

Through the work performed in this study, the surface expression of TLR4 on MDSC was also confirmed, a first for the field in the context of human studies. It was observed that TLR4 expression was reduced on the surface of both MDSC and monocyte controls isolated from healthy controls, pointing to a lack of TLR4 expression on the surface of innate immune subsets during the absence of antigenic challenge. This also suggests that there is an absence of *M.tb*-specific antigens within circulation during latent infection since 80% of the study healthy control population was latently infected with *M.tb*. Adequate control of mycobacteria likely results in the prevention of further immune activation with subsequent TLR4 upregulation on primary phagocytes, like monocytes, by antigens such as LPS, which bind TLR4 with high affinity. Based on the total number of MDSC and monocytes reported on in

Figure 6.10(b) and (c), it appears that most monocytes isolated from TB patients express the TLR4 marker, while only about half of the MDSC isolated from TB patients express it (based on median percentage of total PBMC). In terms of Cav-1 expression, it would appear that Cav-1 is expressed on both monocytes as well as MDSC, again on almost all monocytes, but only on about a quarter of the isolated MDSC from the blood of TB patients. Without further microscopy work to determine possible co-localization of these two surface proteins, it is not possible to conclude whether or not TLR4 and Cav-1 are expressed in the same vicinity of the cell membrane, or whether Cav-1 effector functions may be dependent on the presence of TLR4, as proposed by He *et al.*[320]. The confirmation, however, of the expression of the Cav-1 protein on the surface of MDSC is a promising and novel finding in terms of new directions for the investigation into *M.tb*-specific host immune evasion techniques. If one were to consider the physiological characteristics of Cav-1, it would not be surprising to identify Cav-1 co-localization with TLR4. The Cav-1 protein is enriched in membrane lipid rafts, micro-domains on the cell membrane where many receptors are concentrated. Not only are these lipid rafts rich in cholesterol required for endocytosis, but many receptors translocate to these regions to allow for crosslinking with the T cell receptor (TCR) upon antigen presentation. Lipid rafts have also been reported as regions where glycosylphosphatidylinositol (GPI)-anchored receptors, such as CD14, are internalized into "recycling" endosomes[240,329–332]. Therefore, the co-localization of Cav-1 and TLR4 may be an unexpected occurrence and potentially unrelated to MDSC functions.

The apparent link between TLR4, Cav-1 and CD14 cannot be dismissed based on the evidence supporting the importance of this signaling axis, and the evidence that these markers are indeed expressed in the monocyte and MDSC populations during active TB disease may indicate a novel pathway by which *M.tb* bacilli are internalized by secondary phagocytes, while bypassing traditional phagolysosomal pathways. In order to put the expression of TLR4 on MDSC in context, a study performed by Bunt *et al.*[333] highlighted the importance of the TLR4 signaling pathway in the exacerbation of tumor progression, and recent literature has been summarized by Ray *et al.*[334], focusing more on non-specific bacterial induction of MDSC in the lung. The latest review by Dorhoi and Du Plessis[304] stressed the importance of TLR4 signaling during infectious diseases in the generation of the M-MDSC subpopulation specifically, and with the results of this study identifying a largely M-MDSC-based environment in the peripheral blood of both healthy and *M.tb*-infected individuals, it is very likely that TLR4 signaling plays a crucial role in the life-cycle of the M-MDSC subpopulation. These results also suggest a possible addition to the phenotypic surface marker repertoire of M-MDSC specifically – a valuable finding for a cellular population whose phenotype is still under debate.

Enriched MDSC exhibit a cytokine profile that is conducive to their recruitment and expansion in active TB disease participants following stimulation with PPD.

Considering the observation that the majority of enriched MDSC are of the monocyte lineage, we propose that the M-MDSC subset is responsible for the majority of the cytokine production findings given below.

Enriched MDSC from active TB patients were stimulated with PPD and cultured overnight in order to investigate their response to *M.tb*-specific peptides. As expected, various cytokines known to be involved in the induction and effector functions of the MDSC subset in the tumor microenvironment were significantly upregulated. These included IL-6, IL-10, IL-13, IL-1β, IFN-γ, and TNF-α. The majority of these cytokines are known to be involved in the induction of MDSC, while IL-10 is otherwise one of the main cytokines responsible for MDSC T cell suppressive effector functions via the induction of T_{Reg} cells[181,307,335]. These results are consistent with current literature and have been extensively reviewed in peer-reviewed journals[181,312,336–338]. The PPD-specific upregulation of TNF-α is also consistent with our findings from Chapter 5 where isolated monocytes from latently infected participants were able to be directly stimulated by *M.tb*-specific antigens to produce cytokines like TNF-α. Considering the anti-inflammatory/regulatory nature of MDSC, it is important to comment on the upregulation of two cytokines normally associated with successful *M.tb* control which would be expected to be downregulated: IFN-γ, and TNF-α. However, pro-inflammatory cytokines like IL-6, IL-1 and TNF-α are known to drive the generation of MDSC owing to the chronic inflammatory conditions they promote[304]. Likewise, chronic IFN-γ production, whether from macrophages and T_H1 cells or immature innate cells like MDSC, would likely induce further MDSC activation and recruitment to the site of infection in a feedback loop[339]. This, in part, is supported by evidence in mice that identified enhanced suppressive MDSC functions in bone-marrow-derived MDSC following combined stimulation with LPS and IFN-γ[340].

The chemokines MIP-1α and MIP-1β were also upregulated following stimulation with PPD. Both are involved in the recruitment and regulation of MDSC following the initial recruitment of inflammatory monocytes/MDSC to the site of infection by CCL2, which was not seen to be significantly upregulated in our study when HLA-DR^-CD33^+ MDSC were cultured alone (data not shown)[337,338,341,342]. We did, however, observe an upregulation of CCL2 in latently infected participants in Chapter 5, as well as MIP-1β, which could suggest that the recruitment functions of CCL2 are performed during latency, prior to progression to active disease at which point MDSC are already locally present at the site of disease. As reviewed by Kumar *et al.*, tumor M-MDSC display increased expression of both MIP-1α and MIP-1β in multiple tumor models. MIP-1β has also been observed to function as a chemoattractant for T_{Reg} cells, which are known to be key regulators of protective T_H1 immune responses, and are induced by MDSC-produced IL-10[312,343]. The upregulation of these two chemokines are, therefore, supported by literature in their role during MDSC recruitment.

The above-mentioned cytokines and chemokines are well known to be associated with the MDSC subset. Interestingly, this study highlighted a few upregulated cytokines not previously explored in this subset. These included soluble Fas, IL-22, IL-33, ADAMTS13 and IL-1α. Soluble Fas has previously been shown to be pro-apoptotic through its induction of $CD3^+$ T cell apoptosis, an unconventional mechanism by which MDSC inhibit $CD3^+$ T cell functions for successful host control of *M.tb* infection[344,345]. Additionally, the investigation of Fas in cancer has highlighted a secondary, non-apoptotic role which involves the transmission of proliferation and activation signals. For example, a study performed by Zhang *et al.* observed that overexpression of Fas promoted lung cancer growth *in*

vivo, increased MDSC and T_{Reg} accumulation in the tumor, and promoted *in vitro* chemoattraction of MDSC in a PGE_2-dependent manner[346]. IL-22 has been implicated in CXCL2-dependent migration of MDSC when produced by epithelial T_H22 cells, for which very little information is known, in the mucosa, and increased levels of IL-22 have been documented to be associated with tumor initiation and progression[347,348]. IL-33 is considered a danger-associated molecular pattern or alarmin since it is not released under homeostatic conditions, but rather during stress and inflammation. As such, IL-33 levels are increased in the tumor microenvironment and result in the reduction of MDSC apoptosis via the induction of autocrine GM-CSF secretion, as well as the induction of arginase-1 expression, which both augment MDSC accumulation and suppressive functions, respectively[349,350].

The cytokine ADAMTS13, also known as the von Willebrand factor cleaving protease, is a unique ADAMTS family subgroup that has no known association with HLA-DR^-CD33^+ MDSC expansion or suppressive functions, even though other members of this family have known associations with cancer and angiogenesis[351]. Primarily responsible for appropriate blood coagulation, and the control and structure of the extracellular matrix of the blood vessels, it has been implicated in angiogenesis, with deficiencies observed in humans resulting in thrombotic thrombocytopenic purpura. This disorder has also been demonstrated to be associated with *M.tb* infection-induced septic shock[352,353]. Angiogenesis is the process by which new blood vessels are formed, a normal part of the growth and healing processes within the body. It is also known to play a role in the development of tumors since these structures require nutrients and oxygen like any other bodily structure, and MDSC are well known to be involved in the promotion of this process, among other pro-tumor related functions[312,354–356]. This knowledge highlights the relationship between suppressive myeloid cells and angiogenesis. We, therefore, propose that ADAMTS13 functions similarly to other growth factors like vascular endothelial growth factor (VEGF) which are also important angiogenic factors. Tumor-secreted VEGF is known to interfere with the differentiation and maturation of immature granulocyte-macrophage progenitors, skewing hematopoiesis into the development of immunosuppressive tumor-associated macrophages (TAMs) and MDSC[357]. Considering the shared angiogenic characteristics, ADAMTS13 might be involved in driving the differentiation of myeloid cells towards immature myeloid cell lineages like MDSC and/or TAMs.

In terms of IL-1α, the natural role of this cytokine during *M.tb* infection is known to be mostly pro-inflammatory. In order to expand the MDSC population during chronic infections, MDSC themselves start producing proinflammatory mediators in order to mediate the further expansion of this population in a positive feedback mechanism, as seen in the production of IFN-γ and TNF-α by MDSC stimulated with PPD[336,340,358]. However, it cannot be inferred if the MDSC population is the true producer of this cytokine as our population is not pure, but rather enriched for MDSC. We could, therefore, have observed IL-1α production from monocytes, which are known IL-1α producers.

This study, therefore, successfully enriched the MDSC subset from PBMC and observed a cytokine repertoire that is consistent with literature. Once again, considering the fact that nearly 80% of the enriched MDSC population expressed the CD14 receptor, and thereby are classified as the M-MDSC

subset, we propose that these upregulated cytokines are predominantly produced by the M-MDSC subset in the PBMC fraction of peripheral blood. We were unable to utilize a more PMN-MDSC specific surface receptor like LOX-1 owing to no literature being available on the marker prior to this study's design, so we acknowledge that there may be a possibility for false subset frequency representations. Future studies will utilize the newly identified MDSC subset-specific surface markers for more accurate investigations.

Co-cultured MDSC and CD3$^+$ T cells exhibit a cytokine profile that suggests an MDSC- and PPD-specific suppression of CD3$^+$ T cells.

The hallmark of MDSC function is the suppression of T cells, amongst others, through the production of the enzymes inducible nitric oxide synthase (iNOS) and arginase-1 (ARG1). ARG1 actively competes for L-arginine, which is catabolized to produce ornithine and urea, thereby depleting L-arginine reserves from the environment and inhibiting T cell proliferation. iNOS induces a state of oxidative stress through the production of nitric oxide (NO) and other derivative reactive species. These derivatives include peroxynitrite and hydrogen peroxide, and drive changes within the T cell receptors resulting in defective migration and antigen recognition functions (reviewed by Gabrilovich *et al.*)[336].

Following the enrichment of MDSC from the PBMC fraction of active TB participants, this study investigated the suppressive potential of these cells on T cells in the context of active TB disease and in a contact-dependent manner. Enriched MDSC were co-cultured with CD3$^+$ T cells and stimulated with PPD overnight in two concentration ratios – 1:1 and 1:2.5 (MDSC: T cell). Cytokine production was then compared to PPD-stimulated T cell cytokine production in the absence of enriched MDSC to determine T cell-specific responses. A consensus on the *in vivo* frequency of MDSC is still outstanding. Therefore, based on previous studies, we estimated that the *in vivo* ratio of these cells during chronic inflammatory states would likely fall in the 1:2.5 ratio[178]. When co-culturing at this ratio, only the cytokines IL-1β and soluble Fas were significantly upregulated compared to PPD-stimulated T cells in the absence of MDSC. IL-1β, although it has a central role in pro-inflammatory responses, is also known to be associated with the induction of MDSC accumulation and recruitment, the upregulation thereof in the presence of T cells points towards a T cell-dependent induction of pro-MDSC cytokines from the MDSC present in culture.

As a soluble protein, the membrane-bound form of Fas is created via alternative mRNA splicing and is capable of inhibiting apoptosis induced by the Fas/FasL system[346,359,360]. This study observed an MDSC-associated increase in its production from T cells. It is unknown which cell type is responsible for the increased production of soluble Fas as both MDSC and CD3$^+$ T cells have displayed soluble Fas production when stimulated with PPD on their own (Figure 6.17(a) and Figure 6.18(a) respectively). It is therefore speculated that both cells may be producing the soluble form of this protein as a protective mechanism. Both MDSC and CD3$^+$ T cells are known to express the FasL receptor, which is responsible for the induction of apoptosis following binding membrane-bound Fas, and the production of the soluble form would thereby prevent apoptosis of either of the cell types[345,361]. There were no other significantly

different cytokines expressed when cells were co-cultured in such a ratio, particularly those indicative of T cell suppression (e.g. IFN-γ). This may have been as a result of there being too many T cells in culture for the enriched MDSC to have mounted a successful suppressive effect. Additional host factors that could contribute to the survival or expansion of MDSC could have been lost during the isolation process and therefore not included in the co-culture experiments.

During the 1:1 co-culture experiments, however, there was an observed significant reduction in T cell-specific IFN-γ following stimulation with PPD. This suggests that in the presence of enriched MDSC populations, PPD-specific $CD3^+$ T cell responses are suppressed, resulting in the downregulation in the production of T cell-specific IFN-γ. This is detrimental to host pathogen control, as T cell-specific IFN-γ production is crucial for a successful adaptive response against *M.tb* infection. In contrast, we observed a significant PPD-specific upregulation of the chemokine CCL2, also known as monocyte chemoattractant protein 1 (MCP-1). As mentioned previously, CCL2 was observed to be upregulated in monocytes from latently infected participants in Chapter 5 and is responsible for the initial recruitment of inflammatory monocytes/MDSC to the site of infection. Additionally, a study performed by Du Plessis *et al.* demonstrated that MDSC cultures are associated with increased levels of CCL2 in recently *M.tb* exposed individuals, which supports these findings[178]. The present study of active TB cases confirms the upregulation of CCL2 and highlights its role in inflammatory conditions. It is not possible to conclude whether or not CCL2 production is directly from the monocytic MDSC fraction, however, the finding in this study that the majority of enriched MDSC are of the monocytic phenotype strongly suggests this. It is also possible, however, that the enriched MDSC population contained a fraction of mature monocytes, likewise the monocytes isolated in Chapter 5 could have contained a fraction of M-MDSC owing to the limitations highlighted previously in this discussion.

Some cytokines normally associated with MDSC displayed no significant upregulation during any of the culture experiments.

The cytokine profile of MDSC activation, expansion and effector functions is well characterized in a number of reviews[32,304,336,362]. Many of the more well associated cytokines were not seen to be significantly up- or down-regulated in this study even though they were assessed. Cytokines that were expected to be up-regulated included GM-CSF, IL-4, IL-10, CD40L, CCL1, and CXCL11, while those expected to be down-regulated included IL-2 and IFN-α2.

GM-CSF is expected to have been upregulated owing to it being crucial for the generation of MDSC from the bone marrow during hematopoiesis, while IL-4 and IL-10 are well known to drive the development of tumor-associated macrophages and T_{Reg} subsets, respectively[312,336,363]. No significant change in CD40L was surprising since the CD40-CD40L interaction between MDSC and $CD3^+$ T cells are thought to be responsible for the conversion of $CD4^+$ T cells to induced T_{Reg} cells, and, therefore, indirectly involved with MDSC immunomodulatory functions[364]. The upregulation of the chemokine CCL1 (Chemokine (C-C motif) Ligand 1) is associated with the recruitment, migration and accumulation of MDSC, and polarization of the immune response to that of T_H2. Neutralization of CCL1 has also been

shown to prevent the conversion and suppressive activity of T_{Reg} cells, highlighting its importance in the regulatory functions of the immune system[365–368]. The chemokine CXCL11 (C-X-C motif chemokine 11) is also involved in the recruitment of T_{Reg} cells, as well as the promotion of MDSC invasion of the tumor environment through the induction of fibroblast migration[369,370]. IL-2 and IFN-α2 were expected to be downregulated owing to the known function of MDSC to interfere with IL-2 receptor signaling on $CD3^+$ T cells leading to subsequent desensitization of the T cell receptor (TCR)[312,336], while MDSC reduce $CD4^+$ T cell-responsiveness to IFN-α2 and are themselves reduced in number through IFN-α2-induced pathways[371,372]. While we could speculate the possible reasons behind no observable differences in these eight cytokines/chemokines, it is very likely that this could be due to our small sample size. Alternatively, culture conditions may have lacked many cofactors required for the activation of suppressive effector functions, as well as for the activation of appropriate T cell responses, especially considering the fact that MDSC are poor antigen presenting cells.

We previously postulated that the downregulation of seven cytokines (IL-6, IL-8, IL-13, IP-10, TNF-α, MIP-1α, and MIP-1β) in the whole blood of healthy controls compared to the co-culture of CD14 monocytes and CD3 T lymphocytes may be as a result of a suppressive mechanism activated upon contact with soluble factors normally found within the *in vivo* environment. We also postulated that this suppression may be caused by MDSC. Considering the knowledge that MDSC have a monocytic subset that closely resembles CD14 monocytes, we suspected that this subset of MDSC could be the cause of the observed suppression. When comparing the results from the combined culture of monocytes and T lymphocytes in Chapter 5 to those observed in the co-culture of MDSC and T lymphocytes in Chapter 6, we did not observe the same cytokine production profile. This could be indicative of enhanced suppressive abilities in MDSC expanded during active TB disease, but it could also be indicative of a lack of cell interaction that would normally play a role in cellular activation or differentiation the *in vivo* environment. This brings in to question the use of isolated cells for the investigation of all effector properties, and future studies should consider functional investigations employing mass spectrometry proteomics. In hindsight, this study would have benefitted from the investigation of intracellular cytokine production through flow cytometry for a more cell-specific cytokine production profile. Other reasons could include a lack of clear consensus as to how many MDSC are found, on average, in 1ml of whole peripheral blood, so as to improve our ratio of MDSC to T cells during co-culture when *in vivo* conditions are mimicked. Considering that this study investigated the frequency of MDSC populations in PBMC and not in whole blood, it is possible that cell numbers could have been overestimated, or that cells could have been activated during the isolation process and thus not reflect whole blood conditions.

Concluding Remarks

Myeloid-derived suppressor cells represent a unique population to be investigated in the context of active TB disease. This is a widely researched cell type in the field of oncology and advances in this context may very likely be translatable into the field of tuberculosis. Previous studies on MDSC in active TB disease have focused on whole blood, however the PBMC compartment has proven to be the

optimum source for MDSC characterization which has not yet been performed in the context of active TB disease. From this study, MDSC isolated from the PBMC of active TB participants displayed *M.tb* antigen- and T cell-specific suppressive functions, reducing T cell-specific IFN-γ which is indispensable for the control of *M.tb* infection. These MDSC were also observed to secrete cytokines/chemokines known to be crucial for the expansion, activation and continued survival of additional MDSC, as well as for the differentiation of T_{Reg} cells from the naïve T cell state. This study was able to isolate MDSC from the PBMC of both active TB and healthy control participants, albeit significantly less in the healthy control participant group. This highlights the frequency of this population during active infection, as well as during healthy states. In addition to reporting on the frequency of these cells within the PBMC compartment, this study confirmed the surface expression of both Cav-1 and TLR4 on the surface of MDSC, as well as on the surface of control monocyte populations for the Cav-1 protein specifically. These findings, both in terms of surface receptor expression and the cytokine secretion profile, are a first for the field of TB research and have provided valuable insight into the surface receptor structure of these cells which is considerably under-studied.

CHAPTER 7

Conclusion

Tuberculosis is complex and devastating disease that, while curable, still ranks as the world's deadliest. Initial symptoms of active disease tend to be disregarded for other illnesses such as the flu or other bacterial chest infections, and diagnoses tend to be made only once a patient is severely ill and has likely had time to transmit to close contacts. The non-specific symptoms, initial paucisymptomatic nature of the disease, lacking tools for early diagnosis and stigma all result in low case-detection rates, high rates of transmission and severe progression of disease severity before treatment can be started. The patient, therefore, follows a long and difficult path from the time of eventual diagnosis until the point at which the six month treatment regimen can be successfully completed.

However, clinicians themselves face a long and labour-intense process for the accurate diagnosis of active TB disease. Briefly, the gold standard diagnostic tool for the confirmation of active TB disease is sputum culture, which may take up to six weeks for a result. During this period, patients worsen and transmit disease even further, and on many occasions patients do not return for the diagnostic result. While GeneXpert has improved the time to diagnosis significantly, roll-out of the platform has been complicated by socio-economic factors such as lack of power supplies and appropriate storage facilities for cartridge reagents, particularly in rural regions where the disease burden tends to be higher. Not only do clinicians have to worry about difficult diagnostic methods, but they also face the challenge of ensuring patient adherence to an uncomfortable treatment regimen of six months, during which anti-TB therapies worsen patient adherence due to severe side effects, which include severe nausea. Current efforts to monitor patient response to treatment and potentially predict the outcome involve the conversion of sputum culture to negative at the month 2 time point following treatment initiation.

Current research efforts have focused on the investigation of biomarkers. These biomarkers would include (1) biomarkers for more accurate and time-efficient diagnosis of active TB disease, (2) biomarkers for the prediction of treatment response/outcome for potential treatment shortening options to improve adherence, and (3) functional biomarkers demonstrating unique *M.tb*-specific innate and/or adaptive immune characteristics specific to the immune profile observed at the time of diagnosis, across treatment or at the point at which disease is cured (Figure 7.1). The aim of this dissertation, as a whole, was to investigate potential biomarkers at various stages within this pipeline in an attempt to encompass all aspects involved with the successful cure of a patient with active TB disease.

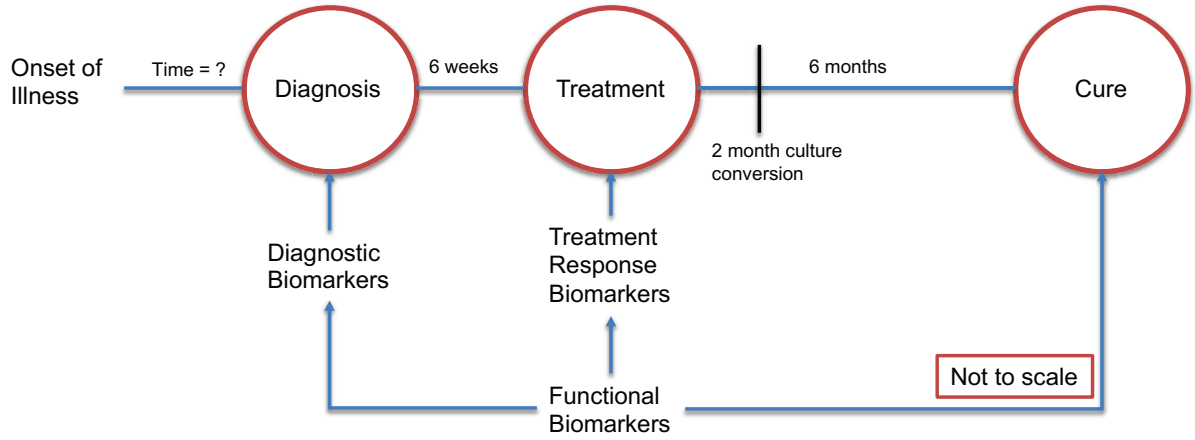

Figure 7.1: Graphical simplification of the pipeline through which patients with active TB disease go, and the biomarker types employed during each phase. The pipeline is not drawn to scale.

We began with the investigation of nine host-specific diagnostic biomarkers, present in serum, in 710 participants who presented to primary health-care clinics with symptoms suggestive of active TB disease (Chapter 2). Serum was selected as the sample type of choice as sputum is known to be a difficult sample to obtain for reasons outlined in previous chapters, and the biomarkers assessed were selected due to their known role as inflammatory and infection biomarkers in other diseases, as well as the ease with which they are able to be measured in the blood[124]. In this chapter, we concluded that univariate use of biomarkers for the prediction of active TB disease was not a feasible option in this setting owing to poor diagnostic abilities, with one exception. It was observed that the biomarker A2M could accurately distinguish between participants with active TB disease and latent infection with a diagnostic accuracy of 92% (95% C.I. 90.0-95.0%), sensitivity of 82.35% (95% C.I. 77.0-87.0%) and specificity of 92.76% (95% C.I. 89.0-96.0%), however the discrimination between latent infection and active TB disease was beyond the scope of this project. Multivariate analyses were thus performed for all 9 biomarkers and combinations thereof. This resulted in the identification of a two-biomarker biosignature (CRP and SAA) that was capable of accurately distinguishing between active TB disease patients and those without active TB disease with a sensitivity of 87.4% (95% C.I. 78.5-93.5%), specificity of 75.7% (95% C.I. 68.8-81.8%) and an area under the curve of 86.6% (95% C.I. 81.9-91.0%), irrespective of HIV infection. When the biosignature was optimized for a sensitivity of greater than or equal to 90%, it was capable of accurately distinguishing between active TB disease patients and those without active TB disease with a sensitivity of 90.8% (95% C.I. 82.7-96.0%), a specificity of 69.6% (95% C.I. 62.4-76.2%) and an area under the curve of 76.5% (95% C.I. 71.0-81.4%). The biosignature was developed in a cohort of participants from multiple African countries, not only from South Africa, which highlights the strong potential of this biosignature to be successful in different geographical locations, a common limitation for most blood-based diagnostic tools. The biosignature performance did not meet the requirements of a non-sputum, blood-based diagnostic tool based on the Target Product Profile guidelines published by the WHO in 2014[127]. The biosignature was, therefore, suitable for use as a point-of-care screening tool instead. The potential of this biosignature was assessed further in combination with other innate immune cytokines that were assessed in the same cohort from the larger AE-TBC study, as was included in the now published seven-biomarker

biosignature developed by Dr Chegou and colleagues[125]. This larger biosignature was capable of diagnosing active TB disease with a sensitivity of 93.8% (95% C.I. 84.0-98.0%) and specificity of 73.3% (95% C.I. 65.2 - 80.1%) irrespective of HIV co-infection and is currently being developed further into a lateral flow device for the screening of patients suspected of having active TB disease at the point-of-care (P.I. Prof Gerhard Walzl). The contribution of the two-biomarker biosignature to the larger seven-biomarker biosignature illustrates the ease with which such a biosignature may be developed into a point-of-care device that would require few special storage conditions and very little training at the clinical staff level for the interpretation of such results. Additionally, the development of a point-of-care device, such as a lateral flow device, would provide an almost instant result, allowing for the swift initiation of the appropriate treatment; not to mention the benefits of a hand-held device for rural communities.

The CRP/SAA biosignature was capable of distinguishing between patients with and without active TB disease irrespective of HIV co-infection. HIV is undoubtedly the most dangerous co-infection in terms of active TB disease owing to the depletion of CD4 T cells crucial for the control of *M.tb* infection. As explained previously, sub-Saharan Africa presents with a variety of non-communicable and infectious diseases that are widely known to increase susceptibility to *M.tb* infection and exacerbate TB disease during co-infection. One such co-infection that is severely understudied on the African continent, and especially in the adult population, is soil-transmitted helminth (STH) infections. Chapter 3 undertook a pilot investigation for STH sensitization (specifically the *Ascaris lumbricoides* species) on a subset of the participants recruited for the AE-TBC study, all of whom were adults and from the South African clinical sites. The result was surprising as approximately 61% of the tested participants were sensitized to *Ascaris lumbricoides* according to specific IgE antibody levels. A positive sensitization was defined by the fluorescent intensity of the light emitted from the bound allergen-specific antibodies translated into a concentration of bound antibody. The higher the intensity of the fluorescent signal, the higher the concentration of bound antibody. Therefore, it is generally considered that any detectable level of fluorescent emission is an indication of circulating antibodies for that specific allergen and possible recent exposure (discussed in detail in the discussion of Chapter 3). When stratified according to active TB disease, approximately 71% of participants with active TB disease were sensitized with *Ascaris lumbricoides*-specific IgE antibodies. While sensitization does not necessarily equate to current infection STH species-specific antibodies are not known (per se) to be detected very long after cleared episodes of infection. These results lead to the investigation of the stability of the developed biosignature upon further stratification of the cohort based on *Ascaris lumbricoides* sensitization. The samples used for this study were QFT plasma samples in order to investigate the potential of using the biosignature in a different sample type, as well as to investigate the effect of *M.tb*-antigen stimulation on the outcome. The biosignature proved robust in discriminating between participants with and without active TB disease in the **unstimulated** samples of the *Ascaris lumbricoides* sensitized/co-infected group, with a sensitivity of 78% (95% C.I. 52.4-93.6%) and specificity of 75% (95% C.I. 50.9-91.3%), while the biosignature performed poorly in the antigen-stimulated samples. The biosignature could have performed better in this instance for various reasons. While Ascaris induces a T_H2 response during the

intestinal phase of its lifecycle, the respiratory phase of the lifecycle potentially exacerbates the inflammatory environment of the lung owing to the tissue damage created by the migration of the larvae through the lining of the airways. This would cause the lung environment to experience a more pronounced pro-inflammatory response resulting in the increased release of acute phase cytokines. These findings further supported the clinical potential of this biosignature, both in high-burden settings and settings where other infectious disease like HIV and *Ascaris lumbricoides* are prevalent. However, these factors seem to go hand-in-hand.

The identification of a robust blood-based biosignature supported the investigation of blood-based biomarkers in other TB research areas. Thus, we turned our attention to the investigation of biomarkers indicative of response to treatment. A previous study (investigating the FACS CAP™ technology) performed in our group investigated the use of PBMC surface markers as biomarkers of response to treatment. The FACS CAP™ technology is expensive and requires advanced expertise and does not offer a feasible approach for translation into the clinical setting. Chapter 4, therefore, investigated the changes of the five most promising markers identified in the FACS CAP™ study in whole blood over the course of anti-TB treatment. As mentioned previously in Chapter 4, many treatment response biomarker studies have investigated the whole blood of patients, however most have focused on the gene expression levels of certain markers, and not their surface expression. The five markers investigated in this study included CD120b (TNFR2), CD126 (IL-6R), CD62L (L-selectin), CD58 (LFA-3) and CD197 (CCR7), all of which were previously identified to have been downregulated over the course of anti-TB treatment, with the exception of CD58 which was upregulated. These five markers were mostly related to the innate immune response, both the activation of the adaptive immune response by innate cytokines, as well as cellular migration of innate cells to the site of infection, with the exception of CD197 which is a memory marker for adaptive immune cells like $CD4^+$ and $CD8^+$ T cells. The surface expression of these markers was investigated on various immune cell subsets, including T- and B- cells, classical and intermediate monocytes, neutrophils, NK cells, and NKT cells. Prior to the subset investigations, the surface expression of each marker was assessed on all cells – only CD58 was differently expressed (downregulated) on all cells over the course of anti-TB treatment, compared to FACS CAP™ where CD58 was upregulated over the course of treatment, pointing towards important differences between whole blood and PBMC assays. This discrepancy could have been as a result of different sample preparation methods altering the expression patterns of markers, i.e. the fixative in the lysing solution or the use of Ficoll-Hypaque could have induced physiological alterations in the cells resulting in heightened activation and, therefore, upregulation of certain markers. During the subset investigations two markers, CD120b and CD58, were differentially expressed (upregulated) over the course of anti-TB treatment on the surface of $CD4^+$ and $CD8^+$ T cells alone, emphasizing once again the importance of a successful T cell response for the control of infection. The upregulation of CD120b on the surface of $CD4^+$ and $CD8^+$ T cells at the end of anti-TB treatment suggests a restoration of TNF-α-mediated protective immunity following successful treatment. Likewise, the upregulation of CD58 expression on these cells at the end of treatment suggests that upon successful anti-TB treatment there is an upregulation of the $CD4^+$ and $CD8^+$-specific T_{SCM} cells, indicating the initiation of memory T cell

development and possibly improved anti-TB responses due to their known association to improve anti-tumor responses in tumor biology[245]. Considering that both of these markers are responsible for important innate immune functions during *M.tb* infection, this highlights the under-researched field of innate immune responses during *M.tb* infection. Future studies should consider the use of larger cohorts and the investigation of additional time points following the initiation of anti-TB treatment for a more detailed representation of biomarker candidate fluctuations. In addition to this, Chapter 4 also investigated the use of a commercially available test, the BD Multitest™ IMK kit, as a potential alternative biomarker candidate. The BD Multitest™ IMK kit is used for the enumeration of absolute cells counts from whole blood and is commonly employed for the enumeration of CD4 counts in HIV. The kit measured the absolute cell counts of CD3 T cells, CD4 T cells, CD8 T cells, naïve T cells, B cells and NK cells, none of which displayed any significant differences over the course of anti-TB treatment in contrast with known literature[373–375]. This suggests that the BD Multitest™ IMK assay may not be sensitive enough to detect *M.tb*-specific changes. Although it may be worthwhile to evaluate other immune subsets not investigated by the BD Multitest™ IMK assay.

During the investigations of diagnostic and treatment response biomarker candidates, the innate immune response and it contributing factors were continually being flagged in the significant results. Considering our desire to still investigate functional biomarker candidates that were linked to both diagnostic and treatment response biomarkers, as well as learn about the immunological mechanism of host immune failure/control, we decided to investigate functional biomarkers involved in the innate immune response to *M.tb* infection, as well as in the direct regulation of subsequent adaptive immune responses. During the investigations performed in Chapter 3 it was observed that the biosignature performed poorly in *M.tb* antigen-stimulated samples compared to unstimulated samples. As a result, the following functional biomarker candidate investigations included the use of *M.tb* antigen-stimulated and unstimulated samples for further comparison.

Chapter 5 investigated 27 cytokines from both the innate and adaptive immune responses, in order to elucidate the innate immune response to *M.tb* antigens in a cohort of latently infected and uninfected individuals. In order to achieve this, neutrophils, monocytes, T cells, monocytes together with T cells, and whole blood were stimulated in QFT Nil and Antigen tubes overnight at concentrations representative of those found *in vivo*. Cytokine measurements of these stimulations revealed a downregulation of IL-6, IP-10, and TNF-α production in whole blood response compared to their production by T cells when stimulated in combination with monocytes in latently infected (QFT+) individuals. The downregulation of TNF-α production was curious owing to the crucial role played by TNF-α during *M.tb* infection for successful granuloma formation and immune activation, not to mention the important role the cytokines IL-16 and IP-10 play in the early stages of immune activation. These data suggest that a suppressive immune cell type exists in the whole blood that is being activated to suppress T cell responses. While such cell types do exist in the form of T_{Reg} cells, we postulate that a suppressive myeloid cell population may also be responsible for this suppression, as well as inducing

the expansion of T_{Reg} cells, for more efficient suppression of host-protective T_H1 responses. We postulate that these cells may be myeloid-derived suppressor cells (MDSC).

MDSC are a heterogeneous population of innate myeloid cells with suppressive properties and have been identified to specifically suppress T cell responses during cancer, and bacterial and viral infections. Since a subset of these cells share the CD14 monocyte marker, it is very likely that the isolated monocyte population used in Chapter 5 contained the monocytic subset of MDSC (M-MDSC) as well. Previous work by Du Plessis and colleagues has identified the expansion of these cells in the whole blood of active TB patients, in a non-specific manner, which supports the hypothesis of their presence in the context of active TB disease[178]. We, therefore, investigated this population further in the PBMC compartment of whole blood in a cohort of 18 active TB patients and 10 latently infected controls, for use as a potential functional biomarker candidate for active TB disease. In Chapter 6, we were able to successfully phenotype MDSC and the three proposed subsets from literature, namely M-MDSC, PMN-MDSC and eMDSC, in both active TB disease patients and healthy controls. MDSC are not known to be expanded in healthy control populations, therefore, the phenotypic confirmation of these cells in our latently infected control group, as well as the evidence of MDSC expansion in recently exposed household contacts supports this finding[178]. This then supported our hypothesis from Chapter 5 that there may well be M-MDSC within the isolated monocyte population, as this chapter made use of latently infected and healthy controls only. Future functional studies would need to be conducted in order to determine whether or not these identified cells are indeed MDSC based on their immunosuppressive properties. We continued to perform co-culture experiments of PPD-stimulated (*M.tb* antigen) MDSC in the presence and absence of T cells in order to compare cytokine readouts to those observed in Chapter 5. PPD-stimulated MDSC in the absence of T cells produced significantly increased amounts of cytokines and chemokines well-known to be associated with MDSC expansion and effector functions, including IL-6, IL-10, and MIP-1β, signifying a positive feedback loop of MDSC expansion, as shown previously[312,376,377]. PPD-stimulated co-culture of MDSC in the presence of T cells (1:1) resulted in the significant downregulation of T cell-specific IFN-γ, compared to T cells stimulated and cultured in the absence of MDSC. In addition to this, the chemokine MCP-1 was significantly upregulated under co-culture conditions which is suggestive of MDSC recruitment. It is speculated that other markers were not found to be suppressed in this study owing to (1) the epitopes present in PPD not activating all of the signaling pathways that would otherwise be activated by the whole organism; (2) MDSC are known to be poor antigen presenting cells, therefore, T cells present within the culture would potentially not be activated as completely as they would have been in whole blood where they would be in the presence of other professional antigen-presenting subsets like monocytes/macrophages. The T cells could, therefore, not be producing the cytokines needed to be suppressed by MDSC in the culture environment; and (3) since the observed majority of MDSC isolated from PBMC where of the monocytic subset, the study could have missed crucial PMN-MDSC suppressive mechanisms. This is likely the case due to the PMN-MDSC subset being recorded as having more suppressive properties compared to the M-MDSC subset[298,307,312,378]. These factors could also be responsible for this study not seeing the same suppressive results as was observed for the non-

specific stimulations using anti-CD3 and anti-CD28 antibodies reported in previous work from our research group[308].

These findings confirmed the *in vitro* suppression of *M.tb*-specific T cells by MDSC. Considering that approximately 90% of the isolated MDSC in this study expressed the CD14 surface marker, supports our hypothesis that M-MDSC may be responsible for the suppressive functions observed both in Chapter 5 and Chapter 6. We propose that MDSC, most likely the M-MDSC subset, present as a promising candidate as a functional biomarker during active TB disease. Future studies should investigate the change in frequency of these cells over the course of anti-TB treatment as a potential treatment response biomarker candidate as well, since the reduction in MDSC numbers may be indicative of restored immunity.

During the phenotypic investigation of the MDSC population in PBMC, two additional surface markers, caveolin-1 and TLR4, were investigated in an attempt to further elucidate their phenotype. In addition to their surface expression, the presence of the two markers in question support a novel hypothesis in which we propose that TLR4 signaling mediates the activation of caveolin-mediated endocytosis of bacteria recognized through TLR4, which may facilitate pathogen uptake into MDSC while bypassing conventional methods. Functionally, TLR4 plays a role in MDSC-mediated downregulation of CD62L on the surface of activated T cells after binding to the alarmin High Mobility Group Box Protein 1 (HMGB1) which further supported its inclusion in our investigations. Since neither marker's expression has been investigated on the surface of MDSC, the confirmation of their expression by flow cytometry has provided a potentially novel functional relationship which should be researched further. While the differences in expression of these two markers was not significant between MDSC and control monocyte populations, the finding is still very important as the presence of this surface protein could have mechanistic research implications should MDSC prove to serve as a protective reservoir for *M.tb*. Future studies will need to be conducted in order to elucidate the functional significance of these markers, as well as the proximity of these markers to one another to determine if crosslinking and subsequent signaling via these markers would be possible. Such studies could potentially investigate the changes in suppressive potential of MDSC in which Cav-1 or TLR4, or both, have been inhibited or knocked-out. Confocal microscopy would be an appropriate tool for investigating the co-expression and/or co-localization of the two markers, particularly in an *in vitro M.tb* infection model, in order to investigate our alternative hypothesis which suggests that *M.tb* could be internalized in MDSC via TLR4-activated, caveolin-mediated endocytosis.

In conclusion, this dissertation has investigated biomarker candidates for multiple phases of the path to the successful cure of active TB disease. The importance of basic translational research is paramount in the field of TB owing to the growing incidence of drug resistant- and multi-drug resistant TB. The need for improved early case-detection rates, shortened time to treatment initiation and shortened treatment regimens will surely help overcome the issue of poor treatment adherence which ultimately leads to the development of drug resistance as well as the heightened transmission thereof. As

mentioned previously, the diagnostic biosignature candidate developed in this dissertation is already being developed further for use in a multi-biomarker biosignature lateral flow device for use at the point-of-care. This dissertation also validated the biosignature candidate in an HIV co-infection and *Ascaris lumbricoides* co-infection setting, confirming its robust nature and highlighting its appropriateness for a diagnostic biosignature in high-burden settings. We also identified two biomarker candidates to be investigated further for use as indicators of treatment response. Should such investigations be successful, efforts could turn to the development of clinical tools capable of indicating individual responses to treatment, either for the shortening of treatment or the conversion to alternative treatment strategies for improved patient outcome. Finally, our investigations lead to the discovery of a potential functional biomarker candidate, MDSC, which could also be translated into a biomarker of treatment response following further investigations. Biomarkers are important aspects in our attempts to identify correlates of risk and protection, and as such are valuable components of TB research. Continued biomarker research promises to provide us with the means to lower disease burden and improve the outcome of sick patients, which is why we believe in this important research.

REFERENCE LIST

1. World Health Organization. *Global tuberculosis report 2018*. (2018).
2. Walzl, G., Ronacher, K., Hanekom, W., Scriba, T. J. & Zumla, A. Immunological biomarkers of tuberculosis. *Nat. Rev. Immunol.* **11**, 343–354 (2011).
3. Korb, V. C., Chuturgoon, A. A. & Moodley, D. Mycobacterium tuberculosis: Manipulator of Protective Immunity. *Int. J. Mol. Sci.* **17**, 131 (2016).
4. Dheda, K., Barry, C. E. & Maartens, G. Tuberculosis. *The Lancet* **387**, 1211–1226 (2016).
5. Nunes-Alves, C. *et al.* In search of a new paradigm for protective immunity to TB. *Nat. Rev. Microbiol.* **12**, 289–299 (2014).
6. Harding, C. V. & Boom, W. H. Regulation of antigen presentation by Mycobacterium tuberculosis: a role for Toll-like receptors. *Nat. Rev. Microbiol.* **8**, 296–307 (2010).
7. O'Garra, A. *et al.* The Immune Response in Tuberculosis. *Annu. Rev. Immunol.* **31**, 475–527 (2013).
8. Pai, M. *et al.* Tuberculosis. *Nat. Rev. Dis. Primer* **2**, 16076 (2016).
9. Sia, J. K. *et al.* Innate Immune Defenses in Human Tuberculosis: An Overview of the Interactions between Mycobacterium tuberculosis and Innate Immune Cells, Innate Immune Defenses in Human Tuberculosis: An Overview of the Interactions between Mycobacterium tuberculosis and Innate Immune Cells. *J. Immunol. Res. J. Immunol. Res.* **2015**, **2015**, e747543 (2015).
10. Turvey, S. E. & Broide, D. H. Innate immunity. *J. Allergy Clin. Immunol.* **125**, S24-32 (2010).
11. Kawai, T. & Akira, S. TLR signaling. *Cell Death Differ.* **13**, 816–825 (2006).
12. Chaplin, D. D. Overview of the immune response. *J. Allergy Clin. Immunol.* **125**, S3-23 (2010).
13. Kleinnijenhuis, J., Oosting, M., Joosten, L. A. B., Netea, M. G. & Van Crevel, R. Innate Immune Recognition of *Mycobacterium tuberculosis*. *Clin. Dev. Immunol.* **2011**, 1–12 (2011).
14. Dorhoi, A. & Kaufmann, S. H. E. Tumor necrosis factor alpha in mycobacterial infection. *Semin. Immunol.* **26**, 203–209 (2014).
15. Fortune, S. M. *et al.* Mycobacterium tuberculosis Inhibits Macrophage Responses to IFN-γ through Myeloid Differentiation Factor 88-Dependent and -Independent Mechanisms. *J. Immunol.* **172**, 6272–6280 (2004).

16. Khan, N., Vidyarthi, A., Javed, S. & Agrewala, J. N. Innate Immunity Holding the Flanks until Reinforced by Adaptive Immunity against Mycobacterium tuberculosis Infection. *Front. Microbiol.* **7**, (2016).
17. Leliefeld, P. H., Koenderman, L. & Pillay, J. How neutrophils shape adaptive immune responses. *Front. Immunol.* **6**, (2015).
18. Verrall, A. J., G. Netea, M., Alisjahbana, B., Hill, P. C. & van Crevel, R. Early clearance of Mycobacterium tuberculosis: a new frontier in prevention. *Immunology* **141**, 506–513 (2014).
19. Orme, I. M., Robinson, R. T. & Cooper, A. M. The balance between protective and pathogenic immune responses in the TB-infected lung. *Nat. Immunol.* **16**, 57–63 (2014).
20. Bermudez, L. E., Wu, M. & Young, L. S. Interleukin-12-stimulated natural killer cells can activate human macrophages to inhibit growth of Mycobacterium avium. *Infect. Immun.* **63**, 4099–4104 (1995).
21. Allen, M. *et al.* Mechanisms of Control of Mycobacterium tuberculosis by NK Cells: Role of Glutathione. *Front. Immunol.* **6**, 508 (2015).
22. Okada, S., Li, Q., Whitin, J. C., Clayberger, C. & Krensky, A. M. Intracellular mediators of granulysin-induced cell death. *J. Immunol. Baltim. Md 1950* **171**, 2556–2562 (2003).
23. Kuwano, Y. *et al.* Interferon-gamma activates transcription of NADPH oxidase 1 gene and upregulates production of superoxide anion by human large intestinal epithelial cells. *Am. J. Physiol. Cell Physiol.* **290**, C433-443 (2006).
24. Roy Chowdhury, R. *et al.* A multi-cohort study of the immune factors associated with M. tuberculosis infection outcomes. *Nature* **560**, 644–648 (2018).
25. Kee, S.-J. *et al.* Dysfunction of Natural Killer T Cells in Patients with Active Mycobacterium tuberculosis Infection. *Infect. Immun.* **80**, 2100–2108 (2012).
26. Godfrey, D. I., Uldrich, A. P., McCluskey, J., Rossjohn, J. & Moody, D. B. The burgeoning family of unconventional T cells. *Nat. Immunol.* **16**, 1114–1123 (2015).
27. Arora, P., Foster, E. L. & Porcelli, S. A. CD1d and Natural Killer T Cells in Immunity to Mycobacterium tuberculosis in *The New Paradigm of Immunity to Tuberculosis* 199–223 (2013). doi:10.1007/978-1-4614-6111-1_11
28. Slauenwhite, D. & Johnston, B. Regulation of NKT Cell Localization in Homeostasis and Infection. *Front. Immunol.* **6**, (2015).

29. Shipp, C., Speigl, L., Janssen, N., Martens, A. & Pawelec, G. A clinical and biological perspective of human myeloid-derived suppressor cells in cancer. *Cell. Mol. Life Sci.* (2016). doi:10.1007/s00018-016-2278-y

30. El Daker, S. *et al.* Granulocytic Myeloid Derived Suppressor Cells Expansion during Active Pulmonary Tuberculosis Is Associated with High Nitric Oxide Plasma Level. *PLoS ONE* **10**, (2015).

31. Kolahian, S. *et al.* The emerging role of myeloid-derived suppressor cells in lung diseases. *Eur. Respir. J.* **47**, 967–977 (2016).

32. Alicea-Torres, K. & Gabrilovich, D. I. Biology of Myeloid-Derived Suppressor Cells. in *Oncoimmunology*, 181–197 (2018). doi:10.1007/978-3-319-62431-0_10

33. Bunt, S. K., Sinha, P., Clements, V. K., Leips, J. & Ostrand-Rosenberg, S. Inflammation induces myeloid-derived suppressor cells that facilitate tumor progression. *J. Immunol. Baltim. Md 1950* **176**, 284–290 (2006).

34. Trikha, P. & Carson III, W. E. Signaling pathways involved in MDSC regulation. *Biochim. Biophys. Acta BBA - Rev. Cancer* **1846**, 55–65 (2014).

35. Knaul, J. K. *et al.* Lung-Residing Myeloid-derived Suppressors Display Dual Functionality in Murine Pulmonary Tuberculosis. *Am. J. Respir. Crit. Care Med.* **190**, 1053–1066 (2014).

36. Siddiqui, S. *et al.* Tuberculosis specific responses following therapy for TB: Impact of HIV co-infection. *Clin. Immunol.* **159**, 1–12 (2015).

37. Adekambi, T. *et al.* Biomarkers on patient T cells diagnose active tuberculosis and monitor treatment response. *J. Clin. Invest.* **125**, 1827 (2015).

38. Hickman, S. P., Chan, J. & Salgame, P. Mycobacterium tuberculosis Induces Differential Cytokine Production from Dendritic Cells and Macrophages with Divergent Effects on Naive T Cell Polarization. *J. Immunol.* **168**, 4636–4642 (2002).

39. D'Elios, M. M., Benagiano, M., Della Bella, C. & Amedei, A. T-cell response to bacterial agents. *J. Infect. Dev. Ctries.* **5**, 640–645 (2011).

40. Bonilla, F. A. & Oettgen, H. C. Adaptive immunity. *J. Allergy Clin. Immunol.* **125**, S33–S40 (2010).

41. da Silva, M. V. *et al.* Complexity and Controversies over the Cytokine Profiles of T Helper Cell Subpopulations in Tuberculosis, Complexity and Controversies over the Cytokine Profiles of T Helper Cell Subpopulations in Tuberculosis. *J. Immunol. Res. J. Immunol. Res.* e639107 (2015).

42. Korn, T., Bettelli, E., Oukka, M. & Kuchroo, V. K. IL-17 and Th17 Cells. *Annu. Rev. Immunol.* **27**, 485–517 (2009).

43. Iwakura, Y. & Ishigame, H. The IL-23/IL-17 axis in inflammation. *J. Clin. Invest.* **116**, 1218–1222 (2006).

44. Gopal, R. *et al.* Interleukin-23 dependent IL-17 drives Th1 responses following Mycobacterium bovis BCG vaccination. *Eur. J. Immunol.* **42**, 364–373 (2012).

45. Gallegos, A. M. *et al.* A Gamma Interferon Independent Mechanism of CD4 T Cell Mediated Control of M. tuberculosis Infection in vivo. *PLOS Pathog* **7**, e1002052 (2011).

46. Wozniak, T. M., Saunders, B. M., Ryan, A. A. & Britton, W. J. Mycobacterium bovis BCG-Specific Th17 Cells Confer Partial Protection against Mycobacterium tuberculosis Infection in the Absence of Gamma Interferon. *Infect. Immun.* **78**, 4187–4194 (2010).

47. Jasenosky, L. D., Scriba, T. J., Hanekom, W. A. & Goldfeld, A. E. T cells and adaptive immunity to Mycobacterium tuberculosis in humans. *Immunol. Rev.* **264**, 74–87 (2015).

48. Caccamo, N. *et al.* Analysis of Mycobacterium tuberculosis-Specific CD8 T-Cells in Patients with Active Tuberculosis and in Individuals with Latent Infection. *PLoS ONE* **4**, (2009).

49. Kozakiewicz, L., Phuah, J., Flynn, J. & Chan, J. The Role of B Cells and Humoral Immunity in Mycobacterium tuberculosis Infection. *Adv. Exp. Med. Biol.* **783**, 225–250 (2013).

50. Maglione, P. J. & Chan, J. How B cells Shape the Immune Response against Mycobacterium tuberculosis. *Eur. J. Immunol.* **39**, 676–686 (2009).

51. Kumar, S. K., Singh, P. & Sinha, S. Naturally produced opsonizing antibodies restrict the survival of Mycobacterium tuberculosis in human macrophages by augmenting phagosome maturation. *Open Biol.* **5**, 150171 (2015).

52. Tebruegge, M. *et al.* Mycobacteria-Specific Cytokine Responses Detect Tuberculosis Infection and Distinguish Latent from Active Tuberculosis. *Am. J. Respir. Crit. Care Med.* **192**, 485–499 (2015).

53. Phalane, K. G. *et al.* Differential Expression of Host Biomarkers in Saliva and Serum Samples from Individuals with Suspected Pulmonary Tuberculosis. *Mediators Inflamm.* **2013**, 1–10 (2013).

54. McNerney, R. & Daley, P. Towards a point-of-care test for active tuberculosis: obstacles and opportunities. *Nat. Rev. Microbiol.* **9**, 204–213 (2011).

55. Schito, M. *et al.* Perspectives on Advances in Tuberculosis Diagnostics, Drugs, and Vaccines. *Clin. Infect. Dis. Off. Publ. Infect. Dis. Soc. Am.* **61 Suppl 3**, S102-118 (2015).

56. Peeling, R. W. & McNerney, R. Emerging technologies in point-of-care molecular diagnostics for resource-limited settings. *Expert Rev. Mol. Diagn.* **14**, 525–534 (2014).

57. Chegou, N. N. *et al.* Tuberculosis assays: past, present and future. *Expert Rev. Anti Infect. Ther.* **9**, 457–469 (2011).

58. World Health Organization. Global tuberculosis report 2015. (2015).

59. Singhal, R. & Myneedu, V. P. Microscopy as a diagnostic tool in pulmonary tuberculosis. *Int. J. Mycobacteriology* **4**, 1–6 (2015).

60. Van Zyl-Smit, R. N. *et al.* Comparison of Quantitative Techniques including Xpert MTB/RIF to Evaluate Mycobacterial Burden. *PLOS ONE* **6**, e28815 (2011).

61. Cruciani, M. *et al.* Meta-Analysis of BACTEC MGIT 960 and BACTEC 460 TB, with or without Solid Media, for Detection of Mycobacteria. *J. Clin. Microbiol.* **42**, 2321–2325 (2004).

62. Kroidl, I. *et al.* Performance of urine lipoarabinomannan assays for paediatric tuberculosis in Tanzania. *Eur. Respir. J.* **46**, 761–770 (2015).

63. Baumann, R. *et al.* Serologic diagnosis of tuberculosis by combining Ig classes against selected mycobacterial targets. *J. Infect.* **69**, 581–589 (2014).

64. Steingart, K. R. *et al.* Xpert® Mtb/Rif assay for pulmonary tuberculosis and rifampicin resistance in adults. *Cochrane Database Syst. Rev.* 1–131 (2013). doi:10.1002/14651858.CD009593.pub2

65. Kirwan, D. E., Cárdenas, M. K. & Gilman, R. H. Rapid Implementation of New TB Diagnostic Tests: Is It Too Soon for a Global Roll-Out of Xpert MTB/RIF? *Am. J. Trop. Med. Hyg.* **87**, 197–201 (2012).

66. Helb, D. *et al.* Rapid Detection of Mycobacterium tuberculosis and Rifampin Resistance by Use of On-Demand, Near-Patient Technology. *J. Clin. Microbiol.* **48**, 229–237 (2010).

67. Aggarwal, A. N., Agarwal, R., Gupta, D., Dhooria, S. & Behera, D. Interferon Gamma Release Assays for Diagnosis of Pleural Tuberculosis: a Systematic Review and Meta-Analysis. *J. Clin. Microbiol.* **53**, 2451–2459 (2015).

68. Trébucq, A. *et al.* Xpert® MTB/RIF for national tuberculosis programmes in low-income countries: when, where and how? *Int. J. Tuberc. Lung Dis.* **15**, 1567–1572 (2011).

69. Skoura, E., Zumla, A. & Bomanji, J. Imaging in tuberculosis. *Int. J. Infect. Dis.* **32**, 87–93 (2015).

70. Simsek, H. *et al.* Comparison of tuberculin skin testing and T-SPOT.TB for diagnosis of latent and active tuberculosis. *Jpn. J. Infect. Dis.* **63**, 99–102 (2010).

71. Essone, P. N. *et al.* Host cytokine responses induced after overnight stimulation with novel M. tuberculosis infection phase-dependent antigens show promise as diagnostic candidates for TB disease. *PloS One* **9**, (2014).

72. Chegou, N. N. *et al.* Potential of Host Markers Produced by Infection Phase-Dependent Antigen-Stimulated Cells for the Diagnosis of Tuberculosis in a Highly Endemic Area. *PLoS ONE* **7**, e38501 (2012).

73. Chegou, N. N. *et al.* Potential of novel Mycobacterium tuberculosis infection phase-dependent antigens in the diagnosis of TB disease in a high burden setting. *BMC Infect. Dis.* **12**, 1 (2012).

74. Cohn, D. L. The Effect of BCG Vaccination on Tuberculin Skin Testing. *Am. J. Respir. Crit. Care Med.* **164**, 915–916 (2001).

75. Burl, S. *et al.* The Tuberculin Skin Test (TST) Is Affected by Recent BCG Vaccination but Not by Exposure to Non-Tuberculosis Mycobacteria (NTM) during Early Life. *PLoS ONE* **5**, (2010).

76. Setiawati, L., Endaryanto, A., Kusumadewi, A. & Lestari, P. Effect of BCG vaccination and non-tuberculous Mycobacterium infection on interferon gamma specific assay and a tuberculin skin test among children with a tuberculosis contact in Surabaya, Indonesia. *Southeast Asian J. Trop. Med. Public Health* **42**, 1460–1468 (2011).

77. Pfyffer, G. E. & Palicova, F. Mycobacterium: General Characteristics, Laboratory Detection, and Staining Procedures *. in *Manual of Clinical Microbiology, 10th Edition* (eds. Versalovic, J. et al.) 472–502 (American Society of Microbiology, 2011).

78. WHO | Policy guidance on drug-susceptibility testing (DST) of second-line antituberculosis drugs. *WHO* Available at: http://www.who.int/tb/publications/2008/whohtmtb_2008_392/en/. (Accessed: 15th June 2016)

79. Barnard, M. *et al.* The Diagnostic Performance of the GenoType MTBDRplus Version 2 Line Probe Assay Is Equivalent to That of the Xpert MTB/RIF Assay. *J. Clin. Microbiol.* **50**, 3712–3716 (2012).

80. Streicher, E. M. *et al.* Mycobacterium tuberculosis population structure determines the outcome of genetic based second-line drug resistance testing. *Antimicrob. Agents Chemother.* AAC.05905-11 (2012). doi:10.1128/AAC.05905-11

81. Viveiros, M. *et al.* Direct Application of the INNO-LiPA Rif.TB Line-Probe Assay for Rapid Identification of Mycobacterium tuberculosis Complex Strains and Detection of Rifampin

Resistance in 360 Smear-Positive Respiratory Specimens from an Area of High Incidence of Multidrug-Resistant Tuberculosis. *J. Clin. Microbiol.* **43**, 4880–4884 (2005).

82. World Health Organization. *Global tuberculosis report 2014*. (2014).
83. WHO. Treatment of Tuberculosis: guidelines for national programmes. *WHO* Available at: http://www.who.int/tb/publications/tb_treatmentguidelines/en/. (Accessed: 2nd June 2016)
84. Riou, C. *et al.* Effect of Standard Tuberculosis Treatment on Plasma Cytokine Levels in Patients with Active Pulmonary Tuberculosis. *PLoS ONE* **7**, (2012).
85. Cliff, J. M., Kaufmann, S. H., McShane, H., Helden, P. & O'Garra, A. The human immune response to tuberculosis and its treatment: a view from the blood. *Immunol. Rev.* **264**, 88–102 (2015).
86. Cliff, J. M. *et al.* Distinct Phases of Blood Gene Expression Pattern Through Tuberculosis Treatment Reflect Modulation of the Humoral Immune Response. *J. Infect. Dis.* **207**, 18–29 (2013).
87. Walzl, G., Ronacher, K., Djoba Siawaya, J. F. & Dockrell, H. M. Biomarkers for TB treatment response: Challenges and future strategies. *J. Infect.* **57**, 103–109 (2008).
88. Wallis, R. S. *et al.* Tuberculosis biomarkers discovery: developments, needs, and challenges. *Lancet Infect. Dis.* **13**, 362–372 (2013).
89. Casey, R. *et al.* Enumeration of Functional T-Cell Subsets by Fluorescence-Immunospot Defines Signatures of Pathogen Burden in Tuberculosis. *PLoS ONE* **5**, e15619 (2010).
90. Doherty, M., Wallis, R. S. & Zumla, A. Biomarkers for tuberculosis disease status and diagnosis: *Curr. Opin. Pulm. Med.* **15**, 181–187 (2009).
91. Sutherland, J. S. *et al.* Differential gene expression of activating Fcγ receptor classifies active tuberculosis regardless of human immunodeficiency virus status or ethnicity. *Clin. Microbiol. Infect.* **20**, O230–O238 (2014).
92. Maertzdorf, J. *et al.* Human gene expression profiles of susceptibility and resistance in tuberculosis. *Genes Immun.* **12**, 15–22 (2011).
93. Veenstra, H. *et al.* Changes in leucocyte and lymphocyte subsets during tuberculosis treatment; prominence of CD3dimCD56+ natural killer T cells in fast treatment responders. *Clin. Exp. Immunol.* **145**, 252–260 (2006).
94. Wallis, R. S. *et al.* Biomarkers and diagnostics for tuberculosis: progress, needs, and translation into practice. *The Lancet* **375**, 1920–1937 (2010).

95. Kaufmann, D. E. *et al.* Upregulation of CTLA-4 by HIV-specific CD4+ T cells correlates with disease progression and defines a reversible immune dysfunction. *Nat. Immunol.* **8**, 1246–1254 (2007).

96. Jones, R. B. *et al.* Tim-3 expression defines a novel population of dysfunctional T cells with highly elevated frequencies in progressive HIV-1 infection. *J. Exp. Med.* **205**, 2763–2779 (2008).

97. Jayakumar, A. *et al.* Serum biomarkers of treatment response within a randomized clinical trial for pulmonary tuberculosis. *Tuberculosis* **95**, 415–420 (2015).

98. Nahid, P. *et al.* Aptamer-based proteomic signature of intensive phase treatment response in pulmonary tuberculosis. *Tuberculosis* **94**, 187–196 (2014).

99. Djoba Siawaya, J. F., Beyers, N., van Helden, P. & Walzl, G. Differential cytokine secretion and early treatment response in patients with pulmonary tuberculosis. *Clin. Exp. Immunol.* **156**, 69–77 (2009).

100. Sloot, R. *et al.* Biomarkers Can Identify Pulmonary Tuberculosis in HIV-infected Drug Users Months Prior to Clinical Diagnosis. *EBioMedicine* **2**, 172–179 (2015).

101. Zak, D. E. *et al.* A blood RNA signature for tuberculosis disease risk: a prospective cohort study. *The Lancet* (2016). doi:10.1016/S0140-6736(15)01316-1

102. Suliman, S. *et al.* Four-Gene Pan-African Blood Signature Predicts Progression to Tuberculosis. *Am. J. Respir. Crit. Care Med.* **197**, 1198–1208 (2018).

103. Tucci, P., González-Sapienza, G. & Marin, M. Pathogen-derived biomarkers for active tuberculosis diagnosis. *Front. Microbiol.* **5**, (2014).

104. John, S. H., Kenneth, J. & Gandhe, A. S. Host biomarkers of clinical relevance in tuberculosis: review of gene and protein expression studies. *Biomarkers* **17**, 1–8 (2012).

105. Oni, T. *et al.* Patterns of HIV, TB, and non-communicable disease multi-morbidity in peri-urban South Africa- a cross sectional study. *BMC Infect. Dis.* **15**, 20 (2015).

106. Bates, M., Marais, B. J. & Zumla, A. Tuberculosis Comorbidity with Communicable and Noncommunicable Diseases. *Cold Spring Harb. Perspect. Med.* **5**, a017889 (2015).

107. Amare, B. *et al.* Quadruple Burden of HIV/AIDS, Tuberculosis, Chronic Intestinal Parasitoses, and Multiple Micronutrient Deficiency in Ethiopia: A Summary of Available Findings, Quadruple Burden of HIV/AIDS, Tuberculosis, Chronic Intestinal Parasitoses, and Multiple Micronutrient Deficiency in Ethiopia: A Summary of Available Findings. *BioMed Res. Int. BioMed Res. Int.*, e598605 (2015).

108. Diedrich, C. R. & Flynn, J. L. HIV-1/Mycobacterium tuberculosis Coinfection Immunology: How Does HIV-1 Exacerbate Tuberculosis? *Infect. Immun.* **79**, 1407–1417 (2011).

109. Montales, M. T., Beebe, A., Chaudhury, A. & Patil, N. Mycobacterium tuberculosis infection in a HIV-positive patient. *Respir. Med. Case Rep.* **16**, 160–162 (2015).

110. Mendonça, M. *et al.* Deficient in vitro anti-mycobacterial immunity despite successful long-term highly active antiretroviral therapy in HIV-infected patients with past history of tuberculosis infection or disease. *Clin. Immunol.* **125**, 60–66 (2007).

111. Oni, T. *et al.* Enhanced diagnosis of HIV-1-associated tuberculosis by relating T-SPOT.TB and CD4 counts. *Eur. Respir. J.* **36**, 594–600 (2010).

112. Rangaka, M. X. *et al.* Clinical, Immunological, and Epidemiological Importance of Antituberculosis T Cell Responses in HIV-Infected Africans. *Clin. Infect. Dis.* **44**, 1639–1646 (2007).

113. Abate, E. *et al.* Asymptomatic Helminth Infection in Active Tuberculosis Is Associated with Increased Regulatory and Th-2 Responses and a Lower Sputum Smear Positivity. *PLOS Negl Trop Dis* **9**, e0003994 (2015).

114. Crompton, D. W. T. & Nesheim, M. C. Nutritional impact of intestinal helminthiasis during the human life cycle. *Annu. Rev. Nutr.* **22**, 35–59 (2002).

115. du Plessis, N. *et al.* Acute helminth infection enhances early macrophage mediated control of mycobacterial infection. *Mucosal Immunol.* **6**, 931–941 (2013).

116. Chatterjee, S. & Nutman, T. B. Helminth-Induced Immune Regulation: Implications for Immune Responses to Tuberculosis. *PLoS Pathog.* **11**, (2015).

117. Hübner, M. P. *et al.* Chronic Helminth Infection Does Not Exacerbate Mycobacterium tuberculosis Infection. *PLOS Negl Trop Dis* **6**, e1970 (2012).

118. George, P. J. *et al.* Helminth Infections Coincident with Active Pulmonary Tuberculosis Inhibit Mono- and Multifunctional CD4 + and CD8 + T Cell Responses in a Process Dependent on IL-10. *PLOS Pathog* **10**, e1004375 (2014).

119. Rafi, W., Ribeiro-Rodrigues, R., Ellner, J. J. & Salgame, P. 'Coinfection-helminthes and tuberculosis'. *Curr. Opin. HIV AIDS* **7**, 239–244 (2012).

120. De Groote, M. A. *et al.* Elucidating novel serum biomarkers associated with pulmonary tuberculosis treatment. *PLoS One* **8**, e61002 (2013).

121. Wang, C. *et al.* Screening and identification of five serum proteins as novel potential biomarkers for cured pulmonary tuberculosis. *Sci. Rep.* **5**, (2015).

122. Zhou, J. Early diagnosis of pulmonary tuberculosis using serum biomarkers. *PROTEOMICS* **15**, 6–7 (2015).

123. Gruys, E., Toussaint, M. J. M., Niewold, T. A. & Koopmans, S. J. Acute phase reaction and acute phase proteins. *J Zhejiang Univ Sci B* **6**, 1045–1056 (2005).

124. Jain, S., Gautam, V. & Naseem, S. Acute-phase proteins: As diagnostic tool. *J. Pharm. Bioallied Sci.* **3**, 118–127 (2011).

125. Chegou, N. N. *et al.* Diagnostic performance of a seven-marker serum protein biosignature for the diagnosis of active TB disease in African primary healthcare clinic attendees with signs and symptoms suggestive of TB. *Thorax* thoraxjnl-2015-207999 (2016). doi:10.1136/thoraxjnl-2015-207999

126. Ruopp, M. D., Perkins, N. J., Whitcomb, B. W. & Schisterman, E. F. Youden Index and Optimal Cut-Point Estimated from Observations Affected by a Lower Limit of Detection. *Biom. J. Biom. Z.* **50**, 419–430 (2008).

127. WHO | High-priority target product profiles for new tuberculosis diagnostics. *WHO* Available at: http://www.who.int/tb/publications/tpp_report/en/. (Accessed: 22nd June 2016)

128. Steingart, K. R. *et al.* Xpert® Mtb/Rif assay for pulmonary tuberculosis and rifampicin resistance in adults. *Cochrane Database Syst. Rev.* 1–166 (2014). doi:10.1002/14651858.CD009593.pub3

129. World Health Organization. Xpert MTB/RIF assay for the diagnosis of pulmonary and extrapulmonary TB in adults and children | Policy Update. (2013).

130. Lawn, S. D., Kerkhoff, A. D., Vogt, M. & Wood, R. Diagnostic and prognostic value of serum C-reactive protein for screening for HIV-associated tuberculosis. *Int. J. Tuberc. Lung Dis.* **17**, 636–643 (2013).

131. Skogmar, S. *et al.* Plasma Levels of Neopterin and C-Reactive Protein (CRP) in Tuberculosis (TB) with and without HIV Coinfection in Relation to CD4 Cell Count. *PLOS ONE* **10**, e0144292 (2015).

132. de Beer, F. C., Nel, A. E., Gie, R. P., Donald, P. R. & Strachan, A. F. Serum amyloid A protein and C-reactive protein levels in pulmonary tuberculosis: relationship to amyloidosis. *Thorax* **39**, 196–200 (1984).

133. Samaha, H. M. S., Elsaid, A. R., Elzehery, R. & Elhelaly, R. C-reactive protein and serum amyloid A levels in discriminating malignant from non-malignant pleural effusion. *Egypt. J. Chest Dis. Tuberc.* **64**, 887–892 (2015).

134. Bajaj, G., Rattan, A. & Ahmad, P. Prognostic value of 'C' reactive protein in tuberculosis. *Indian Pediatr.* **26**, 1010–1013 (1989).

135. Wilson, D., Badri, M. & Maartens, G. Performance of serum C-reactive protein as a screening test for smear-negative tuberculosis in an ambulatory high HIV prevalence population. *PloS One* **6**, e15248 (2011).

136. Yoon, C., Davis, J. L. & Cattamanchi, A. C-reactive protein and tuberculosis screening: a new trick for an old dog? *Int. J. Tuberc. Lung Dis. Off. J. Int. Union Tuberc. Lung Dis.* **17**, 1656 (2013).

137. Boehme, C. C. *et al.* Rapid molecular detection of tuberculosis and rifampin resistance. *N. Engl. J. Med.* **363**, 1005–1015 (2010).

138. Bapat, P. R. *et al.* Differential Levels of Alpha-2-Macroglobulin, Haptoglobin and Sero-Transferrin as Adjunct Markers for TB Diagnosis and Disease Progression in the Malnourished Tribal Population of Melghat, India. *PLOS ONE* **10**, e0133928 (2015).

139. Vandevyver, S., Dejager, L., Vandenbroucke, R. E. & Libert, C. An acute phase protein ready to go therapeutic for sepsis. *EMBO Mol. Med.* **6**, 2–3 (2014).

140. Dalli, J. *et al.* Microparticle alpha-2-macroglobulin enhances pro-resolving responses and promotes survival in sepsis. *EMBO Mol. Med.* **6**, 27–42 (2014).

141. Pawlowski, A., Jansson, M., Sköld, M., Rottenberg, M. E. & Källenius, G. Tuberculosis and HIV Co-Infection. *PLOS Pathog.* **8**, e1002464 (2012).

142. Coussens, A. K. *et al.* Ethnic Variation in Inflammatory Profile in Tuberculosis. *PLoS Pathog.* **9**, e1003468 (2013).

143. Cantwell, M. F., McKenna, M. T., McCray, E. & Onorato, I. M. Tuberculosis and race/ethnicity in the United States: impact of socioeconomic status. *Am. J. Respir. Crit. Care Med.* **157**, 1016–1020 (1998).

144. Chegou, N. N., Black, G. F., Kidd, M., Van Helden, P. D. & Walzl, G. Host markers in QuantiFERON supernatants differentiate active TB from latent TB infection: preliminary report. *BMC Pulm. Med.* **9**, 21 (2009).

145. Wei, J., Xiong, X.-F., Lin, Y.-H., Zheng, B.-X. & Cheng, D.-Y. Association between serum interleukin-6 concentrations and chronic obstructive pulmonary disease: a systematic review and meta-analysis. *PeerJ* **3**, e1199 (2015).

146. Pullan, R. L., Smith, J. L., Jasrasaria, R. & Brooker, S. J. Global numbers of infection and disease burden of soil transmitted helminth infections in 2010. *Parasit. Vectors* **7**, 37 (2014).

147. Karagiannis-Voules, D.-A. *et al.* Spatial and temporal distribution of soil-transmitted helminth infection in sub-Saharan Africa: a systematic review and geostatistical meta-analysis. *Lancet Infect. Dis.* **15**, 74–84 (2015).

148. Ajoge, H. O., Olonitola, S. O. & Smith, D. R. Soil-transmitted helminths are a serious but understudied health concern in South Africa, requiring immediate attention from the scientific community. *F1000Research* (2014). doi:10.12688/f1000research.4812.2

149. Organization, W. H. & others. Global health sector response to HIV, 2000-2015: focus on innovations in Africa: progress report. (2015).

150. REPoRTInG, H. I. V. Global UPDATE. (2014).

151. WHO | Soil-transmitted helminth infections. *WHO* Available at: http://www.who.int/mediacentre/factsheets/fs366/en/. (Accessed: 4th April 2016)

152. WHO | Water related diseases. *WHO* Available at: http://www.who.int/water_sanitation_health/diseases/ascariasis/en/. (Accessed: 4th April 2016)

153. Prevention, C.-C. for D. C. and. CDC - Ascariasis - Biology. Available at: https://www.cdc.gov/parasites/ascariasis/biology.html. (Accessed: 29th January 2018)

154. Babu, S. & Nutman, T. B. Helminth-tuberculosis co-infection: an immunologic perspective. *Trends Immunol.* **37**, 597–607 (2016).

155. Allen, J. E. & Maizels, R. M. Diversity and dialogue in immunity to helminths. *Nat. Rev. Immunol.* **11**, 375–388 (2011).

156. Cooper, P. J. *et al.* Environmental determinants of total IgE among school children living in the rural Tropics: importance of geohelminth infections and effect of anthelmintic treatment. *BMC Immunol.* **9**, 33 (2008).

157. Anuradha, R. *et al.* Anthelmintic Therapy Modifies the Systemic and Mycobacterial Antigen-Stimulated Cytokine Profile in Helminth-Latent Mycobacterium tuberculosis Coinfection. *Infect. Immun.* **85**, e00973-16 (2017).

158. Mishra, P. K., Palma, M., Bleich, D., Loke, P. & Gause, W. C. Systemic impact of intestinal helminth infections. *Mucosal Immunol.* (2014). doi:10.1038/mi.2014.23

159. Abate, E. *et al.* Effects of albendazole on the clinical outcome and immunological responses in helminth co-infected tuberculosis patients: a double blind randomised clinical trial. *Int. J. Parasitol.* **45**, 133–140 (2015).

160. Toulza, F., Tsang, L., Ottenhoff, T. H. M., Brown, M. & Dockrell, H. M. *Mycobacterium tuberculosis* -specific CD4 $^{+}$ T-cell response is increased, and Treg cells decreased, in anthelmintic-treated patients with latent TB: Immunity to infection. *Eur. J. Immunol.* **46**, 752–761 (2016).

161. George, P. J. *et al.* Coincident helminth infection modulates systemic inflammation and immune activation in active pulmonary tuberculosis. *PLoS Negl. Trop. Dis.* **8**, e3289 (2014).

162. Hotez, P. J. *et al.* The global burden of disease study 2010: interpretation and implications for the neglected tropical diseases. *PLoS Negl. Trop. Dis.* **8**, e2865 (2014).

163. Hotez, P. J. *et al.* Helminth infections: the great neglected tropical diseases. *J. Clin. Invest.* **118**, 1311–1321 (2008).

164. Lang, R. & Schick, J. Review: Impact of Helminth Infection on Antimycobacterial Immunity—A Focus on the Macrophage. *Front. Immunol.* **8**, (2017).

165. Abate, E. *et al.* The impact of asymptomatic helminth co-infection in patients with newly diagnosed tuberculosis in north-west Ethiopia. *PLoS One* **7**, e42901 (2012).

166. Bentwich, Z. *et al.* Can eradication of helminthic infections change the face of AIDS and tuberculosis? *Immunol. Today* **20**, 485–487 (1999).

167. Frantz, F. G. *et al.* Helminth coinfection does not affect therapeutic effect of a DNA vaccine in mice harboring tuberculosis. *PLoS Negl. Trop. Dis.* **4**, e700 (2010).

168. Hotez, P. J. & Kamath, A. Neglected tropical diseases in sub-Saharan Africa: review of their prevalence, distribution, and disease burden. *PLoS Negl. Trop. Dis.* **3**, e412 (2009).

169. South Africa. Available at: http://www.unaids.org/en/regionscountries/countries/southafrica. (Accessed: 6th December 2017)

170. WHO | PCT databank. *WHO* Available at: http://www.who.int/neglected_diseases/preventive_chemotherapy/sth/en/. (Accessed: 6th December 2017)

171. WHO | Tuberculosis country profiles. *WHO* Available at: http://www.who.int/tb/country/data/profiles/en/. (Accessed: 6th December 2017)

172. Yu, Z. *et al.* Differences between Human Plasma and Serum Metabolite Profiles. *PLoS ONE* **6**, e21230 (2011).

173. Xu, D. *et al.* Serum protein S100A9, SOD3, and MMP9 as new diagnostic biomarkers for pulmonary tuberculosis by iTRAQ-coupled two-dimensional LC-MS/MS. *PROTEOMICS* **15**, 58–67 (2015).

174. Jacobs, R. *et al.* Host biomarkers detected in saliva show promise as markers for the diagnosis of pulmonary tuberculosis disease and monitoring of the response to tuberculosis treatment. *Cytokine* **81**, 50–56 (2016).

175. Groote, M. A. D. *et al.* Discovery and Validation of a Six-Marker Serum Protein Signature for the Diagnosis of Active Pulmonary Tuberculosis. *J. Clin. Microbiol.* **55**, 3057–3071 (2017).

176. Shang, Z. *et al.* Serum Macrophage Migration Inhibitory Factor as a Biomarker of Active Pulmonary Tuberculosis. *Ann. Lab. Med.* **38**, 9–16 (2018).

177. Jiang, T.-T. *et al.* Serum amyloid A, protein Z, and C4b-binding protein β chain as new potential biomarkers for pulmonary tuberculosis. *PLOS ONE* **12**, e0173304 (2017).

178. du Plessis, N. *et al.* Increased Frequency of Myeloid-derived Suppressor Cells during Active Tuberculosis and after Recent *Mycobacterium tuberculosis* Infection Suppresses T-Cell Function. *Am. J. Respir. Crit. Care Med.* **188**, 724–732 (2013).

179. Van Ginderachter, J. A., Beschin, A., De Baetselier, P. & Raes, G. Myeloid-derived suppressor cells in parasitic infections. *Eur. J. Immunol.* **40**, 2976–2985 (2010).

180. Saleem, S. J. *et al.* Cutting edge: mast cells critically augment myeloid-derived suppressor cell activity. *J. Immunol. Baltim. Md 1950* **189**, 511–515 (2012).

181. Gabrilovich, D. I. & Nagaraj, S. Myeloid-derived suppressor cells as regulators of the immune system. *Nat. Rev. Immunol.* **9**, 162–174 (2009).

182. Chegou, N. N., Heyckendorf, J., Walzl, G., Lange, C. & Ruhwald, M. Beyond the IFN-γ horizon: biomarkers for immunodiagnosis of infection with Mycobacterium tuberculosis. *Eur. Respir. J.* **43**, 1472–1486 (2014).

183. Anuradha, R. *et al.* Modulation of Mycobacterium tuberculosis-specific humoral immune responses is associated with Strongyloides stercoralis co-infection. *PLoS Negl. Trop. Dis.* **11**, e0005569 (2017).

184. Gall, S. *et al.* Associations between selective attention and soil-transmitted helminth infections, socioeconomic status, and physical fitness in disadvantaged children in Port Elizabeth, South Africa: An observational study. *PLoS Negl. Trop. Dis.* **11**, e0005573 (2017).

185. Bopda, J. *et al.* Prevalence and intensity of human soil transmitted helminth infections in the Akonolinga health district (Centre Region, Cameroon): Are adult hosts contributing in the persistence of the transmission? *Parasite Epidemiol. Control* **1**, 199–204 (2016).

186. Müller, I. *et al.* Intestinal parasites, growth and physical fitness of schoolchildren in poor neighbourhoods of Port Elizabeth, South Africa: a cross-sectional survey. *Parasit. Vectors* **9**, 488 (2016).

187. Schüle, S. A. *et al.* Ascaris lumbricoides Infection and Its Relation to Environmental Factors in the Mbeya Region of Tanzania, a Cross-Sectional, Population-Based Study. *PLOS ONE* **9**, e92032 (2014).

188. Fitzsimmons, C. M., Falcone, F. H. & Dunne, D. W. Helminth allergens, parasite-specific IgE, and its protective role in human immunity. *Front. Immunol.* **5**, (2014).

189. Leonardi-Bee, J., Pritchard, D. & Britton, J. Asthma and Current Intestinal Parasite Infection. *Am. J. Respir. Crit. Care Med.* **174**, 514–523 (2006).

190. Elias, D. *et al.* Effect of deworming on human T cell responses to mycobacterial antigens in helminth-exposed individuals before and after bacille calmette–guérin (BCG) vaccination. *Clin. Exp. Immunol.* **123**, 219–225 (2001).

191. Guadalupe, I. *et al.* Evidence for in utero sensitization to Ascaris lumbricoides in newborns of mothers with ascariasis. *J. Infect. Dis.* **199**, 1846–1850 (2009).

192. Mehta, R. S. *et al.* Maternal Geohelminth Infections Are Associated with an Increased Susceptibility to Geohelminth Infection in Children: A Case-Control Study. *PLoS Negl. Trop. Dis.* **6**, e1753 (2012).

193. Chachage, M. *et al.* Helminth-Associated Systemic Immune Activation and HIV Co-receptor Expression: Response to Albendazole/Praziquantel Treatment. *PLoS Negl. Trop. Dis.* **8**, e2755 (2014).

194. Hagel, I. *et al.* Ascaris reinfection of slum children: relation with the IgE response. *Clin. Exp. Immunol.* **94**, 80–83 (1993).

195. Pourriez, J. A three years follow-up of total serum IgE levels in three patients treated for strongyloidiasis. *Parasite* **8**, 359–362 (2001).

196. Iancovici Kidon, M. *et al.* Serum immunoglobulin E levels in Israeli-Ethiopian children: environment and genetics. *Isr. Med. Assoc. J. IMAJ* **7**, 799–802 (2005).

197. Goletti, D., Petruccioli, E., Joosten, S. A. & Ottenhoff, T. H. M. Tuberculosis Biomarkers: From Diagnosis to Protection. *Infect. Dis. Rep.* **8**, (2016).

198. Abbas, A. K., Lichtman, A. H. & Pillai, S. *Cellular and molecular immunology*. (Elsevier, Saunders, 2015).

199. O'Reilly, S., Ciechomska, M., Cant, R., Hügle, T. & van Laar, J. M. Interleukin-6, its role in fibrosing conditions. *Cytokine Growth Factor Rev.* **23**, 99–107 (2012).

200. Scheller, J., Chalaris, A., Schmidt-Arras, D. & Rose-John, S. The pro- and anti-inflammatory properties of the cytokine interleukin-6. *Biochim. Biophys. Acta* **1813**, 878–888 (2011).

201. Garbers, C. *et al.* Species specificity of ADAM10 and ADAM17 proteins in interleukin-6 (IL-6) trans-signaling and novel role of ADAM10 in inducible IL-6 receptor shedding. *J. Biol. Chem.* **286**, 14804–14811 (2011).

202. Wright, H. L., Cross, A. L., Edwards, S. W. & Moots, R. J. Effects of IL-6 and IL-6 blockade on neutrophil function in vitro and in vivo. *Rheumatology* **53**, 1321–1331 (2014).

203. Rincon, M. Interleukin-6: from an inflammatory marker to a target for inflammatory diseases. *Trends Immunol.* **33**, 571–577 (2012).

204. Gabay, C. Interleukin-6 and chronic inflammation. *Arthritis Res. Ther.* **8(2)**, 1–6 (2006).

205. DeLeo, F. R. Attractive shedding. *Blood* **110**, 1711–1712 (2007).

206. Van Snick, J. Interleukin-6: an overview. *Annu. Rev. Immunol.* **8**, 253–278 (1990).

207. Okada, M. *et al.* Anti-IL-6 Receptor Antibody Causes Less Promotion of Tuberculosis Infection than Anti-TNF-α Antibody in Mice. *Clin. Dev. Immunol.* **2011**, (2011).

208. Sodenkamp, J. *et al.* Therapeutic targeting of interleukin-6 trans-signaling does not affect the outcome of experimental tuberculosis. *Immunobiology* **217**, 996–1004 (2012).

209. Nagabhushanam, V. *et al.* Innate Inhibition of Adaptive Immunity: Mycobacterium tuberculosis-Induced IL-6 Inhibits Macrophage Responses to IFN-γ. *J. Immunol.* **171**, 4750–4757 (2003).

210. Kishimoto, T. IL-6: from its discovery to clinical applications. *Int. Immunol.* **22**, 347–352 (2010).

211. Nish, S. A. *et al.* T cell-intrinsic role of IL-6 signaling in primary and memory responses. *eLife* **3**, e01949 (2014).

212. Dienz, O. & Rincon, M. The effects of IL-6 on CD4 T cell responses. *Clin. Immunol.* **130**, 27–33 (2009).

213. Kishimoto, T. Interleukin-6: discovery of a pleiotropic cytokine. *Arthritis Res. Ther.* **8(2)**, 1–6 (2006).

214. Naderi, M., Hashemi, M. & Moradi, N. Association of VNTR polymorphism of tumor necrosis factor receptor 2 (TNFRSF1B) with pulmonary tuberculosis. *Mol. Biol. Res. Commun.* **6**, 23–26 (2017).

215. Mootoo, A., Stylianou, E., Arias, M. A. & Reljic, R. TNF-α in Tuberculosis: A Cytokine with a Split Personality. *Inflamm. Allergy-Drug Targets Former. Curr. Drug Targets-Inflamm. Allergy* **8**, 53–62 (2009).

216. Domingo-Gonzalez, R., Prince, O., Cooper, A. & Khader, S. Cytokines and Chemokines in Mycobacterium tuberculosis infection. *Microbiol. Spectr.* **4**, (2016).

217. Quesniaux, V. F. J. *et al.* TNF in Host Resistance to Tuberculosis Infection. in *Current Directions in Autoimmunity* (eds. Kollias, G. & Sfikakis, P. P.) **11**, 157–179 (KARGER, 2010).

218. Waters, J. P., Pober, J. S. & Bradley, J. R. Tumour necrosis factor in infectious disease. *J. Pathol.* **230**, 132–147 (2013).

219. Faustman, D. & Davis, M. TNF receptor 2 pathway: drug target for autoimmune diseases. *Nat. Rev. Drug Discov.* **9**, 482–493 (2010).

220. Bremer, E. & Bremer, E. Targeting of the Tumor Necrosis Factor Receptor Superfamily for Cancer Immunotherapy, Targeting of the Tumor Necrosis Factor Receptor Superfamily for Cancer Immunotherapy. *Int. Sch. Res. Not. Int. Sch. Res. Not.* **2013**, **2013**, e371854 (2013).

221. Yang, S., Liu, F., Wang, Q. J., Rosenberg, S. A. & Morgan, R. A. The Shedding of CD62L (L-Selectin) Regulates the Acquisition of Lytic Activity in Human Tumor Reactive T Lymphocytes. *PLOS ONE* **6**, e22560 (2011).

222. Schlub, T. E., Badovinac, V. P., Sabel, J. T., Harty, J. T. & Davenport, M. P. Predicting CD62L expression during the CD8+ T-cell response in vivo. *Immunol. Cell Biol.* **88**, 157–164 (2009).

223. Mahnke, K. *et al.* Down-Regulation of CD62L Shedding in T Cells by CD39 + Regulatory T Cells Leads to Defective Sensitization in Contact Hypersensitivity Reactions. *J. Invest. Dermatol.* **137**, 106–114 (2017).

224. Unsoeld, H. & Pircher, H. Complex Memory T-Cell Phenotypes Revealed by Coexpression of CD62L and CCR7. *J. Virol.* **79**, 4510–4513 (2005).

225. Wirth, T. C., Badovinac, V. P., Zhao, L., Dailey, M. O. & Harty, J. T. Differentiation of Central Memory CD8 T Cells Is Independent of CD62L-Mediated Trafficking to Lymph Nodes. *J. Immunol.* **182**, 6195–6206 (2009).

226. Corleis, B. *et al.* Escape of Mycobacterium tuberculosis from oxidative killing by neutrophils: Tubercle bacilli escape neutrophil killing. *Cell. Microbiol.* **14**, 1109–1121 (2012).

227. Borregaard, N. *et al.* Changes in subcellular localization and surface expression of L-selectin, alkaline phosphatase, and Mac-1 in human neutrophils during stimulation with inflammatory mediators. *J. Leukoc. Biol.* **56**, 80–87 (1994).

228. Jeong, Y. H. *et al.* Differentiation of Antigen-Specific T Cells with Limited Functional Capacity during Mycobacterium tuberculosis Infection. *Infect. Immun.* **82**, 132–139 (2014).

229. Mahnke, Y. D., Brodie, T. M., Sallusto, F., Roederer, M. & Lugli, E. The who's who of T-cell differentiation: Human memory T-cell subsets. *Eur. J. Immunol.* **43**, 2797–2809 (2013).

230. Sallusto, F., Lenig, D., Förster, R., Lipp, M. & Lanzavecchia, A. Two subsets of memory T lymphocytes with distinct homing potentials and effector functions. *Nature* **401**, 708–712 (1999).

231. Sanchez-Sanchez, N., Riol-Blanco, L. & Rodriguez-Fernandez, J. L. The Multiple Personalities of the Chemokine Receptor CCR7 in Dendritic Cells. *J. Immunol.* **176**, 5153–5159 (2006).

232. Kahnert, A. *et al.* Mycobacterium tuberculosis Triggers Formation of Lymphoid Structure in Murine Lungs. *J. Infect. Dis.* **195**, 46–54 (2007).

233. Nemeth, J. *et al.* Active tuberculosis is characterized by an antigen specific and strictly localized expansion of effector T cells at the site of infection: Immunity to infection. *Eur. J. Immunol.* **42**, 2844–2850 (2012).

234. Wingren, A. G. *et al.* T cell activation pathways: B7, LFA-3, and ICAM-1 shape unique T cell profiles. *Crit. Rev. Immunol.* **15**, 235–253 (1995).

235. El Menshawy, N., Eissa, M., Abdeen, H. M., Elkhamisy, E. M. & Joseph, N. CD58; leucocyte function adhesion-3 (LFA-3) could be used as a differentiating marker between immune and non-immune thyroid disorders. *Comp. Clin. Pathol.* **27**, 721–727 (2018).

236. Wang, J. H. *et al.* Structure of a heterophilic adhesion complex between the human CD2 and CD58 (LFA-3) counterreceptors. *Cell* **97**, 791–803 (1999).

237. Hanekom, W. A. *et al.* Mycobacterium tuberculosis Inhibits Maturation of Human Monocyte-Derived Dendritic Cells In Vitro. *J. Infect. Dis.* **188**, 257–266 (2003).

238. Henderson, R. A., Watkins, S. C. & Flynn, J. L. Activation of human dendritic cells following infection with Mycobacterium tuberculosis. *J. Immunol. Baltim. Md 1950* **159**, 635–643 (1997).

239. Dobos, K. M., Spotts, E. A., Quinn, F. D. & King, C. H. Necrosis of Lung Epithelial Cells during Infection with Mycobacterium tuberculosis Is Preceded by Cell Permeation. *Infect. Immun.* **68**, 6300–6310 (2000).

240. Fine-Coulson, K., Reaves, B. J., Karls, R. K. & Quinn, F. D. The role of lipid raft aggregation in the infection of type II pneumocytes by Mycobacterium tuberculosis. *PloS One* **7**, e45028 (2012).

241. Scordo, J. M., Knoell, D. L. & Torrelles, J. B. Alveolar Epithelial Cells in Mycobacterium tuberculosis Infection: Active Players or Innocent Bystanders? *J. Innate Immun.* **8**, 3–14 (2016).

242. Sato, K. *et al.* Type II Alveolar Cells Play Roles in Macrophage-Mediated Host Innate Resistance to Pulmonary Mycobacterial Infections by Producing Proinflammatory Cytokines. *J. Infect. Dis.* **185**, 1139–1147 (2002).

243. Bullens, D. M. A. *et al.* Effects of co-stimulation by CD58 on human T cell cytokine production: a selective cytokine pattern with induction of high IL-10 production. *Int. Immunol.* **13**, 181–191 (2001).

244. Leitner, J., Herndler-Brandstetter, D., Zlabinger, G. J., Grubeck-Loebenstein, B. & Steinberger, P. CD58/CD2 Is the Primary Costimulatory Pathway in Human CD28 $^-$ CD8 $^+$ T Cells. *J. Immunol.* **195**, 477–487 (2015).

245. Scholz, G. *et al.* Modulation of mTOR Signalling Triggers the Formation of Stem Cell-like Memory T Cells. *EBioMedicine* **4**, 50–61 (2016).

246. Gattinoni, L. *et al.* A human memory T cell subset with stem cell-like properties. *Nat. Med.* **17**, 1290–1297 (2011).

247. Terstappen, L. W. M. M., Nguyen, M., Lazarus, H. M. & Medof, M. E. Expression of the DAF (CD55) and CD59 antigens during normal hematopoietic cell differentiation. *J. Leukoc. Biol.* **52**, 652–660 (1992).

248. Fuertes Marraco, S. A. *et al.* Long-lasting stem cell–like memory CD8+ T cells with a naïve-like profile upon yellow fever vaccination. *Sci. Transl. Med.* **7**, 282ra48-282ra48 (2015).

249. Stansfield, B. K. & Ingram, D. A. Clinical significance of monocyte heterogeneity. *Clin. Transl. Med.* **4**, (2015).

250. Idzkowska, E. *et al.* The Role of Different Monocyte Subsets in the Pathogenesis of Atherosclerosis and Acute Coronary Syndromes. *Scand. J. Immunol.* **82**, 163–173 (2015).

251. Yang, J., Zhang, L., Yu, C., Yang, X.-F. & Wang, H. Monocyte and macrophage differentiation: circulation inflammatory monocyte as biomarker for inflammatory diseases. *Biomark. Res.* **2**, 1 (2014).

252. Gane, J. M., Stockley, R. A. & Sapey, E. TNF-α Autocrine Feedback Loops in Human Monocytes: The Pro- and Anti-Inflammatory Roles of the TNF-α Receptors Support the Concept of Selective TNFR1 Blockade In Vivo. *J. Immunol. Res.* **2016**, (2016).

253. Wong, K. L. *et al.* The three human monocyte subsets: implications for health and disease. *Immunol. Res.* **53**, 41–57 (2012).

254. Auffray, C. *et al.* Monitoring of Blood Vessels and Tissues by a Population of Monocytes with Patrolling Behavior. *Science* **317**, 666–670 (2007).

255. Maggioli, M. F., Palmer, M. V., Thacker, T. C., Vordermeier, H. M. & Waters, W. R. Characterization of Effector and Memory T Cell Subsets in the Immune Response to Bovine Tuberculosis in Cattle. *PLOS ONE* **10**, e0122571 (2015).

256. Henao-Tamayo, M. I. *et al.* Phenotypic Definition of Effector and Memory T-Lymphocyte Subsets in Mice Chronically Infected with Mycobacterium tuberculosis. *Clin. Vaccine Immunol.* **17**, 618–625 (2010).

257. Sallusto, F., Mackay, C. R. & Lanzavecchia, A. The Role of Chemokine Receptors in Primary, Effector, and Memory Immune Responses. *Annu. Rev. Immunol.* **18**, 593–620 (2000).

258. Lanzavecchia, A. & Sallusto, F. Understanding the generation and function of memory T cell subsets. *Curr. Opin. Immunol.* **17**, 326–332 (2005).

259. van Rensburg, I. C., Kleynhans, L., Keyser, A., Walzl, G. & Loxton, A. G. B-cells with a FasL expressing regulatory phenotype are induced following successful anti-tuberculosis treatment: TB treatment induces FasL regulatory B cells. *Immun. Inflamm. Dis.* **5**, 57–67 (2017).

260. du Plessis, W. J. *et al.* The Functional Response of B Cells to Antigenic Stimulation: A Preliminary Report of Latent Tuberculosis. *PLOS ONE* **11**, e0152710 (2016).

261. Hong, H. S. *et al.* Loss of CCR7 Expression on CD56bright NK Cells Is Associated with a CD56dimCD16+ NK Cell-Like Phenotype and Correlates with HIV Viral Load. *PLoS ONE* **7**, e44820 (2012).

262. Mason, A. T. *et al.* Regulation of NK cells through the 80-kDa TNFR (CD120b). *J. Leukoc. Biol.* **58**, 249–255 (1995).

263. Arokiasamy, S. *et al.* Endogenous TNFα orchestrates the trafficking of neutrophils into and within lymphatic vessels during acute inflammation. *Sci. Rep.* **7**, (2017).

264. Hampton, H. R. & Chtanova, T. The lymph node neutrophil. *Semin. Immunol.* **28**, 129–136 (2016).

265. Beauvillain, C. *et al.* CCR7 is involved in the migration of neutrophils to lymph nodes. *Blood* **117**, 1196–1204 (2011).

266. Förster, R., Davalos-Misslitz, A. C. & Rot, A. CCR7 and its ligands: balancing immunity and tolerance. *Nat. Rev. Immunol.* **8**, 362–371 (2008).

267. Thompson, E. G. *et al.* Host blood RNA signatures predict the outcome of tuberculosis treatment. *Tuberculosis* **107**, 48–58 (2017).

268. Nascimbeni, M., Pol, S. & Saunier, B. Distinct CD4+CD8+ Double-Positive T Cells in the Blood and Liver of Patients during Chronic Hepatitis B and C. *PLoS ONE* **6**, e20145 (2011).

269. Nascimbeni, M., Shin, E.-C., Chiriboga, L., Kleiner, D. E. & Rehermann, B. Peripheral CD4/CD8 Double-Positive T cells are Differentiated Effector Memory Cells With Antiviral Functions. *Blood* 35 (2004). doi:10.1182/blood-2003-12-4395

270. Joosten, S. A. *et al.* Patients with Tuberculosis Have a Dysfunctional Circulating B-Cell Compartment, Which Normalizes following Successful Treatment. *PLOS Pathog.* **12**, e1005687 (2016).

271. Malherbe, S. T. *et al.* Persisting positron emission tomography lesion activity and Mycobacterium tuberculosis mRNA after tuberculosis cure. *Nat. Med.* **22**, 1094–1100 (2016).

272. Roederer, M., Nozzi, J. & Nason, M. SPICE: Exploration and Analysis of Post-Cytometric Complex Multivariate Datasets. *Cytom. Part J. Int. Soc. Anal. Cytol.* **79**, 167–174 (2011).

273. Sagiv, J. Y. *et al.* Phenotypic Diversity and Plasticity in Circulating Neutrophil Subpopulations in Cancer. *Cell Rep.* **10**, 562–573 (2015).

274. Negorev, D. *et al.* Human neutrophils can mimic myeloid-derived suppressor cells (PMN-MDSC) and suppress microbead or lectin-induced T cell proliferation through artefactual mechanisms. *Sci. Rep.* **8**, 3135 (2018).

275. Kleiveland, C. R. Peripheral Blood Mononuclear Cells. in *The Impact of Food Bioactives on Health* 161–167 (2015). doi:10.1007/978-3-319-16104-4_15

276. Flynn, J. L., Chan, J. & Lin, P. L. Macrophages and control of granulomatous inflammation in tuberculosis. *Mucosal Immunol.* **4**, 271–278 (2011).

277. Petruccioli, E. *et al.* Correlates of tuberculosis risk: predictive biomarkers for progression to active tuberculosis. *Eur. Respir. J.* ERJ-01012-2016 (2016). doi:10.1183/13993003.01012-2016

278. WHO | Global tuberculosis report 2017. *WHO* Available at: http://www.who.int/tb/publications/global_report/en/. (Accessed: 11th December 2017)

279. Netea, M. G., Quintin, J. & van der Meer, J. W. M. Trained Immunity: A Memory for Innate Host Defense. *Cell Host Microbe* **9**, 355–361 (2011).

280. Netea, M. G. *et al.* Trained immunity: A program of innate immune memory in health and disease. *Science* **352**, aaf1098 (2016).

281. Vesosky, B., Rottinghaus, E. K., Stromberg, P., Turner, J. & Beamer, G. CCL5 participates in early protection against Mycobacterium tuberculosis. *J. Leukoc. Biol.* **87**, 1153–1165 (2010).

282. Stegelmann, F. *et al.* Coordinate Expression of CC Chemokine Ligand 5, Granulysin, and Perforin in CD8+ T Cells Provides a Host Defense Mechanism against Mycobacterium tuberculosis. *J. Immunol.* **175**, 7474–7483 (2005).

283. Crawford, A., Angelosanto, J. M., Nadwodny, K. L., Blackburn, S. D. & Wherry, E. J. A Role for the Chemokine RANTES in Regulating CD8 T Cell Responses during Chronic Viral Infection. *PLOS Pathog.* **7**, e1002098 (2011).

284. Sadek, M. I., Sada, E., Toossi, Z., Schwander, S. K. & Rich, E. A. Chemokines Induced by Infection of Mononuclear Phagocytes with Mycobacteria and Present in Lung Alveoli during Active Pulmonary Tuberculosis. *Am. J. Respir. Cell Mol. Biol.* **19**, 513–521 (1998).

285. Bystry, R. S., Aluvihare, V., Welch, K. A., Kallikourdis, M. & Betz, A. G. B cells and professional APCs recruit regulatory T cells via CCL4. *Nat. Immunol.* **2**, 1126–1132 (2001).

286. Chiba, K. *et al.* Neutrophils secrete MIP-1beta after adhesion to laminin contained in basement membrane of blood vessels. *Br. J. Haematol.* **127**, 592–597 (2004).

287. Meagher, C. *et al.* CCL4 Protects From Type 1 Diabetes by Altering Islet -Cell-Targeted Inflammatory Responses. *Diabetes* **56**, 809–817 (2007).

288. Joosten, S. A. *et al.* Identification of a human CD8+ regulatory T cell subset that mediates suppression through the chemokine CC chemokine ligand 4. *Proc. Natl. Acad. Sci.* **104**, 8029–8034 (2007).

289. Ashenafi, S. *et al.* Progression of clinical tuberculosis is associated with a Th2 immune response signature in combination with elevated levels of SOCS3. *Clin. Immunol.* **151**, 84–99 (2014).

290. Tecchio, C., Micheletti, A. & Cassatella, M. A. Neutrophil-Derived Cytokines: Facts Beyond Expression. *Front. Immunol.* **5**, (2014).

291. Zucchi, F. C. R. *et al.* Modulation of angiogenic factor VEGF by DNA-hsp65 vaccination in a murine CNS tuberculosis model. *Tuberculosis* **93**, 373–380 (2013).

292. Berard, M., Brandt, K., Paus, S. B. & Tough, D. F. IL-15 Promotes the Survival of Naive and Memory Phenotype CD8+ T Cells. *J. Immunol.* **170**, 5018–5026 (2003).

293. Rausch, A. *et al.* Interleukin-15 mediates protection against experimental tuberculosis: A role for NKG2D-dependent effector mechanisms of CD8+ T cells. *Eur. J. Immunol.* **36**, 1156–1167 (2006).

294. Krupa, A. *et al.* Binding of CXCL8/IL-8 to *Mycobacterium tuberculosis* Modulates the Innate Immune Response. *Mediators Inflamm.* **2015**, 1–11 (2015).

295. Ameixa, C. & Friedland, J. S. Interleukin-8 Secretion from Mycobacterium tuberculosis-Infected Monocytes Is Regulated by Protein Tyrosine Kinases but Not by ERK1/2 or p38 Mitogen-Activated Protein Kinases. *Infect. Immun.* **70**, 4743–4746 (2002).

296. Silva Miranda, M., Breiman, A., Allain, S., Deknuydt, F. & Altare, F. The Tuberculous Granuloma: An Unsuccessful Host Defence Mechanism Providing a Safety Shelter for the Bacteria? *Clin. Dev. Immunol.* **2012**, 1–14 (2012).

297. Hilda, J. N. & Das, S. D. TLR stimulation of human neutrophils lead to increased release of MCP-1, MIP-1α, IL-1β, IL-8 and TNF during tuberculosis. *Hum. Immunol.* (2015).

298. Condamine, T. & Gabrilovich, D. I. Molecular mechanisms regulating myeloid-derived suppressor cell differentiation and function. *Trends Immunol.* **32**, 19–25 (2011).

299. Dufour, J. H. *et al.* IFN- -Inducible Protein 10 (IP-10; CXCL10)-Deficient Mice Reveal a Role for IP-10 in Effector T Cell Generation and Trafficking. *J. Immunol.* **168**, 3195–3204 (2002).

300. Wergeland, I., Assmus, J. & Dyrhol-Riise, A. M. Cytokine Patterns in Tuberculosis Infection; IL-1ra, IL-2 and IP-10 Differentiate Borderline QuantiFERON-TB Samples from Uninfected Controls. *PLOS ONE* **11**, e0163848 (2016).

301. Filippi, C. M. *et al.* Transforming Growth Factor- Suppresses the Activation of CD8+ T-Cells When Naive but Promotes Their Survival and Function Once Antigen Experienced: A Two-Faced Impact on Autoimmunity. *Diabetes* **57**, 2684–2692 (2008).

302. Cottrez, F. & Groux, H. Regulation of TGF- Response During T Cell Activation Is Modulated by IL-10. *J. Immunol.* **167**, 773–778 (2001).

303. Oh, S. A. & Li, M. O. TGF- : Guardian of T Cell Function. *J. Immunol.* **191**, 3973–3979 (2013).

304. Dorhoi, A. & Du Plessis, N. Monocytic Myeloid-Derived Suppressor Cells in Chronic Infections. *Front. Immunol.* **8**, (2018).

305. van der Meer, J. W. The effects of recombinant interleukin-1 and recombinant tumor necrosis factor on non-specific resistance to infection. *Biotherapy Dordr. Neth.* **1**, 19–25 (1988).

306. van der Meer, J. W., Barza, M., Wolff, S. M. & Dinarello, C. A. A low dose of recombinant interleukin 1 protects granulocytopenic mice from lethal gram-negative infection. *Proc. Natl. Acad. Sci. U. S. A.* **85**, 1620–1623 (1988).

307. Bronte, V. *et al.* Recommendations for myeloid-derived suppressor cell nomenclature and characterization standards. *Nat. Commun.* **7**, 12150 (2016).

308. du Plessis, N. *et al.* Increased Frequency of Myeloid-derived Suppressor Cells during Active Tuberculosis and after Recent Mycobacterium tuberculosis Infection Suppresses T-Cell Function. *Am. J. Respir. Crit. Care Med.* **188**, 724–732 (2013).

309. Parton, R. G. & Simons, K. The multiple faces of caveolae. *Nat. Rev. Mol. Cell Biol.* **8**, 185–194 (2007).

310. Mundy, D. I., Li, W. P., Luby-Phelps, K. & Anderson, R. G. W. Caveolin targeting to late endosome/lysosomal membranes is induced by perturbations of lysosomal pH and cholesterol content. *Mol. Biol. Cell* **23**, 864–880 (2012).

311. Hansen, C. G. & Nichols, B. J. Exploring the caves: cavins, caveolins and caveolae. *Trends Cell Biol.* **20**, 177–186 (2010).

312. Kumar, V., Patel, S., Tcyganov, E. & Gabrilovich, D. I. The Nature of Myeloid-Derived Suppressor Cells in the Tumor Microenvironment. *Trends Immunol.* **37**, 208–220 (2016).

313. Vollbrecht, T. *et al.* Chronic progressive Hiv-1 infection is associated with elevated levels of myeloid-derived suppressor cells. *Aids* **26**, (2012).

314. Condamine, T. *et al.* Lectin-type oxidized LDL receptor-1 distinguishes population of human polymorphonuclear myeloid-derived suppressor cells in cancer patients. *Sci. Immunol.* **1**, (2016).

315. Grützner, E. *et al.* Kinetics of human myeloid-derived suppressor cells after blood draw. *J. Transl. Med.* **14**, (2016).

316. Kumar, N. P. *et al.* Role of myeloid derived suppressor cells in tuberculosis infection and disease. *BMC Infect. Dis.* **14**, O18 (2014).

317. Triantafilou, M. & Triantafilou, K. Lipopolysaccharide recognition: CD14, TLRs and the LPS-activation cluster. *Trends Immunol.* **23**, 301–304 (2002).

318. Granucci, F. & Zanoni, I. Role of CD14 in host protection against infections and in metabolism regulation. *Front. Cell. Infect. Microbiol.* **3**, (2013).

319. Juffermans, N. P. *et al.* Serum Concentrations of Lipopolysaccharide Activity–Modulating Proteins during Tuberculosis. *J. Infect. Dis.* **178**, 1839–1842 (1998).

320. He, Z. *et al.* CD14 Is a Co-Receptor for TLR4 in the S100A9-Induced Pro-Inflammatory Response in Monocytes. *PLOS ONE* **11**, e0156377 (2016).

321. Roth, J., Vogl, T., Sorg, C. & Sunderkötter, C. Phagocyte-specific S100 proteins: a novel group of proinflammatory molecules. *Trends Immunol.* **24**, 155–158 (2003).

322. Foell, D., Wittkowski, H., Vogl, T. & Roth, J. S100 proteins expressed in phagocytes: a novel group of damage-associated molecular pattern molecules. *J. Leukoc. Biol.* **81**, 28–37 (2007).

323. Feng, P.-H. *et al.* S100A9+ MDSC and TAM-mediated EGFR-TKI resistance in lung adenocarcinoma: the role of RELB. *Oncotarget* **9**, 7631–7643 (2018).

324. Källberg, E. *et al.* S100A9 Interaction with TLR4 Promotes Tumor Growth. *PLoS ONE* **7**, e34207 (2012).

325. Mazzoni, A. *et al.* Myeloid Suppressor Lines Inhibit T Cell Responses by an NO-Dependent Mechanism. *J. Immunol.* **168**, 689–695 (2002).

326. Marvel, D. & Gabrilovich, D. I. Myeloid-derived suppressor cells in the tumor microenvironment: expect the unexpected. *J. Clin. Invest.* **125**, 3356–3364 (2015).

327. Vogl, T. *et al.* Mrp8 and Mrp14 are endogenous activators of Toll-like receptor 4, promoting lethal, endotoxin-induced shock. *Nat. Med.* **13**, 1042–1049 (2007).

328. Björk, P. *et al.* Identification of human S100A9 as a novel target for treatment of autoimmune disease via binding to quinoline-3-carboxamides. *PLoS Biol.* **7**, e97 (2009).

329. Nichols, B. Caveosomes and endocytosis of lipid rafts. *J. Cell Sci.* **116**, 4707–4714 (2003).

330. Triantafilou, M., Morath, S., Mackie, A., Hartung, T. & Triantafilou, K. Lateral diffusion of Toll-like receptors reveals that they are transiently confined within lipid rafts on the plasma membrane. *J. Cell Sci.* **117**, 4007–4014 (2004).

331. Lingwood, D. & Simons, K. Lipid rafts as a membrane-organizing principle. *Science* **327**, 46–50 (2010).

332. Zaas, D. W., Duncan, M., Rae Wright, J. & Abraham, S. N. The role of lipid rafts in the pathogenesis of bacterial infections. *Biochim. Biophys. Acta BBA - Mol. Cell Res.* **1746**, 305–313 (2005).

333. Bunt, S. K., Clements, V. K., Hanson, E. M., Sinha, P. & Ostrand-Rosenberg, S. Inflammation enhances myeloid-derived suppressor cell cross-talk by signaling through Toll-like receptor 4. *J. Leukoc. Biol.* **85**, 996–1004 (2009).

334. Ray, A., Chakraborty, K. & Ray, P. Immunosuppressive MDSCs induced by TLR signaling during infection and role in resolution of inflammation. *Front. Cell. Infect. Microbiol.* **3**, (2013).

335. Gabrilovich, D. I., Velders, M. P., Sotomayor, E. M. & Kast, W. M. Mechanism of immune dysfunction in cancer mediated by immature Gr-1+ myeloid cells. *J. Immunol. Baltim. Md 1950* **166**, 5398–5406 (2001).

336. Gabrilovich, D. I., Ostrand-Rosenberg, S. & Bronte, V. Coordinated regulation of myeloid cells by tumours. *Nat. Rev. Immunol.* **12**, 253–268 (2012).

337. Wesolowski, R., Markowitz, J. & Carson, W. E. Myeloid derived suppressor cells – a new therapeutic target in the treatment of cancer. *J. Immunother. Cancer* **1**, 10 (2013).

338. Di Mitri, D., Toso, A. & Alimonti, A. Molecular Pathways: Targeting Tumor-Infiltrating Myeloid-Derived Suppressor Cells for Cancer Therapy. *Clin. Cancer Res. Off. J. Am. Assoc. Cancer Res.* **21**, 3108–3112 (2015).

339. Ribechini, E., Greifenberg, V., Sandwick, S. & Lutz, M. B. Subsets, expansion and activation of myeloid-derived suppressor cells. *Med. Microbiol. Immunol. (Berl.)* **199**, 273–281 (2010).

340. Greifenberg, V., Ribechini, E., Rössner, S. & Lutz, M. B. Myeloid-derived suppressor cell activation by combined LPS and IFN-gamma treatment impairs DC development. *Eur. J. Immunol.* **39**, 2865–2876 (2009).

341. Huang, B. *et al.* CCL2/CCR2 pathway mediates recruitment of myeloid suppressor cells to cancers. *Cancer Lett.* **252**, 86–92 (2007).

342. Qian, B.-Z. *et al.* CCL2 recruits inflammatory monocytes to facilitate breast-tumour metastasis. *Nature* **475**, 222–225 (2011).

343. Schlecker, E. *et al.* Tumor-infiltrating monocytic myeloid-derived suppressor cells mediate CCR5-dependent recruitment of regulatory T cells favoring tumor growth. *J. Immunol. Baltim. Md 1950* **189**, 5602–5611 (2012).

344. Peter, M. E. *et al.* The CD95 receptor: apoptosis revisited. *Cell* **129**, 447–450 (2007).

345. Sinha, P. *et al.* Myeloid-derived suppressor cells express the death receptor Fas and apoptose in response to T cell–expressed FasL. *Blood* **117**, 5381–5390 (2011).

346. Zhang, Y. *et al.* Fas Signal Promotes Lung Cancer Growth by Recruiting Myeloid-Derived Suppressor Cells via Cancer Cell-Derived PGE2. *J. Immunol.* **182**, 3801–3808 (2009).

347. Zou, Q. & Zhuang, Y. IL-22-producing Th cells regulate myeloid-derived suppressor cells in Helicobacter pylori-associated immunopathogenesis (IRC5P.456). *J. Immunol.* **192**, 125.5-125.5 (2014).

348. Perusina Lanfranca, M., Lin, Y., Fang, J., Zou, W. & Frankel, T. Biological and pathological activities of interleukin-22. *J. Mol. Med. Berl. Ger.* **94**, 523–534 (2016).

349. Xiao, P. *et al.* Interleukin 33 in tumor microenvironment is crucial for the accumulation and function of myeloid-derived suppressor cells. *OncoImmunology* **5**, e1063772 (2016).

350. Lu, B., Yang, M. & Wang, Q. Interleukin-33 in tumorigenesis, tumor immune evasion, and cancer immunotherapy. *J. Mol. Med.* **94**, 535–543 (2016).

351. Kumar, S., Rao, N. & Ge, R. Emerging Roles of ADAMTSs in Angiogenesis and Cancer. *Cancers* **4**, 1252–1299 (2012).

352. Toscano, V. *et al.* Thrombotic thrombocytopenic purpura associated with primary tuberculosis. *Infection* **23**, 58–59 (1995).

353. Pène, F. *et al.* Septic Shock and Thrombotic Microangiopathy Due to Mycobacterium tuberculosis in a Nonimmunocompromised Patient. *Arch. Intern. Med.* **161**, 1347–1348 (2001).

354. Mazzieri, R. *et al.* Targeting the ANG2/TIE2 axis inhibits tumor growth and metastasis by impairing angiogenesis and disabling rebounds of proangiogenic myeloid cells. *Cancer Cell* **19**, 512–526 (2011).

355. Condamine, T., Ramachandran, I., Youn, J.-I. & Gabrilovich, D. I. Regulation of Tumor Metastasis by Myeloid-derived Suppressor Cells. *Annu. Rev. Med.* **66**, 97–110 (2015).

356. Umansky, V., Blattner, C., Gebhardt, C. & Utikal, J. The Role of Myeloid-Derived Suppressor Cells (MDSC) in Cancer Progression. *Vaccines* **4**, (2016).

357. Kusmartsev, S. *et al.* Oxidative Stress Regulates Expression of VEGFR1 in Myeloid Cells: Link to Tumor-Induced Immune Suppression in Renal Cell Carcinoma. *J. Immunol.* **181**, 346–353 (2008).

358. Atretkhany, K.-S. N. *et al.* TNF Neutralization Results in the Delay of Transplantable Tumor Growth and Reduced MDSC Accumulation. *Front. Immunol.* **7**, (2016).

359. Cheng, J. *et al.* Protection from Fas-mediated apoptosis by a soluble form of the Fas molecule. *Science* **263**, 1759–1762 (1994).

360. Takabatake, N. *et al.* Circulating levels of soluble Fas ligand and soluble Fas in patients with chronic obstructive pulmonary disease. *Respir. Med.* **94**, 1215–1220 (2000).

361. Lettau, M., Paulsen, M., Kabelitz, D. & Janssen, O. Storage, expression and function of Fas ligand, the key death factor of immune cells. *Curr. Med. Chem.* **15**, 1684–1696 (2008).

362. Veglia, F., Perego, M. & Gabrilovich, D. Myeloid-derived suppressor cells coming of age. *Nat. Immunol.* **19**, 108–119 (2018).

363. Ostrand-Rosenberg, S. & Sinha, P. Myeloid-Derived Suppressor Cells: Linking Inflammation and Cancer. *J. Immunol. Baltim. Md 1950* **182**, 4499–4506 (2009).

364. Pan, P.-Y. *et al.* Immune stimulatory receptor CD40 is required for T-cell suppression and T regulatory cell activation mediated by myeloid-derived suppressor cells in cancer. *Cancer Res.* **70**, 99–108 (2010).

365. Roland, C. L. *et al.* Cytokine levels correlate with immune cell infiltration after anti-VEGF therapy in preclinical mouse models of breast cancer. *PloS One* **4**, e7669 (2009).

366. Sceneay, J., Parker, B. S., Smyth, M. J. & Möller, A. Hypoxia-driven immunosuppression contributes to the pre-metastatic niche. *Oncoimmunology* **2**, e22355 (2013).

367. Eruslanov, E. *et al.* Expansion of CCR8+ inflammatory myeloid cells in cancer patients with urothelial and renal carcinomas. *Clin. Cancer Res. Off. J. Am. Assoc. Cancer Res.* **19**, 1670–1680 (2013).

368. Hoelzinger, D. B. *et al.* Blockade of CCL1 inhibits T regulatory cell suppressive function enhancing tumor immunity without affecting T effector responses. *J. Immunol. Baltim. Md 1950* **184**, 6833–6842 (2010).

369. Shaw, A. K. *et al.* TGFβ Signaling in Myeloid Cells Regulates Mammary Carcinoma Cell Invasion through Fibroblast Interactions. *PLoS ONE* **10**, (2015).

370. Polimeno, M. *et al.* Regulatory T cells, interleukin (IL)-6, IL-8, vascular endothelial growth factor (VEGF), CXCL10, CXCL11, epidermal growth factor (EGF) and hepatocyte growth factor (HGF) as surrogate markers of host immunity in patients with renal cell carcinoma. *BJU Int.* **112**, 686–696 (2013).

371. Mundy-Bosse, B. L. *et al.* Distinct myeloid suppressor cell subsets correlate with plasma IL-6 and IL-10 and reduced interferon-alpha signaling in CD4+ T cells from patients with GI malignancy. *Cancer Immunol. Immunother. CII* **60**, 1269–1279 (2011).

372. Stanojević, I. *et al.* Interferon alpha-induced reduction in the values of myeloid-derived suppressor cells in melanoma patients. *Vojnosanit. Pregl.* **72**, 342–349 (2015).

373. Axelsson-Robertson, R. *et al.* Frequency of Mycobacterium tuberculosis-specific CD8+ T-cells in the course of anti-tuberculosis treatment. *Int. J. Infect. Dis.* **32**, 23–29 (2015).

374. Garand, M. *et al.* Functional and Phenotypic Changes of Natural Killer Cells in Whole Blood during Mycobacterium tuberculosis Infection and Disease. *Front. Immunol.* **9**, (2018).

375. Kumar, N. P., Moideen, K., Viswanathan, V., Kornfeld, H. & Babu, S. Effect of standard tuberculosis treatment on naive, memory and regulatory T-cell homeostasis in tuberculosis-diabetes co-morbidity. *Immunology* **149**, 87–97 (2016).

376. Lee, C.-R. *et al.* Myeloid-Derived Suppressor Cells Are Controlled by Regulatory T Cells via TGF-β during Murine Colitis. *Cell Rep.* **17**, 3219–3232 (2016).

377. Nagaraj, S., Youn, J. & Gabrilovich, D. I. Reciprocal relationship between myeloid-derived suppressor cells and T cells. *J. Immunol. Baltim. Md 1950* **191**, 17–23 (2013).

378. Gabrilovich, D. I. Myeloid-Derived Suppressor Cells. *Cancer Immunol. Res.* **5**, 3–8 (2017).